RECONSTRUCTING DEBRIS TRANSPORT PATHWAYS ON CONSTRUCTIONAL RIDGES: WAHIANOA GLACIER, MT RUAPEHU

A thesis presented in partial fulfillment of the requirements for the degree of Master of Science in Quaternary Science, at Massey University, Palmerston North, New Zealand.

Stephanie Mandolla

April 2007

The Wahianoa Glacier of Mt Ruapehu, New Zealand, looking north-west. The glacier is confined by Girdlestone Peak (left), and Mitre Peak (right).

Abstract

Reconstructing debris transport pathways on constructional ridges: Wahianoa Glacier, Mt Ruapehu

Stephanie Mandolla

It is generally accepted that Mt Ruapehu, Tongariro National Park, New Zealand, was heavily glaciated during the Pleistocene. Eight small glaciers can still be found on the summit of this active volcano. However, the glaciers have been retreating at a fast rate during the last few centuries. The scientific community has placed its main focus on the volcanic aspects of the region. Although most authors refer to the landforms that appear to be of glacial origin as 'moraines', no actual glacial studies have been undertaken so far to provide the necessary evidence that is needed to support this hypothesis.

The aim of this study is to use established field techniques in glacial geomorphology to (1) identify the extent of glacial deposits using diagnostic criteria and (2) to reconstruct the transport pathways of the Wahianoa Glacier. Four main diagnostic criteria have been used: clast morphology, macrofabrics, grain size distribution and the surface texture of grains. The Wahianoa valley has a very pronounced U-shape and is likely to be of glacial origin. The valley consists of two elongate debris ridges that are made out of unconsolidated, poorly sorted diamict of varying lithologies.

This study has identified that the activity and the composition of the volcano has lead to complex glacial processes. Glacial ice has advanced over a deformable bed and the glacier itself was probably extensively covered by supraglacial debris. The area has been identified as a pre-historic pathway for lahars and the volcano erupts frequently to produce fresh volcanic deposits. As the active vent has changed its position during the eruptive history of the volcano, the quantity and the location of the source rock that fed the glacier has varied greatly. This study is an initial attempt at unfolding the glacial

history of Mt Ruapehu. This is based on field analysis of glacigenic sediments, rather than topographic and aerial photo analysis. The results show great complexity and the potential for further studies of other moraine systems on Mt Ruapehu.

ACKNOWLEDGEMENTS

I extend my sincere thanks and appreciation to my supervisor, Dr Martin Brook, for the support and feedback given throughout the year.

I wish to thank Dough Hopcroft, for the help with the SEM analysis.

Special thanks to John Procter for giving his permission to reproduce some of his findings.

I also like to thank Dr Bernd Striewski for his help with the sedigraph analysis.

Many thanks to David Feek for the help and organisation of field and laboratory equipment.

I also wish to thank my family for their unfailing support and understanding.

Lastly, I would like to thank Erin Nolan for the many hours we have spent together in the field and for helping to make Ohakune an exciting place during the summer months.

****

TABLE OF CONTENTS

LIST OF FIGURES

LIST OF TABLES

Chapter 1

INTRODUCTION

1.1 MT RUAPEHU

Mt Ruapehu is an active andesite stratovolcano with a multiple vent system. Five summit craters have been identified: East Crater, West Crater, North Crater, Dome Crater, and Girdlestone Crater/Wahianoa Cone (Donoghue, 1991; Williams, 2001). The current vent is in the form of a crater lake. The volcano was built over the past 250k yrs in at least four cone-building episodes (Donoghue & Neall, 2001; Hackett, 1985; Hackett & Houghton, 1989). The Ruapehu massif is comprised of products from both effusive and explosive eruptions. These contrasting lithologies result in structural instability and different erosion rates. The ring plain consists mainly of reworked debris, coarse laharic volcaniclastic deposits and air fall tephra units (Hackett & Houghton, 1989; Procter, 2003).

1.1.2 The present day glaciers of Mt Ruapehu

With a height of 2797m Mt Ruapehu is the highest mountain on the North Island of New Zealand. Due to its altitude it also allows the formation of glaciers. These are the only glaciers found on the North Island. The locations and the extent of these glaciers are shown in figure 1.1. The Whangaehu and the Mangatoetoenui Glaciers are situated on the eastern slopes of Ruapehu and are fed by the Summit Plateau. The Whakapapanui Glacier to the north is the remnant of the once much more advanced Whakapapa Glacier to the north-west (Heine, 1962). The Mangaturuturu Glacier can be found on the western slopes and is the result of over spilling nevé from the Crater Basin Glacier. The Wahianoa and the Mangaehuehu Glaciers on the south and south-east are the only glaciers that are not fed by the summit nevé.

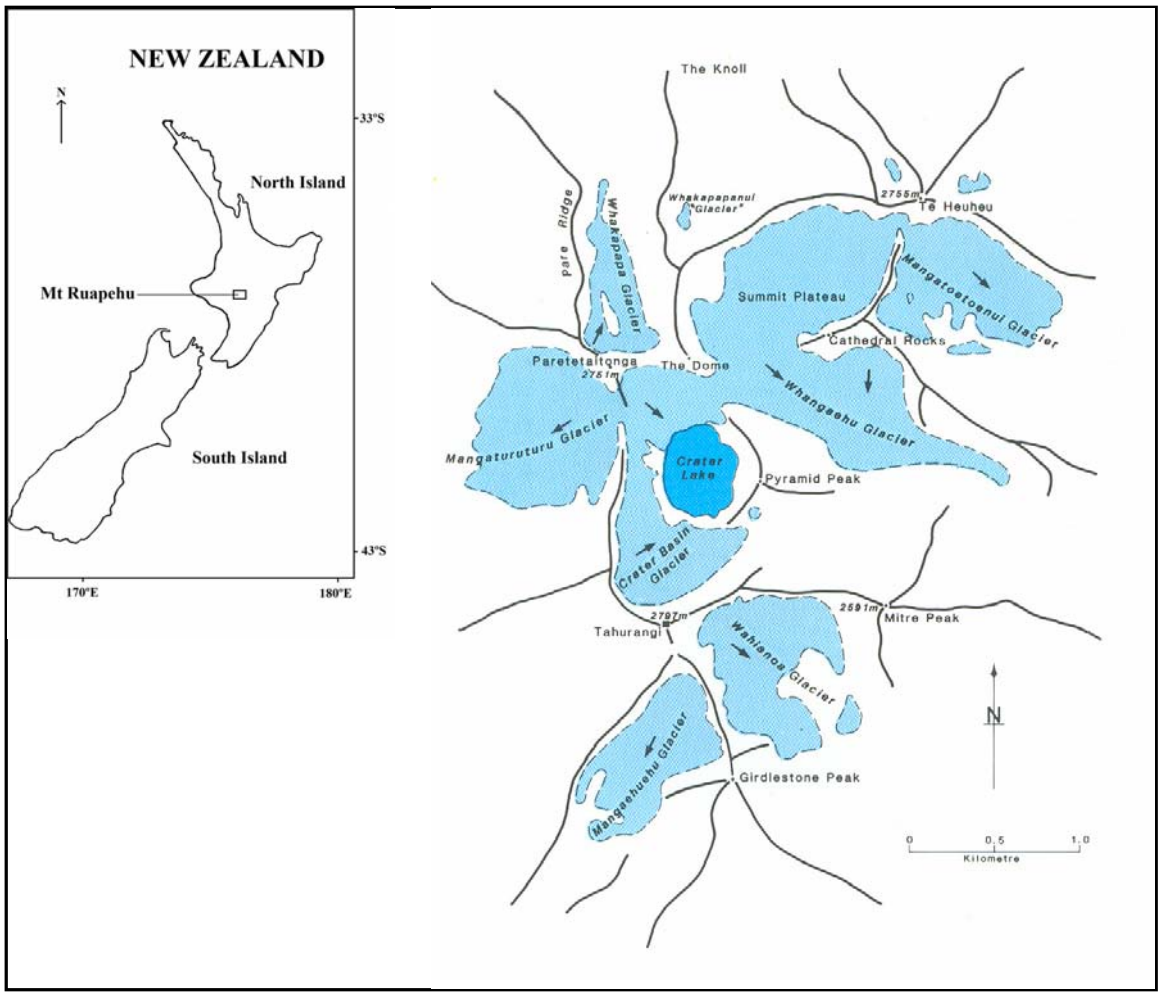

Figure 1.1 Plainview of the summit area of Mt Ruapehu, showing the locations and the extent (as in 1988) of the present day glaciers. The arrows indicate the direction of ice flow (Williams, 2001).

1.1.3 Former glaciation on Mt Ruapehu

Hackett (1985) has identified several glacial valleys on Mt Ruapehu. Figure 1.2 shows the outline of the Ruapehu massif and the locations of these valleys. Because the largest moraines cut into and build upon the two oldest volcanic formations, Hackett suggested that these moraines are younger than 0.23ma. Although it is generally accepted that the present day glaciers were more advanced during the Pleistocene, no definitive account has been given so far. This is mainly due to the fact that volcanic processes have made it difficult to interpret the evidence (McArthur & Shepherd, 1990). For example: laharic and till deposits are both unconsolidated and poorly sorted diamictons and both can produce striae (McArthur & Shepherd, 1990; Donoghue & Neall, 2001). Therefore, the existence

and the extent of a former, more advanced glaciation on Ruapehu was subject of controversy for a very long time (Willett, 1950). However, McArthur and Shepherd (1990) have concluded that glacial features have formed during two main glacial episodes, which they have linked to the last two stadials of the Otira Glaciation[1]. This was based on the reconstruction of the equilibrium line altitude (ELA), which was correlated with those of the Tasman Valley on the South Island.

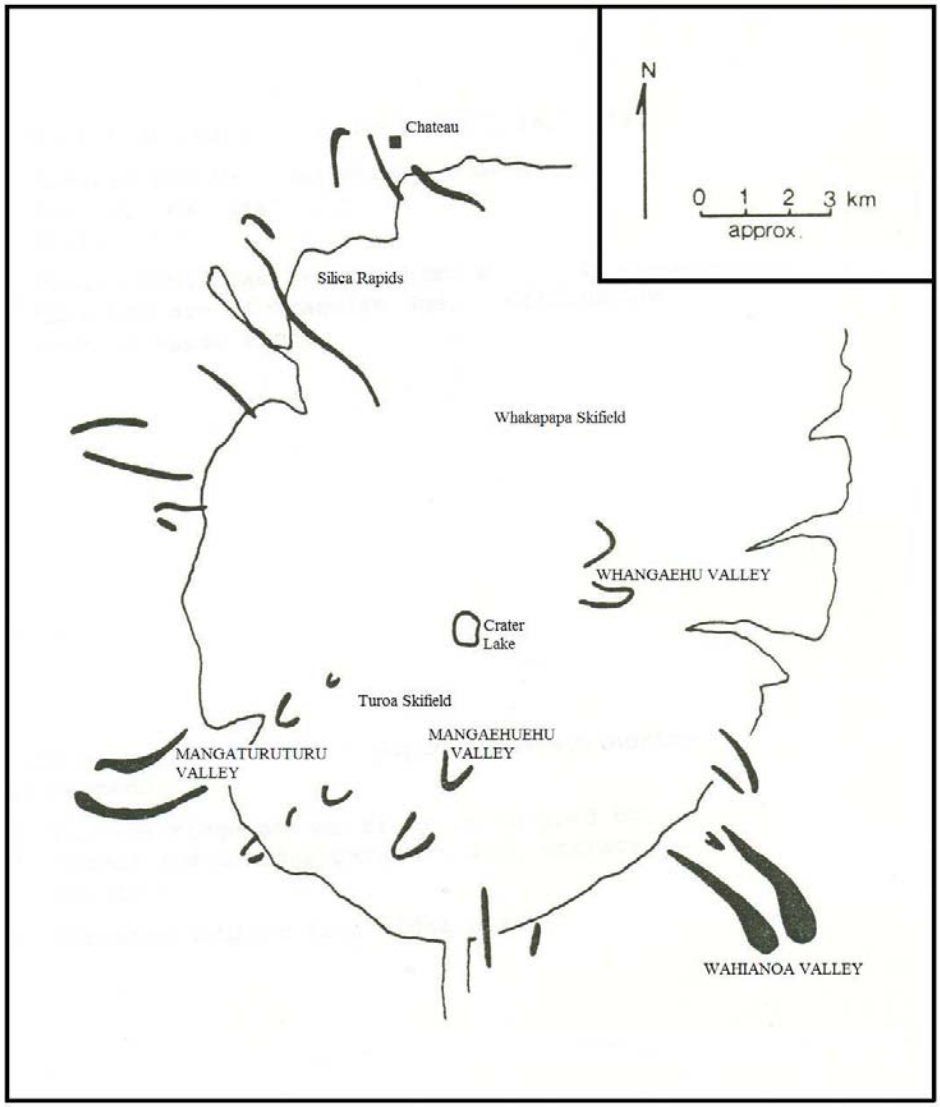

Figure 1.2: Distribution of glacial moraines on Mt Ruapehu as identified by Hackett (adapted from Hackett, 1989).

[1] The Otira Glaciation spanned around 70-10ka yrs BP (Marine Oxygen Isotope stages 2-4) (McGlone *et al.,* 1993).

1.2 OBJECTIVES

The focus of this study is the Wahianoa Valley (Fig. 1.3) on the southeastern slopes of Mt Ruapehu. Very little research has been done so far to unfold the glacial history of Ruapehu. The objectives of this study are:

1) To provide evidence for the hypothesis that the Wahianoa debris ridges are true glacial moraines and are not the result of volcanic and/or fluvial activity.
2) To reconstruct the transport pathways of the Wahianoa Glacier.
3) To identify the extent of glacial deposits in the Wahianoa valley.
4) To apply established field techniques in glacial geomorphology.

The outcomes of this study will include:

1) Provide evidence that the two debris ridges of the Wahianoa Valley are true moraines.
2) A reconstruction of the transport pathways of the Wahianoa Glacier.
3) Provide information on the extent of glacigenic deposits.
4) Showing the relationship between glacial transport and deposition by providing information on:
    - clast shape and roundness;
    - macrofabrics of clasts;
    - the overall grain-size distribution;
    - surface texture of individual grains.
5) Provide information on the implications of an active volcano on a glacial system.

Figure 1.3 The Wahianoa Valley, Mt Ruapehu, New Zealand, looking north-west. The Wahianoa Glacier can be seen in the background between Girdlestone Peak (left) and Mitre Peak (right). The Valley forms a very pronounced U-shape. The two debris ridges are believed to be lateral moraines.

1.3 THE STUDY AREA

1.3.2 Wahianoa Glacier

Like all glaciers of Mt Ruapehu, the Wahianoa Glacier has retreated dramatically during the last century. Figure 1.4 shows the retreat of the Mangaehuehu Glacier from the early 1900s to 2006. In 1988 the Wahianoa Glacier covered an area of about 0.47km^2, its mean thickness was estimated at 15m and its volume at 0.0074km^3 (Keys, 1988). During the last two decades the glacier has shrunk further. However, no published surveys of glacier extent are available since 1988. The peak above the headwall of the Wahianoa Glacier is the highest point of Mt Ruapehu. Tahurangi Peak (2797m) is also the highest point on the North Island. The glacier is confined by two pyramids: Girdlestone Peak (2658m) to the West and Mitre Peak (2591m) to the East. Keys (1988) estimated the lowest elevation of the Wahianoa Glacier at 2240 ± 40m above sea level (a.s.l.). The glacier feeds several tributary streams that merge into the Wahianoa River and later into the Whangaehu River.

Figure 1.4 The retreat of the Mangaehuehu Glacier. (A) shows the glacier in the early 1900s. The glacier was strongly crevassed during this time; (B) shows a photograph of the same glacier in the 1970s. A major bluff has become visible. A steep lateral moraine on the eastern side can be seen; (C) this photo was taken late summer 2006 and is looking up the headwall. Barely any ice is left below the bluff (A + B from Williams, 2001).

1.3.3 The Wahianoa Valley

The Wahianoa valley has a very pronounced U-shape and is one of the most prominent features of the area. A U-shaped valley is generally associated with glacial activity (Kirkbride & Matthews, 1997). Therefore, it is likely that the ridges that are formed longitudinally along each side of the valley are lateral moraines, as postulated by McArthur & Shepherd (1990). The debris ridges are comprised of unconsolidated and poorly sorted diamict of varying lithologies, which is typical for a till deposit (Hambrey, 1994). On the top of the debris ridges, individual clasts and boulders show many features that can be

associated with past glacial activities, such as striae and faceted surfaces (Fig. 1.5). The ridges extend about 5.6km (horizontal distance) down the mountain to an elevation of about 1200m.

Figure 1.5 Evidence of glacial activity on Mt Ruapehu. One side of the boulder (A) has been highly polished and shows striae. A clast (B) displays a very smooth-surfaced groove; The megaclast shown in (C) has a flat and highly polished surface. The surface is strongly striated; Clast (D) is also strongly striated but also has a faceted surface.

The first peak on the eastern ridge is the Tufa Trig Station at an elevation of 1347m. At this point, the ridge is slightly convex and forms the furthest extent of the debris ridge deposit (Fig. 1.6). It is difficult to determine if this area is the terminal moraine because no conclusive deposits can be found. It is likely that the terminal moraine has been washed away by fluvial and/or volcanic processes. Closer to the glacier the ridges are stratified with layers of lava flows. The thickness of these flows varies greatly between the debris ridges. On the western ridge, lava flows are abundant but relatively thin, whereas the eastern ridge shows fewer but more extensive units. At higher altitude these thick lava flows are exposed as major bluffs.

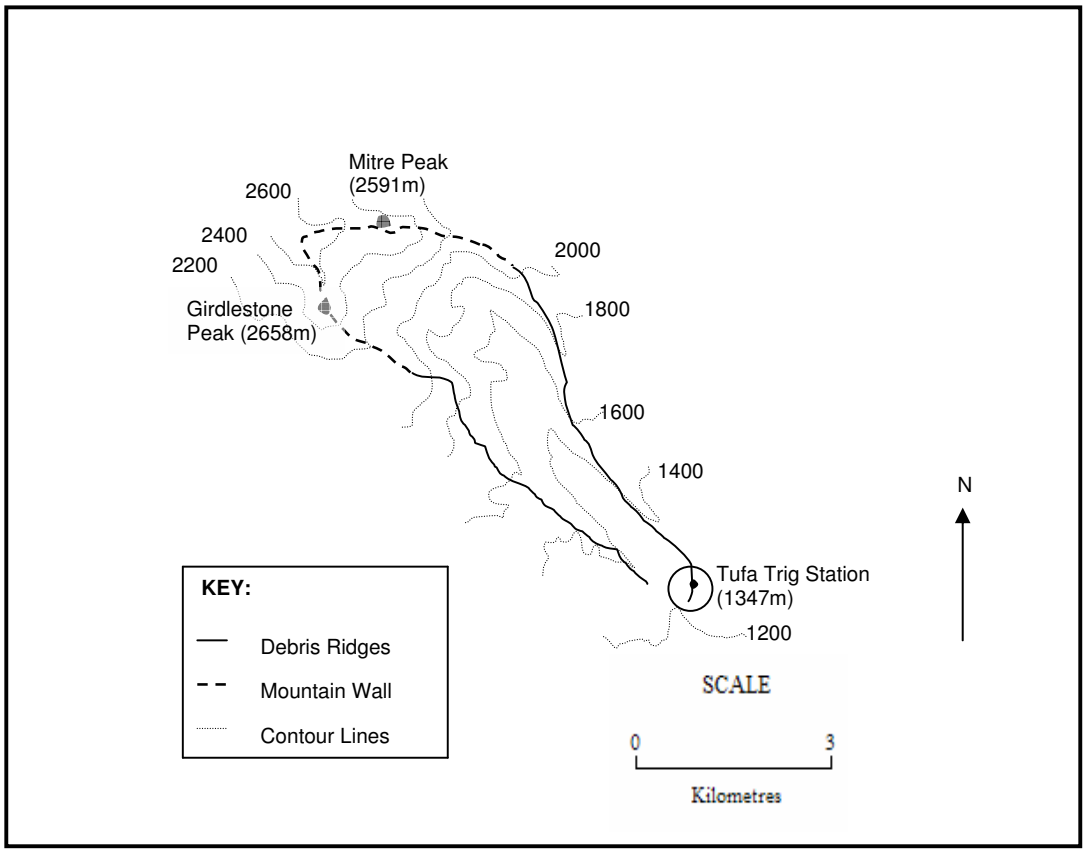

Figure 1.6 Sketch map of the Wahianoa Valley showing an outline of the debris ridges and the Mountain wall. In the area of the Tufa Trig Station the ridge is slightly convex and forms the furthest extent of the debris ridge deposit.

The height of the debris ridges varies. At the Tufa Trig Station the ridge deposit has a height of nearly 150m. The first peak on the western ridge is somewhat higher and the deposit has a height of 175m at that point (Fig. 1.7). Both debris ridges gain in height with altitude. Where the lava flows form bluffs on the eastern ridge, the deposit reaches a height of about 320m, whereas the western ridge is only about 200m at that particular location. These heights were identified by using the New Zealand Map Sheet (NZMS) 260 T20.

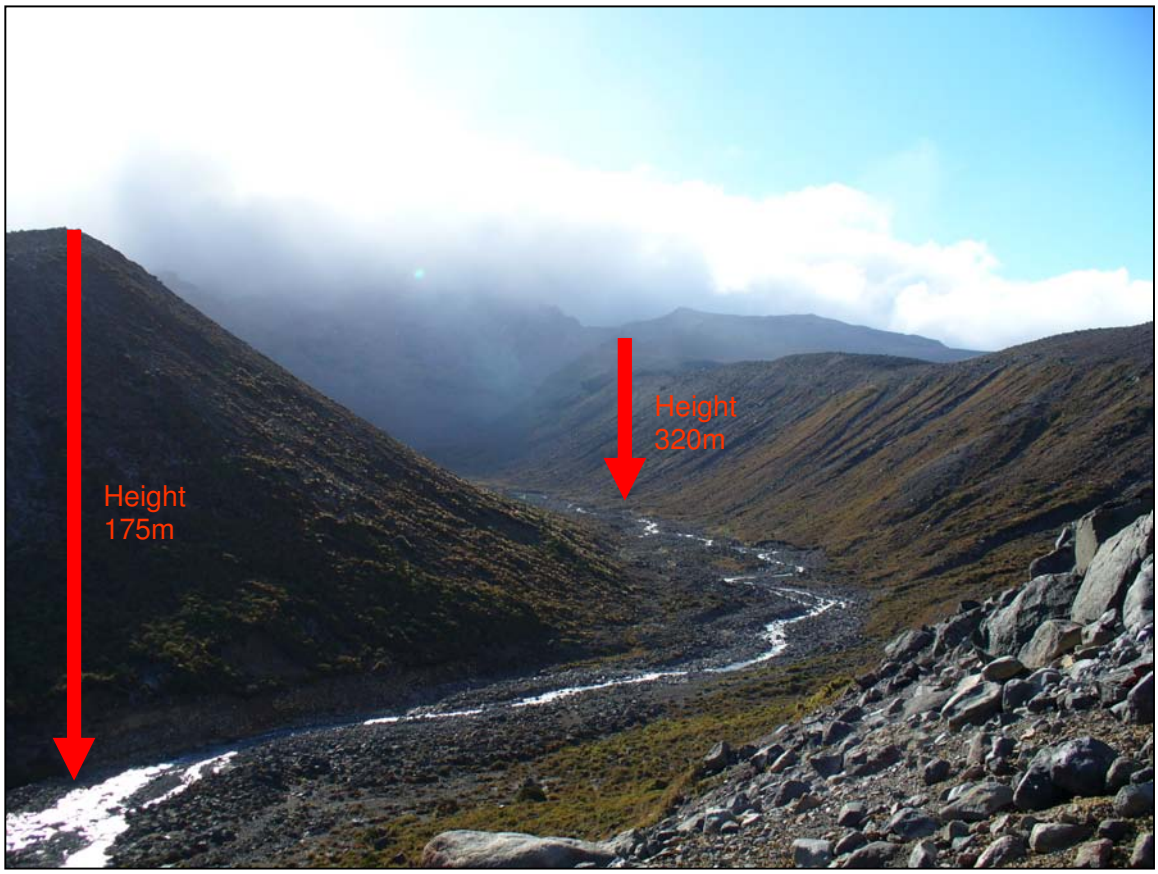

Figure 1.7 The debris ridges of the Wahianoa Valley, looking northwest. The height of the ridges ranges between about 150m at the Tufa Trig Station (to the right of the photo) and about 320m at the area where the lava flows form bluffs on the eastern ridge.

1.3.4 The morphology of the Wahianoa Valley

The morphology and the direction of the Wahianoa debris ridges vary greatly. The overall direction of the valley is south-east. However, at cross-sections E-F and G-H (Fig. 1.8) the ridges have a more southward direction. The depth of the valley decreases down-valley. As mentioned before, the headwall of the Wahianoa Glacier is confined by Girdlestone Peak and Mitre Peak (Fig. 1.8 A-B). The debris ridges originate at these two peaks. Cross-section C-D shows that the slopes (ice proximal side) of the debris ridges are nearly vertical at that location. The eastern ridge is also extremely narrow at this point. Further down-valley (Fig. 1.8 E-F), the slope of the western ridge becomes much gentler than the eastern ridge. The width of the eastern debris ridge increases dramatically at cross-section G-H and the ridge is much higher than the western deposit. From this point onwards the two ridges become narrower and have a southeastern direction. The height of both ridges also

decreases with decreasing altitude. At the furthest extent of the deposits, the eastern ridge curves slightly inwards (to the west).

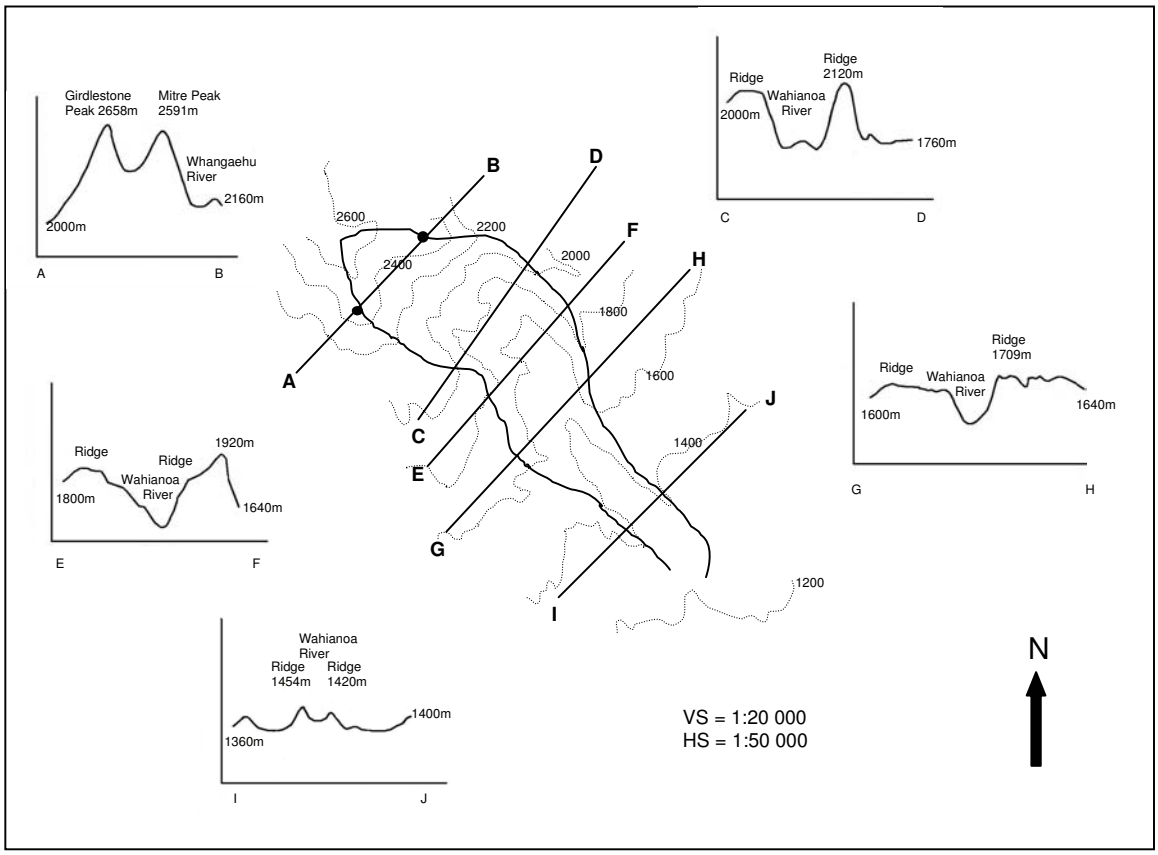

Figure 1.8 Cross-sections from various locations along the Wahianoa debris ridges. The heights and the slope angles of the two lateral ridges change dramatically along the valley.

1.3.5 Lahars on Ruapehu

At present the active crater of Ruapehu is filled with a lake, which frequently overflows. Furthermore, a volcanic eruption generally leads to the melting of the summit ice and snow. These events typically generate lahars. Ruapehu has a very long history of lahars and the Wahianoa valley has been identified as a pre-historic pathway for such events (Donoghue, 1991; Hodgson, 1993; Neall *et al.*, 1999; Donoghue & Neall, 2001) (Fig. 1.9). Therefore, it can be assumed that the deposits of the Wahianoa valley have been modified to some degree or even washed away. During a time of glaciation it is very likely that lahars would occur more frequently and are possibly more severe, since more ice is available.

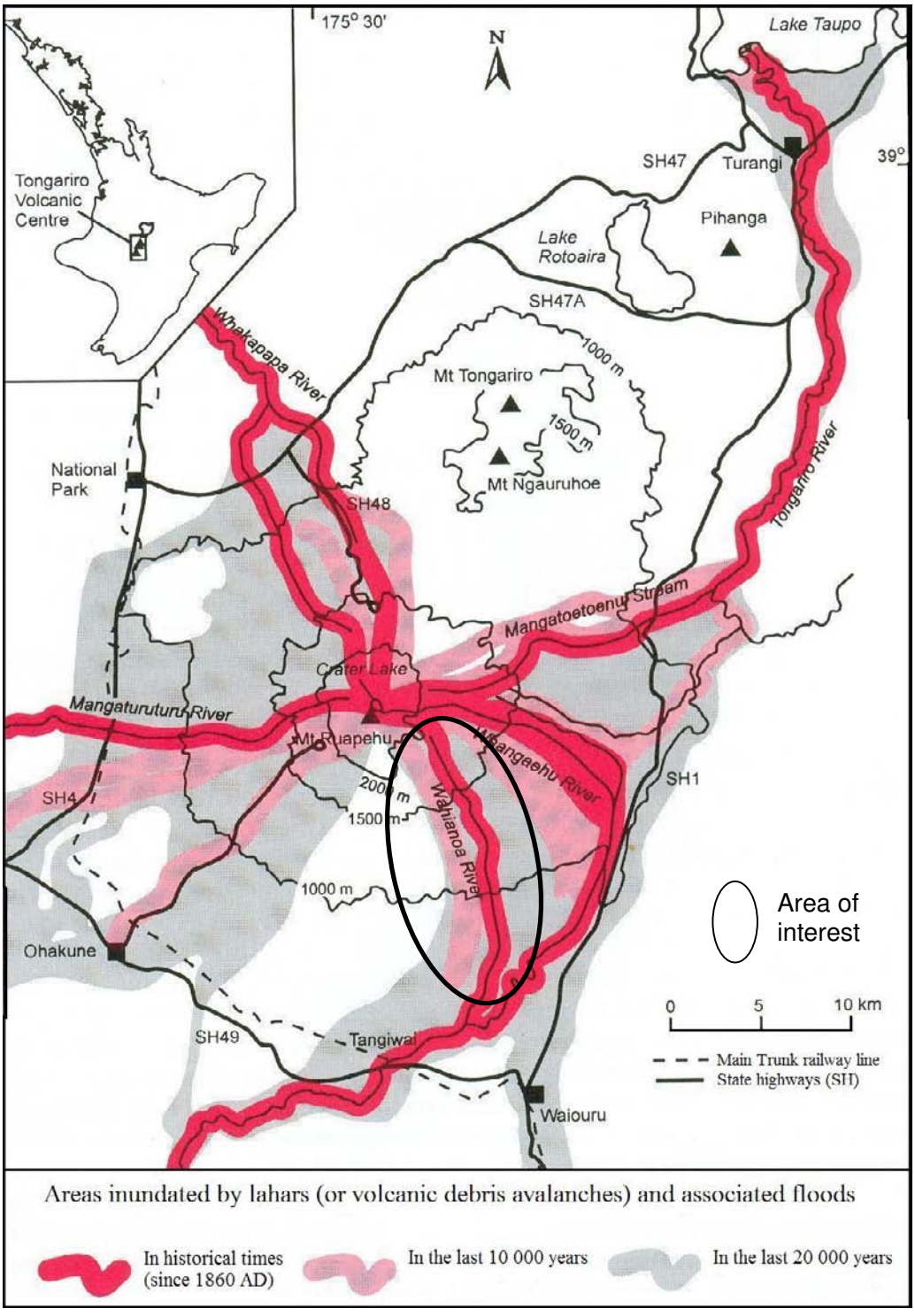

Figure 1.9 Volcanic hazards map showing the distribution of lahars of Ruapehu for the last 20 000 years. It clearly shows that the Wahianoa River has been a transport pathway for lahars in the past (Neall *et al*., 1999).

1.3.6 Lava flows and tephras on Ruapehu

There are numerous lava flows visible in the upper slopes of the Wahianoa Valley (Fig. 1.10). Some of the lava flows show typical columnar jointing. The lava flows on the eastern ridge are thicker and more extensive than on the western ridge. The photograph (Fig. 1.10) also shows that the layers of lava flows alternate with very loose material and so form a sandwich-like deposit. These pyroclastic fragments consist of volcanic ash, lapilli and basaltic pumice. These unconsolidated sediments will have led to a high rate of debris supply for the glacier, since they are highly erodible. Not all tephras found on Ruapehu are derived from this volcano. Ruapehu produces mainly andesite tephras but rhyolitic tephras from the Taupo and Okataina Volcanic Centres have also been found. For example: the Kaharoa Tephra is from the Okataina Volcanic Centre and is dated as 636 ± 12 cal. yr BP (Alloway *et al.,* 2007), whereas the Pahoka Tephra (older than 9 820 ± 80 years BP - ^{14}C) is andesitic and is the product of an eruption on Mount Tongariro (Donoghue *et al.,* 1995).

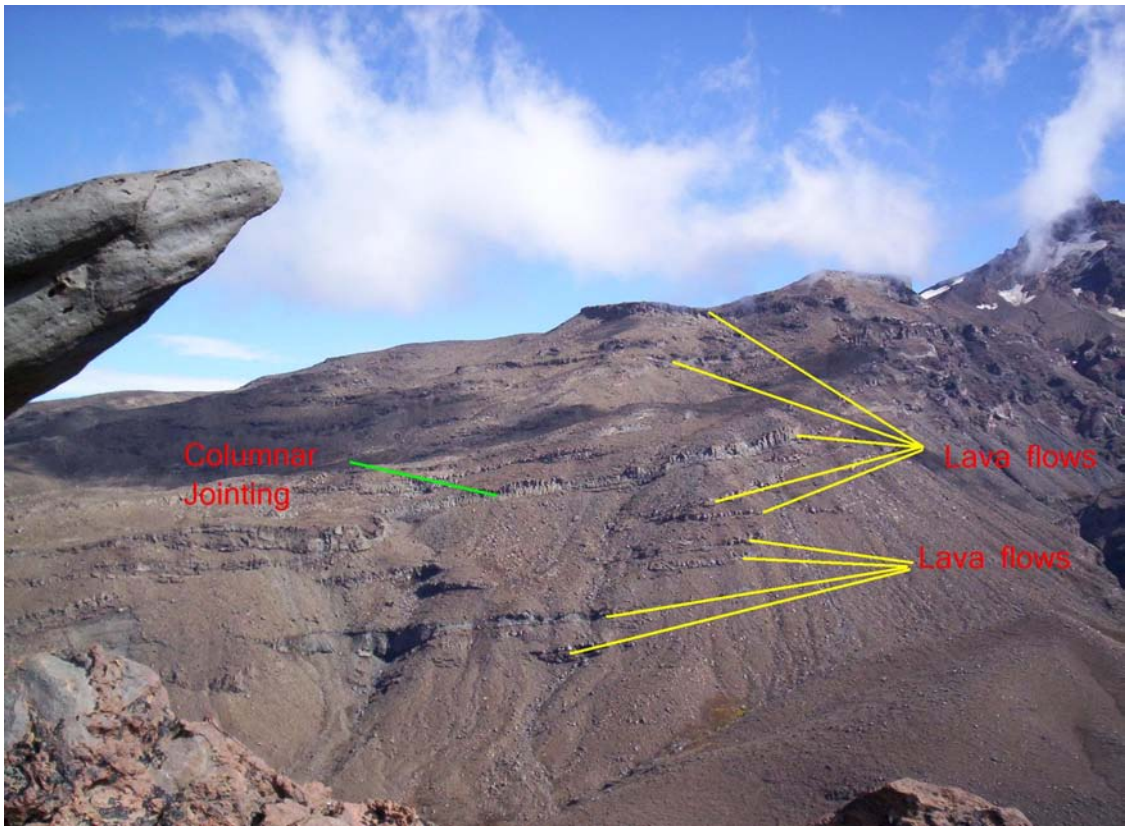

Figure 1.10 Lava flows and columnar jointing on the higher slopes of the Wahianoa Ridges, looking west.

There is a variety of available literature on the tephrochronology, geochemistry, stratigraphy and volcanic hazards of the volcanoes of the central North Island and especially about the Tongariro Volcanic Center (TVC). The lava flows and air fall ash of the southeastern ring plain is of particular importance for this study, since the lithology of the subglacial bedrock and the supply of supraglacial debris plays an important role in the formation of moraines (Bennett & Glasser, 1996).

Hackett (1985) and Hackett and Houghton (1989) had defined four major cone-forming episodes. These can be seen in figure 1.11. The Te Herenga Formation (>130k yrs BP) is the oldest one and is only found on the northern section of the mountain. The Wahianoa Formation (120k to 60k yrs BP) makes up the southeastern sequences and is of the most relevance to the present study. The Mangawhero Formation can be subdivided into a southwestern segment and into an eastern segment. The formation is dated at 60k to 15k yrs BP. The Whakapapa Formation represents the most recent lava sequences, younger than 15k years BP (Cole *et al.*, 1986).

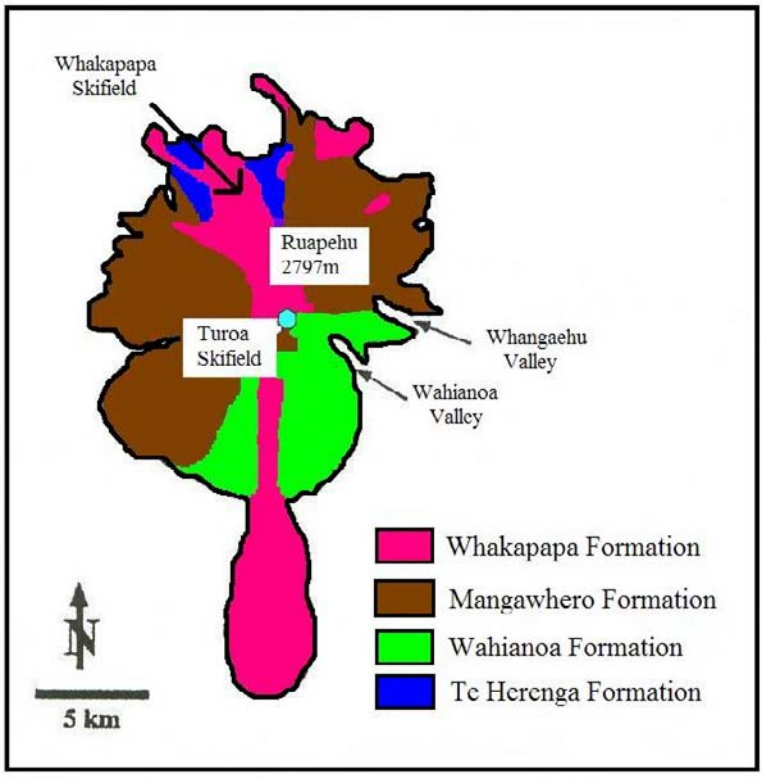

Figure 1.11 Distribution of formations that represent major cone forming events (adapted from Hackett, 1985)

1.3.7 The Wahianoa Formation (120k to 60k yrs BP)

According to Hackett (1985) the Wahianoa Formation consists of extensive lava flows that form major bluffs, tuff breccias, and finer grained tuffaceous material. The deposits have been altered by hydrothermal activity and by the intrusion of several plugs and dykes. The rock face of Mitre Peak is intruded by at least one large dyke (Hackett, 1985). The formation is thickest in the upper Whangaehu valley and the upper boundary of the formation is visible at Girdlestone Peak. The upper portion of the peak consists of the younger Mangawhero Formation (60k to 15k yrs BP), which sits unconformably over the Wahianoa Formation. The lava flows typically show blocky and platy jointing, which produces angular and sheet-like fragments when eroded (Hackett, 1985). This is important for this study, since supraglacial debris does not alter much in a glacial system.

Hackett and Houghton (1989) have provided some detail about the stratigraphy of the Rangipo Planeze, which is the area between the Wahianoa valley and the Whangaehu valley. Procter (2003) mapped the area in great detail. His study included the eastern ridge of the Wahianoa valley. The following diagrams show some of his findings (Fig. 1.12 A + B and fig. 1.13). Figure 1.12 A shows the study area. The locations numbered 1 to 4 and 10 to 13 are of greatest value for this study, since they are directly on or near the eastern ridge of the Wahianoa valley. Figure 1.12 B shows the geological units of the Rangipo Planeze. Procter identified two different lava flows, a block & ash-flow unit, two volcanic diamictons and most importantly two till deposits, which he called Till A and Till B. He describes them as an “unconsolidated, very poorly sorted diamicton” (Procter, 2003).

Procter (2003) also calculated that Till A covers an area of 2 187 300 m^2 and has a volume of 0.088 km^3. Till B has a total volume of 0.029 km^3 and covers a somewhat smaller area of 1 739 425 m^2. These calculations were done by using Geographic Information System (GIS). During this process, a geological map was superimposed onto a Digital Elevation Model (DEM). Figure 1.13 shows the stratigraphy of the geological units found on the Rangipo Planeze. The geology of the Wahianoa valley is important for this study, since lithology plays a major part in the rate and mode of erosion (Hambrey & Ehrmann, 2004).

Because air fallen deposits are much softer than lava flows, they are more erodible. Lava flows often form fractured blocks or sheet-like clasts that are very angular (Hackett, 1985; Procter, 2003). This is determined by the composition and the temperature of the magma when it rises (Schmincke, 2004). The block & ash-flow deposit is described as a poorly sorted, monolithic, unconsolidated breccia (Procter, 2003). The volcanic diamict 1 was also identified in this study. It is an easily recognisable deposit found on the upper portion of the eastern ridge (Fig. 1.14). Its matrix is cemented and very weathered. The clasts are mainly grey coloured andesites and range in size. No deposit was found on the western ridge.

Till A makes up the lower end of the eastern ridge deposit. Till B can be found on the eastern side, next to the same ridge. This is an area where the deposit forms a smaller channel that runs parallel to the main ridge. Procter (2003) associated this with the retreat of the Wahianoa Glacier. Because of the great differences in the lithology and the stratigraphy of the study area, it can be expected that the till deposits show great variations in clast morphology and clast fabrics.

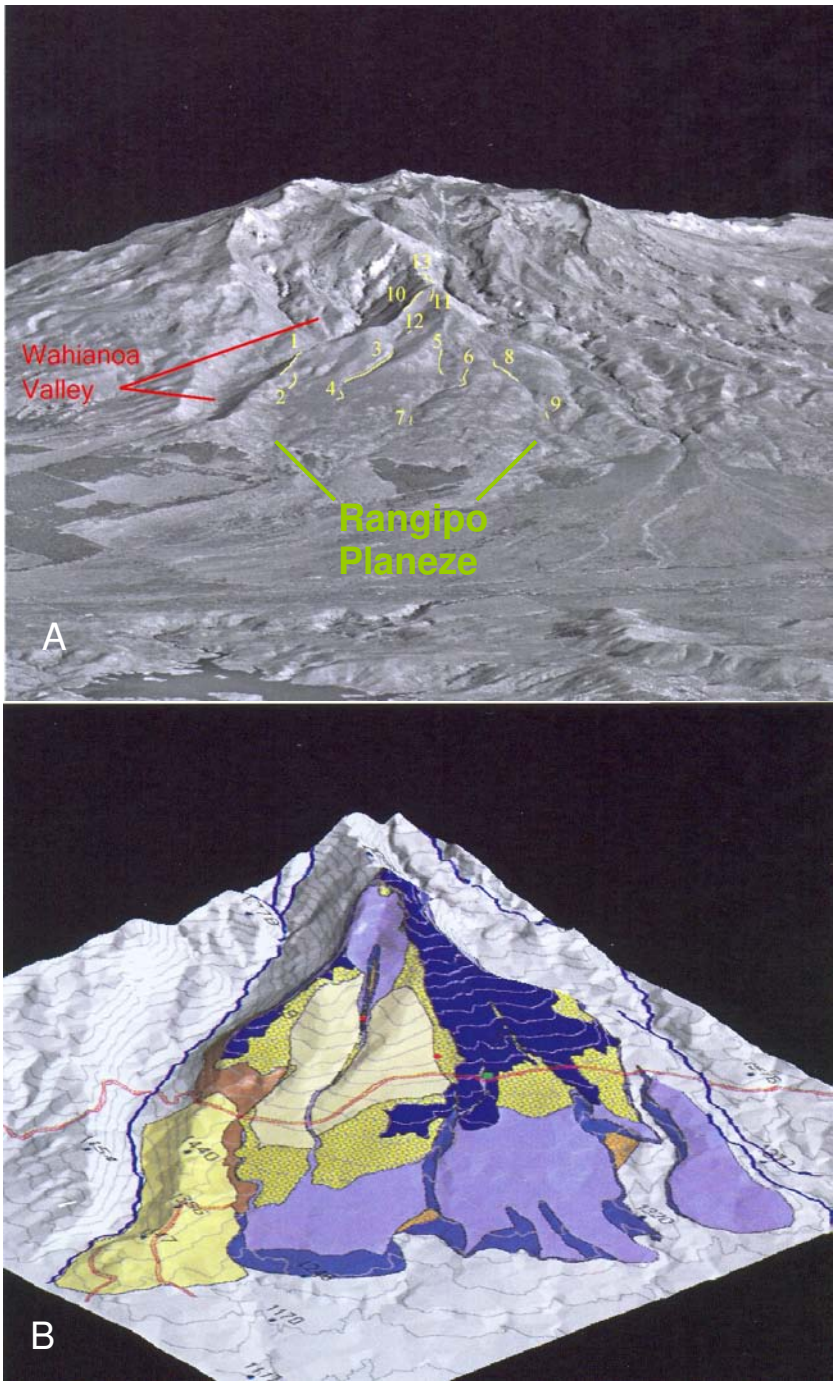

Figure 1.12 (A) is an ortho-photo draped over a DEM at 20 m resolution and shows an oblique view of the Rangipo Planeze. The numbers show the locations of the stratigraphic columns of figure 1.13. (B) was created with GIS and shows the geology of the Rangipo Planeze. The key for this map is the same as in figure 1.13. Both maps are looking to the northwest (Procter, 2003).

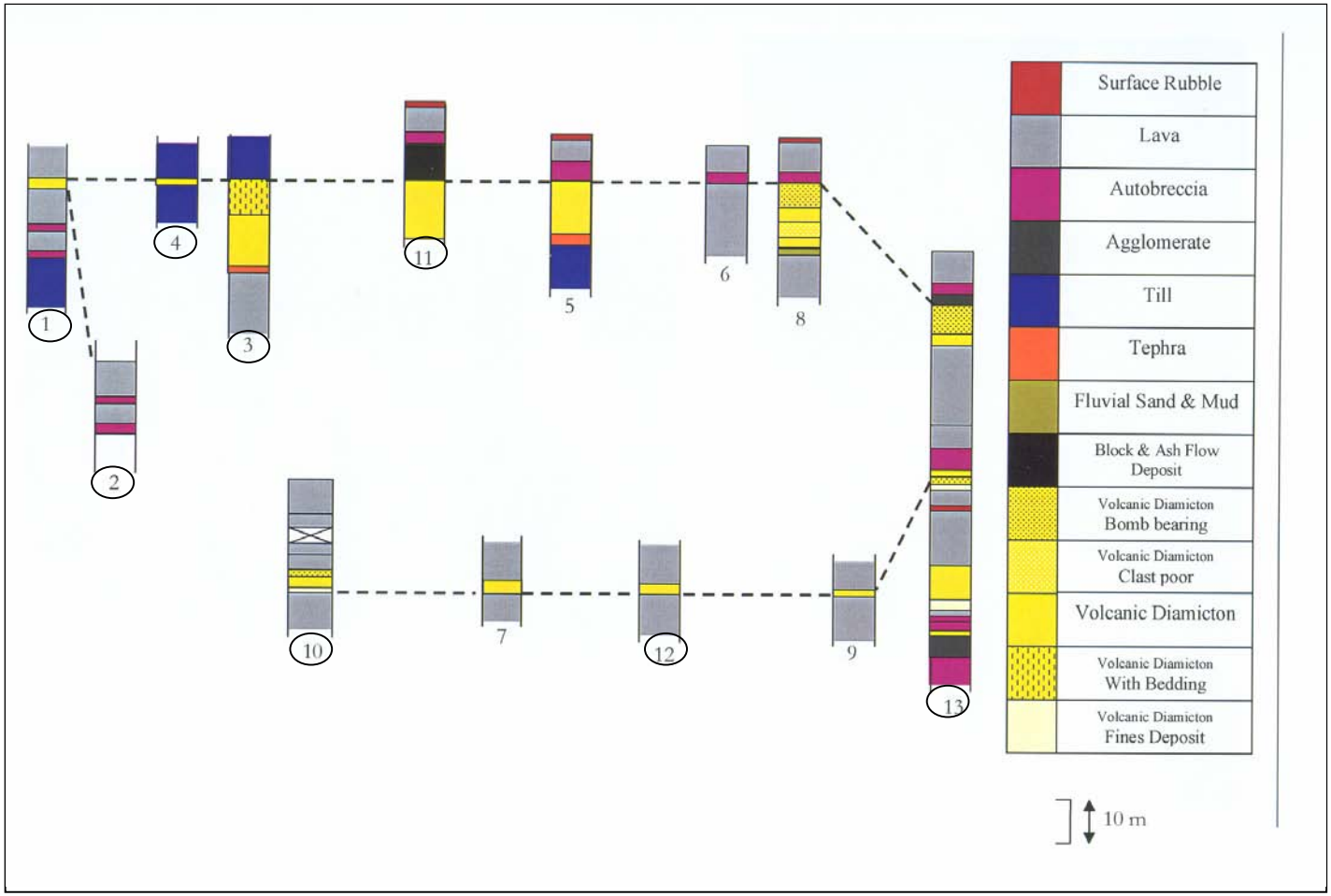

Figure 1.13 The stratigraphy of the geological units found on the Rangipo Planeze. Numbers refer to locations in figure 1.12 A. The circled locations are found on or near the eastern ridge of the Wahianoa Valley and are important for this study (Procter, 2003).

Figure 1.14 Volcanic diamicton found on the upper region of the eastern ridge deposit. The matrix is cemented and highly weathered. The clasts range in size and are mainly grey coloured andesites.

1.4 OUTLINE OF THE THESIS

The first chapter of this thesis has introduced the reader to the study area and to some of the important geological processes that occur. The second chapter will highlight the work of previous researchers that have studied the glaciers or the glacial landforms of Mt Ruapehu. Only a limited amount of work has been done so far. The glacial system and the processes involved in glacial transport and deposition are discussed in chapter three. Although this research does not look at the glacial dynamics of the Wahianoa Glacier, the basic concepts need to be highlighted in order to understand the origin of the deposits. The results of this study are presented in chapter four to seven. Each resource chapter starts with a section that introduces the reader to the method and to previous studies. This is followed by the methodology, data analyses and the data presentation of the results. Chapter four presents the findings of clast morphology. Chapter five is concerned with the orientation of clasts found in the Wahianoa valley. Grain-size distribution is presented in chapter six and the findings of the surface textures of individual grains are explained in chapter seven. The findings of this research and the possible causes are discussed in chapter eight. Chapter nine forms the conclusion for this project, which revisits the main objectives that are stated in the introduction. Further research opportunities are presented in the same chapter.

Chapter 2

LITERATURE REVIEW

2.1 GLACIAL STUDIES ON MOUNT RUAPEHU

2.1.2 Introduction

The European History in New Zealand started in the late eighteenth century, with the main colonisation of Pakeha taking place during the early nineteenth century. Studies in glaciology started relatively late in New Zealand, compared with Europe. This was mainly due to the fact that European explorers in New Zealand (Fig. 2.1) had to overcome many problems. Many scientists have mentioned the existence of moraines on Mt Ruapehu (e.g. Park, 1925; Hackett & Houghton, 1989, Donoghue & Neall, 2001) but not much attention has been given to these in the past. For a long time the extent of glacial ice on the North Island was very controversial (Willett, 1950). This was because many landforms that were thought to be of glacial origin were in fact products of volcanic activity (Grange, 1931; Te Punga, 1953). Adkin (1912) was the first to suggest that the Tararua Ranges were glaciated. This hypothesis has long been proven to be correct (Brook, *et al.,* 2005; Brook & Brock, 2005).

Figure 2.1 An early exploration party rests on the slopes of Mt Tongariro (Greenway, 1998).

2.1.3 Early observations of the glaciers on Mt Ruapehu

Benedict Friedländer (1898) gave a very detailed account of the volcanoes of the Tongariro National Park. Although his notes focused on the volcanic nature of the mountains, he also mentioned the existence of glaciers on Mt Ruapehu. Friedländer states: "*Ruapehu surpasses the snow-line considerably-i.e., that height above which more snow falls than can be melted…On mountains like this the excess of snow is counterbalanced, …, in that a part of the snow travels to lower altitudes – partly as avalanches, partly as glaciers – to be melted below."* (Friedländer, 1898). Although Friedländer was uncertain about the number and locations of craters on Ruapehu, he assumed that the summit neve′ is responsible for Crater Lake. He concluded that the summit neve′ melts and leaks into the crater because of hot gases rising from below.

2.1.4 Early theories of extensive glaciation in New Zealand

James Park was the first scientist to mention glacial landforms on and around Mt Ruapehu (1909). Park published several papers and books (1909a-d, 1910, 1915, 1925, 1926) dealing with the spatial extent of Pleistocene glaciation in New Zealand. Park believed that most of the South Island once was covered by a major ice sheet. Regarding the North Island, Park believed that glaciers from Mt Ruapehu extended far into neighbouring valleys (Park, 1925) to form two major moraines that were situated to the west and south of the volcano (Park, 1909, 1910) (Fig. 2.2). According to Park (1909), these till deposits consisted of andesitic blocks, which he referred to as 'erratics', and a silt/clay matrix. The largest rocks were found near Taihape and Utiku (Fig. 2.3), where they also showed the greatest concentration.

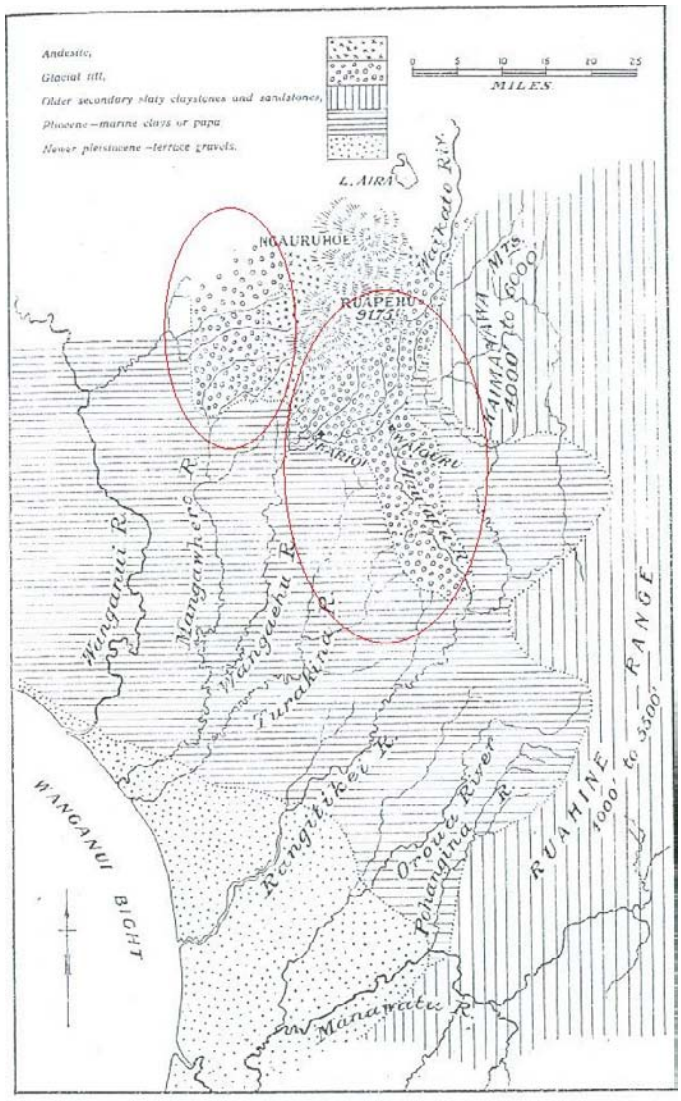

Figure 2.2 Geological sketch-plan showing position of glacial till (in red circles) south of Ruapehu (Park, 1909).

Park found several andesitic boulders in the Hautapu Valley (Fig. 2.3), about 80 km southeast of Mount Ruapehu (1909) and one erratic boulder (Fig. 2.4) near Mangaweka at the Rangitikei River about 100km southeast of Mount Ruapehu (Park, 1915). The erratic boulder showed striae parallel to its a-axis. Park (1909) was convinced that the andesitic boulders further upstream and the erratic boulder were part of a large sheet of glacial boulder-clay (till). Park (1915) concluded that a glacial ice sheet, which originated on the south-west slopes of Mt Ruapehu, transported large amounts of debris down the Hautapu Valley and terminated in the Rangitikei Valley.

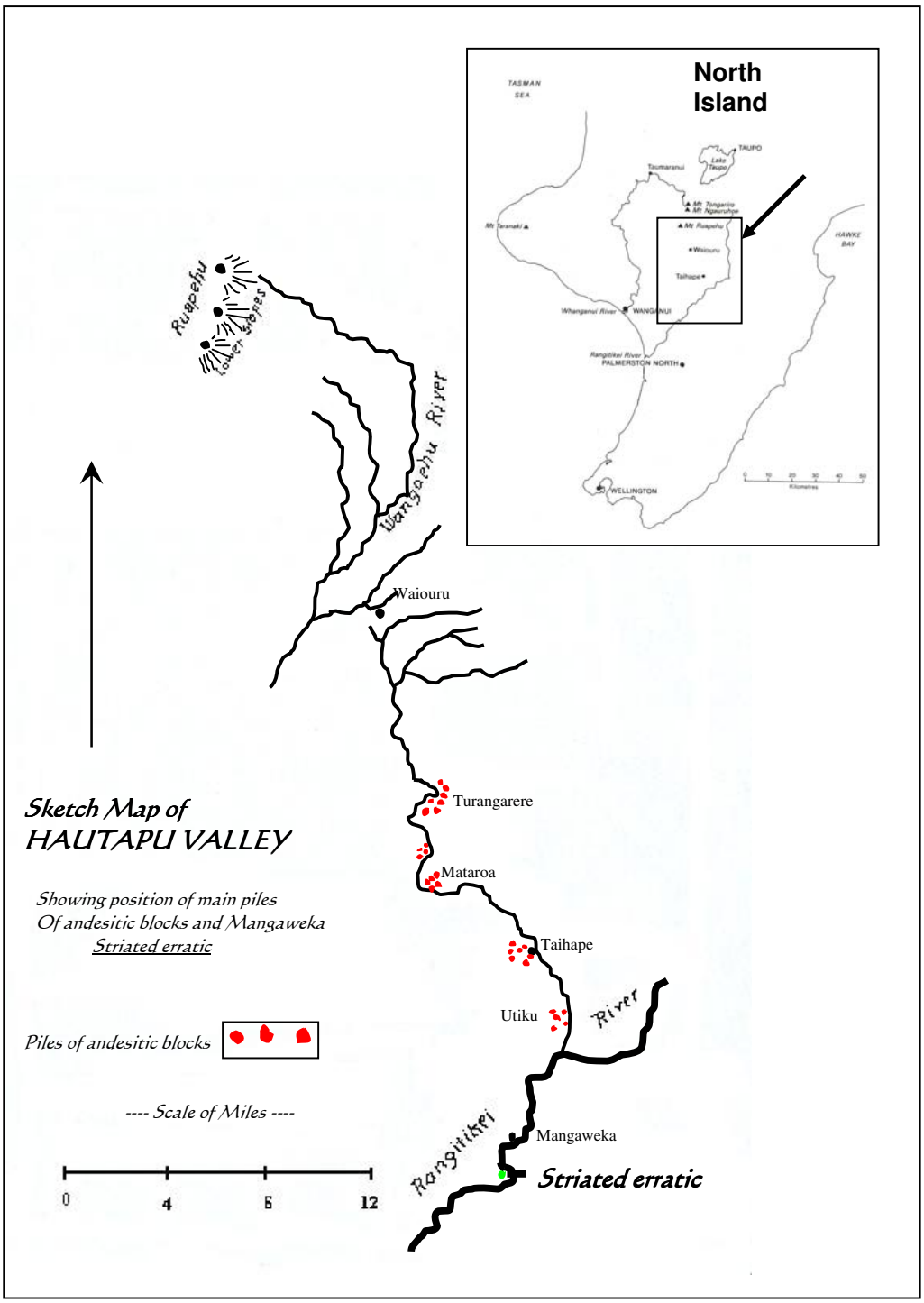

Figure 2.3 Sketch map of the Hautapu Valley where Park found andesitic blocks and a striated erratic, which he describes as a sheet of glacial boulder-clay (adapted from Park, 1915).

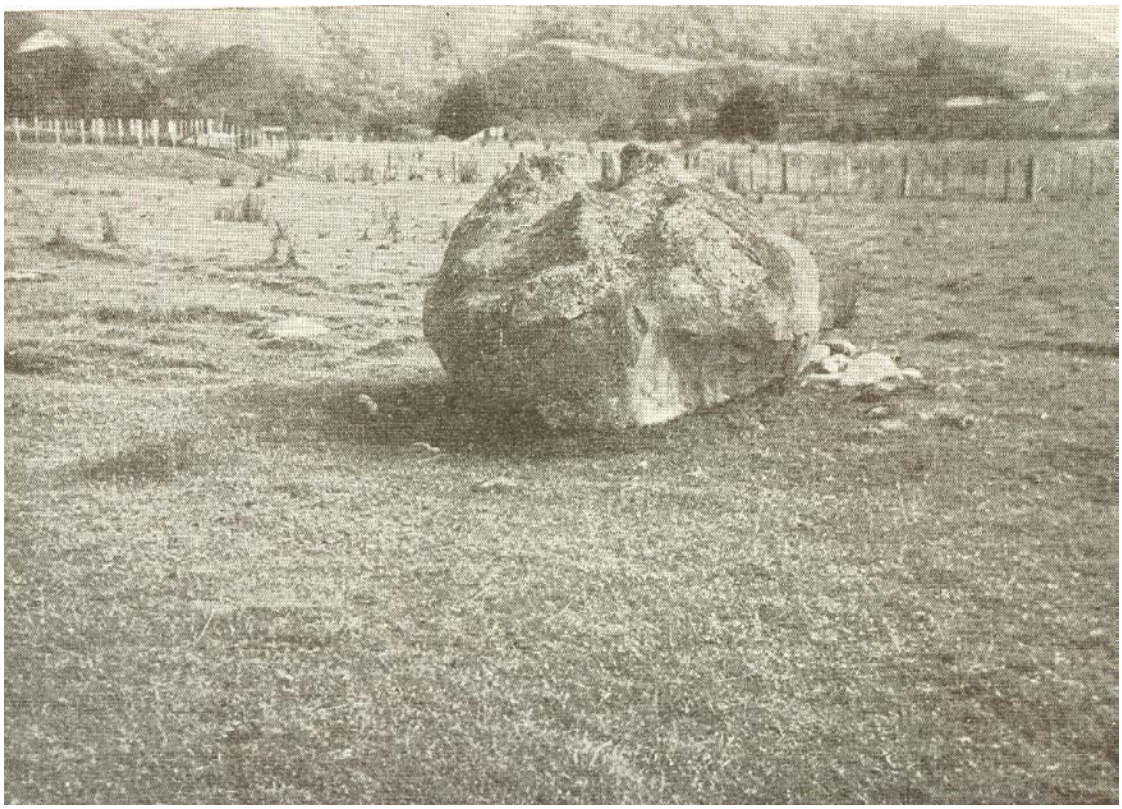

Figure 2.4 Park's photograph of the andesite erratic that showed striations. The boulder was found near Mangaweka (Te Punga, 1953).

On the Waimarino Plain, about 15km north-west of Mount Ruapehu, Park (1926) identified two deposits of debris-hummocks. They showed various heights and were composed of large angulated andesitic blocks. Park believed that these mounds were the remnants of a terminal moraine. He states: *"The Waimarino mounds were formed during the final retreat of the glacier [Waimarino glacier], their material being piled up in ice-caves and notches along the edge of the ice-front"* (Park, 1925). It is now known that Mount Ruapehu has produced debris avalanches in the past in this region and that these mounds are derived from one such event (9500ya). This avalanche originated from the northwest slopes of Mount Ruapehu and traveled 12km down the Whakapapa catchment (Neall *et al.,* 1999; Neall, 2001).

Marshall (1909) claimed that no glacial evidence was found in the areas Park discussed in his reports; however, he did agree that a cooler period of increased glaciation in New Zealand occurred in the Pleistocene. Marshall (1909) thought that the existing glaciers were extended to lower elevation and that many glaciers existed where there are none at the present time. In regard to the North Island and Mount Ruapehu, Marshall was convinced that there were no signs of glaciation, except in those areas where the current glaciers existed.

Taylor (1927) visited the northwestern slopes of Mt Ruapehu in January 1923 and gave an account of the extent of the Whakapapa Glacier at that time. He estimated the location of the glacier snout to be at c.7 500ft (2286m). Taylor (1927) also noticed the existence of several cirques to the north of the glacier. He believed that freeze-thaw action had lead to these features. Because of the nature of the environment Taylor did not find any unequivocal evidence but he remained convinced of the existence of Pleistocene glaciation on Ruapehu.

With the aim to further investigate the cause of the Tangiwai lahar disaster (24 December 1953), Odell climbed the north-west side of Mount Ruapehu in May 1954 and made some additional observations on the glaciers of the mountain. Odell (1955) estimated the snout of the Whakapapa Glacier to be at an elevation of 7000ft (2134m), 150m lower than Taylor's estimation in 1927. This difference is likely to be a matter of miscalculation, since both observers estimated the elevation of the lowest glacial ice without any instruments to measure the altitude.

Odell (1955) agreed that there was little evidence of the spatial extent of Pleistocene glaciation on Mt Ruapehu, though he did not dispute the theory. Odell (1955) believed that the contrasting lithologies of the volcano have inhibited the formation of vast morainic material. Odell (1955) made some further observations, noticing that the eastern side of the mountain showed older morainic deposits at lower elevations than elsewhere on the mountain. Odell also suggested that the northern side of Mt Ruapehu receives more solar

radiation and that the ablation rate of the glaciers was therefore greater on the northern side of the mountain.

2.1.5 Glacier fluctuations on Mt Ruapehu

Many scientists have noted a rapid retreat of the glaciers on Mt Ruapehu and subsequently have made observations regarding this process. Krenek (1959) was extremely concerned about the fast retreat of the glaciers during 1955 and 1956, noting the retreat of the Whangaehu and Mangatoetoenui glaciers was greater in 1954-1955 than during the previous fifteen years. Krenek (1959) constructed detailed sketch maps of some of the glaciers, and tried to postulate reasons for the accelerated retreat and down wasting of the glaciers. Figure 2.5 shows the retreat of the Whakapapa Glacier. The temperature and rainfall at the Chateau Tongariro (northern slopes) during the winter of 1954 and the summer of 1955 were much higher than usual (Fig. 2.6). June 1954 was much warmer than average and therefore little snow was added to the glaciers. July and August of 1954 had more rainfall, although the temperatures were the same as usual. September and October were much drier than on average. Therefore, very little snow was added to the glaciers. The months starting from October 1954 to May 1955 were extremely warm, which possibly caused an earlier start of ablation. The months February and May had a lot of rainfall. This will have further enhanced the down wasting of the glaciers. Krenek (1959) correlated this change in climate to the changes of the glaciers of Mt Ruapehu.

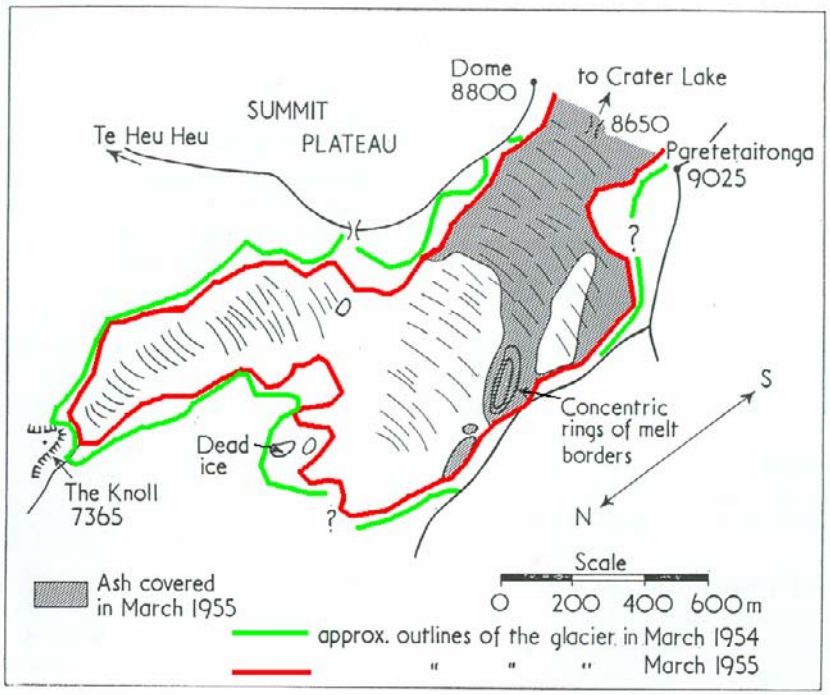

Figure 2.5 Sketch map of the Whakapapa Glacier (adapted from Krenek, 1959).

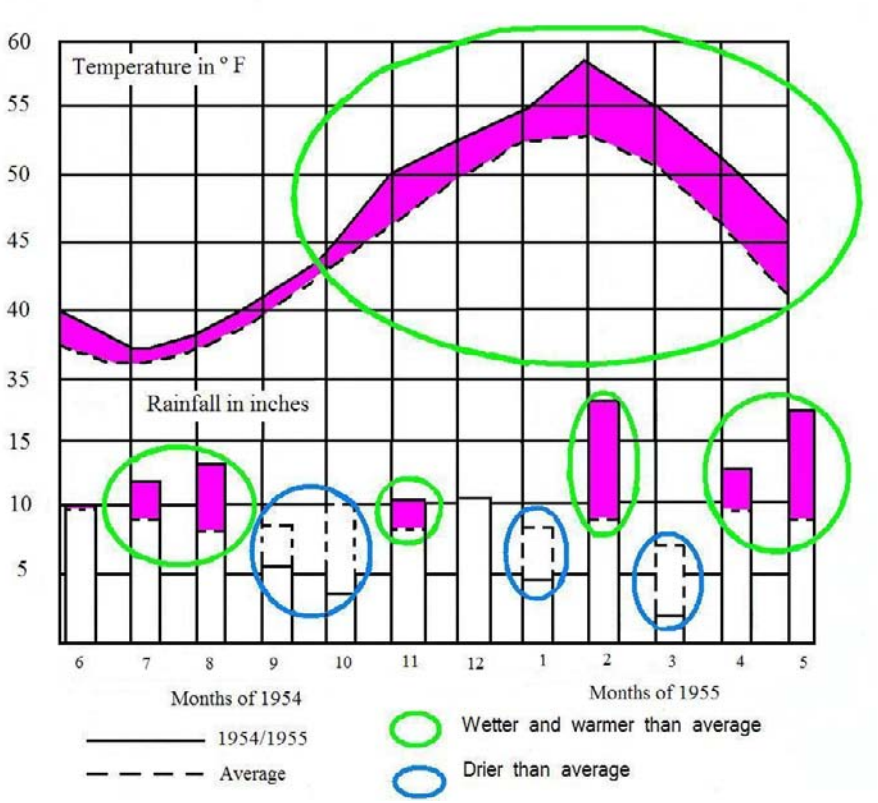

Figure 2.6 Temperatures and rain fall at Chateau Tongariro, June 1954 to May 1955 (adapted from Krenek, 1959).

2.1.6 Photographic studies of glacier fluctuations on Mt Ruapehu

A network of photographic stations was installed during 1960 and 1962 that overlooked some of the glaciers of Mt Ruapehu (e.g., the Whakapapanui Glacier), in order to study the fluctuations of the glaciers. Figure 2.7 shows the Whakapapanui glacier (left) and the Whakapapaiti glacier (right). Before the summer of 1957-1958 these two glaciers were joined and thought of as one glacier, which was called the Whakapapa Glacier. By the end of the autumn of 1958 it became obvious that the Whakapapa Glacier is fed by two systems, as rock started to appear in between.

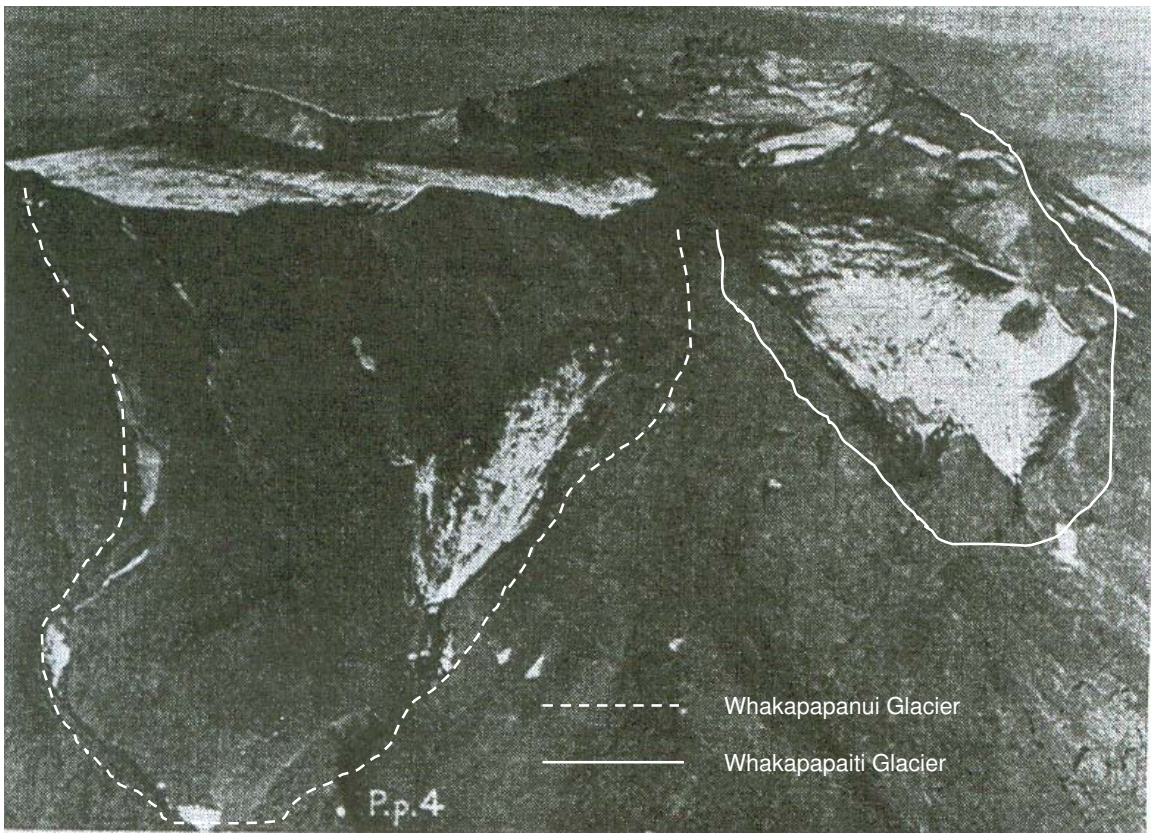

Figure 2.7 The Whakapapanui Glacier (left) and the Whakapapaiti Glacier (right) on the northwestern face of Mount Ruapehu. Tahurangi (2797m) in the background (Heine, 1962).

In addition to photographic evidence, Heine (1962) collected mean temperatures and the amount of rainfall between 1957 and 1962 from the Chateau Tongariro weather station. The study showed that the above-normal temperatures during the spring seasons were responsible for the lower amount of glacial ice that was left in autumn. Heine (1962) postulated that instead of snowfall, the increased temperatures caused a greater rainfall,

which further enhanced the ablation rate of the glaciers (Thayyen *et al.,* 2005). Figure 2.8 shows the major retreat of the Whakapapanui glacier during the autumn months of 1960, 1961, and 1962 as observed by Heine (1962).

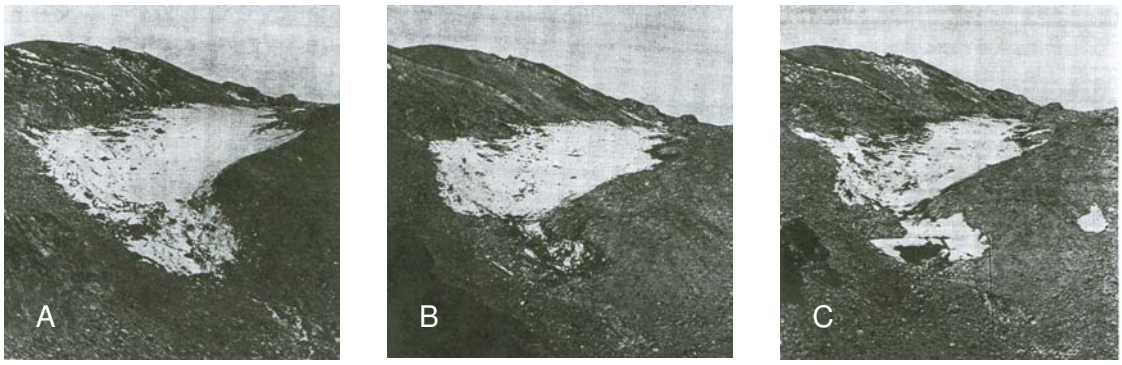

Figure 2.8 Documented changes of the Whakapapanui Glacier (39º 16' S 175º 33' 40" E) during (A) 17 April 1960, (B) 25 April 1961, and (C) 19 March 1962 (Heine, 1962).

Kells and Thompson (1968 and 1970) attempted a reconnaissance survey of the Whakapapanui Glacier, which included the application of field techniques in micrometeorology and in glaciology. The aim of the Ruapehu Research project was to study the glacier hydrological budget and the glacier-climate relationship. The ablation and accumulation rate of the glacier was found by measuring the temperature within the layer of neve′ and adjacent air. To measure the net accumulation, the thickness of the nevé was found by digging small pits into the glacier's surface. The density was then calculated by:

Density of nevé = Mass (weight in grams)/Volume (π r 2 x depth)

It was suggested that the exposed ice is less than 4ka (Kells & Thompson, 1968) and the project wanted to provide evidence for this hypothesis by radio carbon dating organic dirt cones. The study aimed to collect data over a period of five years (starting winter 1968), however, it appears as if unforeseen circumstances have prevented the completion of the project as no further data is available after 1969.

During the one year of research, Kells and Thompson (1970) have identified a positive budget in the Whakapapanui Glacier, which was the first in twenty years. It was suggested that the lower level of Lake Taupo was the result of this trend, as more precipitation fell in

the form of snow during winter 1969. Kells and Thompson (1970) further discussed the implications of the 1969 eruption of Ruapehu on the mass balance of the Whakapapanui Glacier. Numerous lahars occurred during the eruption, which left thick layers of mud behind on the Whangaehu, Whakapapaiti, Whakapapanui and Mangaturuturu Glaciers (Ruscoe, 1978). It was suggested (Kells & Thompson, 1970) that the mud layer could act as an insulator of the underlying ice and decreases the rate of ablation during the following years. However, it was also postulated that the mud layer could be removed by the melt water, which would return the glacier's mass balance to its prior trend.

2.1.7 The first study of glacial moraines on Mt Ruapehu

McArthur and Shepherd (1990) are the only scientists so far that have studied the end moraines of Mt Ruapehu. McArthur and Shepherd (1990) made careful field observations and analysed aerial photographs, with the aim of placing these end moraines into the timeframe of Quaternary glaciation. They concluded that all moraines have formed over at least two periods of ice advances. Furthermore, they identified that the moraines were probably deposited during the last two stadials of the Otira Glaciation, as they are situated on lava flows that are younger than 60k yrs. It has been suggested that deposition of the moraines took place between 14k and 25 500 yrs ago (Procter, 2003), though no attempts of dating the moraines has yet been undertaken.

2.2 THE GLACIER CHRONOLOGY OF NEW ZEALAND

There is abundant evidence that climate variations have occurred in New Zealand during the Quaternary but the best record exists only for the late Pleistocene (Fig. 2.9) (Salinger, 2001). The evidence is mainly derived from pollen, marine cores, speleothem, fluvial aggradation/degradation, ice cores, loess, aeolian quartz (Selby, 1985) and the reconstruction of glacier advances/regressions, by calculating equilibrium-line altitudes (ELAs), studying glacier mass balance (section 3.1.3) and glacial landforms. When correlating the different evidences to time markers, such as tephras and the paleomagnetic record, a chronological record can be constructed.

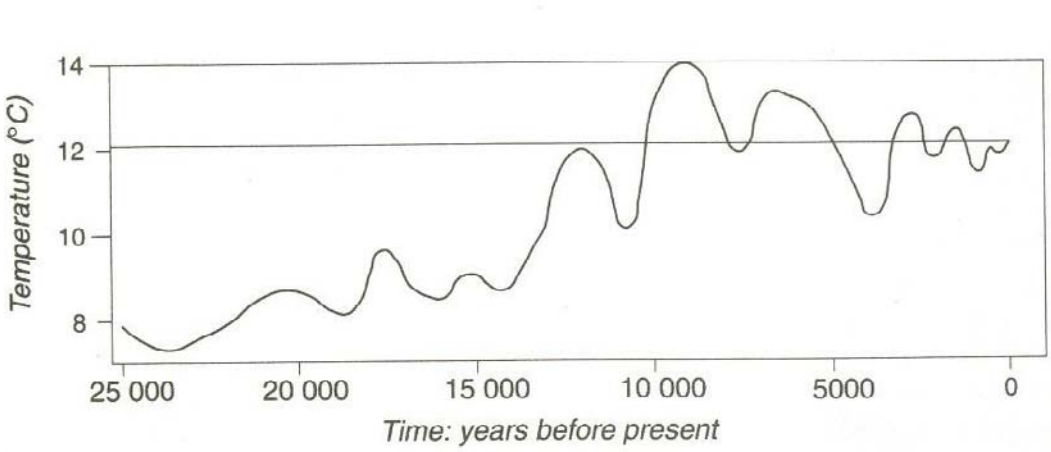

Figure 2.9 Average temperature variations over time for New Zealand for the last 25k yrs. From pollen, glacial and speleothem data (After Salinger & McGlone, 1990).

2.2.2 Glaciers and climate - the use of ELAs

Early glacial studies focused on the reconstruction of ELAs in New Zealand (e.g. Taylor, 1926; Willett, 1950). Porter (1975) identified a similar climatic trend as the northern hemisphere by calculating ELAs from an area in the Tasman River-Lake Pukaki drainage basin of the Southern Alps. Although the results from New Zealand compared closely to those from middle- and lower-latitudes, Porter (1975) points out that a strict comparison cannot be made. This is mainly due to factors, such as isostatic and tectonic effects that are often not included in the analysis.

Lamont *et al.,* (1999) studied the relationship between glaciers of the Southern Alps and climate by looking at atmospheric circulation and glacier mass balances. The investigation took over a period of 21 years and looked at 48 index glaciers. The main climatic factors that determine the altitudes of the annual equilibrium lines are summer temperature and the total precipitation (Lamont *et al.,* 1999). Fitzharris *et al.* (1997) argued that variations of annual ELAs in New Zealand are due to atmospheric circulation patterns that derive from the Pacific. Lamont *et al.,* (1999) produced a "sloping roof" model, which shows the average trend surfaces of ELAs across the Southern Alps (Fig. 2.10). These surface trends were then correlated with the atmospheric circulation patterns from that time. The results have shown that a steeper sloping trend across the Southern Alps is associated with anomalous southwest to westerly flow and a less steep slope with anomalous south,

southeast and easterly flow. Therefore, the results have proven that glacier mass balances and atmospheric circulation are strongly related.

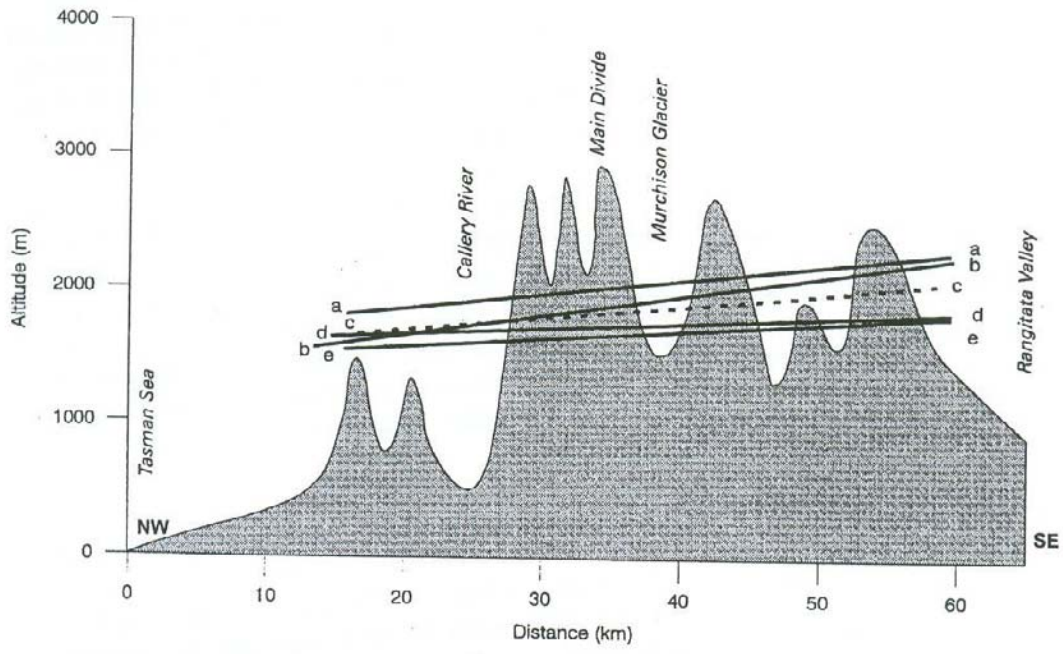

Figure 2.10 The "sloping model': a topographic profile across the central Southern Alps showing trend surface slopes for (a) a year with high ELAs, (b) a year with the steepest slope, (c) long-term ELAs, (d) a year with the least steep slope, and (e) a year with a low ELAs (Lamont *et al.,* 1999).

2.2.3 Glaciers and climate - the use of moraine sequences

The use of moraine chronologies in climate reconstruction is generally an accepted approach (Burrows, 1975). However, Kirkbride and Brazier (1998) question the validity of this method. It was argued that moraine systems are too complex and often not studied sufficiently to serve as valid evidence in climate reconstruction. Kirkbride and Brazier (1998) argue that moraines are often seen to simply represent times of glacier expansion and hence a time of cooler climate. Factors such as the availability of datable material, post erosional destruction and the sensitivity of the glacier system to change is generally not included.

2.2.4 Glacial chronology

Table 2.1 shows New Zealand's late Pleistocene glacial advances and interglacials. The table was constructed from data compiled from the South Island. It is known that there were at least three glacials and interglacials during the late Pleistocene (Salinger, 2001). The exact timing of these events is still the focus of present studies (Almond *et al.,* 2001). Most research concentrates on the Otira Glaciation, which spanned Marine Oxygen Isotope stages 2-4, around 70-10ka yrs BP, off which the peak (18-20ka yrs BP) is generally referred to as the Last Glacial Maximum LGM (McGlone *et al.,* 1993).

Table 2.1 Correlation of New Zealand late Pleistocene glacial and interglacials (After Salinger & McGlone, 1990).

Stages	*North Westland Glacials*	*West Coast Cliffs*	*Upper Buller Glacials*	*Waimakariri River Glacials*	*Rakaia River Glacials*	*Wanganui Taranaki Interglacials*	*Date (B.P.)*
ARANUIAN INTERGLACIAL							
	Kumara3			Poulter 2	Acheron 2		13 000
	Late Kumara 2_3			Poulter 1	Acheron 1		15 000
OTIRA			*Minor*	*Interstadial*			17 000
	Kumara 2_2			Blackwater 3	Bayfield 3		18 000
GLACIATION			*Minor*	*Interstadial*			19 000
	Kumara 2_1		Black Hill	Blackwater 2	Bayfield 2		22 000
				Blackwater 1	Bayfield 1		27 000
			Important	*Interstadial*			c. 40 000
				Otarama	Tui Creek 3		
					Tui Creek 2		
					Tui Creek 1		70 000
OTURI INTERGLACIAL	?	Awatuna 2				Hauriri	80 000?
						Inaha	100 000
		Awatuna 1				Rapanui	120 000
WAIMEA GLACIATION	Kumara 1		Tophouse	Woodstock	Woodlands		140 000
TERANGI INTERGLACIAL	Karoro ?					Ngarino	210 000
WAIMAUNGA GLACIATION	Hohonu		Kikiwa	Avoca			310 000
WAIWHERO INTERGLACIAL		Albion 3				Brunswick Braemore	

Moar and McKellar (2001) provide a detailed pollen record for the northern and southern ends of Greens Beach, north of Lake Ianthe, South Westland. The pollen record showed dominance in species that occur during times of climate-transitions. Two sections were radiocarbon dated at 29600 ±850 and 38000 +4450 -2850yrs BP, which places this area to the last interglacial (Kaihinu).

Shulmeister *et al.* (2005) studied the Cobb Valley, North-West Nelson, New Zealand, and presented a new glacial chronology of the last glacial transition in the area. Shulmeister *et al.* (2005) suggest that the last deglaciation of the Otira Glaciation commenced no earlier than 18-19ka. The following 3-4kyrs was a time of numerous short-term still-stands and/or minor re-advances. By 14ka the ice had completely retreated from the valley. The findings do not correspond with the Northern Hemisphere Younger Dryas chronozone[2], which suggests that inter-hemispheric climate forcing was not the key process of New Zealand glaciation during the last glacial interglacial transition.

One of the most comprehensive studies (the NZ-INTIMATE project) of the glacial chronology that includes the North Island was completed by Alloway *et al.* (2007). The study presents a climate event stratigraphy for the past 30kyrs and is based on data compiled from various sources, such as the Kaipo and Otamangakau wetlands, marine core MD97-2121 southeast of North Island, spelothems on northwest South Island, Auckland maars and the Okarito wetland on southwestern South Island. The data was correlated with well known tephra marker beds from the Taupo Volcanic Centre and the Okataina Volcanic Centre, but also with the glacial records, the spelothem record, fluvial terraces, loess and aeolian quartz. The study identified three major climatic events: (1) The last glacial coldest period LGCP began at about 28ka BP and ended at about 18ka BP at Termination l. The LGCP was interrupted by a warmer phase between 27ka and 21ka BP. (2) The last glacial-interglacial transition LGIT is dated between 18ka and 11600ya BP. This phase experienced a lateglacial warm period from about 14800 to 13500ya BP and a lateglacial climate reversal taking place between 13500 and 11600ya BP. The third climatic event took

[2] Northern Hemisphere Younger Dryas was a brief period of cold climate and is dated at 12.75 to 11.2ka (Shulmeister *et al.,* 2005).

place during Holocene interglacial conditions. There were two warmer phases took place between 11600 and 10800ya BP and 6800 and 6500ya BP. Alloway *et al.* (2007) further concluded that the lateglacial reversal in New Zealand began somewhat later than the start of the Antarctic Cold Reversal[3]

2.2.5 The Little Ice Age

The Little Ice Age (LIA) was a period that encompassed considerable climatic variability and is therefore difficult to place into a correct time frame (McKinzey *et al.,* 2005). Not many studies have focused on the LIA in New Zealand (Winkler, 2004) and hence, most data is based on glaciers of the Northern Hemisphere (e.g. Zemp *et al.,* 2006). Lawrence (1969) was one of the first to observe more recent climatic variations in New Zealand. Lawrence postulated that the rises and falls of lake waters are related to climatic changes and therefore changes in glacier behaviour. Lawrence (1969) suggested that the lakes in the Rotorua area, central North Island, rose between AD 1715 and 1790 and drowned Maori villages that were located close to the lake shores due to the melting of glacier ice from Mt Ruapehu.

Chinn *et al.* (2005) have compared recent glacier advances in Norway and New Zealand as both countries experienced a period of mass gain at the same time (between the early 1980s and 2000) and both lie in similar climatic zones. The aim of the study was to identify common causes for this advance. The results have shown that the glacier advance was associated with increases in the strength of westerly atmospheric circulation. This increased the total precipitation in both countries and decreased the ablation season temperatures in Norway.

Winkler (2004) suggests a LIA maximum for New Zealand around AD 1725-1740 and a readvance around 1860 and 1890/95. These results are based on a study completed at Mt Cook National Park, South Island, New Zealand (Winkler, 2004). Lichenometric data was collected from four glaciers. The Mueller, Hooker and Eugenie Glaciers experienced major glacier front oscillations directly following the LIA maximum. The three glaciers

[3] Antarctic Cold Reversal was a period of time when the warming trend since the LGM temporarily halted.

readvanced during the late nineteenth century and again early twentieth century. The Tasman Glacier behaved somewhat different to the other three. The glacier readvanced to its LIA maximum and overtopped preexisting LIA moraines, making it impossible for dating.

Chapter 3

DEBRIS IN TRANSPORT

3.1 THE GLACIAL SYSTEM

3.1.2 The formation of glaciers

The formation of a glacier depends on temperature, precipitation and relief (Ehlers, 1996). Air temperature is the most influential factor in the mass balance of a glacier and is highly dependent on the global position (Zemp *et al.*, 2006). With decreasing latitude the altitude of possible glaciation increases (Kaser, 2006). Precipitation in the form of snowfall is important for the formation of glaciers. However, if the summer temperatures are low enough to prevent or reduce ablation, little snowfall is required to maintain a glacial system. The relief and the aspect are also important factors that contribute to the formation of glaciers and in maintaining the glacier balance (Evans & Cox, 2005). The highest mountain will not support a glacier if its slopes are too steep and north-facing mountain slopes are generally sunnier and warmer in New Zealand than the south-facing sides.

3.1.3 The mass balance of a glacier

Only where the amount of snow exceeds the amount of ablation can a glacier form. The area of net accumulation is called the *accumulation zone* (Fig. 3.1), and the *ablation zone* is the area of net loss. Ablation mainly occurs at the terminus of the glacier and can occur in all three phase changes: vapour (evaporation, sublimation), liquid (melt water at surface and base of glacier), and solid (calving and windblown snow). The balance between these two zones is called the *mass balance.* The mass balance is responsible for the spatial distribution of the glacier.

The area that separates the ablation and accumulation zone is *the equilibrium line*. At the end of a budget year, the mass balance is zero at this particular point (Zemp, *et al.*, 2006). The equilibrium line is not a physical feature and is very responsive to climate variability. Therefore, mass balance measurements of glaciers are used as indicators of climate changes, since glacial behaviour and climate are linked (Lamont *et al.*, 1999). However, the

response time of glaciers to climate changes varies greatly (Chinn *et al.*, 2005). For example, the ablation rate in debris covered glaciers is often smaller than in glaciers with clean ice, since the debris can act as an insulator. Singh *et al.* (2000) found that the melt rate of the Dokriani Glacier in the Garhwal Himalayas, which is covered by a layer of fine debris, is 1.25 times smaller than that for clean ice. Pelto & Hedlund (2001) claim that physical characteristics, such as slope gradient, ice thickness, accumulation rate and the terminus velocity, determine the response time of some of the North Cascade glaciers, rather than microclimate. Bahr *et al.* (1998) have identified that often larger glaciers respond to climate changes much slower than smaller glaciers.

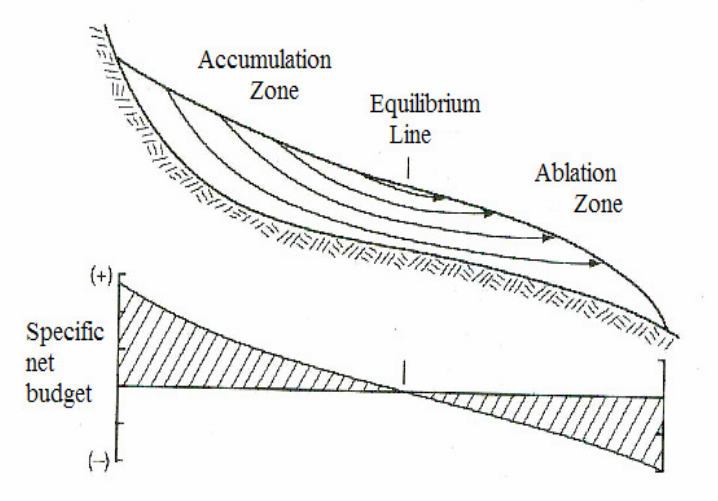

Figure 3.1 A schematic cross section of a typical valley glacier, showing the relationship between accumulation and ablation zones and the equilibrium line (Hooke, 2005).

3.1.4 Glacier flow

Snow accumulates in the accumulation zone. As each layer of snow is buried, the process of compaction occurs. Over time, the snow metamorphoses into ice and the gradient of the glacier becomes steeper until ice flow is initiated. The movement of glacial ice can take place within the ice and/or at the basal zone (Benn & Evans, 1998). This transfers the ice to the ablation zone, where it eventually will be lost due to ablation. The rate at which glacial ice moves is dependent on local environmental conditions, the amount of debris transported in the glacier and especially the surface slope gradient. The variations in velocities mainly

occur when the pressure of the ice in the accumulation zone becomes larger than the resistance in areas of the ablation zone.

The topography on which the glacier exists causes variations of the velocity of ice flow within the glacier. Valley glaciers are generally confined by valley walls, which typically increase the rate of friction due to greater resistance. Therefore, the glacial ice moves slower in these areas (Martini *et al.*, 2001, Menzies, 2002). In addition, the lithology is an important agent in glacier flow. Harder rocks cause greater friction than softer ones as they exert more resistance to the ice movement. Many valley glaciers form U-shaped valleys. Figure 3.2 shows a schematic interpretation of the velocity variations within the Wahianoa Glacier at the time of its fullest extent, following the work of Martini *et al.* (2001). The ice would have moved fastest at the centre of the basal- and supraglacial zones. Generally, the flanks of the valley cause an increase in friction and the ice moves much slower along the sides.

The morphology of the Wahianoa valley (section 1.3.4) shows that the western ridge has a gentler slope. This probably caused an *asymmetrical channel flow,* which means that the ice possibly moved slower on the western side (Benn & Evans, 1998). Furthermore, the debris ridges are more restricted (narrower) down valley. This is generally associated with an increase in velocity, as the ice discharge of the glacier has to be sustained in this situation (Benn & Evans, 1998). A further reason to suggest that the velocity of the Wahianoa Glacier could have been relatively high is that the ice moved over a deformable bed. This typically causes a decrease in friction.

Ice flows in three different manners: (a) by *internal deformation* (creep and large-scale folding and faulting); (b) by *basal sliding* over hard bedrock; and (c) by *subglacial deformation* (Ehlers, 1996).

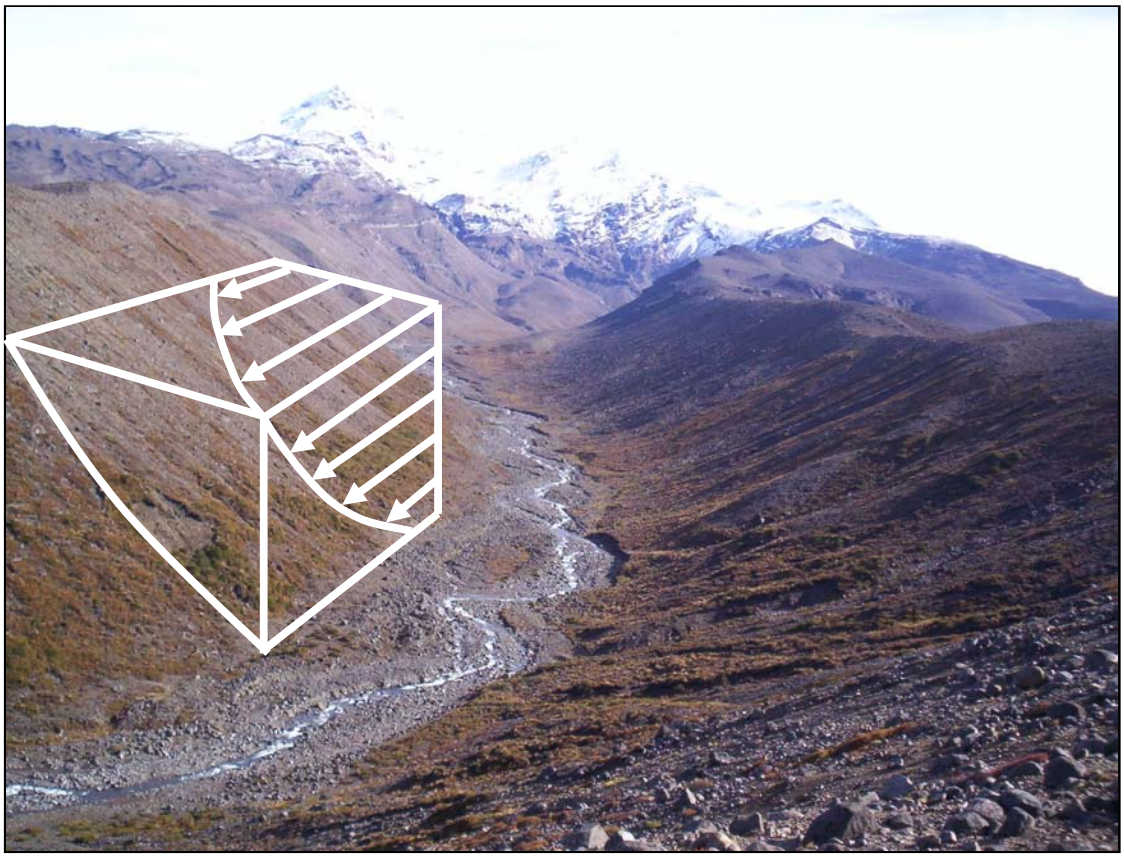

Figure 3.2 Theoretical horizontal and vertical velocity variations within the Wahianoa Glacier at a time of its greatest extent. The length of the arrows indicates the velocity of glacial ice. The ice would have moved fastest in the center of the basal- and supraglacial zones. However, less friction would have been caused in this situation because the glacier moved over a deformable bed.

3.1.4.1 Internal Deformation

The density of ice increases with time and depth. For example: freshly fallen snow has a surface density of only 0.03g cm^{-3} and true glacial ice will reach a surface density of about 0.83g cm^{-3} (Jacka, 2006). This transformation from snow to ice is due to increasing pressure from freshly fallen snow above. The stress exerted onto the ice crystals results in permanent deformation, which is generally referred to as *creep.*

Because ice is a solid close to its melting point, its rheology is an intermediate between a plastic and a viscous material (a viscous fluid). This behaviour is referred to as *power law flow*. Creep involves the deformation and displacement of ice crystals and its rate is a function of shear stress. Shear stress is a function of applied normal stress, which itself is a

function of ice thickness and surface slope. The greater the shear stress the greater is the rate of creep. This relationship is known as *Glen's Flow Law* and is given by:

$$\dot{\varepsilon} = A\tau^{n}$$

where $\dot{\varepsilon}$ is the rate of deformation, τ is the applied stress, and A and n are constants (Benn & Evans, 1998). The shear stress is greatest in the basal zone of a glacier because of the thickness of the ice. Therefore, the rate of glacial creep is greatest here. In warm glaciers the rate of creep is typically higher than in cold glaciers, since ice behaves more plastically with increased temperature. The basal shear stress is given by:

$$\tau_b = \rho\ g\ h\ sin\alpha$$

where τ_b is basal shear stress, ρ is the ice density, g is acceleration due to gravity, h is the depth of the glacial ice, and α is the glacier's surface slope (Lawson & Fitzsimons, 2001).

The rate of creep also varies within a glacier (Fig. 3.3). This is dependent on the two flow states: compressional flow (usually in the ablation zone, where ice becomes thinner and glacial movement is reduced) and extensional flow (mainly in the accumulation zone, where the mass increases and the rate of glacial movement). This leads to the formation of characteristic crevasse patterns (Fig. 3.4) (Hambrey, 1994). The formation of crevasses is due to tensile (extensional) stresses within the glacier, as a result of topographic interactions.

3.1.4.2 Basal Sliding

Internal deformation takes place in all glaciers, whereas basal sliding occurs mainly in glaciers that move over hard bedrock. The process of basal sliding is most efficient in warm glaciers where meltwater acts as a lubricant, reducing friction and enhancing flow of ice over subglacial bedrock. In temperate glaciers, this process is most efficient in spring and early summer (Iken *et al.*, 1983). In cold based glaciers the ice is frozen to the substrate and can therefore not slide over it. As no hard bedrock has been identified at the basal zone of the Wahianoa basin, basal sliding is of little interest to this study.

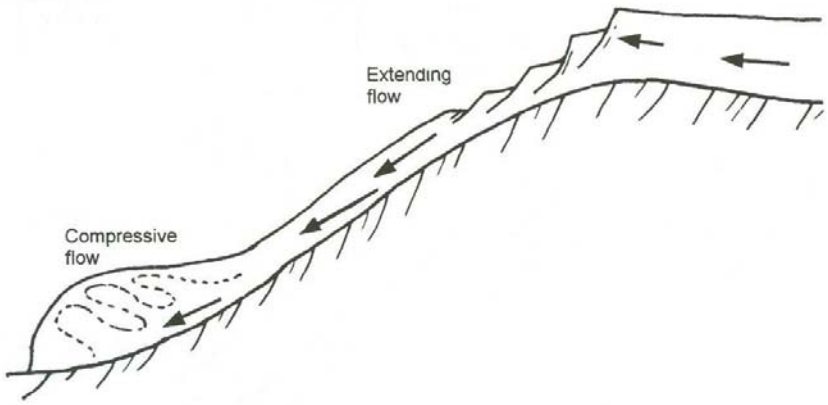

Figure 3.3 Longitudinal diagram of a glacier, showing extending and compressive flow. The arrows indicate flow velocities. The formation of crevasses is due to the variations of tension and compression in the glacier (Martini *et al.*, 2001).

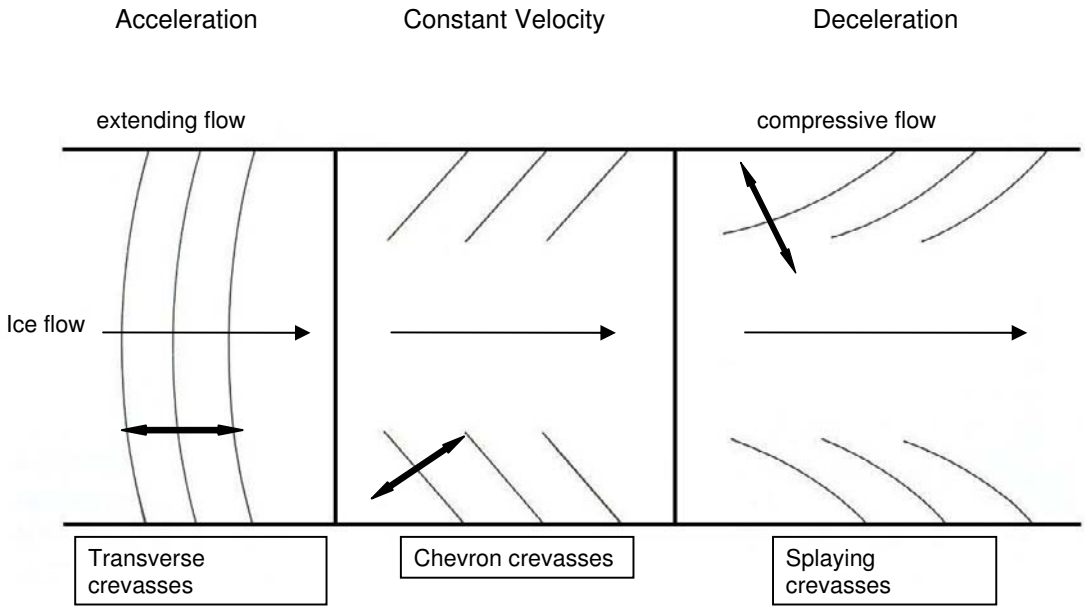

Figure 3.4 Crevasse patterns in a valley glacier. A schematic interpretation that shows extensional and compressional flow and indications of flow rate. The arrows indicate the directions of maximum tensile stresses and are directly responsible for the formation of crevasses (adapted from Nye, 1957).

3.1.4.3 Subglacial Deformation

Many glaciers move over unconsolidated sediment and have done so in the past (Boulton & Hindmarsh, 1987). The sediment beneath the ice typically consists of particles of varying sizes and lithologies. Very little work has been done on subglacial deformation in general and none in New Zealand (Lawson & Fitzsimons, 2001).

Subglacial deformation occurs where glacial ice, which is near its pressure melting point, moves over a layer of unconsolidated sediment. This layer of sediment is generally saturated with water and therefore has a high pore-water pressure. Because the upper layer of the till is saturated with water, it deforms more readily than the basal ice and glacial flow is supported by the shearing forces that take place within this deformable layer (Boulton & Hindmarsh, 1987). The deforming sediments become part of the moving ice mass and the layer below (in which no movement occurs) becomes the stable till (Fig. 3.5). Therefore, the deformable sediment, together with the ice mass, slides over this rigid substrate and a more rapid ice motion is generally achieved (Boulton & Jones, 1979; Brown *et al*., 1987).

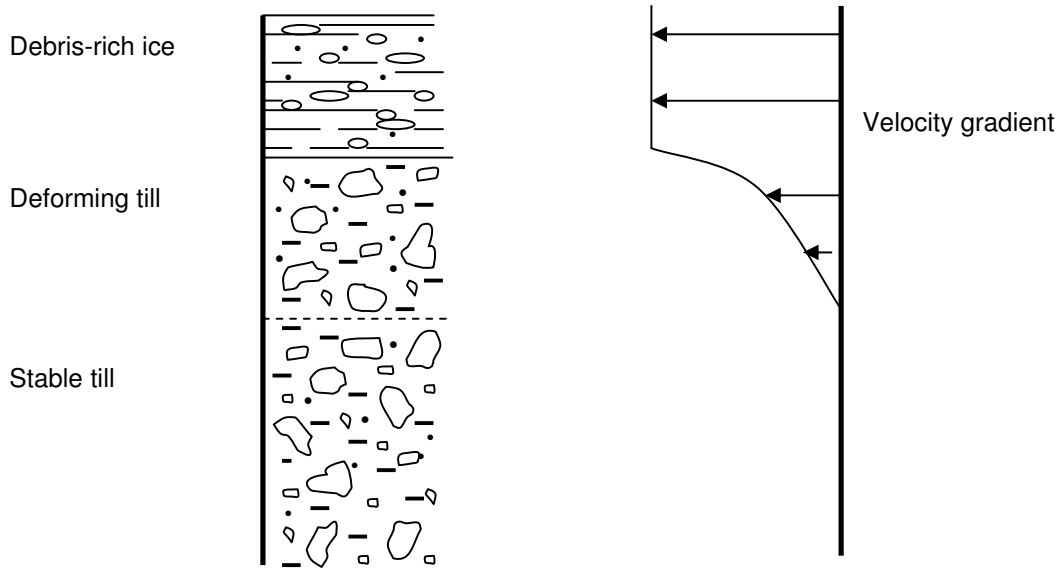

Figure 3.5 Deformable bed model. A layer of saturated till becomes part of the moving ice mass. In this layer the strain rates are high and the sediments deform rapidly. The debris

rich ice and the deforming till move over a layer of stable sediments without deformation (after Boulton, 1979).

It has been suggested that deforming layers of till can move downwards (*excavational* deformation) or upwards (*constructional* deformation) through a sequence if there is a net accumulation beneath a glacier (Hart *et al.*, 1990; Hart, 1995a). Both types of subglacial deformation have been identified by Hart (1996) at a site of Aberdaron, North Wales. Hart (1996) postulated that subglacial fluvial processes influenced the type of deformation by causing different bed conditions.

3.2 PROCESSES INVOLVED IN GLACIAL TRANSPORT

Glaciers are able to transport vast volumes of debris for very long distances. Clasts can be transported on the surface of the glacier, within the glacial ice or at the glacier bed. In general, supraglacial and englacial debris undergoes little modification, as they are exposed to fewer stresses. However, strong forces act on subglacial debris due to their interaction with the glacier bed and the overburden pressure of the ice (Bennett & Glasser, 1996). Firstly, the clasts become detached from their source by *glacial erosion.* This is followed by the *entrainment* of clasts in the glacial ice. This leads to *glacial transport*, where the debris is carried along the length of the glacier. In mountain glaciers the ablation zone and especially the terminus can be completely laden with debris. Glaciers possess the ability to transport very large boulders to the lower reaches of the glacial system (Hambrey, 1994). These are generally referred to as 'erratics', which are often of a different lithology than the rocks in their depositional environment. The processes that are involved in glacial transport are described below.

3.2.2 Glacial erosion

Glacial erosion fractures and removes material from the bedrock and takes place at the ice-rock interface. Consequently, it is extremely difficult to observe directly. However, it is also one of the most important processes involved in the glacial system because it permanently alters the landscape. As ice is generally softer than bedrock, erosion is not caused by the glacial ice directly. It is the interaction between the subglacial debris and the bedrock that causes erosion; generally most efficient where basal sliding occurs. Therefore,

basal temperature is an important factor that determines the rate and severity of erosion. However, some erosion can also take place in cold glaciers due to internal creep. Girdlestone Peak, Mt Ruapehu, is a glacial *horn*, the direct result of glacial erosion in mountains (Fig. 3.6). Its pyramidal shape was caused by the erosion by the Wahianoa Glacier and the Mangaehuehu Glacier (Williams, 2001).

3.2.2.1 Abrasion

Abrasion is the direct interaction of subglacial debris with the bedrock (Fig. 3.7). It occurs when particles move across the bedrock and cause a general wear of the rock and/or the scouring of the rock surface (Benn & Evans, 1998). For example: larger clasts often scratch the surface of the bedrock which leads to the formation of striae, which are small grooves on the rock surface. The abrading rock needs to be harder than the bedrock (Drewry, 1986), and there must be a constant supply of abrading rock fragments (Martini *et al.*, 2001). When the entrained fragments and the bedrock abrade together, a large quantity of rock flour will be produced. Rock flour generally polishes the bedrock and gives meltwater a 'milky' colour.

The variables that control abrasion are: (1) the *rate of basal sliding*, which is controlled by the basal thermal regime - if the velocity of the moving ice is high, more particles are being dragged along the bed. Therefore, the rate of abrasion will be high; (2) the *concentration of basal debris within the ice* - if the concentration of basal debris is high, the frictional drag between the bed and the ice will also increase. This has the effect that the rate of basal sliding will be reduced and therefore the rate of glacial abrasion; (3) the *basal contact pressure*, which is the pressure between the basal clast and the bed rock - the greater the pressure, the greater the rate of abrasion; and (4) the *hardness of the bed rock and the abrading clasts* – some rocks withstand abrasion more than others (Bennett & Glasser, 1996).

Figure 3.6 Girdlestone Peak has been sculpted into a glacial *horn*. It was shaped by the Wahianoa Glacier, seen on the right of the photograph and by the Mangaehuehu Glacier. The latter is situated on the southwestern side of the mountain (behind the ridge on the left side of the photograph).

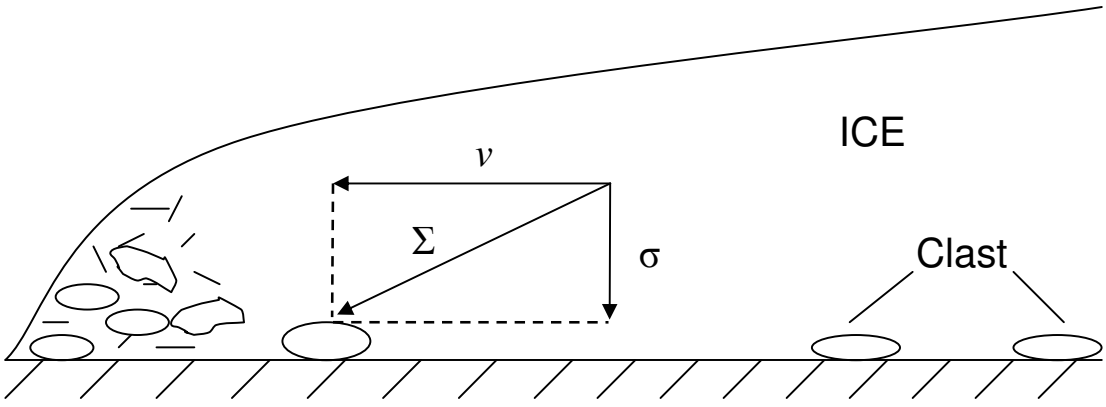

Figure 3.7 Schematic presentation of a glacier in motion and the processes that are required for abrasion to occur. The combined forces of weight (σ) and the movement (*v*) of the glacier ice push against a clast or the bedrock, as indicated by the vector sum $\Sigma = v + \sigma$ (Martini, *et al.,* 2001).

Several models have been developed over the years that try to explain subglacial erosion. Benn & Evans (1998) provide a very detailed account of these. The Boulton model (1974) assumes that effective normal pressure is the most important variable in subglacial erosion. According to this model, abrasion rate increases with increased pressure. However, at a certain point, when the pressure causes too much friction (depends on the weight of the overlying ice minus the basal water pressure) between the bed and the rock fragments, the particles will stop moving all together and become lodged (Fig. 3.8). It has been argued that this model is only applicable where the concentration of basal debris is high and if the interface between the particles and the bed consists out of cavities and contact points (Benn & Evans, 1998; Knight, 1999).

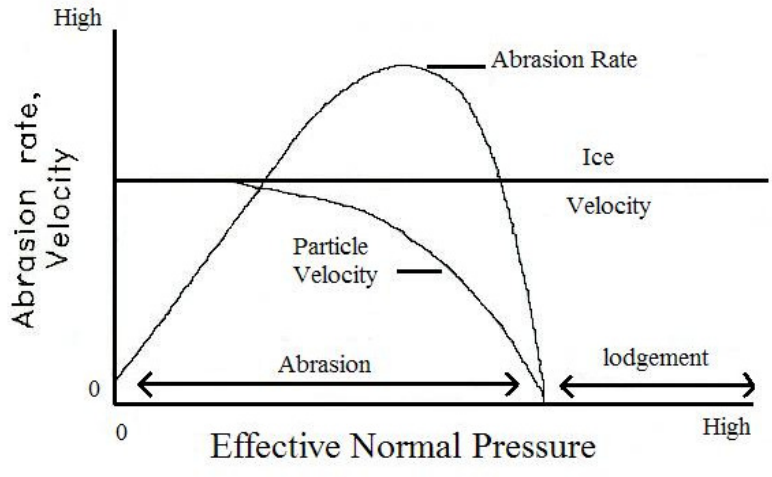

Figure 3.8 Theoretical graph constructed by Boulton (1974) showing the relationship between abrasion and lodgement. The abrasion rate increases with increasing pressure until a critical point has been reached. This critical value depends on the velocity. The highest rate of abrasion depends on the hardness of the fragment and on the velocity (Knight, 1999).

The Hallet (1979b) friction model argues that the basal sliding velocity is independent of the basal water pressure and the ice thickness because of the buoyant properties of the particles when imbedded into the ice (Benn & Evans, 1998; Knight, 1999). The buoyant weight equals the weight of the rock fragment minus the weight of the same volume of ice (Benn & Evans, 1998). The rock particles are said to be buoyant because they are constantly surrounded and supported by glacial ice. The resulting contact force between the

rock fragment and the bed is determined by the rate of downward movement and the buoyant weight, which are the functions of ice velocity. The rate of abrasion (Hallet, 1979b) is given by

$$\dot{A} = \alpha_{ch}\, C_r u_c F_c$$

where $\dot{A}$ is the rate of abrasion, α_{ch} is a constant that is dependent on the geometry of the striator and the hardness of the bed and the clasts, C_r is the debris concentration, u_c is the velocity of the clast and F_c is the effective contact force (Iverson, 2002). This model is generally accepted as the more realistic of the two (Knight, 1999). However, the Hallet model only applies to glacial environments where basal debris concentration is low and individual clasts are completely imbedded into the glacial ice.

3.2.2.2 Plucking

Plucking ("quarrying") is the process that removes rock fragments from subglacial bedrock. It involves the fracturing of bedrock and the entrainment of these rock fragments into the ice. When a glacier moves over any kind of substratum, immense forces are created. If there are any obstructions in the bedrock, the ice will exert compressive forces on these due to adhesive forces formed between the ice and the obstacles (Martini *et al.,* 2001). However, the tensile strength of a rock is generally much stronger than that of the ice. Therefore, plucking can only occur if the rock fragment has been weakened due to prior stress exerted (Price, 1973). Tensile stresses can also develop when the moving ice is frozen to the bed.

Temporary stress concentrations exerted on clasts and bedrock can result in rock fracturing (Benn & Evans, 1998). Martini *et al.* (2001) suggest that the repeated retreat and advance of a glacier can cause the bedrock to weaken, which can cause it to fail. In addition, subglacial freeze-thaw action can enhance this process. Weaknesses in rock can also develop well before the formation of a glacier, due to general weathering processes. Morland & Morris (1977) investigated if the stress field generated in bedrock by moving glacial ice is enough to cause rock fracturing. They concluded that bedrock failure can only occur if there are some weaknesses (i.e. jointing) in the rock prior to the glacial processes.

Bennett and Glasser (1996) give a detailed account of three theories that have been developed to explain fracturing in bedrock as glacial ice overrides the rock: (1) *discontinuous rock mass failure* (Addison, 1981) occurs where a rock mass contains weaknesses due to differences in basal ice pressures. These stress fields are transferred to the bedrock underneath and are concentrated on the lee side if an obstacle exists that contains air cavities; (2) the *heat-pump effect* (Kirkbride, 2002) is caused when the differences in ice pressure produces small cold patches in the base. This occurs because pressure reduces the pressure melting point and the ice melts. On the other hand, this process consumes latent heat and the ice mass becomes colder. The adhesive forces between the rock and the ice are stronger in these areas and plucking is more likely to occur; (3) *hydraulic jacking* (Iken, 1981) is the process where fluctuations in the basal water pressure causes the expansion and the propagation of bedrock fractures. Hydrostatic pressure causes the base of the glacier to lift, which causes the plucking off fragments that were frozen to the bed.

After the plucking of rock particles from the bedrock the fragments become entrained into the glacial ice. However, erosion and entrainment do not always occur in conjunction with each other. Sometimes the products of erosion are removed from the glacial system via meltwater before they can be entrained within glacial ice (Knight, 1999). The processes discussed above cause the propagation of fractures in basal rock and consequently the entrainment of subglacial material into basal ice. Friction between subglacial bedrock and ice, when reduced, enhance the mechanism of entrainment (Benn & Evans, 1998).

3.2.2.3 Meltwater erosion

In temperate glaciers subglacial meltwater plays a major role in erosion and transport of debris. It can flow underneath glacial ice as a very thin layer and/or through subglacial tunnels (both Nye and Röthlisberger channels). Water is capable of entering rock pores and rock joints and therefore enhances the break-up of rock. Water is also chemically reactive and is a great medium to transport fine particles that are in suspension or that move by saltation. Glacial meltwater erosion can result due to *mechanical* or *chemical* processes.

If sediment laden water flows over a substrate, the particles in the fluid will abrade the rock. The rate of this type of *mechanical erosion* is dependent on (1) the debris concentration. Generally, the higher the debris concentration, the higher the rate of abrasion; (2) fluvial abrasion is more efficient in turbulent water. The frequency of abrading particles making contact with the substratum increases if the water velocity is higher; (3) the hardness of the particles in question influences the efficiency of abrasion. If the particles in the meltwater are harder than the basal rock, they are more likely to cause abrasion; (4) Fluvial abrasion is also dependent on the properties of the water channel and therefore the angle of attack. As in rivers, abrasion is most intensive in bends or where there are large obstacles in the path for collisions to occur (Drewry, 1986; Bennett & Glasser, 1996).

Chemical erosion is the process by which meltwater erodes bedrock by chemical solution (Tranter, 2006). Soluble elements in the rock dissolve in the water and therefore leave the glacial system. The efficiency of chemical erosion depends on the lithology and the properties of the meltwater system (Knight, 1999). Chemical erosion is more effective in a subglacial water system than in many subaerial ones because the solubility of gases in water increases in lower temperatures. This causes the water to become more acidic and therefore more reactive. Furthermore, glacial meltwater is often rich in rock flour. This drastically increases the surface area of reactive particles and makes erosion more affective. Lastly, glacial meltwater tends to flow through the glacier system very fast. Therefore, the meltwater is less likely to become chemically saturated and remains more reactive.

3.2.3 Glacial entrainment and transport

Glacial transport is very complex and is affected by ice properties, sediment source and sediment supply (Kirkbride, 2002). Goodsell *et al.* (2005) have identified that ice deformation and associated ice structures play an important part in glacial debris transport by studying the processes that control the formation of medial moraines and dirt cones. Due to their very high altitudes, the Karakoram Mountains and the western Himalayas have areas of permafrost and very high precipitation rates. Most of these glaciers are extremely long and their snouts can advance to semi-arid regions (Owen, 1994). This leads to very

complex glacial systems. Furthermore, due to a great sediment supply from these mountains, the glaciers are often strongly debris covered, which alters glacial dynamics and response time, due to reduced ablation. The amount of supraglacial and englacial debris entering a glacier is determined by the nature and the extent of extraglacial terrains, but the amount of subglacial debris is primarily determined by the thermal regime and by the properties of the substratum (Kirkbride, 2002).

Glacial abrasion and plucking are only two processes that add sediment to the glacial system. In valley glaciers rock falls (mostly due to frost shattering) from surrounding mountain walls are additional sources of sediment input. These are even more efficient in seismically active areas, such as in the Andes, the Himalayas and New Zealand (Hewitt, 1988). Avalanche debris (rock, soil, ice and snow) and debris flows are also typical in these environments. However, rock falls add the largest volumes to a glacial system (Hambrey, 1994). A further type of sediment input is aeolian transport via wind and/or volcanic eruptions. Glacial ice can contain particles that have been transported for many hundreds of kilometers (Ehlers, 1996). The glaciers of Ruapehu would have contained large amounts of volcanic ash during their greatest advance. However, the glaciers have retreated to such an extent that only recent ash deposits will be enclosed in the glacial ice.

3.2.4 High-level Transport Zone

The sediment transport pathway that transports supraglacial or englacial debris is called the *passive transport zone* (Boulton, 1978) or the *high-level transport zone* (Kirkbride, 2002). As the debris is transported on the surface or within the ice, it undergoes very little modification and the characteristics of the parent rock are preserved (Fig. 3.9). Debris that is transported in the high-level transport zone derives from different supraglacial sources, such as rock falls, debris avalanches, volcanic ash, aeolian transported particles, aerosols and sometimes extraterrestrial material, such as meteorites (Kirkbride, 2002). Generally, if debris falls onto the glacier's surface above the ELA, the clasts will be buried to become englacial debris. However, if sediment falls onto the surface below the ELA, no burial takes place and the debris remains on the glacier's surface (Fig. 3.9) (Bennett & Glasser, 1996).

3.2.5 Low-level Transport Zone

Once a clast has been removed from the basal shear zone by glacial erosion it becomes entrained into the ice and transported to areas of deposition. As the subglacial debris is transported, it is exposed to great forces and undergoes significant modification. Therefore, this type of transport pathway is termed the *active transport zone* (Boulton, 1978) or the *low-level transport zone* (Fig. 3.9) (Kirkbride, 2002). However, Benn *et al.* (2003) argue that the distinction between the passive and active transport zone is oversimplified by Boulton (1978), as some supraglacial sediment can undergo modification in the passive transport zone (Owen *et al*., 2002). Furthermore, clasts do not have to remain in their designated transport zone. Supraglacial and englacial debris can enter the basal zone by burial or by crevasses.

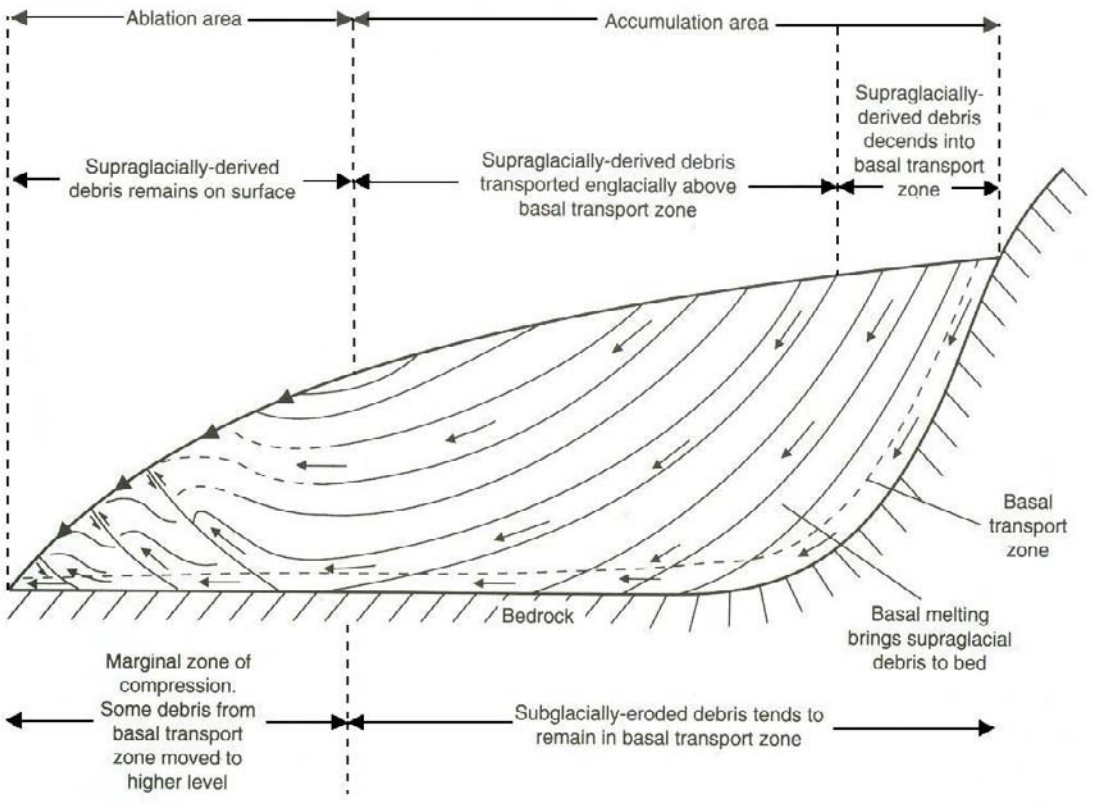

Figure 3.9 The transport pathways of debris through a valley glacier. High-level transport zone, where supraglacial debris is transported on the surface of the glacier and englacial debris within the ice. Debris does not come into contact with bedrock. Low-level transport zone, where subglacial debris is transported along the basal zone. Debris undergoes great modification because of contact with glacier bed (Boulton, 1978).

3.2.6 Clast modification

In general, supra and englacial debris typically exhibit low roundness, show very variable sphericity, and have a deficiency of fines (Hambrey, 1994). Subglacial debris undergoes great modification due to high stresses in the basal transport zone (Fig. 3.10). The clasts are more rounded and their shapes are elongated and platy (Benn & Ballantyne, 1994). During high-level transport, the chance of interparticle collision is very small (Kirkbride, 2002). Therefore, supraglacial debris contains particles that are coarser than 1Ø and lack in fine particles (Hambrey, 1994). Debris that is transported close to the glacier sole is exposed to pressure melting and regelation due to ice deformation around bed obstacles (Kirkbride, 2002). This causes the particles to collide and enhances the modification of the sediment. Therefore, subglacial debris generally contains a larger fraction of finer particles.

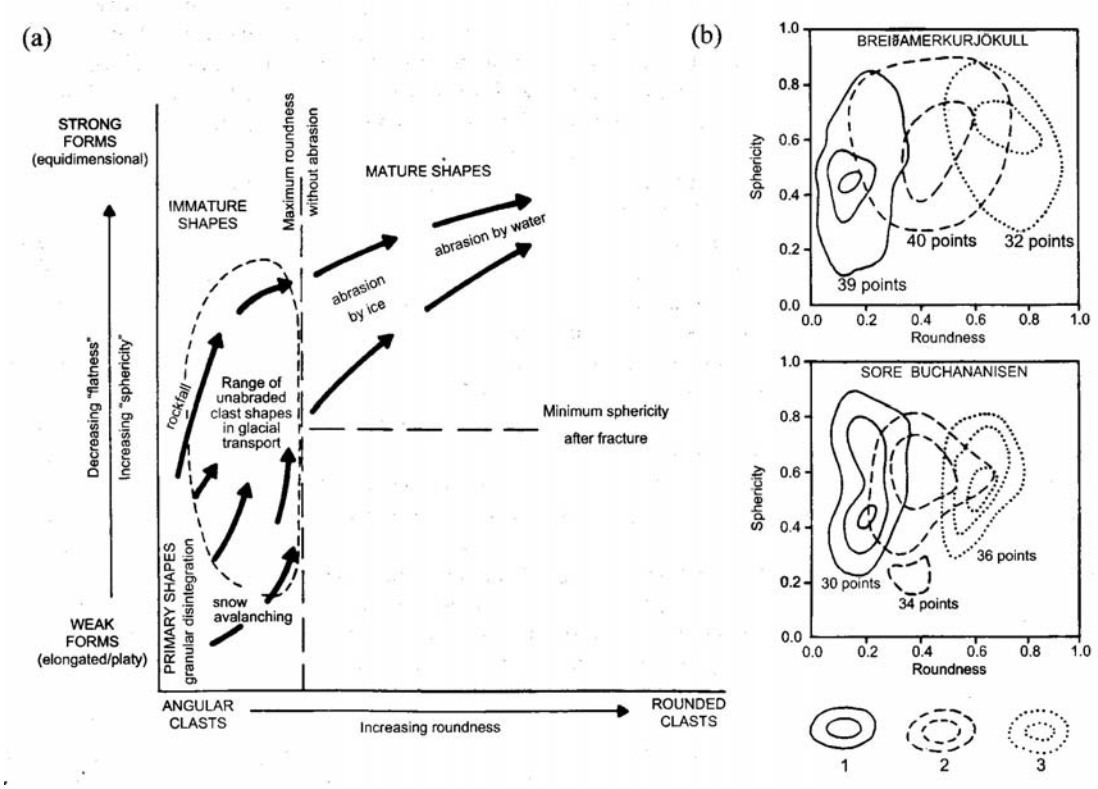

Figure 3.10 Modification of clast shape during glacial transport. (a) Results from 88 samples of 50 clast each from Tasman and Mueller Glacier, New Zealand. Supraglacial debris exhibit immature shapes. Whereas debris that has undergone glacial abrasion shows greater roundness and an elongated and platy shape (Kirkbride, 2002). (b) Krumbein form-roundness plots of clasts from high-level and low-level transport zones. 1=englacial debris; 2=basal debris; 3=lodgement till (after Boulton, 1978)

Kjaer (1999) investigated the effect of subglacial transport on sediment properties of the Myrdalsjökull ice-cap, Iceland. The study included grain-size distribution, clast morphology and geochemical and mineral magnetic properties. The investigation showed that only a very short transport distance (only about 250m of transport distance) was required for clasts to reach a mature state (Fig. 3.11). Beyond this point, other factors influence clast modification.

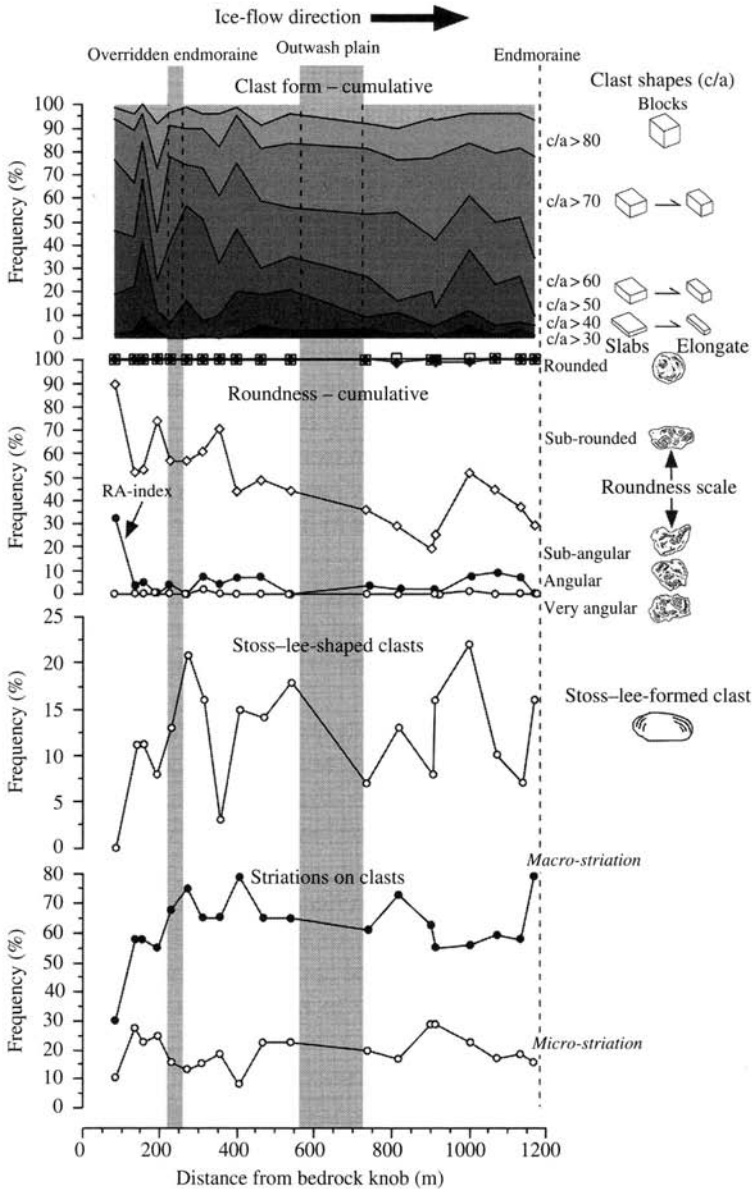

Figure 3.11 Variations in clast morphology with distance along the transport pathway of the Myrdalsjökull ice-cap, Iceland. Shaded area indicates major geomorphological features serving as guidelines (Kjaer, 1999).

3.2.7 Lateral Moraines

Lateral moraines are composite supraglacial and subglacial features that form when supraglacial debris accumulates between glacial ice and the rock wall (Hambrey, 1994). Lateral moraines often have a mud-grade matrix due to the effect of comminution that takes place between the ice and the rock wall (Hambrey, 1994). Figure 3.12 A illustrates the formation of a lateral moraine due to the dumping of glacial debris. Although the bulk of debris derives from the glacier, some may also fall onto the moraine from the rock wall (Bennett & Glasser, 1996). Figure 3.12 B shows the formation of lateral moraines due to seasonal deposition, where debris is often temporarily stored between the ice margin and the dump moraine. This occurs due to short-term ice retreat during the summer months, when the ablation rate is high.

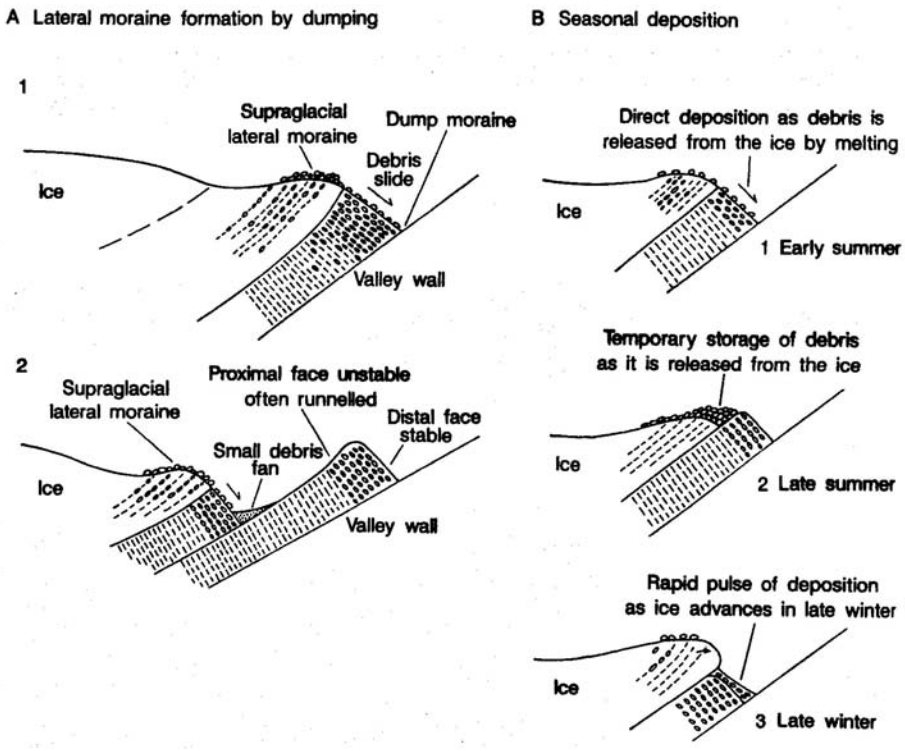

Figure 3.12 The formation of lateral moraines by dumping of supraglacial debris. (A) Lateral moraine formation, showing scree-like bedding. (B) Seasonal deposition (Modified from Small, 1987).

As noted before, lateral moraines may undergo numerous periods of aggradation and erosion. Therefore, the depositional histories of a glacier is generally preserved within the till deposit, which is reflected in typical sedimentary facies of the lateral moraines (Benn *et al.,* 2003). Figure 3.13 demonstrates the internal stratigraphy of a large lateral moraine, showing a talus cone that delivers debris directly to the till deposit. If the moraine is influenced by ice-marginal meltwater streams that flow laterally to the glacier, small kame terraces may develop (Bennett & Glasser, 1996). These are flat-topped ridges that are composed of bedded glaciofluvial debris.

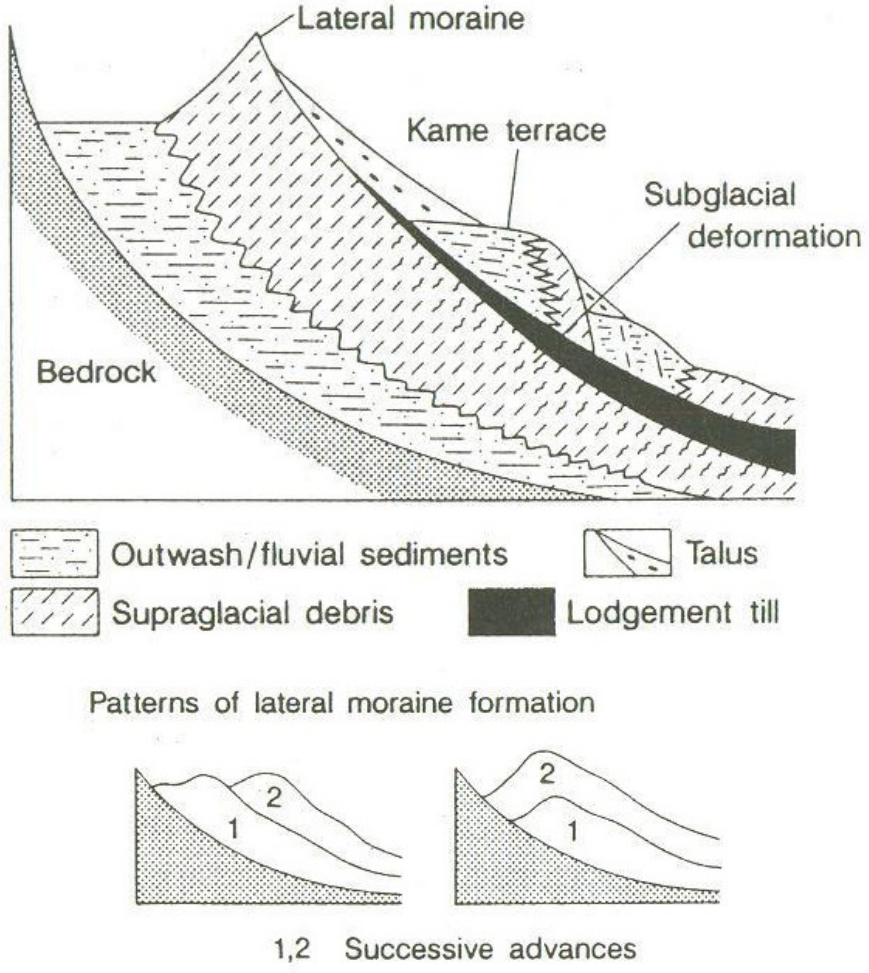

Figure 3.13 Schematic internal stratigraphy of large lateral moraines (Bennett & Glasser, 1996).

3.3 DEBRIS TRANSPORT OF THE WAHIANOA GLACIER

It is likely that the Wahianoa Glacier was strongly debris mantled, because of the unstable nature of the Ruapehu massif. Furthermore, frequent eruptions of the volcano and its neighbours, will have resulted in a large supply of supraglacial debris of volcanic origin. The formation of moraines is also generally associated with a large supply of supraglacial debris, which accumulates along the margins of the glacier (Benn, *et al.*, 2003). The Wahianoa River is currently erodings into the base of the Wahianoa valley. The river possibly played a major role in the glacial system and mechanical and chemical erosion might have occurred. The glacier primarily moved over unconsolidated sediment, which must have caused subglacial deformation. Subglacial deformation is linked with fast ice motion because a water saturated layer of till is coupled to the ice and both move together over a stable layer of till.

Chapter 4

CLAST MORPHOLOGY

4.1 INTRODUCTION

Clast morphology deals with the shape, roundness and texture of clasts. The morphological characteristics of glacial sediments are determined by processes, such as debris transport and deposition. These processes were discussed in detail in chapter three. Supraglacial and englacial sediment is not modified to a great extent, since they simply travel on or within the glacial ice. However, subglacial sediment is often exposed to great forces and shows a great degree of modification. Therefore, clast morphology is an important source of information when reconstructing the debris transport pathway of a glacier.

4.1.2 Previous studies in clast morphology

The significance of clast shape and roundness of sedimentary particles was identified a long time ago (Wadell, 1932). It took several years to define shape and roundness and to develop appropriate classifications (e.g. Wadell, 1932, 1933, 1935). Krumbein (1941) defines clast shape as *"a measure of the ratio of the surface area of a particle to its volume"*, whereas clast roundness as *"a measure of the curvature of the corners and edges expressed as a ratio to a whole, independent of its form"*. Krumbein (1941) also concentrated on developing efficient methods to measure clast morphology and to analyse the data. Powers (1953) proposed a new roundness scale that defined six classes (Fig. 4.4) and required the user to make visual assessments (Hubbard & Glasser, 2005). The scale starts at 0.12 (very angular) and finishes at 1.00 (well rounded).

Ballantyne (1982) was one of the first to realise that glacial clasts that have undergone different modes of erosion, exhibit systematic morphological characteristics. The study showed that supraglacial clasts have a slabby shape. Whereas subglacial derived clasts do not. Benn and Ballantyne (1993) further investigated the relationship between shape/roundness and the mode of transport in a glacial setting by using control samples. It was identified that scree deposits show little modification. The clasts are typically very

angular and angular. On a triangular shape continuum the clasts are elongated and slabby. Benn and Ballantyne (1993, 1994) also discovered that till deposits produce the reverse results. To distinguish the two types of clasts and therefore the mode of transport, they called the point where the clasts can be differentiated on the clast shape continuum (c/a axial ratio ≤ 0.4) the C_{40} index. In situations where the C_{40}/RA ratios show high values it can be assumed that the mode of transport was passive and where the ratios are low actively (chapter 3).

Since the discovery of the relationship between clast shape and roundness and the mode of glacial transport, many studies have applied this method in various glacial environments. For example Bennett *et al.* (1997) studied the clast modification and the influence of lithology in high-arctic environments. The study concluded that co-variance plots (clast shape and roundness) (Benn & Ballantyne, 1994) provide valuable discriminator of most glacial facies. The results did not suggest that lithology influences clast morphology to a great extent. But it was suggested that the clast possibly have not reached a mature state.

Many studies have used clast morphology in conjunction with other diagnostic criteria. Kjaer (1999) studied till properties of the retreating Myrdalsjökull ice cap, Iceland, to reconstruct the subglacial transport pathway. The following criteria were used: grain-size distribution, clast morphology, geochemistry and mineral magnetic analysis. Kjaer (1999) proposed that only a very short transport distance (first 250m) is required for glacigenic sediment to reach a mature state. Beyond this distance, other factors influence particle characteristics

Hambrey & Ehrmann (2004) studied the clast morphology of five glaciers from the Mt Cook area, New Zealand. This study had the aim to test the hypotheses that supraglacial debris in the Southern Alps is mainly derived from rock falls and that clasts are reworked by glaciofluvial processes. Hambrey & Ehrmann (2004) further proposed that sediments from alpine catchments have distinctive characteristics. The majority of the results have supported the hypotheses postulated in this study. The glaciers of the Southern Alps transport vast volumes of supraglacial debris. Streams play a major role in reworking

glacigenic sediment. However, the clasts that were studied did not exhibit any distinctive features.

Clast morphology has also been used to identify unknown debris ridge deposits in southern Africa. Mills and Grab (2005) have used clast morphology in conjunction with grain-size distribution and macrofabrics to specify the geomorphological processes that have produced the ridge deposits. All criteria applied in this study have led to the conclusion that the debris ridge in question is in fact a latero-push or dump moraine. The clasts measured were elongated and platy and angular to very angular (section 4.2 and 4.3), which has been related to supraglacial derived till (Mills & Grab, 2005).

4.2 CLAST SHAPE

The shape of a clast is determined by its relative dimensions (Evans & Benn, 2004). A clast exhibits three axes that are perpendicular to each other. The longest axis is called *a*-axis, the intermediate *b*-axis and the shortest *c*-axis (Fig. 4.1). The measurements of the three axes can be used to determine the overall shape of the clast. This is done by calculating the ratios of the *b/a* and *c/b* axes and the disc-rod index (DRI), which is determined by (a-b)/(a-c). The resulting data can then be plotted up on a ternary diagram, which is a triangular shape continuum (Fig. 4.2). The end-members of this continuum are 1) a "sphere" ("blocks") where a = b = c; 2) a "prolate" ("elongates") where a > b = c; and 3) an "oblate" ("slabs") where a = b > c.

To show the co-variance of the characteristics of the clasts, the RA index (% of VA + A clasts, see section 4.3) versus the C_{40} index (% of clasts with *c/*a axial ratio ≤ 0.4) can be plotted on a scatter diagram (Fig. 4.3). In the example below, The C_{40} index was identified by Benn & Ballantyne (1993) and has been proven (together with the RA index) to be an invaluable 'tool' in the distinction of supraglacial/englacial sediment, which has been transported passively (low C_{40}/low RA) and basal/subglacial sediment, which has been transported actively (high C_{40}/high RA).

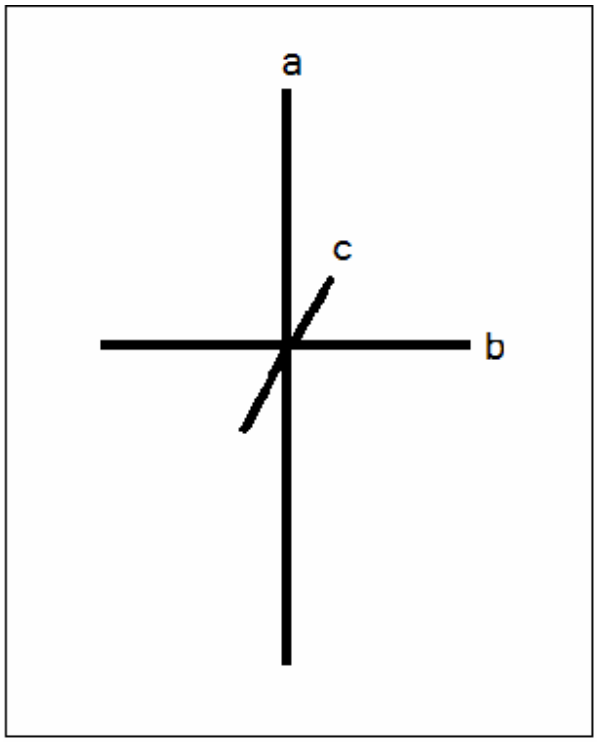

Figure 4.1 The three orthogonal (at right angles to each other) axes of a clast. The *a*- axis is the longest axis, the *b*- axis the intermediate axis and the *c*- axis is the shortest axis.

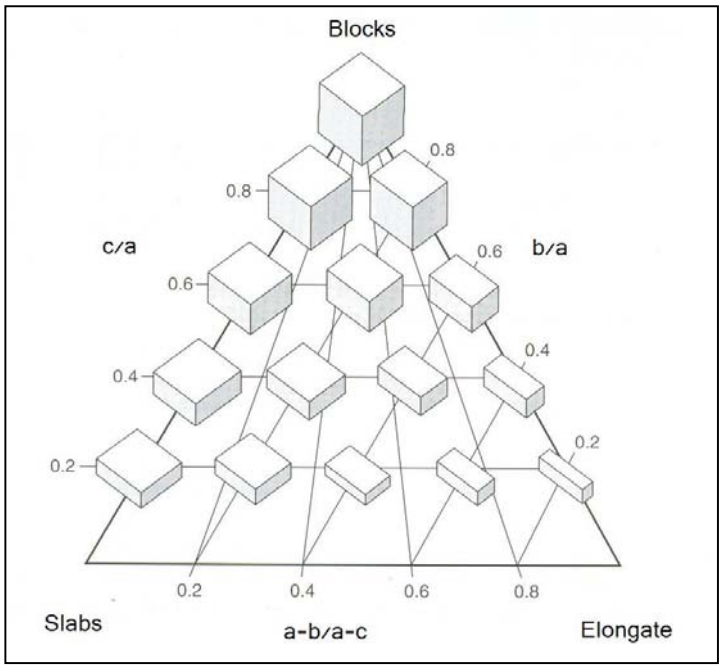

Figure 4.2 A ternary diagram where c/a is plotted against b/a and a-b/a-c (DRI). The end-members of the triangular shape continuum are: blocks (a=b=c), elongates (a>b-c) and slabs (a=b>c) (Evans & Benn, 2004).

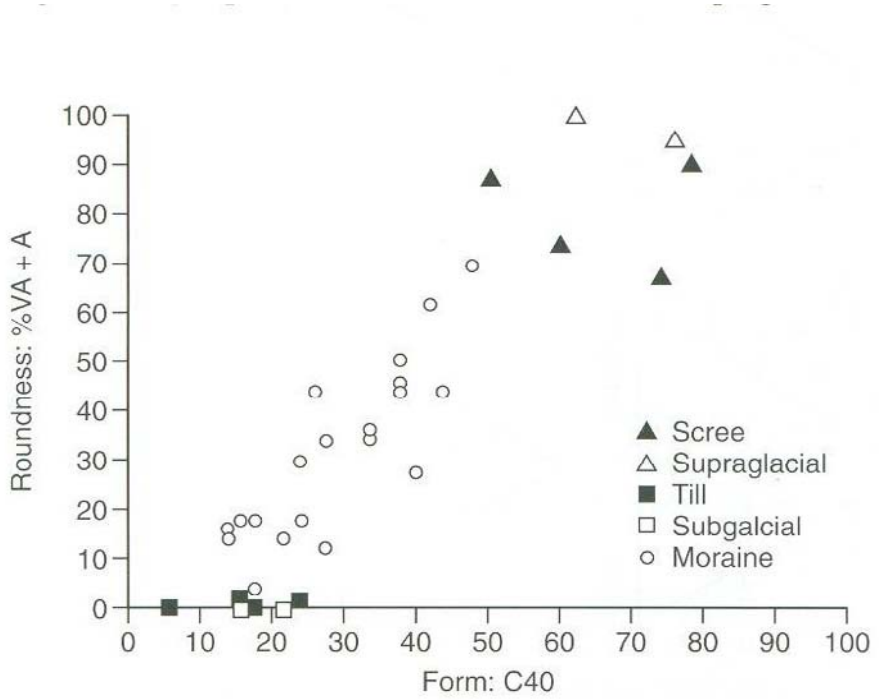

Figure 4.3 Scatter diagram that shows the clast shape (C_{40} index) and roundness (RA index) data from a glacier in Norway. The control samples are from scree and supraglacial debris (passive transport) and from till and subglacial debris (active transport). The moraine deposit plot well between the control samples, which suggest that these deposits have been transported in both transport pathways (Evans & Benn, 2004).

4.3 ROUNDNESS

The roundness of a clast is determined by the amount of wear that shows on the edges and faces of the clast. For example: if the faces and edges of a clast are unworn, than they will feel extremely sharp. This clast is described as 'very angular'. A clast will feel very smooth if it does not exhibit any faces or edges. This clast is classified as 'well rounded'. The roundness of a clast provides valued information about the nature of weathering, transportation and deposition. A well rounded particle will have undergone great stresses and processes to have caused it to loose all its faces and edges. Roundness is an indicator of the amount of modification the clast has undergone. In a glacial environment the greatest wear is shown in clasts that have been transported actively in the subglacial or basal zone. Table 4.1 gives a descriptive presentation of clast roundness categories. Figure 4.4 shows visual images that help with the classification of clast roundness.

Table 4.1 Descriptive criteria for clast roundness categories (Evans & Benn, 2004).

CLASS	DESCRIPTION
Very Angular (VA)	Edges and faces unworn; delicate protuberance
Angular (A)	Edges and faces unworn
Sub Angular (SA)	Faces unworn, edges worn
Sub Rounded (SR)	Edges and faces worn but clearly distinguishable
Rounded (R)	Edges and faces worn and barely distinguishable
Well Rounded (WR)	No edges or faces distinguishable

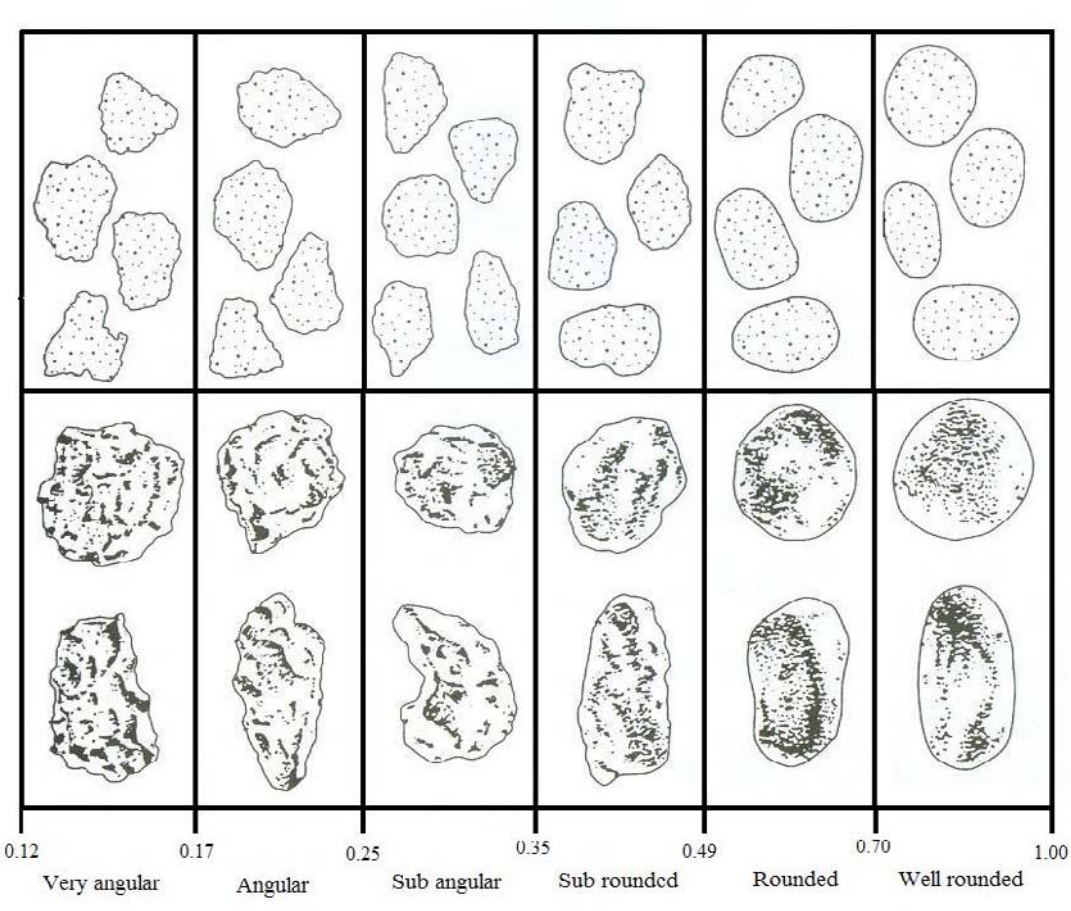

Figure 4.4 Visual images that help with the determination of clast roundness.

4.4 METHODOLOGY

4.4.2 Data collection

The main purpose of this study is to provide evidence for the assumption that the Wahianoa debris ridges are truly of glacial origin. This is done by attempting to reconstruct the transport pathway of the Wahianoa Glacier. Therefore, it is important to identify the shape and roundness of clasts in order to reconstruct their mode of transport. Not much work has been done in developing optimum sampling strategies in glacial morphological studies (Evans & Benn, 2004). Therefore, the methods used in this case study are based mainly on suggestions made by Evans & Benn (2004) and by Hubbard & Glasser (2005). In addition to the above, the methods were designed appropriately to the environment and time spent in the field. Figure 4.5 illustrates the field procedures used for this analysis.

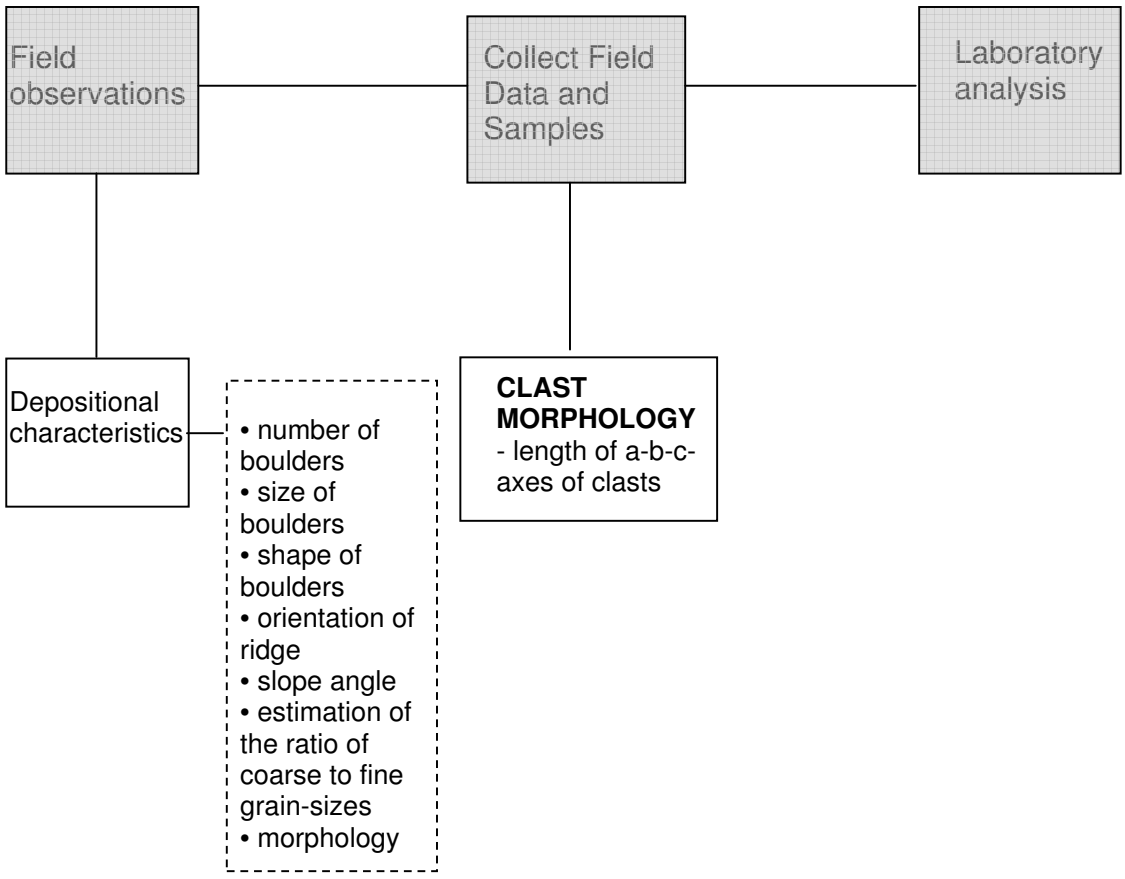

Figure 4.5 Flow diagram illustrating the field procedures used to identify the morphology of clasts from the Wahianoa valley.

The two debris ridges were divided into numerous transects, starting at the highest points that were accessible at that particular time (Fig. 4.8). In each transect 20 individual clasts were analysed. To represent samples from the whole population, clasts were chosen randomly from a wider area within each transect. The samples were measured directly in the field. The length of the three orthogonal axes was identified with the use of calipers and the data was then recorded for later processing (Fig. 4.6).

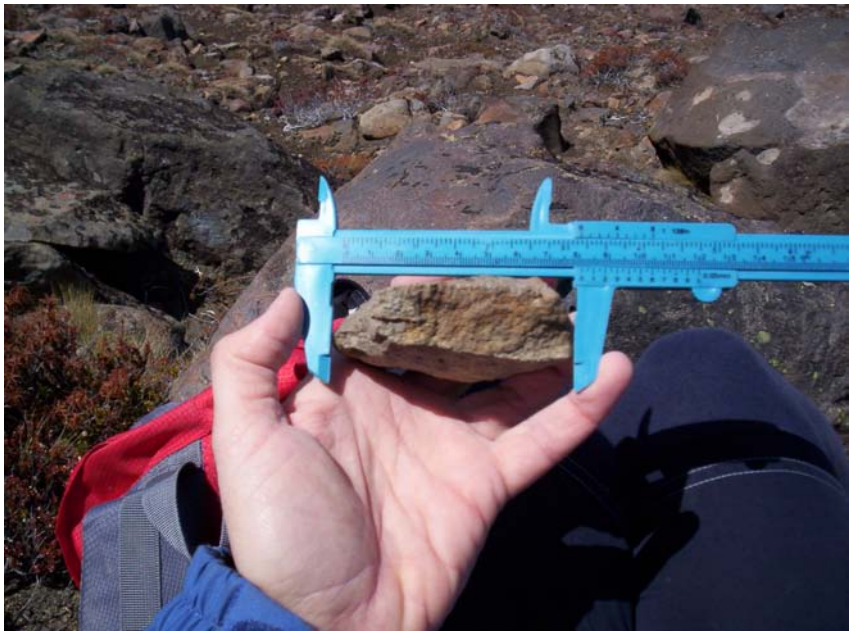

Figure 4.6 The measurement of the *a*-axis of a clast, using calipers.

The samples in transects a and b were collected half way up the sides of the debris ridges and the samples from transect e from the surface of a smaller lobe at the distal end of the eastern ridge. Transects c and d represent samples from the centre of the debris ridges. Both ridges show lobes that appear to be smaller ice channels that are branching off the main deposits. On the eastern side there is one bigger lobe running almost parallel to the ridge, whereas the true right shows at least three smaller lobes. These are nearly perpendicular to the major ridge deposit. Out of time constrains, only the second lobe on the true right was observed. These four transects where named samples 1-4f (Fig. 4.8).

After measuring the axes of each clast, its roundness was determined. This was achieved by using the visual images of Figure 4.4 and by feeling the edges of the clast (Fig. 4.7). Roundness is a very subjective criteria and is open for interpretation. Therefore, it is imperative that only one and always the same person collects this information. This is done to serve the purpose of consistency. Once the three axes were measured and the roundness determined, the clast was then thrown away in order to avoid using the same sample twice.

Figure 4.7 Determining the roundness of a clast. This is done by comparing the clast with the visual images of figure 4.4 and by judging the degree of wear of the edges of a clast.

To achieve comparable results, the individual clasts had to be of similar sizes. It was suggested (Evans & Benn, 2004) to choose samples with an *a*-axis between 35 mm and 125 mm and this was followed as much as possible in this research. It should be mentioned here that clast sizes are variable in the area of interest and it was not always easy to find clasts in the desired size range. In addition, care had to be taken to distinguish between deposits that were the direct result of volcanic activity (e.g. lava bombs) and sediments that had been modified by glacial processes. This was extremely difficult, since all rocks are igneous and have been derived from Mount Ruapehu and its surrounding neighbours. Furthermore, there have been numerous eruptions since the LGM and therefore, older deposits are overlain by younger ones.

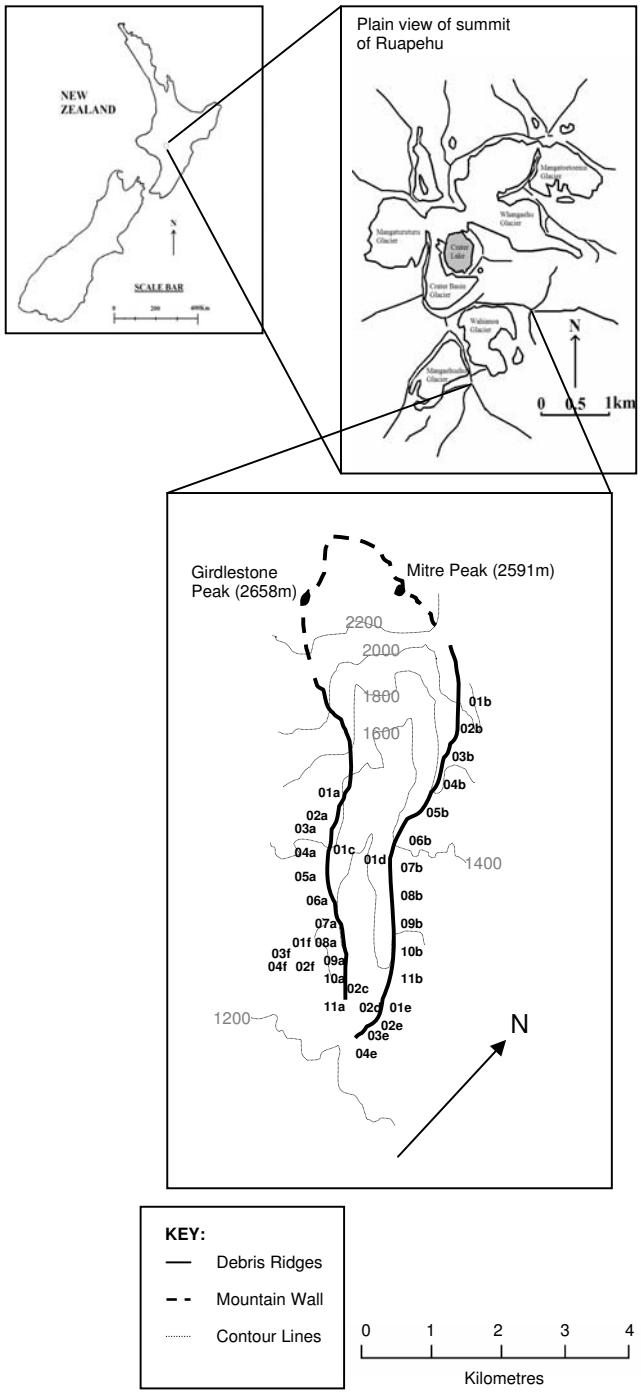

Figure 4.8 Schematic map of the Wahianoa debris ridges. It shows the locations and numbers of all transects used in this study.

4.4.3 Data analysis

After the collection of the field data, the information was then analysed according to Benn and Ballantyne (1993). The c/a and b/a ratios and the DRI were calculated and plotted on a ternary diagram. This was done with the help of a plotting spreadsheet (TRI-PLOT) that was used in Excel. The resulting graphical representation of the data was then used to identify any pattern that illustrates the overall shape of the clasts in a particular area. The C_{40} index was then calculated to show the percentages of clasts that may have been transported in the passive transport zone.

The roundness was presented graphically in the form of histograms. The histograms were produced in Excel and show the class of roundness and the number of individual clasts. Once the histograms were drawn, the ratios of very angular and angular clasts were calculated. The purpose of calculating the RA index was to identify the degree of wear exhibited by the clasts and therefore to identify the mode of transport. In order to be able to compare shape and roundness of clasts, the ternary diagrams and histograms were placed next to each other.

4.5 RESULTS – CLAST MORPHOLOGY

Figures 4.9 and 4.10 show the shape and roundness of clasts found in the Wahianoa Valley. Figure 4.9 shows the results of clasts that represent the western ridge. No particular pattern can be identified. The C_{40}/RA indices of this particular group of clasts show low to medium values. The majority of clasts appear to be sub angular and sub rounded with a slight tendency to angularity. The c/a and b/a ratios also show middle values. Therefore, it is impossible to identify a particular shape that these clasts represent.

The clasts of the eastern ridge show very different results compared to the ones from the western ridge (Fig. 4.9). The values for shape mostly fall between the blocky and elongated end-members of the triangular shape continuum. Therefore, it can be assumed that either the mode of transport was different or there was a difference in sediment source on that side of the valley.

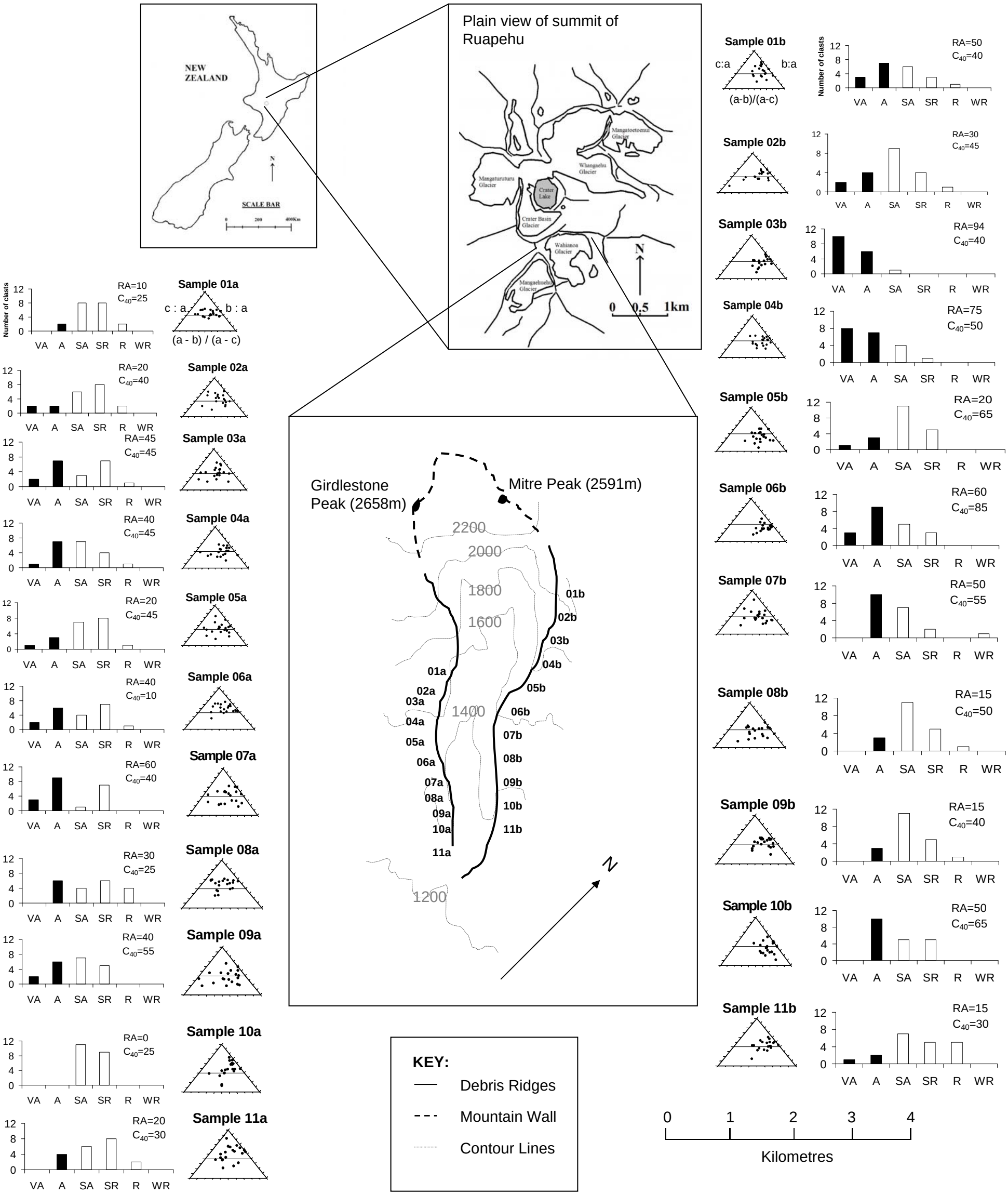

Figure 4.9 Clast morphology results for the debris ridges of the Wahianoa valley. The ternary diagrams show clast shape and the histograms show clast roundness. The location of each transect is shown in the sketch map. RA refers to the percentage of VA and A clasts in each sample. C_{40} refers to the percentage of clasts with c/a axial ratios ≤ 0.4.

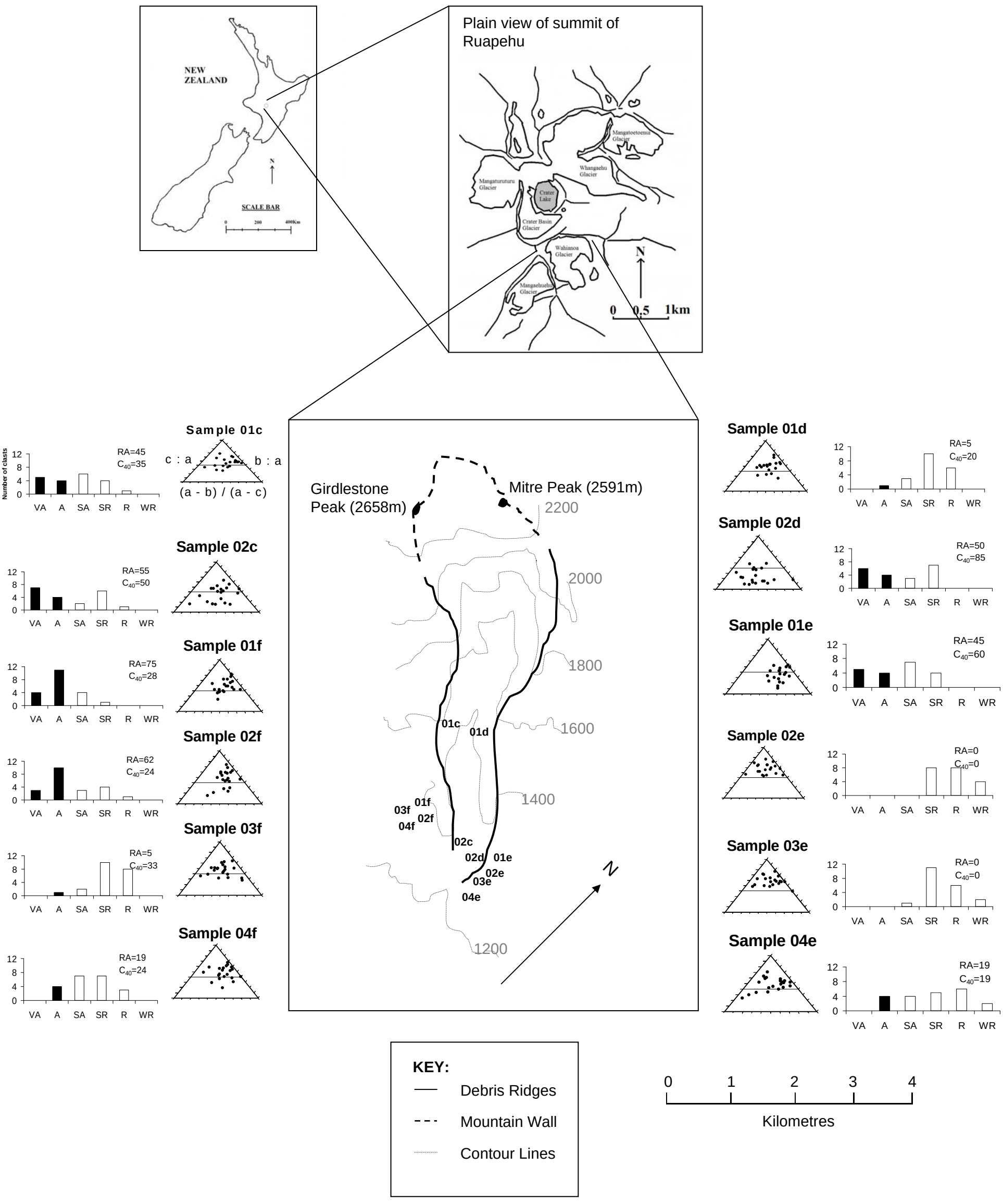

Figure 4.10 Clast morphology results for base and lobe samples. Samples 01c, 02c and 01d, 02d refer to transects located at the base of the debris ridges. Samples 01e to 04e refer to transects that are situated on a small lobe at the furthest extent of the eastern ridge. Samples 01f to 04f are transects located at one of several smaller lobes that run nearly perpendicular from the western ridge.

As mentioned in the introductory chapter (section 1.3), the stratigraphy between the two ridges varies greatly. The lava flows on the eastern ridge show a greater thickness than on the western ridge. It is likely that the difference in lithology has caused the difference in clast shape. In addition, the C_{40}/RA ratios show great variation. Therefore, it is very difficult to make any conclusive statements about the mode of transport. However, when comparing the results of the two ridges, the C_{40}/RA values on the eastern side are slightly higher than those on the western side.

Figure 4.10 shows the results of a small lobe (samples 01e-04e) that might be a terminal moraine. It is extremely difficult to make any concrete conclusions in this regard since there is no deposit that shows clear indications of this. Because the current fluvial system indicates episodes of major flooding (Fig. 4.11) it is likely that, if a terminal moraine has ever existed, it might have been washed away. Samples 2e and 3e show very promising values, however, because samples 1e and 4e do not, a conclusive statement about the mode of transport cannot be made.

Figure 4.10 also represents clasts found at the base of the debris ridges (samples 01c/02and 01d/02d). Again, they show great variation in shape and roundness. Sample 1d was located below the bluffs of lava flows that can be found on the eastern ridge. These lava flows typically show columnar jointing and therefore tend to be quite angular. The C_{40} is reasonably high. However, the RA only shows 50. Therefore, the relationship between shape and roundness does not provide enough evidence to come to a concrete conclusion. Sample 2d was collected from an outcrop at the base of the western ridge. It should be mentioned here that the outcrop was caused by some run-off water. Therefore, it is likely that the clasts have been influenced by water action.

Figure 4.11 Wahianoa River floodplain. (A) Looking down on the floodplain from the eastern ridge. (B) Looking down-valley (southeast) from the riverbed. (C) Looking down on the floodplain from the western ridge.

As mentioned before, there are several smaller lobes that run either parallel or perpendicular to the main debris ridges (Fig. 4.14-4.16). The samples 1f -4f on figure 4.10 are the results from the second lobe of the western ridge. The lobes on that side are very interesting and appear to be overflows of the main glacier. This conclusion is based on the fact that these lobes show signs of small individual glacial systems.

When following the ridge crest of the western ridge, it becomes obvious that there are individual accumulations of mega clasts (Fig. 4.12). In between these accumulations the ridge slopes down and up again close to the next stack of boulders. The sediment size in between these accumulations decreases greatly and no boulders are visible. As someone follows the ridges, the number and size of boulders appears to increase. Some erratic

boulders where found relatively far away from the main ridge (Fig. 4.13). In addition to the erratics, there were further depositional evidences that are typical for glacial activity. For example: large boulders deposited on top of small ones and vice versa.

Figure 4.12 Accumulations of megaclasts in between the lobes on the western ridge deposit (looking east). Clasts appear to have been 'dumped' and stacked up. Faces of individual clasts are worn. Dark coloured boulder on the right is possibly a lava bomb.

Figure 4.13 Two erratic boulders found at the end of the true left ridge of the second lobe that run nearly perpendicular to the main debris ridge on the true right. NB. Note the ski pole for scale in the upper photograph.

The results for shape and roundness of these deposits are similar to all the others. The C_{40}/RA values vary greatly. However, the clasts closer to source show a much greater angularity than those further away. An additional feature is that all clasts appear to be blockier rather than slabby or elongated. Again, the lithology is likely to be responsible for these non-conclusive results. This is in addition to the fact that the glacier has moved over unconsolidated material. The processes involved in glacier motion over deformable bedrock were discovered only recently (Hambrey, 1994, Benn & Evans, 1998, and Knight, 1999).

4.6 SUMMARY

In summary, the results of the shape and roundness of the clasts of the Wahianoa Valley are not very conclusive and do not support the aim of this project. During this investigation it has become very clear that the glacial deposits of Mount Ruapehu are extremely complex. There are many factors that appear to have influenced the deposits. One main issue that has been identified is that the glacier moved over unconsolidated sediment. The sediment source varies greatly in quantity and lithology. This is due to the fact that the glaciers are located on an active volcano. This fact will be further investigated in the main discussion of this thesis (chapter 9).

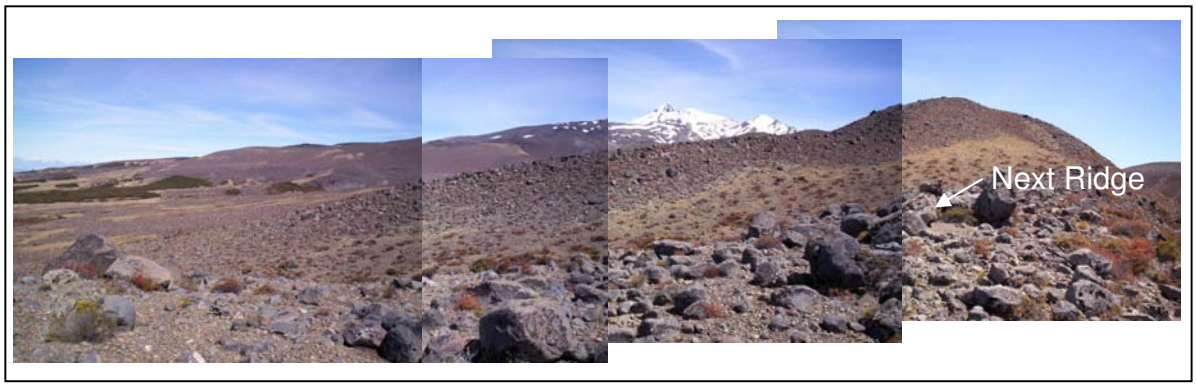

Figure 4.14 First channel on the true right, looking up valley with Girdlestone Peak and Mitre Peak in background. The crest of the next ridge (second channel) visible.

Figure 4.15 First channel on the true right, looking down valley.

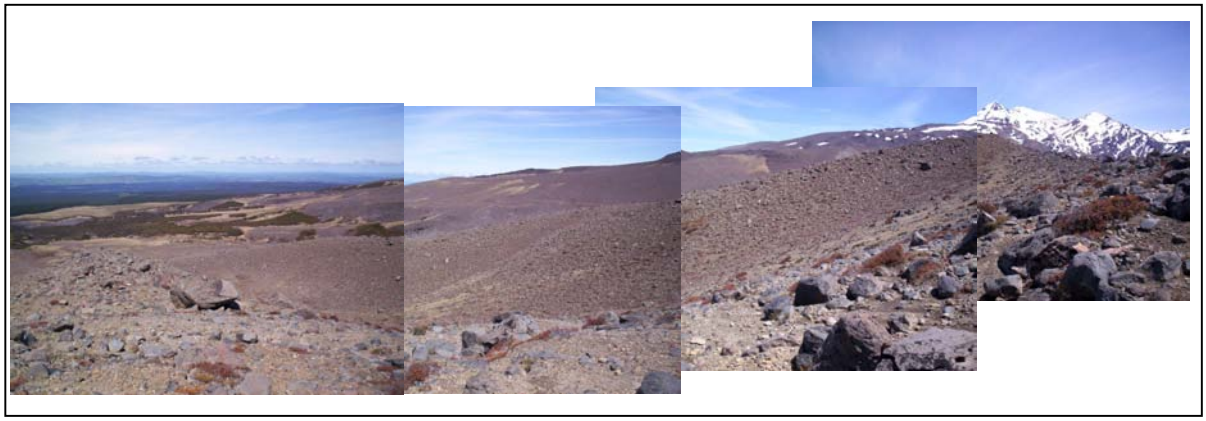

Figure 4.16 Standing on the true left ridge of the second channel, looking northwest. Girdlestone Peak and Mitre Peak in background.

Chapter 5

FABRIC ANALYSIS OF CLASTS

5.1 INTRODUCTION

Fabric analysis is the study of the orientation (declination) and the dip angle (inclination) of particles (Andrews, 1971). Hubbard & Glasser (2005) differentiate between macrofabrics (gravel-sized clasts *in situ*), mesofabrics (clasts in size range 2-10mm) and microfabrics (sediment in size range < 2mm). Measuring the declination and inclination of the a-axis of elongate clasts from till deposits can help identifying the direction of ice movement and glacier behaviour for paleoenvironmental analysis (Drewry, 1986).

5.1.2 Previous studies

Miller (1884) was one of the first researchers to publish work on till-clast orientation. He observed that clasts have a preferred orientation along their longest axis (a-axis). *"The longer axis of the stone is often directed in the line of glaciation, and the pointed end is frequently, but not always, toward the ice"* (Miller, 1884, p.167). Other early investigators (Bell, 1888; Upham, 1891) came to similar conclusions but the importance of their investigations of till fabrics were overlooked at the time (Holmes, 1941). During the 1930's the study of the orientation of glacigenic diamictons became more recognised. Richter's (1932, 1933, 1936) work was some of the most influential work of that time as he was able to confirm earlier conclusions by presenting his results in a more quantitative way. In addition to the observations made by earlier investigators, Richter also identified that some clasts in tills are orientated transverse to ice flow and that striae form parallel to ice flow.

Holmes (1941) statistical work on till fabrics of the central New York state of the USA is considered by Andrews (1971) as possibly the most complex work ever done on clast fabric. Holmes (1941) was able to interpret the modes of glacial transport and deposition by studying till fabrics. Holmes (1941) also realised that clast shape and roundness influences fabric strength as wedge formed clasts with prominent flat surfaces aligned in the direction of ice flow. During the following years the techniques used in till fabric analysis were

applied by many researchers (Karlstrom, 1952; West & Donner, 1956; Wright, 1957; Harrison, 1957a and 1957b; Glen *et al.,* 1957).

More recent studies (e.g., Lawson, 1979; Hicock, 1991; Benn, 1995; Hooyer & Iverson, 2000; Larsen & Piotrowski, 2003) have focused on the processes that control clast fabric. Dowdeswell *et al.* (1985) have used fabric analysis to identify the modes of transport and deposition in different glacial environments. Hart (1994) investigated the effects of subglacial deformation on till fabric. With the introduction of eigenvectors and eigenvalues (Mark, 1973) the potential for the identification and description of glacigenic diamictons has developed further (Bennett, *et al.,* 1999).

Recent work has concentrated mainly on *a*-axis fabrics, as the *a*-axis rotates under exerted stress and aligns in the direction of ice-flow and hence provides information about former depositional processes (Hooyer and Iverson, 2000). However, the orientation of the *a*-axis provides only two dimensional fabric information, whereas the a-b plane is typically orientated up-flow to minimise particle resistance (Hubbard & Glasser, 2005). Rose (1989) measured *a*-axis fabrics of fluted moraines on the foreland of Austre Okstindbreen, Norway. The *a*-axis fabrics showed a strong convergence towards the ice-proximal part of the flute and diverged away at the ice-distal end (Fig. 5.1). This process was interpreted as a response to large lodged boulders on the glacier bed.

The fabric strength relative to clast size was investigated by Kjaer and Krüger (1998). Fabric data from basal tills of Fakse Banke and Klintholm, Denmark, were sampled. A further analysis was completed at Slettjökull, Iceland. Kjaer and Krüger (1998) measured the *a*-axis and *b*-axis of individual clasts and calculated the eigenvalues (S_1, S_2 and S_3) and eigenvectors (V_1, V_2 and V_3), which are statistical parameters that show the fabric strength and the directional properties of the data (Benn, 1994). The results are shown in figure 5.2. It was concluded that clast size does influence fabric strength as clasts that are longer than 2-3cm show greater preference for parallel orientation than clasts do with a shorter *a*-axis.

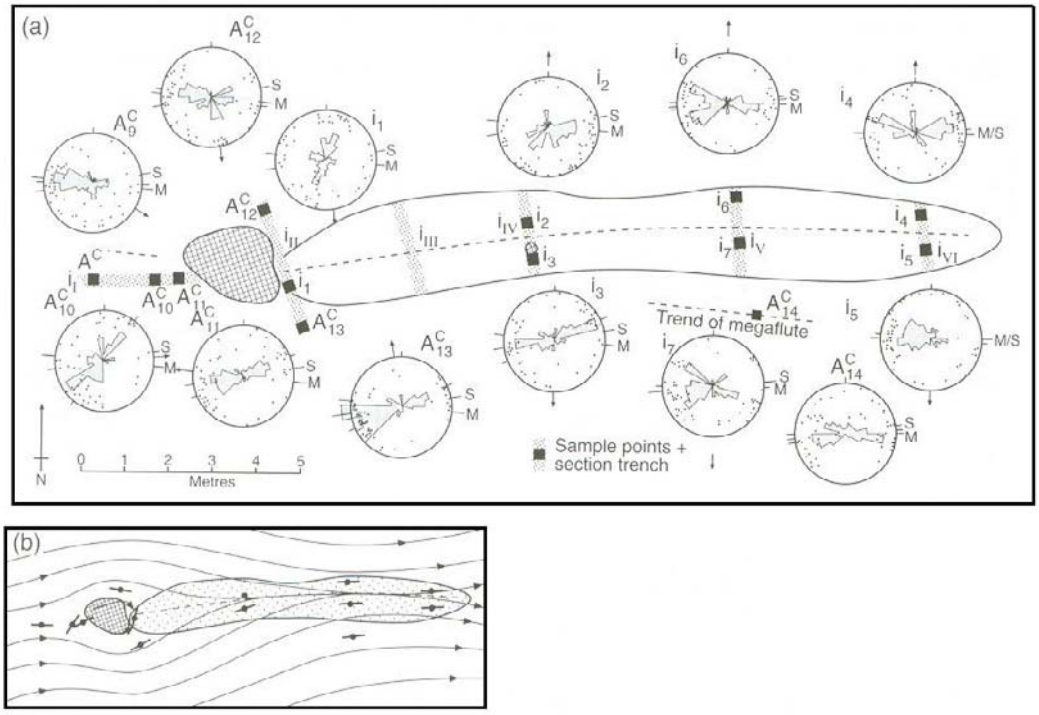

Figure 5.1 (a) *A*-axis fabrics in a flute on the foreland of Austre Okstindbreen, Norway. (b) Reconstructed flow patterns from preferred a-axis orientations. These have been interpreted as ice flow directions, or patterns of strain within the till (Rose, 1989).

Li *et al.* (2006) suggest that subglacial tills have stronger fabric than supraglacial till. This was shown in a study (Li *et al.,* 2006) of till deposits and other sediments in the upper Urumqi River, Tian Shan, China. Fabric data (*a*-axis and *a-b* plane) from four profile sections was collected, in addition to morphological data [*c/a* and (*a-b*)/(*a-c*)]. The eigenvalues and eigenvectors were then calculated. The results from the Upper Wangfeng profile is shown as contour data in figure 5.3. The results of the study have shown that clasts from till deposits have stronger *a*-axis and *a-b* plane fabric than those from non-glacial deposits. Furthermore, the study has also confirmed the hypothesis that subglacial till fabric is stronger than supraglacial one.

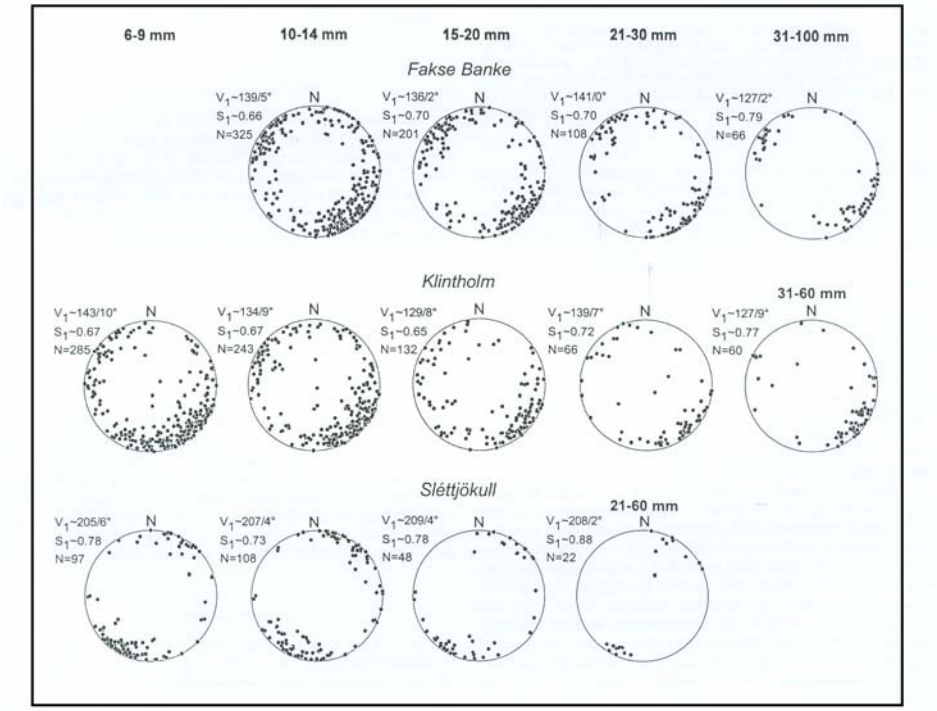

Figure 5.2 Fabric data from individual clast-size fractions from Fakse Banke, Klintholm, Denmark, and Slettjökull, Iceland. The data is presented as scatter diagrams on the lower hemisphere of a Lambert equal-area projection (Kjaer & Krüger, 1998).

5.2 METHODOLOGY

Till fabric analysis can provide valuable information about the directions of glacial ice movement and the modes of transport and deposition. Furthermore, the fabric analysis of glacigenic diamictons can give some indication of the strains the clasts were exposed to before deposition (Hubbard & Glasser, 2005). Generally, englacial sediments are exposed to fewer stresses than subglacial sediments. Therefore, no preferred orientation may be found in englacial diamictons. However, the stresses increase closer to the basal zone and clasts are forced to re-orientate (Drewry, 1986). Therefore, most studies (e.g. Kjaer & Krüger, 1998; Li *et al.,* 2006) focus on subglacial till and clasts *in situ.* Because the Wahianoa debris ridges consist of unconsolidated material (sandy matrix with interbedded clasts), it was not feasible to dig pits or trenches. Therefore, the aim was to measure the declination and inclination of clasts found on the surface of the ridges. The purpose of this study is to reconstruct the transport pathways of the Wahianoa Glacier. As no previous work has been done on Ruapehu in that field, the main interest lies in the identification of the direction of ice movement.

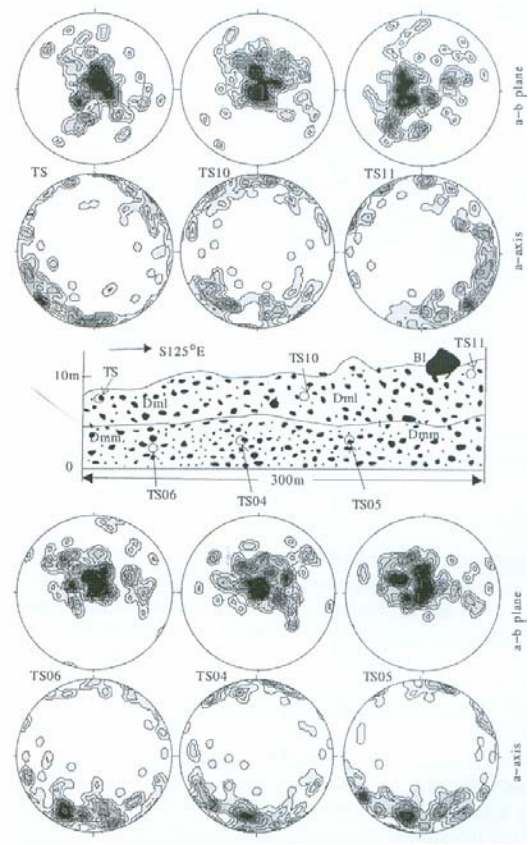

Figure 5.3 Sampling sites and its density contours of till clasts fabric of the Upper Wangfeng, upper Urumqi River, China, profile (Li *et al.,* 2006).

As noted above, the initial aim was to measure the declination and the inclination of smaller clasts found on the debris ridges. However, as the deposits are unconsolidated and therefore susceptible to slope movement, it was more desirable to investigate the orientation of megaclasts, since these are less likely to have moved from their original place of deposition. Furthermore, some areas of the ridge crests and slopes have been altered by humans to some degree, such as the construction of the popular 'Round the Mountain Track'.

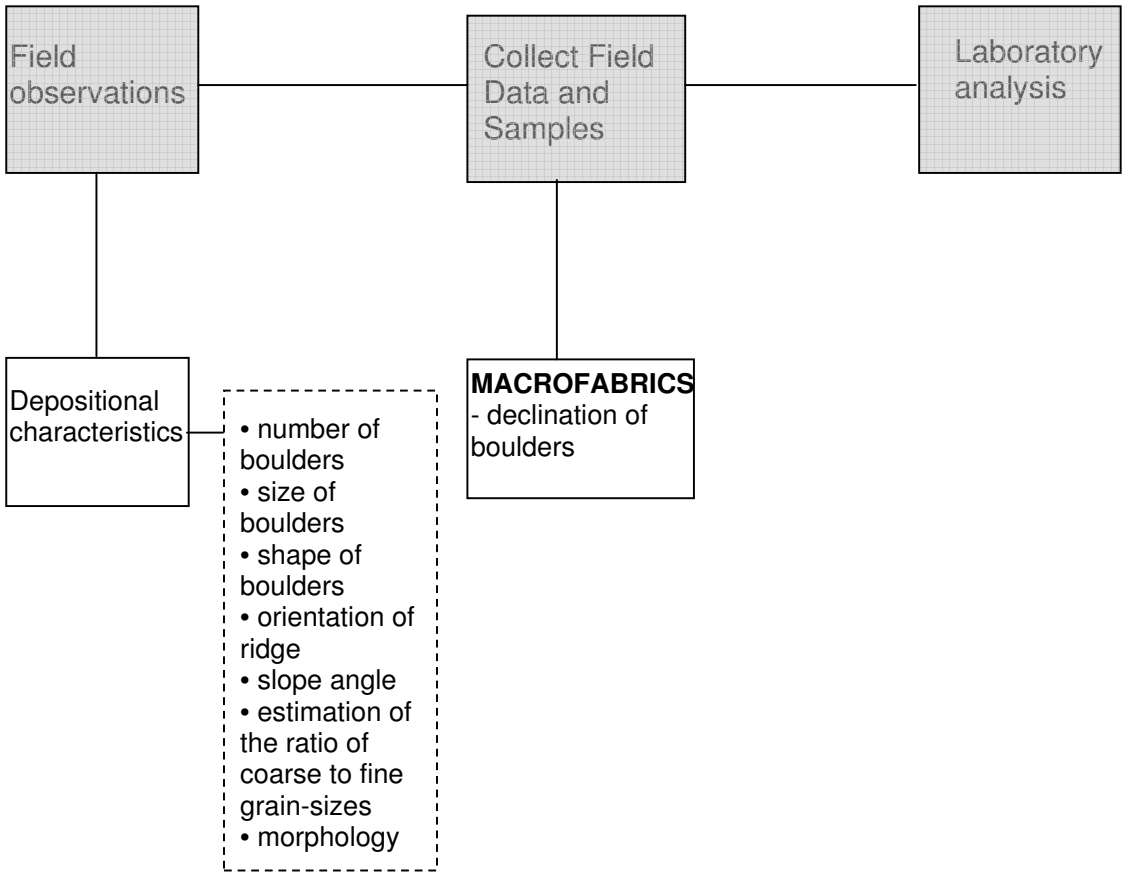

Figure 5.4 Flow diagram illustrating field procedures used to identify the orientation of boulders from the Wahianoa valley.

5.2.2 Sampling procedure

Figure 5.4 illustrates the field procedures used in the analysis of clast macrofabrics. A clinometer was used for the measurement of the declination of boulders on the Wahianoa Valley debris ridges (Fig. 5.5 A). At first, a suitable boulder was identified (Fig. 5.5 B). A suitable megaclast is one with a defined a-axis as those clasts are more likely to show parallel orientation (Kjaer & Krüger, 1998). Hubbard & Glasser (2005) have suggested measuring the declination in the direction of the dip. Although this study is not focusing on the dip angle (out of reasons discussed above) and it is less important in a bi-directional analysis, it was still attempted as much as possible.

Figure 5.5 Method for fabric analysis. (A) A clinometer is used to measure the declination of the orientation of clasts. A suitable clast (B) is one with a defined a-axis. A pencil is aligned to the a-axis and placed on the surface (C) or next to the clasts (D). The clinometer is held next to the pencil and the declination of the clasts is read off (C) and (D).

The orientation of the *a*-axis was marked by placing a pencil parallel to the axis (Fig. 5.5 C - E). If the surface of the boulder was not flat enough to hold the pencil in place (or too windy), the pencil was either placed next to the boulder or an imaginary line had to be used (Fig. 5.5 E). Once the a-axis was defined, the clinometer was held horizontally next to the pencil or the imaginary line. It is important to ensure that the compass needle is free to rotate to give a correct reading. The orientation was then read off to the nearest 5º and noted in a field notebook for later analysis. This method was done simultaneously with the method for clast morphology. Therefore, the boulders were located in a close range of the same transects. The measurements of twenty boulders were taken on each sample site. A total of over five hundred measurements were completed. If boulders or clasts showed striae, the orientation of these were also noted. However, too few were found for a valid analysis.

5.2.3 Data analysis

The declination and inclination of clasts are generally more useful as they provide 3-D fabric data. Furthermore, the eigenvalues and eigenvectors can be calculated to show fabric strength (Li, *et al.,* 2006). As this study only looks at the orientation of clasts, the data is presented as a rose diagram. A rose diagram provides a good visual image and is less time consuming to produce. However, it only shows the strength of preferred orientations and not any hidden patterns of dip orientations (Hubbard & Glasser, 2005).

After the completion of the fieldwork, the data was entered into the computer. For this study the Oriana Programme (Version 2.02c) was used. This programme produces satisfying visual images and provides sufficient basic statistics. Figure 5.6 shows an example of a rose diagram produced in Oriana and the statistics this program calculates. This particular diagram shows *bi-directional* data, which is also called *axial* data. A rose diagram is like a histogram that has been wrapped around a circle. The sections are generally wedge-shaped. For this study each wedge has a width of 10º of the total circle. The length of each wedge shows the number of observations within this particular range. Bi-directional data shows undirectional lines. This means that both ends of the lines represent the direction. For example: in figure 5.6 five samples out of the total of twenty

five, have a declination that lies between 120º and 130º. Therefore, the line has a direction of 120º/130º and 300º/310º. The arc around the circle shows the confidence for the mean direction. For this study it is of 95%.

The mean vector (μ) shows the mean direction of the boulders. In the example below it is 90.29º. As this is bi-directional data, the orientation is in both directions: 90.29º and 270.29º (90.29º + 180º). Another variable of interest to this study is the length of the mean vector (r). It shows the mean angle (μ) and its length. The length of the mean vector lies between 0 and 1. If r has a larger value then the results are more clustered around the mean vector. The circular standard deviation shows how 'spread' the data is around their average values. Therefore, it gives a good indication of the degree of variability within the samples. The Rayleigh test shows the concentration around the mean vector. It is calculated by $Z = n r^2$, where n is the number of observations and r is the length of the mean vector. A large Z value means a high concentration around the mean. In this situation it is less likely that the data is uniformly distributed and hence show evidence of preferred orientation (Fisher,1993). These are the main statistics that were used in this study.

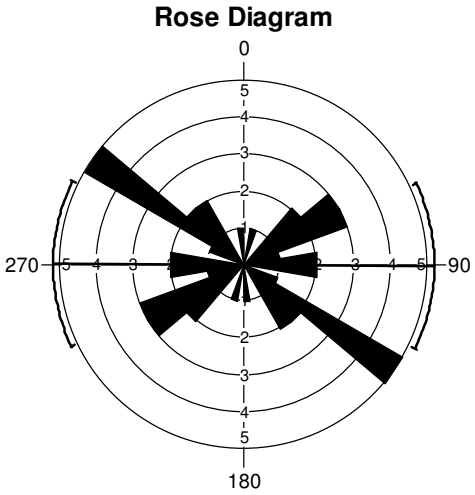

Basic Statistics

Data Type	Axial
Number of Observations	25
Mean Vector (μ)	90.29°
Length of Mean Vector (r)	0.302
Circular Standard Deviation	44.323°
Rayleigh Test (Z)	2.282

Figure 5.6 An example of a rose diagram produced with statistical computer programme Oriana. The wedges show the number of observations within a range. The diagram is bi-directional where the lines represent direction at both ends. The arc around the circle is the confidence arc, which is of 95% for this study. The circle represents the compass-directions where 0º or 360º is north. The programme also calculates some basic statistics of which the mean vector is one of the most important one.

5.3 RESULTS – MACROFABRICS

5.3.2 Wahianoa debris ridges

The results for the debris ridges of the Wahianoa Glacier are presented in the following pages. Tables 5.1 to 5.2 show the statistical data collected in this study. Figure 5.7 shows the declinations identified in each transect. These are presented as rose diagrams. The location of each transect is also shown in the same figure. The arcs around the circles are *95% confidence arcs*. The wedges are divided in 10º intervals of the entire circle. The size of the wedges shows the number of observations in each range.

Table 5.1 Basic statistics of the orientation of boulders on the eastern side (true left).

SAMPLE NUMBER	NUMBER OF OBSERVATIONS	MEAN VECTOR (μ)	LENGTH OF MEAN VECTOR (r)	CIRCULAR STANDARD DEVIATION	RAYLEIGH TEST (Z)
01b	20	97.65º	0.21	50.65º	0.88
02b	20	115.80º	0.22	50.16º	0.93
03b	17	179.34º	0.25	47.80º	1.05
04b	20	16.89º	0.31	43.98º	1.89
05b	20	19.67º	0.22	50.11º	0.94
06b	20	24.86º	0.24	48.61º	1.12
07b	20	80.60º	0.08	64.18º	0.13
08b	20	83.94º	0.43	37.04º	3.76
09b	22	105.10º	0.48	34.75º	5.05
10b	21	82.26º	0.40	38.94º	3.31
11b	20	100.43º	0.49	33.95º	4.91

Table 5.2 Basic statistics of the orientation of boulders on the western side (true right).

SAMPLE NUMBER	NUMBER OF OBSERVATIONS	MEAN VECTOR (μ)	LENGTH OF MEAN VECTOR (r)	CIRCULAR STANDARD DEVIATION	RAYLEIGH TEST (Z)
01a	20	79.13º	0.07	65.97º	0.10
02a	20	91.83º	0.26	46.86º	1.38
03a	20	0.50º	0.12	59.17º	0.28
04a	20	134.44º	0.29	44.98º	1.70
05a	20	122.12º	0.07	66.59º	0.09
07a	9	6.12º	0.35	41.55º	1.10
08a	19	146.17º	0.32	43.35º	1.92
09a	21	20.40º	0.35	41.73º	2.52
10a	20	174.03º	0.28	45.46º	1.61
11a	20	130.39º	0.04	71.27º	0.04

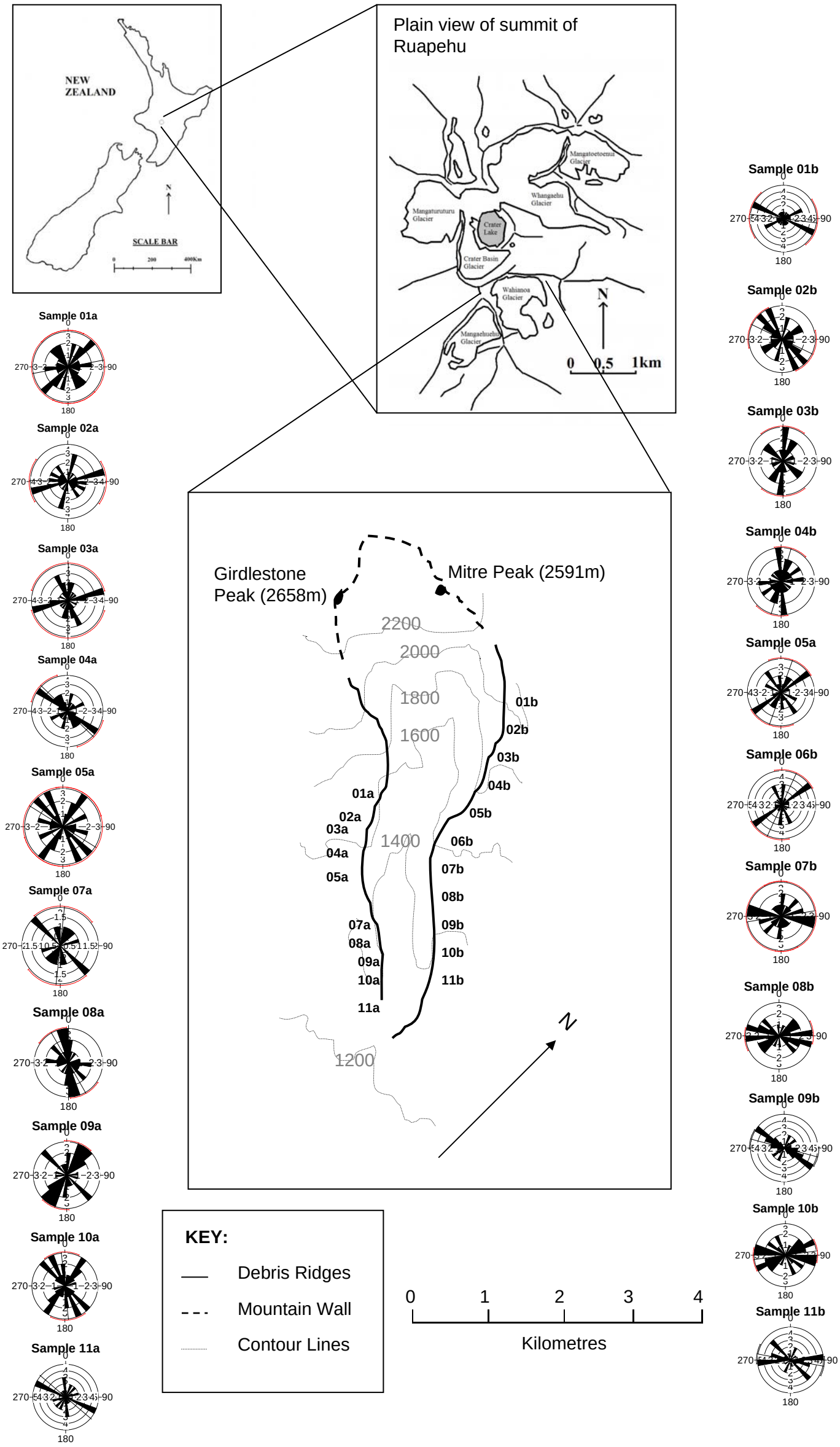

Figure 5.7 Macrofabrics results for the two debris ridges of the Wahianoa valley. The location of each transect is shown on the sketch map of the area.

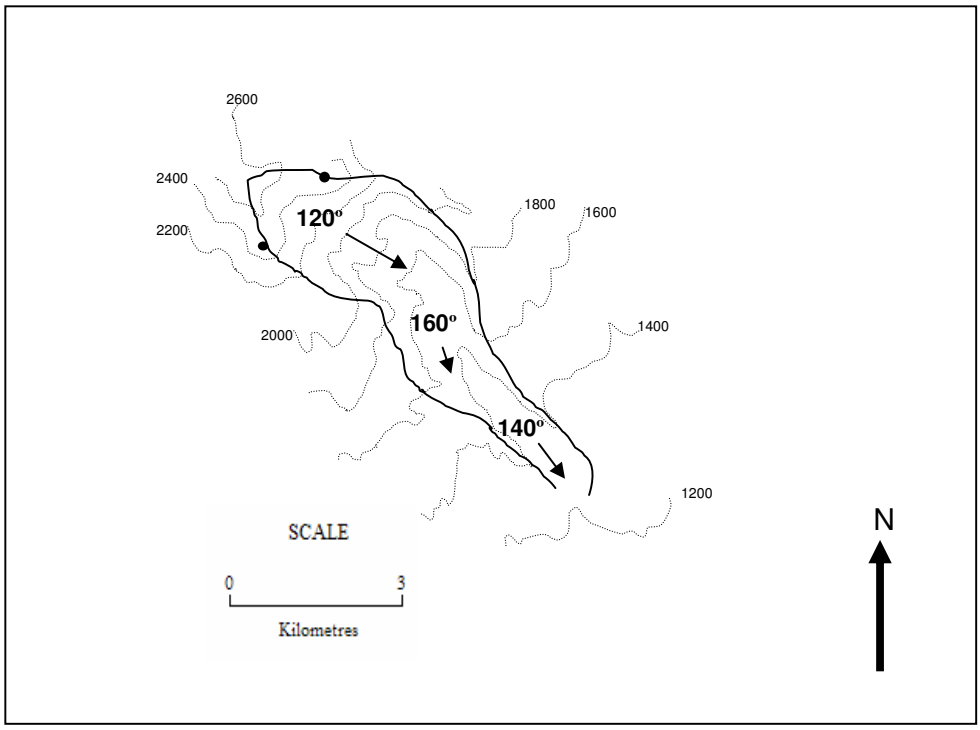

Figure 5.8 Sketch map of the Wahianoa Valley debris ridges showing the estimated directions within the valley. The ridges have a more eastward direction at the headwall than at the terminus and the centre is aligned in a more southward direction.

When looking at figure 5.7, it becomes apparent that the declinations do not follow an obvious pattern. However, the *mean directions* of the eastern ridge have an overall western/eastern trend (mean direction 149.23º/329.23º), whereas the boulders on the western ridge appear to be orientated more north/south and north-west/south-east (mean direction 81.93º/261.93º). The overall orientation of the debris ridges is in a south-east direction (~ 140º). Therefore, the net direction of the western ridge is similar to the net direction of the debris ridges. Figure 5.8 highlights that the ridges do not follow one direction only. At the glacier headwall, the ridges point more eastward than at the terminus. At the centre the ridges point more southwards. The configuration of the debris ridges should be the result of the direction of the ice movement. Figure 5.9 shows summarising diagrams of all the declinations and the mean directions of the western and eastern ridges.

Declinations of all samples from western moraine

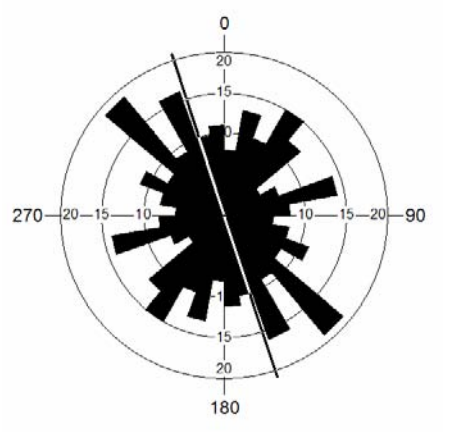

Number of observations	190
Mean vector (μ)	161.94°
Length of Mean Vector (r)	0.08
Circular Standard Deviation	64.25°
Rayleigh Test (Z)	1.24

Mean declination of the western moraine

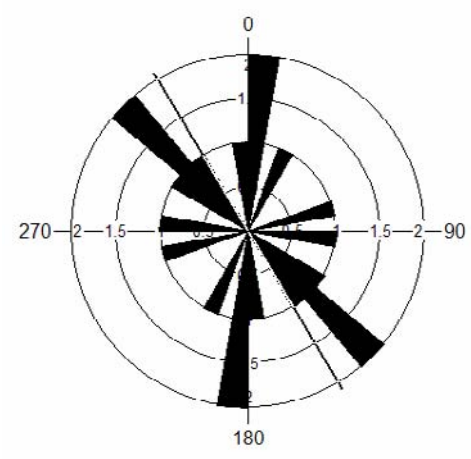

Number of Observations	10
Mean Vector (μ)	149.23°
Length of Mean Vector (r)	0.32
Circular Standard Deviation	43.267°
Rayleigh Test (Z)	1.022

Declinations of all samples from eastern moraine

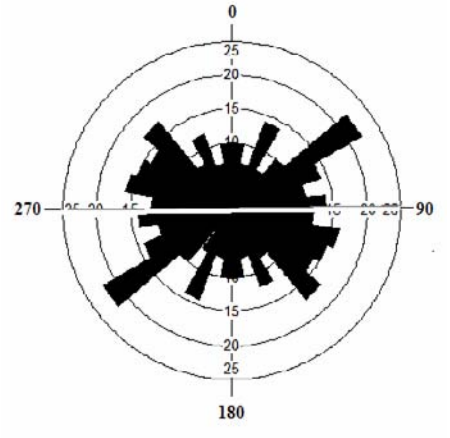

Number of observations	220
Mean Vector (μ)	88.99°
Length of Mean Vector (r)	0.12
Circular Standard Deviation	58.46°
Rayleigh Test (Z)	3.42

Mean declination of the eastern moraine

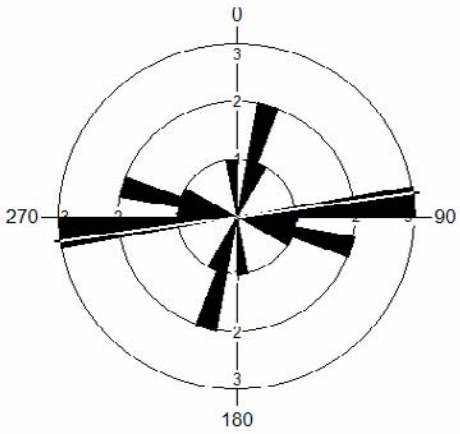

Number of Observations	11
Mean Vector (μ)	81.93°
Length of Mean Vector (r)	0.283
Circular Standard Deviation	45.549°
Rayleigh Test (Z)	0.878

Figure 5.9 Rose diagrams showing all declinations of the moraines and their mean orientation.

5.3.3 Small debris lobes-western ridge

Figure 5.10 shows the fabric data from two smaller lobes that run almost perpendicular to the western ridge. The statistical parameters of the lobes are presented in Table 5.3. Field measurements suggest that these particular lobes have an overall direction of about 170º to 180º. The mean direction of the four transects is 173º/353º. This is also similar to the direction of the centre part of the debris ridges (Fig. 5.8). There are a minimum of four lobes on the western ridge. It is likely that the lobes have formed due to overflowing ice. This could have been caused due to a difference in debris supply or due to topographical reasons. As Ruapehu was possibly covered by an ice cap rather than by individual alpine glaciers, the ice flow would have been more radial and not valley restricted.

Table 5.3 Basic statistics of the orientation of megaclasts of two small debris lobes on the western side.

SAMPLE NUMBER	NUMBER OF OBSERVATIONS	MEAN VECTOR (μ)	LENGTH OF MEAN VECTOR (r)	CIRCULAR STANDARD DEVIATION	RAYLEIGH TEST (Z)
1f	21	6.33º	0.21	50.27º	0.97
2f	21	14.30º	0.49	33.97º	5.15
3f	21	126.27º	0.57	30.33º	6.84
4f	21	171.24º	0.21	50.73º	0.91

5.3.4 Small debris lobe-eastern ridge

There is one small lobe at the distal end of the eastern ridge. Figure 5.10 shows the fabric data from clasts found on this lobe. Samples 1e, 2e and 4e have a mean direction of 154º/334º. Table 5.4 presents the statistical parameters. This deposit is likely to be a small push moraine that has formed during one of the last advances of the glacier and could therefore be one of the youngest deposit that has formed. It is interesting that these transects have a similar mean direction as the debris ridges. This is especially obvious in transects 4e and 3e, which are the most advanced areas of the ridge.

Table 5.4 Basic statistics of the orientation of megaclasts of a small debris lobe.

SAMPLE NUMBER	NUMBER OF OBSERVATIONS	MEAN VECTOR (μ)	LENGTH OF MEAN VECTOR (r)	CIRCULAR STANDARD DEVIATION	RAYLEIGH TEST (Z)
01e	20	0.91º	0.31	43.54º	1.98
03e	20	123.44º	0.48	34.70º	4.61
04e	21	156.71º	0.56	30.81º	6.61

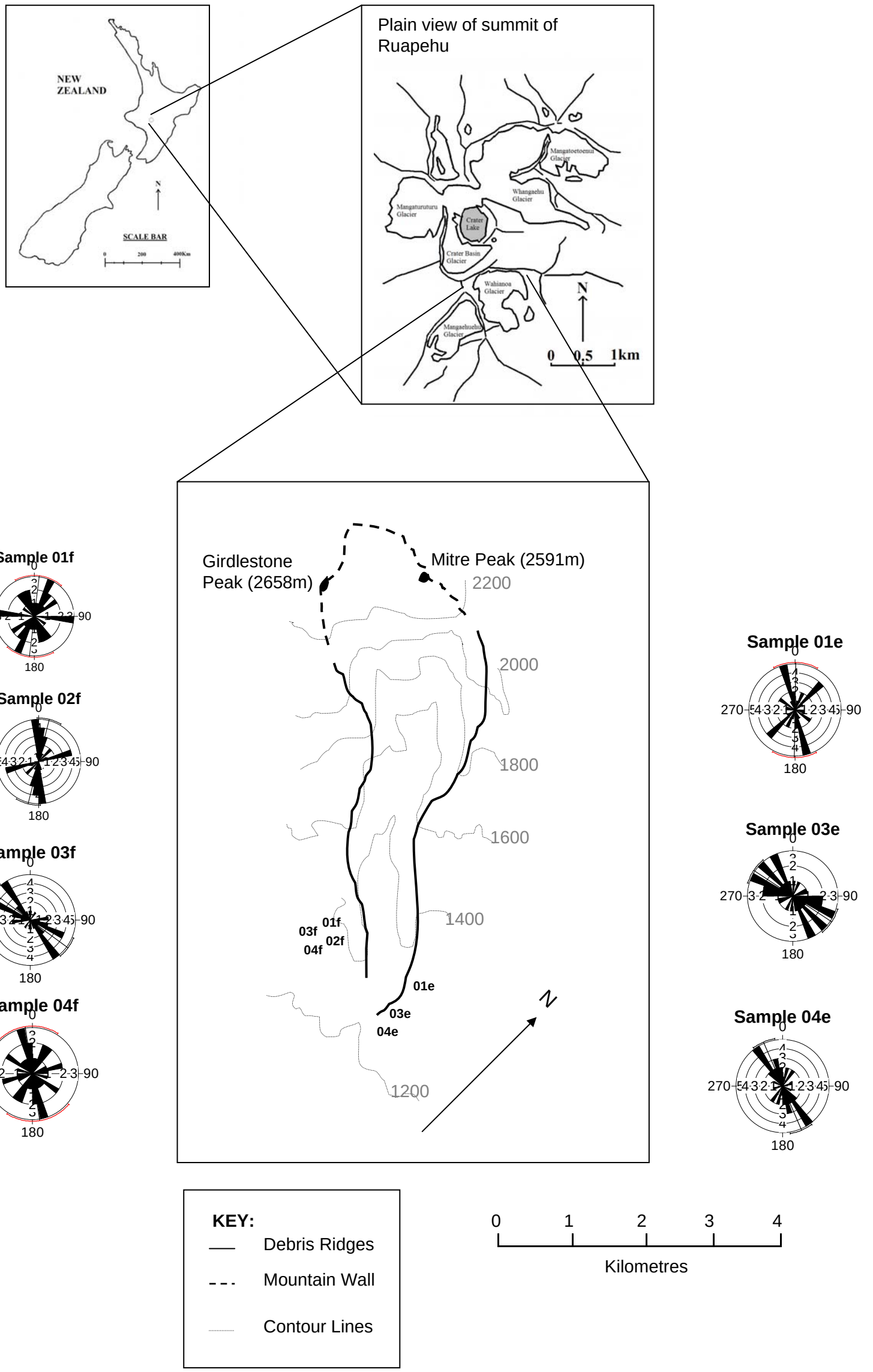

Figure 5.10 Macrofabric results for one of several smaller lobes that run nearly perpendicular from the western ridge (01f to 04f) and for one small lobe at the furthest extent of the eastern ridge (01e, 03e and 04e).

5.4 SUMMARY

Although the orientations of clasts in the Wahianoa Valley appear to be quite random, the mean directions have actually uncovered some patterns that show similarities to the orientations of the debris ridges. Nevertheless, the limited fabric analysis has identified a great complexity of the Wahianoa debris ridges and it appears that the glacier had several changes in dominant ice-flow direction. This may have been caused by different debris supplies and the topographic confinements at higher elevations. It would be desirable to complete a further analysis of the area that would produce eigenvectors and eigenvalues, as they display three-dimensional patterns of dip angles and clast orientation, together with fabric strength (Benn, 1994).

Chapter 6

GRAIN-SIZE DISTRIBUTION

6.1 INTRODUCTION

Erosion and weathering processes produce particles of different sizes (Boggs, 2001). Therefore, a study in grain-size distribution of a sedimentary deposit gives an insight in its geological history. In basic terms, the further a particle has been transported, the smaller it becomes. The study of the grain-size distribution of a sedimentary deposit can help to identify the processes that have produced the deposit. The sizes of particles range from microscopic scales to boulders of several meters in diameter. The size distribution of large particles can be identified readily by measuring the orthogonal axes (*a*-, *b*- and *c*-axes) with calipers or a ruler. To specify the mean diameter (*d*), the following equation is used $d = (a + b + c)/3$. To identify the size range of small particles, a sample is usually collected from the field and taken to the laboratory for analysis.

Depending on the type of sediment, different techniques can be applied (Table 6.1). Unconsolidated fine sediment is generally air-dried and sieved. The resulting statistical data provides information about the size distribution patterns of the sediments. Other techniques are based on the settling velocities of particles in a medium. To measure the concentration of silt and clay particles in a sample, different types of automated particle-size analysers can be used. These are based on various principles, such as changes in light intensities, light diffraction, X-ray beams and so on. This study of the grain-size distribution of sediments from the Wahianoa debris ridges used the dry sieving technique for the sizes 1mm to 0.06mm and X-ray beams for the finer fractions (up to 0.0002mm).

Table 6.1 Methods of measuring sediment grain-size (Boggs, 2001)

Type of sample	Sample grade	Method of analysis
Unconsolidated sediment and disaggregated sedimentary rock	Boulders Cobbles Pebbles	Manual measurement of individual clasts
	Granules Sand Silt Clay	Sieving, settling-tube analysis, image analysis
		Pipette analysis, sedimentation balances, photothydrometer, Sedigraph, laser-diffractometer, electro-resistance (e.g., Coulter counter)
Lithified sedimentary rock	Boulders Cobbles Pebbles	Manual measurement of individual clast
	Granules Sand Silt Clay	Thin-section measurement, image analysis
		Electron microscope

6.1.2 The phi scale

Because particles in sedimentary deposits generally have a size range from a few microns to a few meters, data is often presented on a logarithmic scale (Boggs, 2001; Evans & Benn, 2004). The universally used grain-size scale is the Udden-Wentworth scale (Boggs, 2001). The scale converts particle sizes to a logarithmic scale. The *phi* (Ø) *scale* (Krumbein, 1938) is the most commonly used transformation scale:

$$Ø = -\log_2 d$$

where Ø is the phi size and d is the grain diameter. For example, a grain with a diameter of 2mm has a phi size of -1. This is the power required to raise the base of the logarithm to 2 (Boggs, 2001; Evans & Benn, 2004). Table 6.2 shows the phi scale and the qualitative descriptions of the of the particle sizes that were used in this study. The phi scale was first proposed by Udden in 1898 and modified by Wentworth in 1922.

Table 6.2 Particle size conversion table and nomenclature (after Wentworth, 1922)

Micro metres	Phi	Particle size category	Particle size sub-category
707-500	0.5-1	Sand	Coarse sand
354-250	1.5-2	Sand	Medium sand
177-125	2.5-3	Sand	Fine sand
88.4-62.5	3.5-4	Sand	Very fine sand
44.2-31.3	4.5-5	Silt	Coarse silt
22.1-15.6	5.5-6	Silt	Medium silt
11.0-7.81	6.5-7	Silt	Fine silt
5.52-3.91	7.5-8	Silt	Very fine silt
2.76-1.95	8.5-9	Clay	Coarse clay
1.38-0.98	9.5-10	Clay	Medium clay
0.69-0.49	10.5-11	Clay	Fine clay

6.1.3 Statistical measures used in grain-size analyses

The data of grain-size distributions are generally presented in a line graph or frequency curve. This provides a good visual presentation of the distribution of a grain population. Statistical terms are often used to qualitatively describe the grain-size distribution of a sample (Boggs, 2001). As it is impossible to count each individual grain of a population, average values for the main fractions are used (Folk & Ward, 1957). The *mean* measures the central tendencies of a population. *Sorting* measures the range of grain sizes that are present in a grain population and the magnitude of the spread of these sizes around the mean (Boggs, 2001). The mathematical expression of sorting is the standard deviation of a grain population.

The *skewness* of a statistical population is a measure of asymmetry. A normal distribution is expressed in a typical bell-shaped frequency curve. In this type of curve the skewness is said to be symmetrical. However, most particle size populations are normally distributed and form an asymmetry or skew. A positively skewed curve is one that skews right. This type of skew is also called *fine* skewed, as it has a ‘fine particle tail’. A negatively skewed curve skews left and is called *coarsely* skewed, which has a ‘coarse particle tail’.

The *kurtosis* is an indication of the peakedness of a curve. Leptokurtic and platykurtic are the two extremes of kurtosis. Leptokurtic refers to strong peakedness in a frequency curve.

Platykurtic represents a gentler peak. Mesokurtic is a degree of kurtosis that falls in between leptokurtic and platykurtic.

6.1.4 Previous studies

The study of grain-size distributions has been widely used. As particle size reflects transport energy, it is an important indicator of the environment of deposition (Landim & Frakes, 1968). The work done by Folk and Ward (1957) has been one of the most influential investigations done so far. At the time of the investigation grain size and sorting of sediments was poorly understood. Folk and Ward (1957) studied the Brazos River Bar (Texas) to identify certain particle size parameters. The further aim was to study how size fractions behave with transport. Statistical measures were modified from earlier work (e.g. Inman, 1952). The true values for mean, sorting, skewness and kurtosis cannot be calculated in grain populations as it is impossible to know the exact number of grains, especially finer grains. Therefore, certain percentiles have to be chosen to identify average values. Folk and Ward (1957) have found values that are still being used in current research (e.g. Mills & Grab, 2005).

Greenwood (1969) used size-frequency statistics to differentiate between marine-lain and aeolian sands. In his study, Greenwood states that sediment parameters must be quantitative, must discriminate between environments, be constant through time and should preferably be universal (Greenwood, 1969). He attempted various analyses to identify the most satisfying method that helps with the distinction between environments. Greenwood identified that the most important measures are skewness, the mean, the standard deviation and kurtosis. Variations within these measures are indicative for different environments. However, the study of grain-size distributions should always be used in conjunction with other parameters.

Landim and Frakes (1968) tested the efficiency of using statistical parameters to differentiate between different depositional environments. The study followed the methods developed by Folk and Ward (1957). Landim and Frakes (1968) analysed samples from alluvial fan, till and outwash deposits. This investigation was literature based only. No

samples were collected from the field directly, as the aim was to test the validity of using statistical parameters. The method has shown some positive results. It was concluded that it is more useful to use standard deviation, mean and skewness to differentiate between till and alluvial fan deposits. For distinguishing between till and outwash deposits, kurtosis, mean and standard deviation are more appropriate. Landim and Frakes (1968) also suggested that the use of statistical parameters in grain-size analyses could be used for unknown deposits.

Haldorsen (1981) tried to link grain size composition of tills to the processes that produce the sediments. Haldorsen simulated different erosion processes with a ball mill and identified that most sand fractions form due to crushing and silt fractions due to abrasion. However, Hoey (2004) argues that it is now widely accepted that particle size can rarely be related directly to processes and that other evidence needs to be included. Therefore, this study uses grain-size distribution in conjunction with clast morphology, macrofabrics and Scanning Electron Microscope analysis of microtextures on individual grains, rather than relying on one criterion alone.

Many grain distributions are bimodal or multimodal. This makes it even more difficult to relate grain size to processes (Sharp *et al.* 1994). Figure 6.1a shows a multi-modal grain-size distribution. Figure 6.1b shows scatter diagrams where standard deviations and fraction are plotted against mean grain size. The samples were collected from basal ice from Variegated Glacier, Alaska. Individual modes were identified in the distributions, which were then interpreted with reference to known sub-glacial processes.

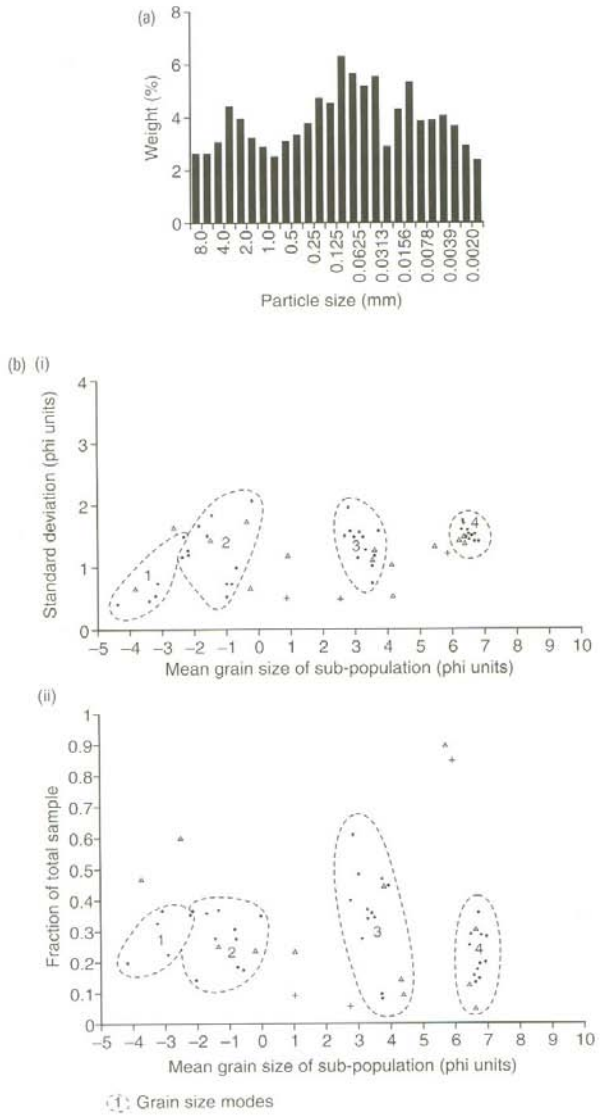

Figure 6.1 (a) A histogram of a multi-modal distribution. The sediments were collected from a basal till sample (Benn and Gemmell, 2002). (b) Standard deviation and fraction of total sample in a given mode as a function of mean grain size of each sub-population in basal ice samples from Variegated Glacier, Alaska (Sharp *et al.* 1994).

Boulton (1978) studied the processes that occur during glacial transport and what affect these have on glacigenic sediments. Boulton concluded that supraglacial and englacial debris is transported in a more passive way and is not exposed to traction and shear stresses. Therefore, supraglacial and englacial debris generally consist of coarser grain-size fractions and angular clasts. In contrast, subglacial debris is transported in the basal zone,

where clasts are more exposed to traction and shear stresses. Subglacial debris typically consists of finer size fractions and more rounded clasts (Boulton, 1978).

Mills and Grab (2005) used various diagnostic criteria to interpret periglacial and glacial landforms in southern Africa and particle size was one of those criteria. Three trenches were dug into ridges of unconsolidated diamictons. Mills and Grab (2005) used statistical parameters to interpret the distribution of grain size. They identified that the results from the trenches vary greatly from samples found *in situ* away from the trenches. The statistics were calculated by using the Folk and Ward method (1957). This study is very valuable as it provides evidence from more than one diagnostic criterion, which are macrofabrics and clast morphology.

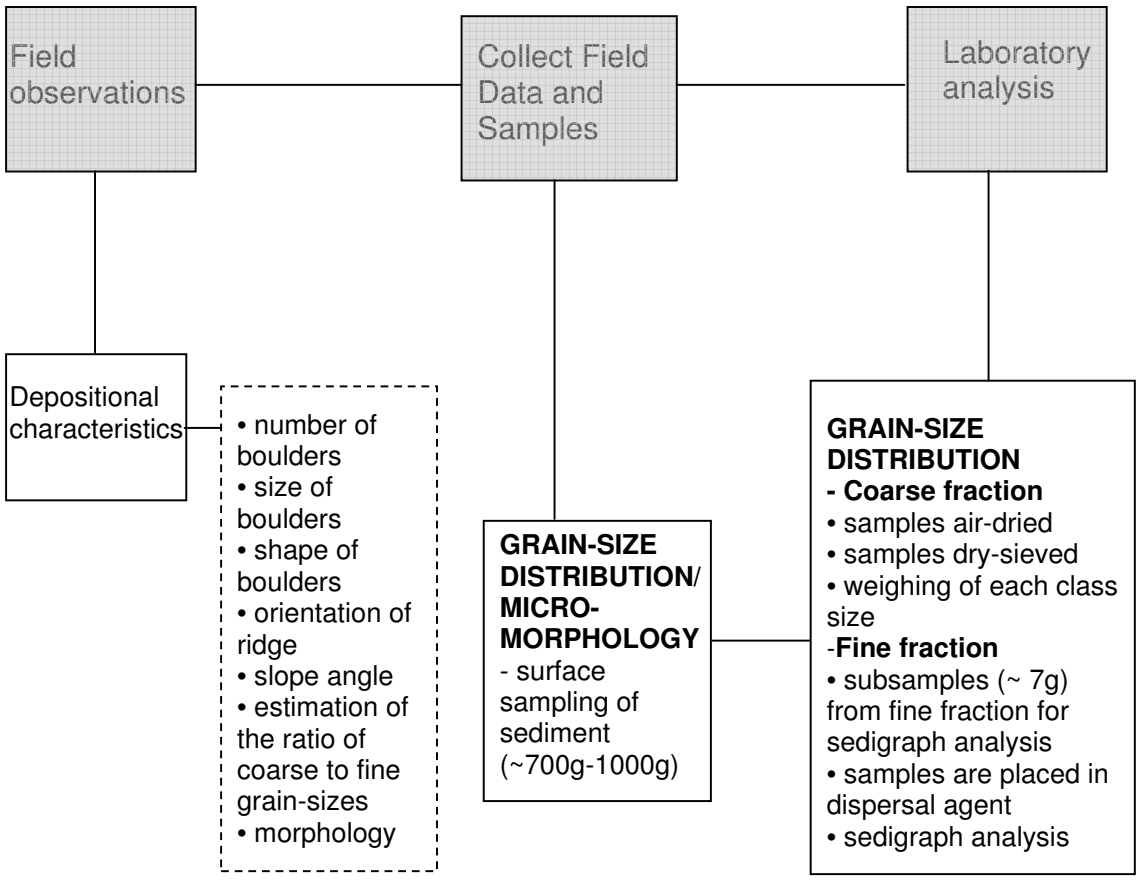

Figure 6.2 Flow diagram illustrating the field procedures and laboratory techniques used to identify the grain-size distribution of the Wahianoa valley.

6.2 METHODOLOGY

6.2.2 Sample collection

Figure 6.2 illustrates the method used in this analysis. Ten till samples for the study of the grain-size distribution were collected from each of the two lateral ridges. Figure 6.3 shows the locations of transects. The same transects that were used for the previous methods (chapters 4 and 5) have been used. In addition, some further samples were taken from outcrops at the base of the ridges. The majority of data for this project was collected from the crest and the slopes of the debris ridges in shallow pits. The purpose of this part of the study is to collect information about sediment source, transport and depositional processes. In each transect a small hole was dug about 5 to 10cm deep to expose 'clean' sediment. This was done to avoid the contamination from weathered surface material. The sediments were placed into small, clean labeled plastic bags (15 x 20cm) and taken to the laboratory.

6.2.3 Sample preparation

Each sample had a weight of about 500 to 700g each. The samples were air-dried for several days in an oven and then sieved with an automatic sieve shaker (Fig. 6.4). The sediments were sieved at half-phi intervals from 0.5 Ø to > 4 Ø. The finer fractions were further analysed with a sedigraph (Micromeritics Sedigraph 5100). After the sieving process, each sample was weighed.

Western debris ridge (01a-11a) and base sample (01c) - circle

Outcrop on western ridge (02c-1 – 02c-16))

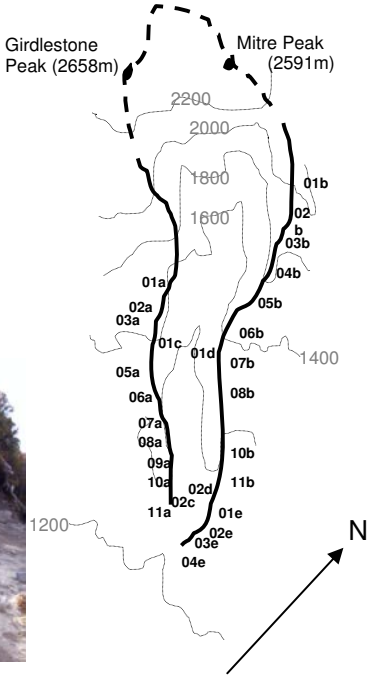

Eastern debris ridge (01b-11b) and base sample (01d) - circle

Outcrop on eastern ridge - circle (02d-1 – 02d-7)

Small lobe at the end of the main eastern ridge - circle (01e-03a)

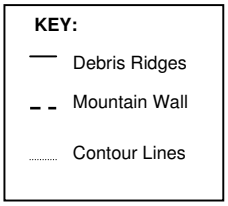

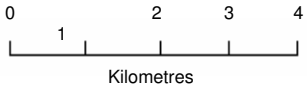

Figure 6.3 Locations of transects used in this research. (A) Transects 01a to 011a are located along the western ridge. Transect 01c is also shown (circled area). (B) Transects 01b to 011b are found along the eastern ridge. Transect 01d is shown in the circled area. (C) Outcrop at the base of the western ridge (samples 02c-1 to 02c-16). Picture shows layered tephra deposits. (D) Outcrop at the base of the eastern ridge (samples 02d-1 to 02d-7). (E) Transects 01e to 03e were collected from a small lobe at the furthest extent of the eastern ridge (circled area).

Figure 6.4 A sieve shaker (EFL 2 mk3). The sediments were air dried and sieved at half-phi intervals from 0.5 Ø to > 4 Ø.

For the sedigraph analysis, a sub-sample was taken from the fine fraction (> 4 Ø) of each sample. To ensure that the sub-sample represents the entire population, the sediment was split until the desired amount (c.7g) was achieved. The samples were placed into a dispersal agent (10% sodiumpyrophoshate) and vigorously stirred with an automatic magnetic stirrer over night. This was done to ensure that the sediment was sufficiently dispersed for the sedigraph analysis. Each of the homogeneous suspensions was then placed into a small column of the sedigraph. A sedigraph measures the concentration of the sediment at different depths in the column with the help of a finely collimated x-ray beam (Boggs, 2001; Evans & Benn, 2004). The sedigraph analysis measured the concentrations of the particle diameters 62.50μm to 0.18 μm (4 Ø to 11 Ø).

6.2.4 Analysing sedimentary data

The grain-size distribution is generally presented in a histogram, a ternary plot or a line graph. A histogram is used to show the percentage of the retained sieve size versus the sediment size. A ternary plot shows the percentages or the ratios of the sand, silt and clay fractions. To present the trend of a particle population, a line graph or frequency curve is used. In this case the cumulative percentage of the weight retained is drawn against the sediment size. Most sediment populations produce a typical skew (Hoey, 2004), which means that there is a large number of one particular data range present.

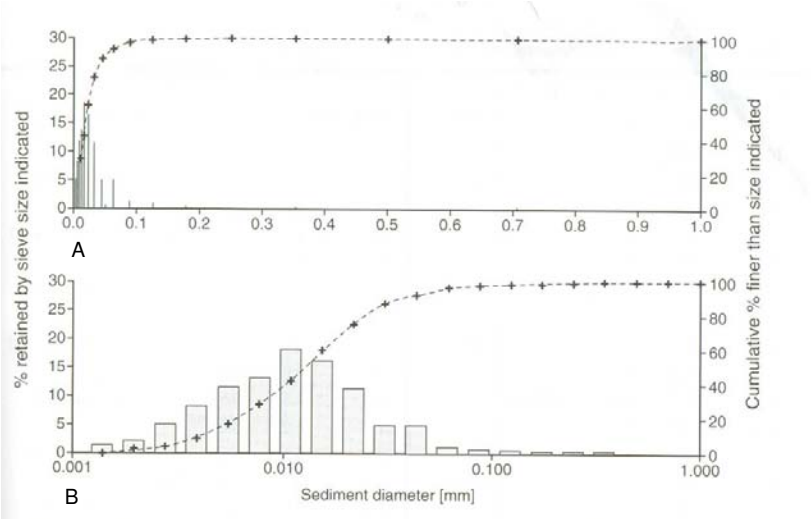

Figure 6.5 Graph (A) shows the grain-size distribution from a sediment sample from the Soler Glacier, Chile (Glasser & Hambrey, 2002). It uses an arithmetic scale (x-axis). The sizes range from fine to coarse on the x-axis. Graph (B) shows the same data but drawn on a logarithmic x-axis.

Because of the large range of particles, a logarithmic or geometric scale is generally used. Figure 6.5 shows the grain-size distribution for 'Sand subfacies 1', which was sampled by Glasser and Hambrey (2002) from the Soler Glacier in Chile. The upper graph (A) shows the data plotted on an arithmetic x-axis, whereas the lower graph (B) is plotted on a logarithmic x-axis. The logarithmic scale provides more detail as there is a high concentration of fine sediments (positive skewness).

This study describes the proportion of grains in particular size classes of each sediment sample and its statistical descriptions. The statistics were calculated with the GRADISTAT Programme (Version 4.0) that can be used in Excel (Blott & Pye, 2001). The GRADISTAT is a very efficient programme and gives the researcher numerous options for calculations and presentations. This research followed the calculations and qualitative descriptions that were developed by Folk and Ward (1957). Table 6.3 shows the statistical formulae and the qualitative descriptions of standard deviation (sorting), skewness and kurtosis. $Ø_{nn}$ is the phi size for which $_{nn}$% of the distribution is coarser (Hoey, 2004).

Table 6.3 Statistical formulae used in the calculation of grain size parameters by GRADISTAT. Logarithmic (original) Folk and Ward (1957) graphical measures (in phi).

Mean	Standard Deviation	Skewness	Kurtosis
$M_Z = \frac{\phi_{16} + \phi_{50} + \phi_{84}}{3}$	$\sigma_I = \frac{\phi_{84} - \phi_{16}}{4} + \frac{\phi_{95} - \phi_5}{6.6}$	$Sk_I = \frac{\phi_{16} + \phi_{84} - 2\phi_{50}}{2(\phi_{84} - \phi_{16})} + \frac{\phi_5 + \phi_{95} - 2\phi_{50}}{2(\phi_{95} - \phi_5)}$	$K_G = \frac{\phi_{95} - \phi_5}{2.44(\phi_{75} - \phi_{25})}$

Sorting (σ_I)		Skewness (Sk_I)		Kurtosis (K_G)	
Very well sorted	< 0.35	Very fine skewed	$^{+}$0.3 to $^{+}$1.0	Very platykurtic	< 0.67
Well sorted	0.35 – 0.50	Fine skewed	$^{+}$0.1 to $^{+}$0.3	Platykurtic	0.67 – 0.90
Moderately well sorted	0.50 – 0.70	Symmetrical	$^{+}$0.1 to $^{-}$0.1	Mesokurtic	0.90 – 1.11
Moderately sorted	0.70 – 1.00	Coarse skewed	$^{-}$0.1 to $^{-}$0.3	Leptokurtic	1.11 – 1.50
Poorly sorted	1.00 – 2.00	Very coarse skewed	$^{-}$0.3 to $^{-}$1.0	Very leptokurtic	1.50 – 3.00
Very poorly sorted	2.00 – 4.00			Extremely leptokurtic	> 3.00
Extremely poorly sorted	> 4.00				

6.3 RESULTS – GRAIN-SIZE DISTRIBUTION

The results for the grain-size distribution of the Wahianoa Valley debris ridges are firstly presented in line graphs that show the cumulative percentages of the weight retained of each class size versus the particle size (phi). The individual weight percentage of each size class is drawn in a histogram. The sample numbers refer to the same numbers as in the previous sections of this study (Fig. 6.3). The particle size sub-categories are included in the cumulative curves. The statistical parameters of each sample are presented in tables 6.4 to 6.7.

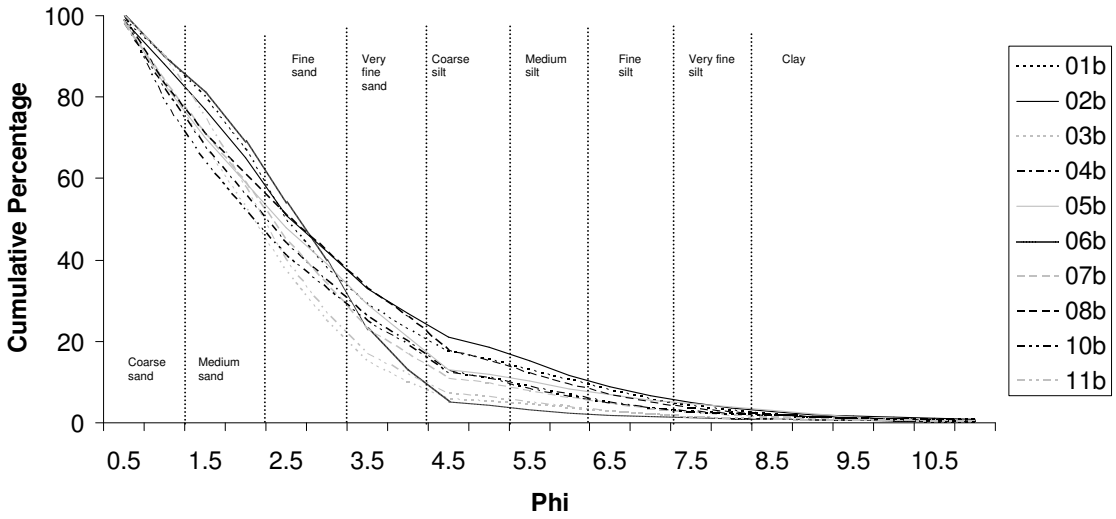

Figure 6.6 Cumulative curve of the eastern ridge. Transect 01b is located closest to the glacier and transect 11b at distal end. Between 75 and 90% of all grain populations is of sand size.

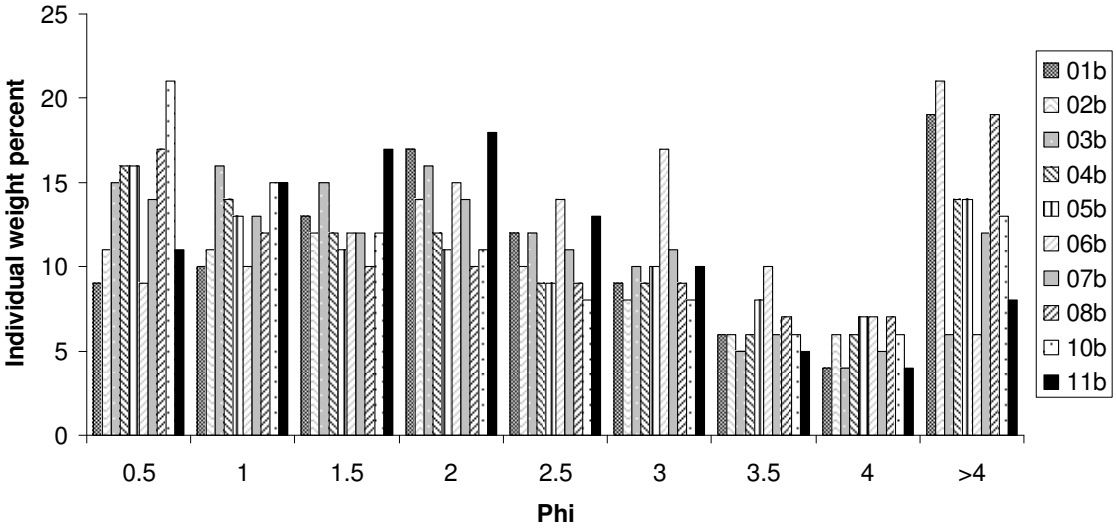

Figure 6.7 Histogram that shows the individual weight percent of the samples from the eastern ridge. A greater proportion of all samples is concentrated between coarse and fine sand.

Table 6.4 Table showing the statistic and qualitative descriptions for the samples of the eastern ridge.

	02b	01b	03b	04b	05b	06b	07b	08b	10b	11b
SAMPLE TYPE	Unimodal, poorly sorted	Unimodal, poorly sorted	Unimodal, poorly sorted	Unimodal, poorly sorted	Bimodal, poorly sorted	Bimodal, poorly sorted	Bimodal, poorly sorted	Unimodal, poorly sorted	Unimodal, poorly sorted	Unimodal, poorly sorted
TEXTURAL GROUP	Muddy sand	Muddy sand	Sand	Sand	Sand	Sand	Sand	Muddy sand	Sand	Sand
SEDIMENTS NAME	Coarse silt, medium sand	Coarse silt, medium sand	Poorly sorted, coarse sand	Poorly sorted, coarse sand	Poorly sorted, coarse sand	Poorly sorted, fine sand	Poorly sorted, coarse sand	Coarse silt, coarse sand	Poorly sorted, coarse sand	Poorly sorted, medium sand
MEAN	2.07	2.02	1.63	1.81	1.88	2.03	1.81	1.96	1.68	1.72
MEAN-VERBAL DESCRIPTION	Fine sand	Fine sand	Medium sand	Medium sand	Medium sand	Fine sand	Medium sand	Medium sand	Medium sand	Medium sand
SORTING	1.68	1.57	1.12	1.49	1.58	1.13	1.38	1.70	1.49	1.10
SORTING-VERBAL DESCRIPTION	Poorly sorted	Poorly sorted	Poorly sorted	Poorly sorted	Poorly sorted	Poorly sorted	Poorly sorted	Poorly sorted	Poorly sorted	Poorly sorted
SKEWNESS	0.32	0.31	0.16	0.29	0.26	-0.04	0.21	0.28	0.36	0.15
SKEWNESS-VERBAL DESCRIPTION	Very fine skewed	Very fine skewed	Fine skewed	Fine skewed	Fine skewed	Symmetrical	Fine skewed	Fine skewed	Very fine skewed	Fine skewed
KURTOSIS	1.22	1.45	0.91	1.02	1.04	0.89	1.05	1.04	0.98	1.00
KURTOSIS-VERBAL DESCRIPTION	Leptokurtic	Leptokurtic	Mesokurtic	Mesokurtic	Mesokurtic	Platykurtic	Mesokurtic	Mesokurtic	Mesokurtic	Mesokurtic

Table 6.5 Table showing the statistic and qualitative descriptions for the samples of the western ridge.

	01a	02a	03a	05a	06a	07a	08a	09a	10a	11a
SAMPLE TYPE	Trimodal, poorly sorted	Polymodal, poorly sorted	Bimodal, poorly sorted	Unimodal, poorly sorted	Unimodal, poorly sorted	Unimodal, poorly sorted	Unimodal, poorly sorted	Unimodal, poorly sorted	Bimodal, poorly sorted	Unimodal, poorly sorted
TEXTURAL GROUP	Muddy sand	Muddy sand	Muddy sand	Sand	Muddy sand	Sand	Sand	Sand	Muddy sand	Sand
SEDIMENTS NAME	Coarse silt, coarse sand	Coarse silt, coarse sand	Coarse silt, medium sand	Poorly sorted, medium sand	Coarse silt, medium sand	Poorly sorted, medium sand	Poorly sorted, coarse sand	Poorly sorted, medium sand	Medium silt, coarse sand	Poorly sorted, medium sand
MEAN	2.48	2..36	1.93	1.87	2.09	1.80	1.74	1.88	2.05	2.18
MEAN-VERBAL DESCRIPTION	Fine sand	Fine sand	Medium sand	Medium sand	Fine sand	Medium sand	Medium sand	Medium sand	Fine sand	Fine sand
SORTING	1.95	1.97	1.56	1.46	1.70	1.08	1.69	1.29	1.79	1.41
SORTING-VERBAL DESCRIPTION	Poorly sorted	Poorly sorted	Poorly sorted	Poorly sorted	Poorly sorted	Poorly sorted	Poorly sorted	Poorly sorted	Poorly sorted	Poorly sorted
SKEWNESS	0.30	0.32	0.25	0.32	0.28	0.08	0.40	0.24	0.30	0.16
SKEWNESS-VERBAL DESCRIPTION	Fine skewed	Very fine skewed	Fine skewed	Very fine skewed	Fine skewed	Symmetrical	Very fine skewed	Fine skewed	Fine skewed	Fine skewed
KURTOSIS	1.05	1.14	1.20	1.40	1.27	1.00	1.35	1.36	1.38	1.22
KURTOSIS-VERBAL DESCRIPTION	Mesokurtic	Leptokurtic	Leptokurtic	Leptokurtic	Leptokurtic	Mesokurtic	Leptokurtic	Leptokurtic	Leptokurtic	Leptokurtic

6.3.2 The results for the eastern ridge (samples 01b - 011b)

Figures 6.6 and 6.7 show the results for the eastern ridge of the Wahianoa valley. Table 6.4 presents the statistical information. The samples are derived from 10 transects along the ridge and show a great similarity in the grain-size distribution. Figure 6.6 shows that the majority of the samples from that ridge deposit are of sand size. Less than 25% of all samples consist of particles that are finer than silt. Coarse to fine sand shows the greatest concentration. Figure 6.7 shows the individual weight percentages for the coarser size classes (0.5 to >4 phi) of all collected samples. As all samples show great similarities, it can be assumed that similar processes and lithologies have lead to this deposit.

6.3.3 The results from the western ridge (samples 01a - 011a)

The following two figures (Fig. 6.8 and 6.9) and table 6.5 show the results for the western ridge. The line graph shows a small difference in the upper and lower parts of the deposits. The samples closest to the glacier contain a slightly larger portion of fines than the eastern ridge. The lower part of the ridge appears to be more heterogeneous than the others, as the individual percentages within each size class vary. However, the overall trend in the grain-size distribution of both ridges is very similar.

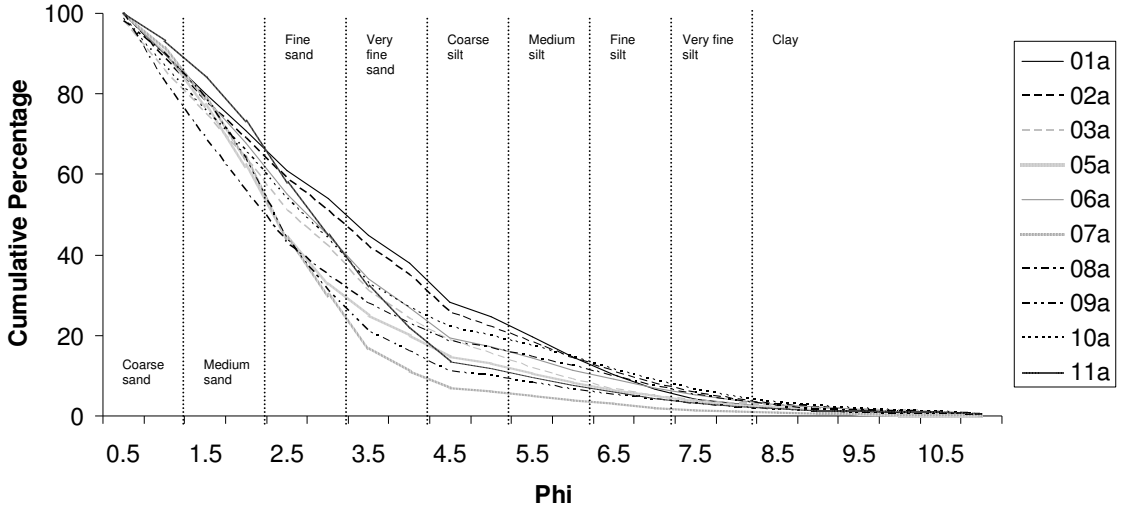

Figure 6.8 Cumulative curve showing the results for the western ridge. Sample 01a is located closest to the glacier and sample 11a is at the distal end.

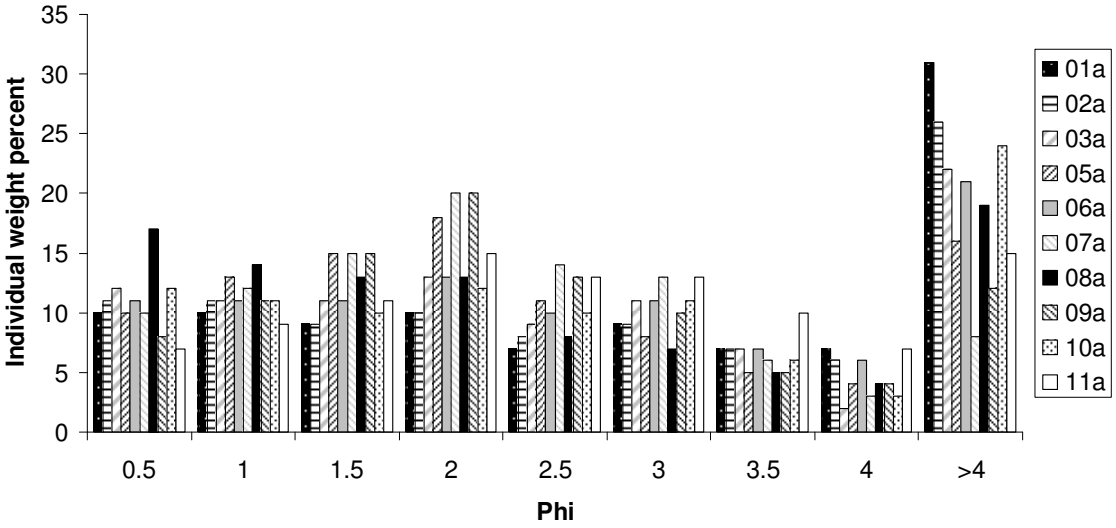

Figure 6.9 Histogram that shows the results for the western ridge. Samples from the distal end (07a to 11a) show some greater variations in size than the remaining samples. The weight percentages of the fine fraction (>4 phi) varies substantially.

6.3.4 The results for two samples (01c and 01d) from the base close to the glacier

Some further samples were collected from the base of the ridges close to the glacier. Figures 6.10 and 6.11 show the results of these two grain populations. Tables 6.6 presents the statistical information. The overall trend of the cumulative curve is similar to the ones from the samples of the main ridges. Both samples are of medium to fine sand. The finer fractions are coarse to fine silt. Although the samples were collected from both ridges, the samples are very similar. Therefore, the lithologies and processes that have led to the deposits must have been very alike.

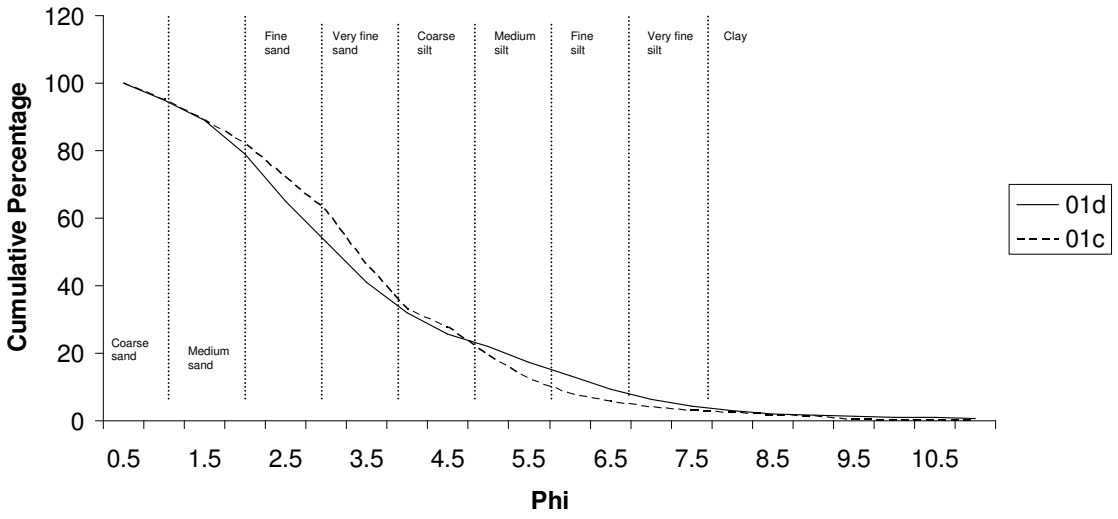

Figure 6.10 Cumulative curve showing the results of two samples that were collected from the base of the upper part of the ridges. Sample 01d represents the population from the eastern ridge and 01c from the western ridge. There is not much difference within the two samples. Both are of sand size.

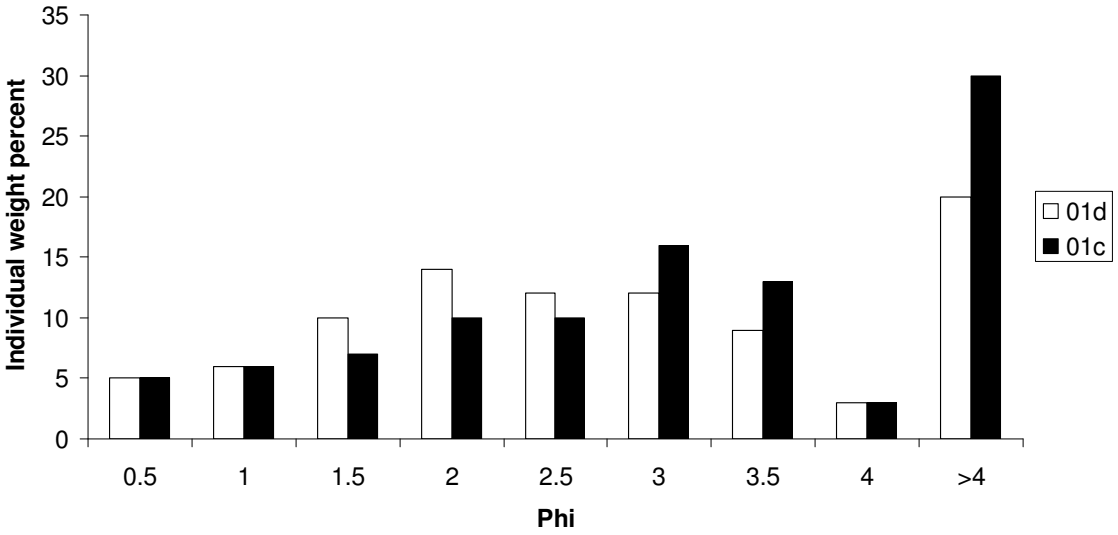

Figure 6.11 Histogram showing the results of two samples that were collected from the base of the upper part of the ridges. The results show great similarities. Although the sample from the western ridge is slightly finer than the sample from the eastern ridge.

Table 6.6 Table showing the statistic and qualitative descriptions for the cutting section of the eastern ridge.

	01d	01c	02d-1	02d-2a	02d-2b	02d-3	02d-4	02d-5	02d-7
SAMPLE TYPE	Bimodal, poorly sorted	Bimodal, poorly sorted	Unimodal, poorly sorted	Unimodal, moderately sorted	Bimodal, poorly sorted	Trimodal, very poorly sorted	Bimodal, poorly sorted	Bimodal, poorly sorted	Bimodal, very poorly sorted
TEXTURAL GROUP	Muddy sand	Muddy sand	Sand	Sand	Muddy sand	Muddy sand	Muddy sand	Sand	Muddy sand
SEDIMENTS NAME	Coarse silt, medium sand	Very coarse silt, fine sand	Poorly sorted, fine sand	Moderately sorted, fine sand	Very coarse sand, fine sand	Coarse silt, very fine sand	Coarse silt, fine sand	Poorly sorted, coarse sand	Coarse silt, fine sand
MEAN	2.50	2.77	2.55	2.28	3.08	4.66	2.88	1.68	3.44
MEAN-VERBAL DESCRIPTION	Fine sand	Fine sand	Fine sand	Fine sand	Very fine sand	Very coarse silt	Fine sand	Medium sand	Very fine sand
SORTING	1.66	1.64	1.20	0.83	1.58	2.28	1.26	1.48	2.08
SORTING-VERBAL DESCRIPTION	Poorly sorted	Poorly sorted	Poorly sorted	Moderately sorted	Poorly sorted	Very poorly sorted	Poorly sorted	Poorly sorted	Very poorly sorted
SKEWNESS	0.30	0.15	0.12	0.17	0.38	0.49	0.16	0.33	0.32
SKEWNESS-VERBAL DESCRIPTION	Fine skewed	Fine skewed	Fine skewed	Fine skewed	Very fine skewed	Very fine skewed	Fine skewed	Very fine skewed	Very fine skewed
KURTOSIS	1.43	1.31	1.32	1.02	1.55	0.88	1.40	1.08	1.09
KURTOSIS-VERBAL DESCRIPTION	Leptokurtic	Leptokurtic	Leptokurtic	Mesokurtic	Very leptokurtic	Platykurtic	Leptokurtic	Mesokurtic	Mesokurtic

Table 6.7 Table showing the statistic and qualitative descriptions for the outcrop samples of the western ridge and for the samples of the small lobe at the maximum extent of the eastern ridge.

	02c-1	02c-8	02c-16	01e	02e	03e
SAMPLE TYPE	Unimodal, moderately sorted	Unimodal, moderately sorted	Unimodal, poorly sorted	Unimodal, poorly sorted	Unimodal, poorly sorted	Unimodal, poorly sorted
TEXTURAL GROUP	Sand	Sand	Sand	Sand	Sand	Muddy sand
SEDIMENTS NAME	Moderately sorted, fine sand	Poorly sorted, medium sand	Poorly sorted, coarse sand	Poorly sorted, coarse sand	Poorly sorted, medium sand	Coarse silt, medium sand
MEAN	2.89	1.92	1.20	1.80	1.75	2.16
MEAN-VERBAL DESCRIPTION	Fine sand	Medium sand	Medium sand	Medium sand	Medium sand	Fine sand
SORTING	0.90	1.13	1.34	1.59	1.45	1.62
SORTING-VERBAL DESCRIPTION	Moderately sorted	Poorly sorted	Poorly sorted	Poorly sorted	Poorly sorted	Poorly sorted
SKEWNESS	0.16	0.05	0.56	0.33	0.25	0.24
SKEWNESS-VERBAL DESCRIPTION	Fine skewed	Symmetrical	Very fine skewed	Very fine skewed	Fine skewed	Fine skewed
KURTOSIS	1.63	0.96	1.52	1.33	1.25	1.20
KURTOSIS-VERBAL DESCRIPTION	Very leptokurtic	Mesokurtic	Very leptokurtic	Leptokurtic	Leptokurtic	Leptokurtic

6.3.5 The results from two outcrops from each ridge (samples 02d-1 – 02d-7 eastern ridge and samples 02c-1 – 02c-16 western ridge)

Figures 6.12 to 6.15 and tables 6.6 to 6.7 show the results of two cutting sections that were collected from the eastern and western ridges. The samples from the eastern ridge (02d-1 to 02d-7) were collected just above the river bed (Wahianoa River). The outcrop has become visible due to a small stream that flows down the slope of the eastern ridge. These samples are very different to the other samples, as they contain a very large portion of fines (mainly silt). The samples 02d-2a and 02d-2b are derived from the same layer. However, as they exhibit different colours, they are treated as two individual samples here. 02d-2a is also slightly coarser than 02d-2b.

All outcrop samples were collected from the distal end of the ridges. Therefore, it can be assumed that they have traveled the furthest. Furthermore, the samples are derived from deposits close to the base of the ridges. It is therefore very likely that subglacial processes may have lead to their formation, which also could explain why these samples are much finer than the ones from the surface samples of the ridges.

The outcrop samples from the western ridge (samples 02c-1. 02c.8 and 02c-16) also show a larger portion of fines. However, because of seasonal conditions these samples were collected much later in the year and only three samples are presented here. The outcrop was found above a thick layer (c. 3m) of conglomerate, where the river cuts into the ridge. This outcrop also showed several layers of tephras. The samples presented here are from the lowest, middle and top layers of this particular outcrop. These layers were interbedded within at least three different tephras. Some of these tephras are of rhyolitic origin and some of andesitic. As the results indicate, the outcrop samples vary greatly. The lowest (02c-1) and therefore oldest is much finer than the remaining two. This sample is primarily of fine sand. The middle sample (02c-8) is slightly coarser and contains mainly medium to fine sand grains. The sample from top layer (02c-16) and therefore youngest is much coarser than the lower layers. It contains coarse to medium sand mainly. It appears that bed 02c-16 is an andesitic tephra (section 8.1.5).

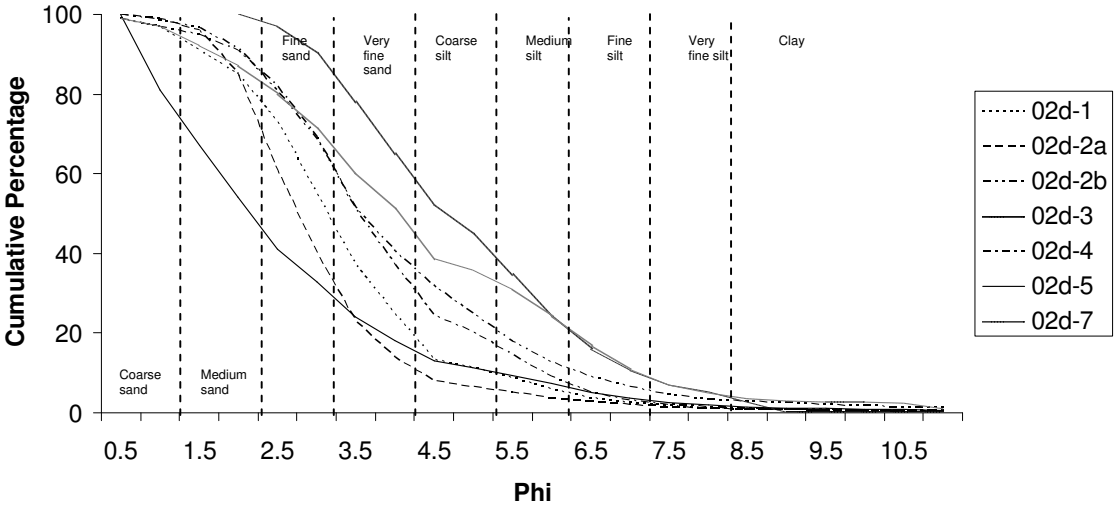

Figure 6.12 Cumulative curve showing the results from numerous samples that were collected from a cutting section on the eastern ridge. The samples are much finer than any of the other samples (about 60 to 50%).

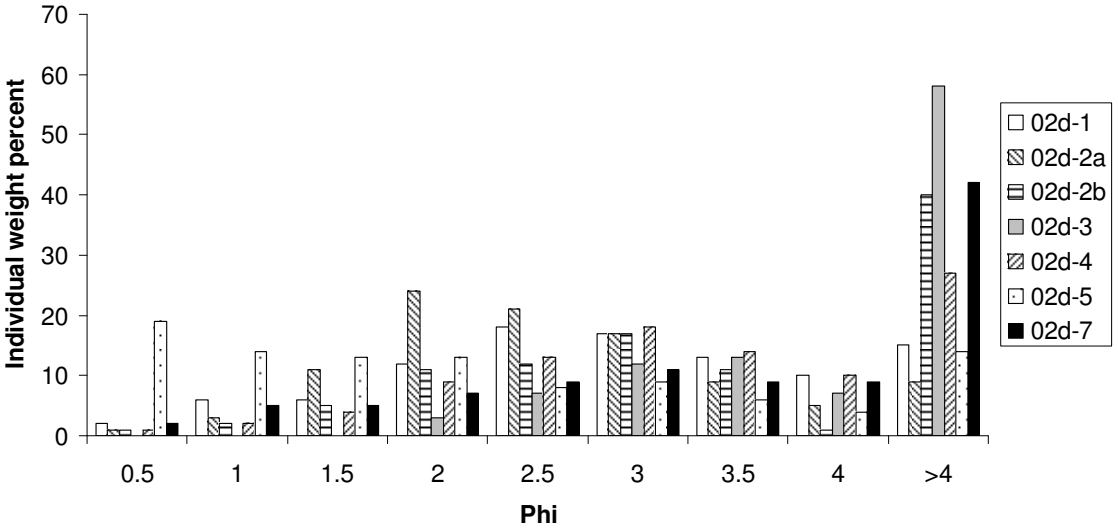

Figure 6.13 Histogram that shows the results for outcrop samples that were collected near the base on the eastern lower end. Most of the grain populations show a very large fraction of fines. However, there are some variations within the groups.

The outcrop samples are very different compared to the other samples. Different processes must have occurred on both sides to produce these differences. The lithologies appear to be varied as the western ridge contains numerous layers of different types of tephras. The western ridge changes direction at the point of the outcrop, where it also forms the highest

point. The outcrop on the eastern ridge shows no evidence of tephras and is more homogeneous. However, it is difficult to determine from this study alone if there are no tephras preserved on the eastern ridge, as this was the only outcrop that was studied and it would have been beyond the aim of this investigation.

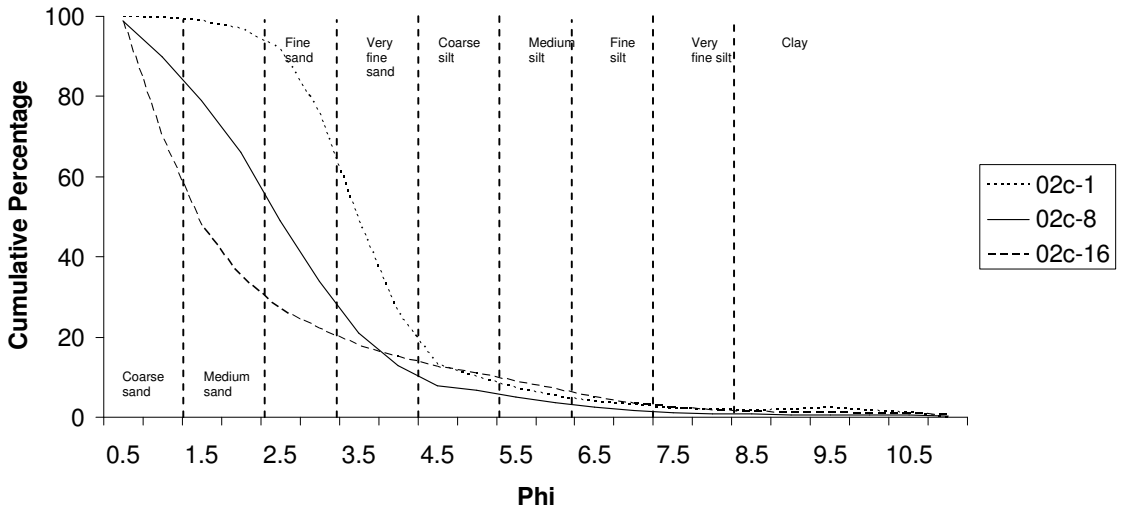

Figure 6.14 Cumulative curve showing the results for the three outcrop samples that were collected on the western ridge. All samples are of sand size. However, there are great variations within the grain populations.

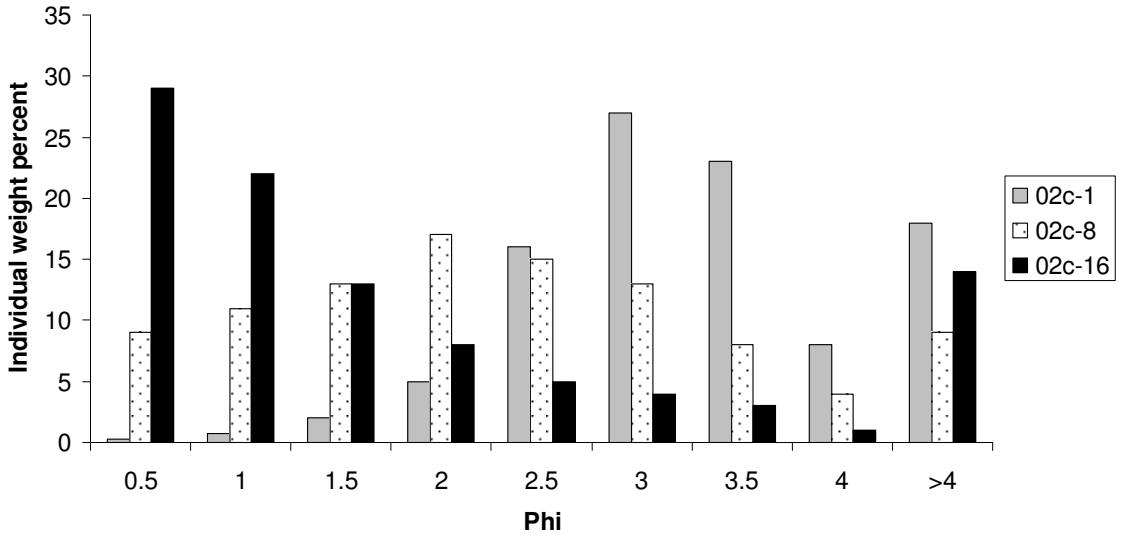

Figure 6.15 Histogram showing the individual weight percentages of each size class. There are great variations within the three populations. The oldest (02c-1) layer of the samples has the highest proportion of fine grains and the oldest (02c-16) has the coarsest fractions. However, all samples are of sand size.

6.3.6 The results from a small lobe on the eastern ridge (samples 01e - 03e)

Three sediment samples (Fig. 6.16 and 6.17) were collected from a small lobe on the eastern ridge, which is currently the furthest extent of the ridge deposits. The overall trend is similar to the one from the main deposits (two lateral ridges). About eighty percent of the grain populations are of sand size (coarse to fine sand). Sample 03e represents the furthest extent of this particular deposit and is finer than the other two samples. However, the study of the grain-size distribution of a sedimentary deposit is interested in the trends and averages of grain populations and not in the behaviour of individual samples.

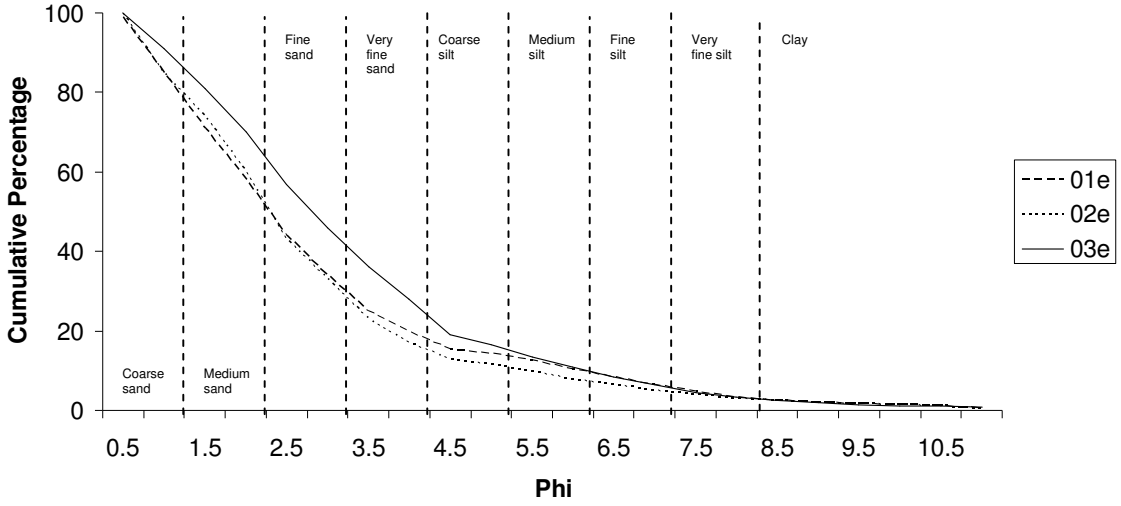

Figure 6.16 Cumulative curve showing the results of three samples that were collected from a small lobe on the eastern ridge. The lobe is currently the furthest extent of the ridge deposit (down valley). The graph shows a very similar trend to the main ridge deposits. About 80% of the grain populations are of sand size.

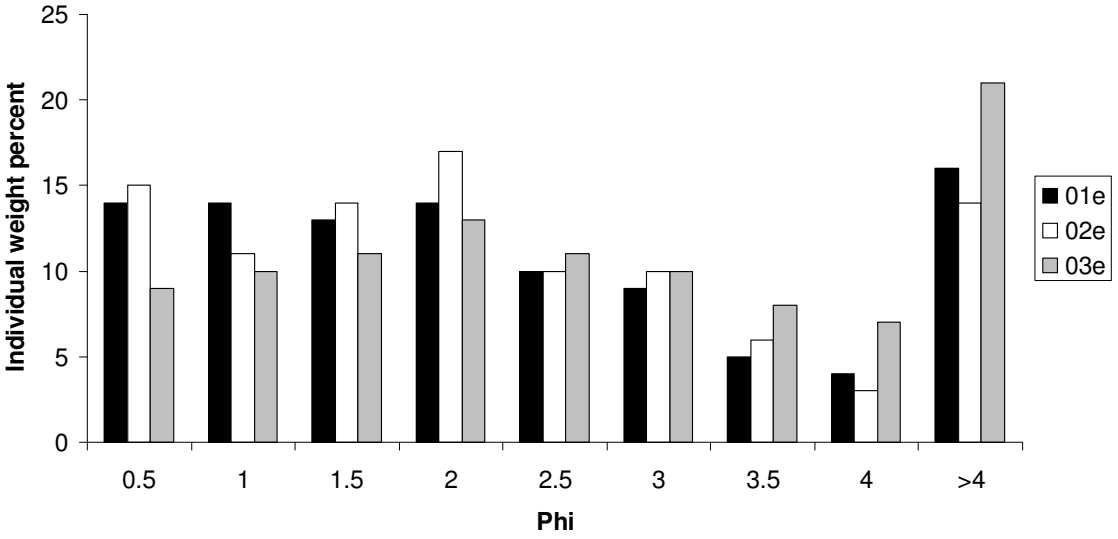

Figure 6.17 Histogram showing the individual weight percentages of each size class from the samples that were collected from a small lobe on the eastern ridge. The histogram shows that the populations are of coarse to fine sand. Less than 20% of all grain populations are finer than silt.

6.3.7 Statistical analysis

Tables 6.4 to 6.7 show the statistic measures and their qualitative descriptions for all collected samples. The mean values for the samples from the western ridge (01a-11a), the eastern ridge (01b-11b), the outcrop samples from the western ridge (02c-1 – 02c-16) and the small lobe samples from the eastern ridge (01e-03e) all fall into the fine to medium sand size range. However, the outcrop samples from the eastern ridge (02d-1 – 02d-7) have mean values that can be qualitatively described as fine sand to very coarse silt.

The grain populations of the Wahianoa Valley are poorly sorted, as nearly all samples have a sorting value that ranges between 1 and 2 phi. Skewness ranges from 0.3 to 0.56 for all samples of the Wahianoa debris ridges, which indicates that they are fine to very fine skewed. Few samples are symmetrical. Kurtosis ranges between 1.05 and 1.63, which means that the grain populations are primarily leptokurtic and mesokurtic.

6.4 SUMMARY

The results presented suggest that similar processes have lead to the formation of the Wahianoa debris ridges. The matrix of the ridges primarily consists of coarse (55.7%) to medium (22.9%) sand. According to Boulton (1976) and Benn and Evans (1998), supraglacially derived till has a silt-clay content <15%. Therefore, the results for the grain-size distribution further support the hypothesis that the Wahianoa Glacier was strongly debris mantled. All results show a similar trend (very fine skewed to fine skewed and leptokurtic and mesokurtic), however, the results for the samples that were collected from two outcrops near the base at the maximum end of the ridges, show greater variations. The outcrop of the western ridge shows some tephra beds that are undisturbed. This suggests that these deposits have formed prior to a glacial advance (section 8.1.5) and therefore in a non-glacial environment.

Chapter 7
MICROMORPHOLOGY OF SURFACE GRAINS

7.1 INTRODUCTION

Debris transported subglacially can be exposed to great stresses with clast modification greater in the basal transport zone (Boulton, 1979). In general, clasts transported in this zone tend to be blocky and rounded (see chapters 3 and 4). At a smaller scale, the development of surface textures on clasts is strongly dependent on lithology (Hambrey, 1994). Harder rock, such as granite, schist and gneiss typically show fewer striae than softer, fine-grained rock, such as mudstones and carbonates (Kuhn *et al.*, 1993). Hence, the modification of glacigenic sediments also takes place at micro-scale. The study of surface textures of sand and silt-sized grains in glacial geomorphology has only started to develop over the last three decades (Evans & Benn, 2004) using Scanning Electron Microscope (SEM) systems.

Research conducted so far using SEM on grain surfaces is limited and has mainly concentrated on analyses of quartz grains (e.g. Whalley & Krinsley, 1974; Mazzullo & Ritter, 1991), as quartz is one of the most abundant resistant minerals found in areas of Pleistocene ice sheet glaciation in Europe and North America. Figure 7.1 shows examples of quartz grains that have undergone glacial transport and typically show conchoidal fractures, abrasion features, chattermarks, adhering particles, medium to high relief and sharp angular features (Mazzullo & Ritter, 1991; Campbell & Thompson, 1991; Mahaney & Kalm, 2000; Mahaney *et al.,* 2004). The present study of surface features of till grains is primarily concerned with the identification of any textures that can be linked to a glacial mode of transport and deposition. As Mt Ruapehu is an andesitic volcano and consists mainly of mafic minerals, it was considerably difficult to compare the results with previous research. This is because the vast majority of previous SEM analyses of glacigenic sediments have been undertaken on quartz (e.g. Rogerson & Hudson, 1983).

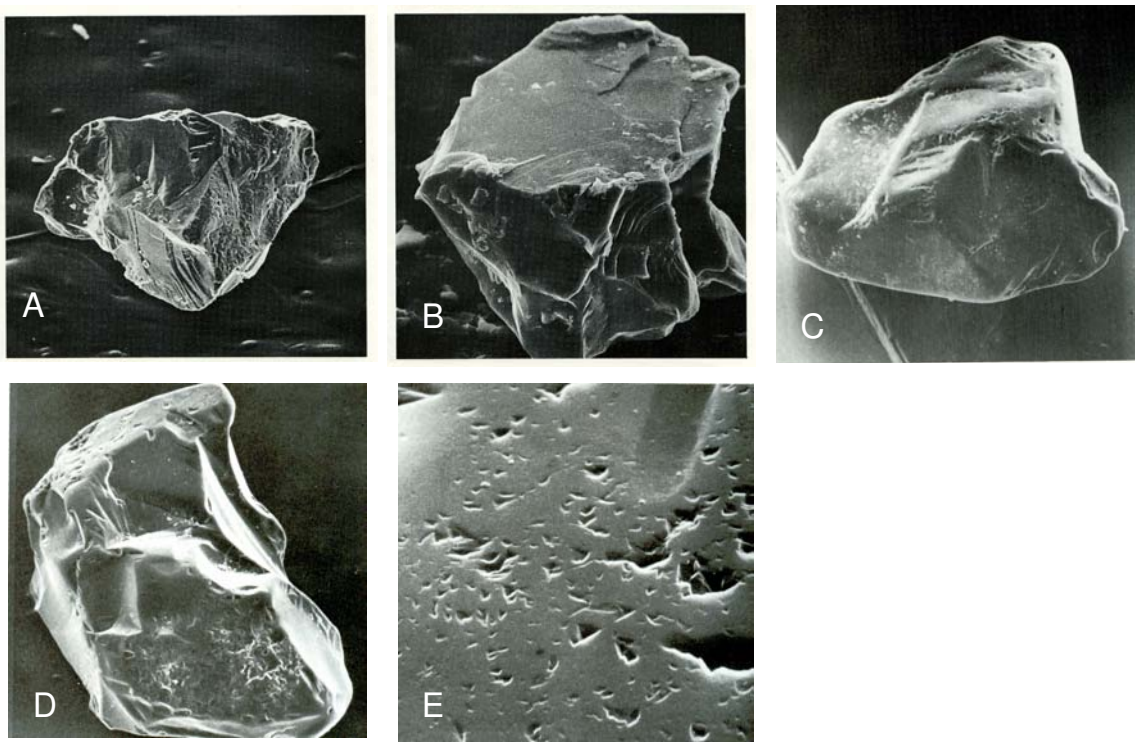

Figure 7.1 Glacial micro-morphological textures on quartz grains from different locations. (A) Angular grain with conchoidal fractures and sharp edges *(delta in fjord at margin of modern glacier, Norway);* (B) Cleavage plane, adhering particles, conchoidal fractures *(modern glacier, Switzerland);* (C) Conchoidal breakage, rounded edges *(Argentine continental shelf. Late Pleistocene);* (D) Irregular outline solution and re-precipitation, few conchoidal breakage patterns and round edges *(Argentine continental shelf. Late Pleistocene);* (E) Precipitation and V-shaped depressions *(Argentine continental shelf. Late Pleistocene)* (Krinsley & Doornkamp, 1973).

7.1.2 Previous studies

The usefulness of the SEM in grain surface analysis comes from its great resolving power. A modern light microscope has a resolution of 200nm, whereas the SEM can distinguish fine detail up to 3nm (Flegler *et al.,* 1993). Numerous studies that deal with the microtextures of sediments and the discrimination of depositional environments have been published (e.g., Hamilton & Krinsley, 1967; Krinsley & Doornkamp, 1973; Whalley & Krinsley, 1974; Bull, 1981).

As previously noted, the majority of research has focused on surface textures of quartz grains to identify depositional environments as well as ice thickness (Mahaney, 1995). Figure 7.2 shows the wide variety of microtextures of grains from tills from different

localities. The tills are derived from landscapes glaciated by ice sheets of varying thicknesses. The results appear to show that the wide range of surface microtextures increases with ice thickness (Fig. 7.2). It also shows that certain microtextures are absent at lower ice thicknesses. Sub-parallel linear fractures, conchoidal fractures, curved grooves, straight grooves, crescentic gouges and arc-shaped steps are absent in till samples from glaciers with an estimated ice thickness of less than 200m. This is an interesting observation, as these features are highly abundant in the samples where the ice thickness is higher. Relief appears to become greater with increasing ice thickness.

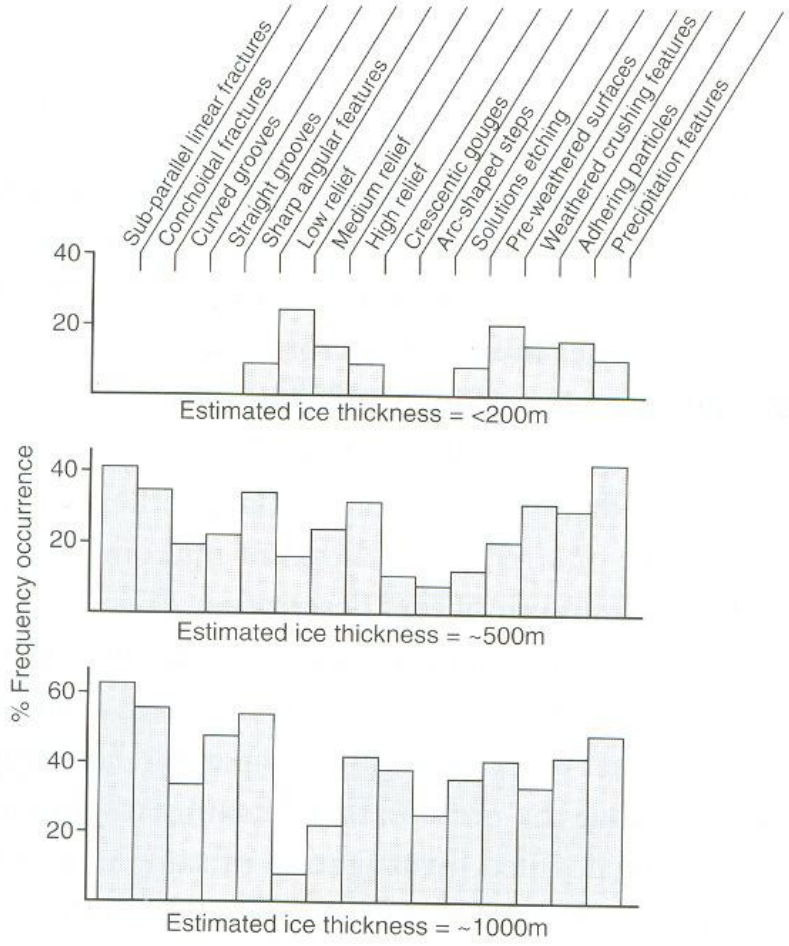

Figure 7.2 Frequency plots showing the variation in microtextures of till grains from Antarctica, Svalbard, North America, Ellesmere Island and the European Alps. The tills were deposited by glaciers of different thicknesses. The results appear to show that an increased variety of microtextures occurs with ice thickness (Mahaney, 1995).

Despite the wide range of studies that have undertaken a microtexture analysis, the usefulness of microtextures as paleo-depositional discriminator is still not fully accepted (Mahaney & Kalm, 2000, 2001). Mahaney and Kalm (2000) claim that many earlier studies (e.g. Whalley & Krinsley, 1974) have relied mainly on the analysis of sediments that were found close to glacial environments and that it is likely that these sediments have been reworked and mixed with sediments from other depositional environments. To test the hypothesis that glacial SEM microtextures are distinguishable from fluvial depositional environments, Mahaney and Kalm (2000) compared a large number of glacial grain samples (that had undergone basal, fluvial and glaciofluvial transport) from the Pleistocene with non-cemented sandstone of Middle Devonian age. The study showed distinctive differences (Fig. 7.3). The glacially transported grains showed large numbers of conchoidal and subparallel linear fractures, whereas the Devonian sand showed dominance in low relief. The till grains showed high relief and adhering particles, whilst mechanically-upturned edges, deep troughs, linear steps, curved grooves and straight grooves were the only microtextures found in the till samples. The glaciofluvial sand and the Devonian sand grains showed strong edge rounding and V-shaped percussion cracks.

.

Microtextures have also been studied under thin-sections, which highlights deformation features (van der Meer, 1993). Figure 7.4 shows a thin-section of a study that investigated the importance of subglacial shear in till genesis (Khatwa & Tulaczyk, 2001). The study compared Pleistocene till from England with modern till (UpB till) from beneath Ice Stream B, West Antarctica. It was identified that microstructures were less abundant and diverse in modern till than in the Pleistocene till. Khatwa and Tulaczyk (2001) concluded that the same till-forming processes, such as subglacial deformation, can produce distinctly different till microtexures.

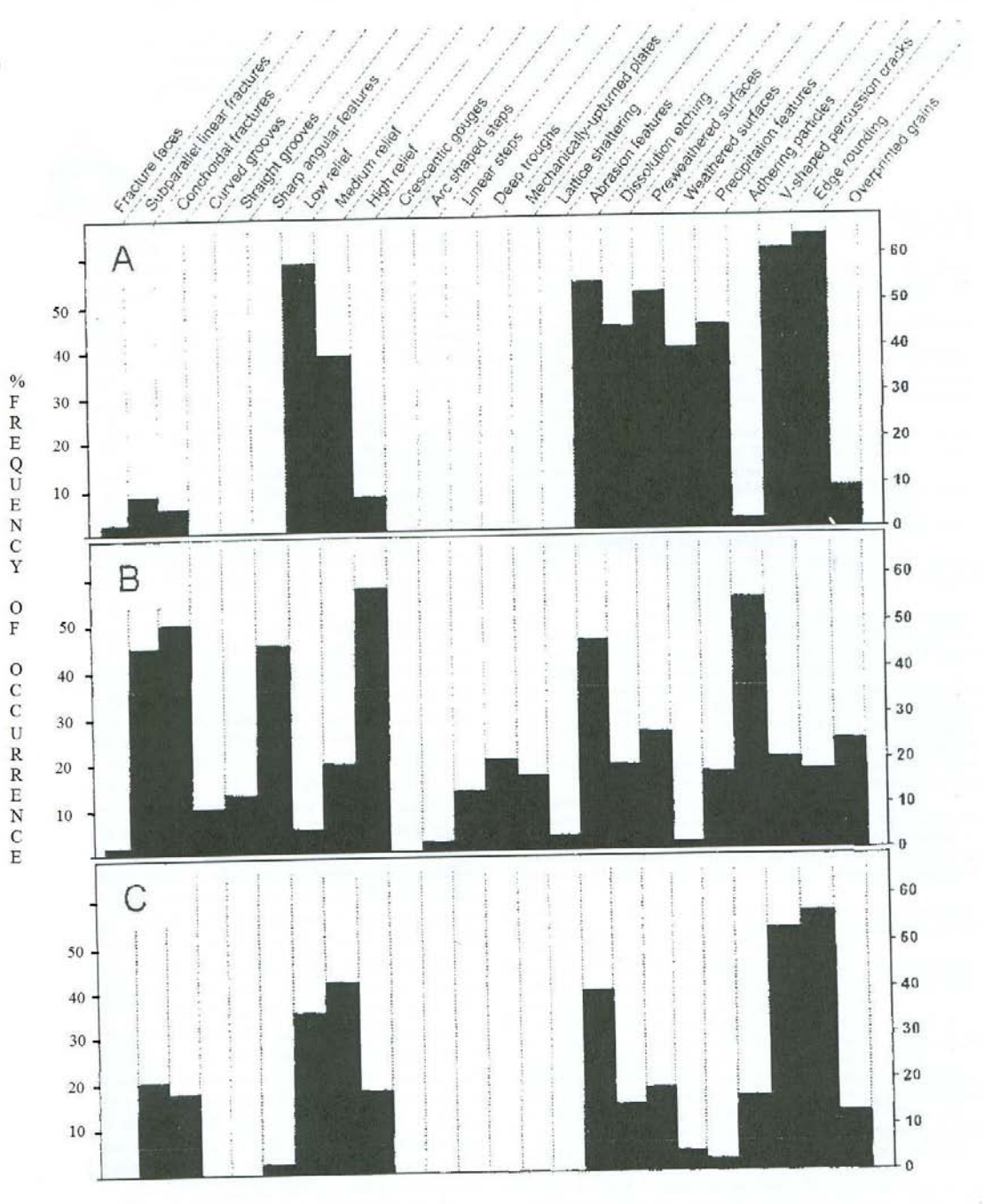

Figure 7.3 SEM frequency plots of occurrence of different microtextures in: A. Devonian sands; B. Weichselian Tills; and C. Weichselian glaciofluvial sands (Mahaney & Kalm, 2000).

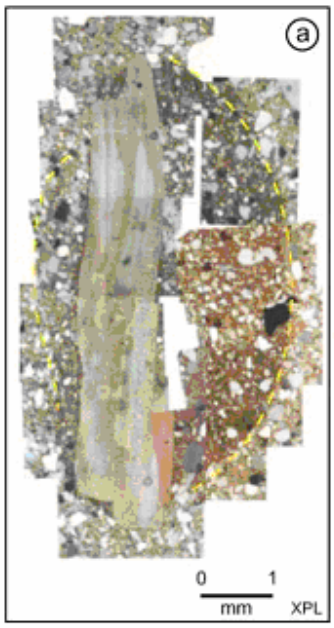

Figure 7.4 Microstructural data from Pleistocene sediment samples: (a) bioclast fragment exhibiting adherent matrix structure (from sample WR3A) (Khatwa & Tulaczyk, 2001).

7.2 METHODOLOGY

In the study of SEM microtextures it is important to collect data from numerous grains that represent the supposed depositional environment. Furthermore, it is essential to use more than one microtexture in the interpretation of the paleoenvironmental conditions (Krinsley & Doornkamp, 1973). Quartz grains are generally used because common surface themes have been recognised from different depositional environments (Krinsley & Doornkamp, 1973). However, as mentioned before, the study of microtextures in sedimentary deposits is still in development. The aim of this part of the study is to investigate the surface textures of individual grains found on the surface of the lateral ridge deposits of the Wahianoa valley. The first part of the analysis included the bulk of minerals that were found. The second part looked solely at magnetite crystals.

7.2.2 Sample preparation

This study used the standard methods for this technique following Krinsley & Doornkamp (1973) (Fig. 7.5). A small amount of grains from the coarse sand fraction (1mm-0.5mm) were sub-sampled from the sediments that were collected for the grain-size distribution (chapter 6). The grains were first studied on the light microscope and as the grains were

heavily coated with contaminants, they were cleaned using the method introduced by Tamm in 1922, (Blakemore *et al.*, 1987). 10.92g of oxalic acid together with 16.11g of ammonium oxolate was dissolved in distilled water to make a solution of 1 litre. The samples were placed into this solution and gently shaken and then left overnight. The grains were then placed into an ultrasonic bath until all contaminants were removed. Lastly, the grains were thoroughly rinsed with distilled water and then oven-dried.

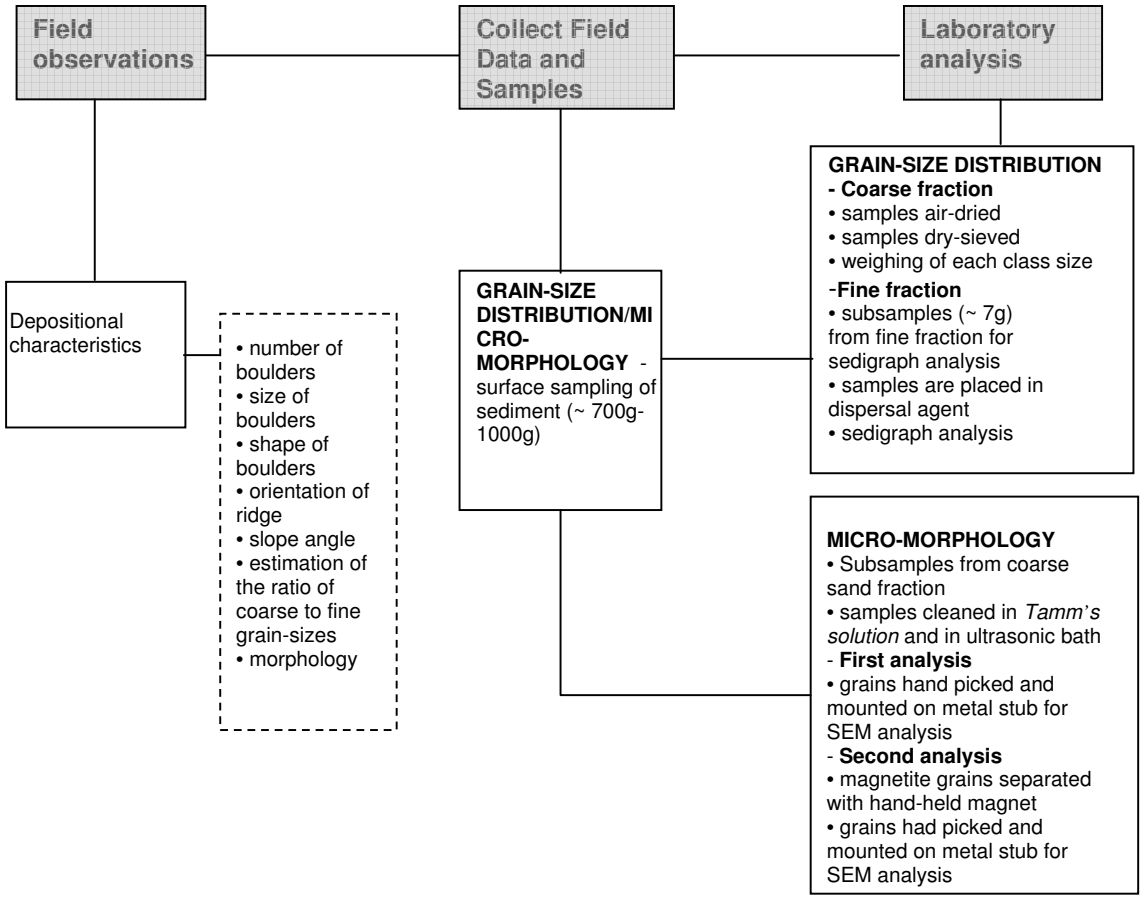

Figure 7.5 Flow diagram illustrating the field procedures and laboratory techniques used to identify the micro-morphology of individual grain from the Wahianoa valley.

The crystals were handpicked with the help of a binocular microscope and then mounted onto a metal stub. The first series of observations was done by choosing a variety of grains, though pumiceous grains where avoided as they have lower strength due to high vesicularity. The second part of the study examined magnetite only. The reason for selecting magnetite grains was to enhance the possibility of distinguishing microtextures that were caused due to glacial activity and not during eruption processes. Magnetite is

easily separated and has no cleavage. The magnetite grains were separated with a hand-held magnet and then handpicked and mounted on stubs. The mounted grains were coated with a thin layer of gold before the stub was placed in the SEM for analysis. It was unrealistic to analyse each individual grain under extreme high magnification because of the time each analysis takes and the large quantity of samples. Although the SEM has a magnification range of 20-150000X (Flegler *et al.,* 1993), most grains were studied at a lower magnification of 100X.

7.2.3 Image analysis

The resulting images from the SEM analysis were examined for microtextures and the percentage of frequency occurrence of each feature was calculated and plotted on a histogram, following the categories of microtextures introduced by Mahaney and Kalm (2000). The main concern for this part of the research was that all grains found on the surface of the debris ridges of the Wahianoa valley could potentially be ash deposits that have simply been emplaced during an eruption and have not undergone glacial transport. Therefore, some additional microfeatures that were identified by Donoghue (1991), were included (vesiculated, vesiculated glassy coating, abrasion features and sharp edges).

The SEM is mainly used in volcanology to identify the chemistry of minerals, their lattice structures, particular shapes of crystals and the extent of vesicularity. This study looked at microtextures that are common in glacial environments but also at features that are typical for volcanic ash. Unfortunately, some of these features are similar or even the same. Andesitic tephras contain a high fraction of pyroxenes (Donoghue, 1991), which tend to develop conchoidal fracture patterns, which is a microtexture that has been identified to be typical for glacial depositional environments (Mahaney & Kalm, 2000). Sharp edges are also common in volcanic ash. It is this feature that makes volcanic ash so abrasive and dangerous. Figure 7.6 shows ash particles that were identified by Donoghue (1991). It shows typical features that are presented in tephras. The Tufa Trig Formation contains all tephras that have erupted from c. 1800yr BP to the present from Mt Ruapehu.

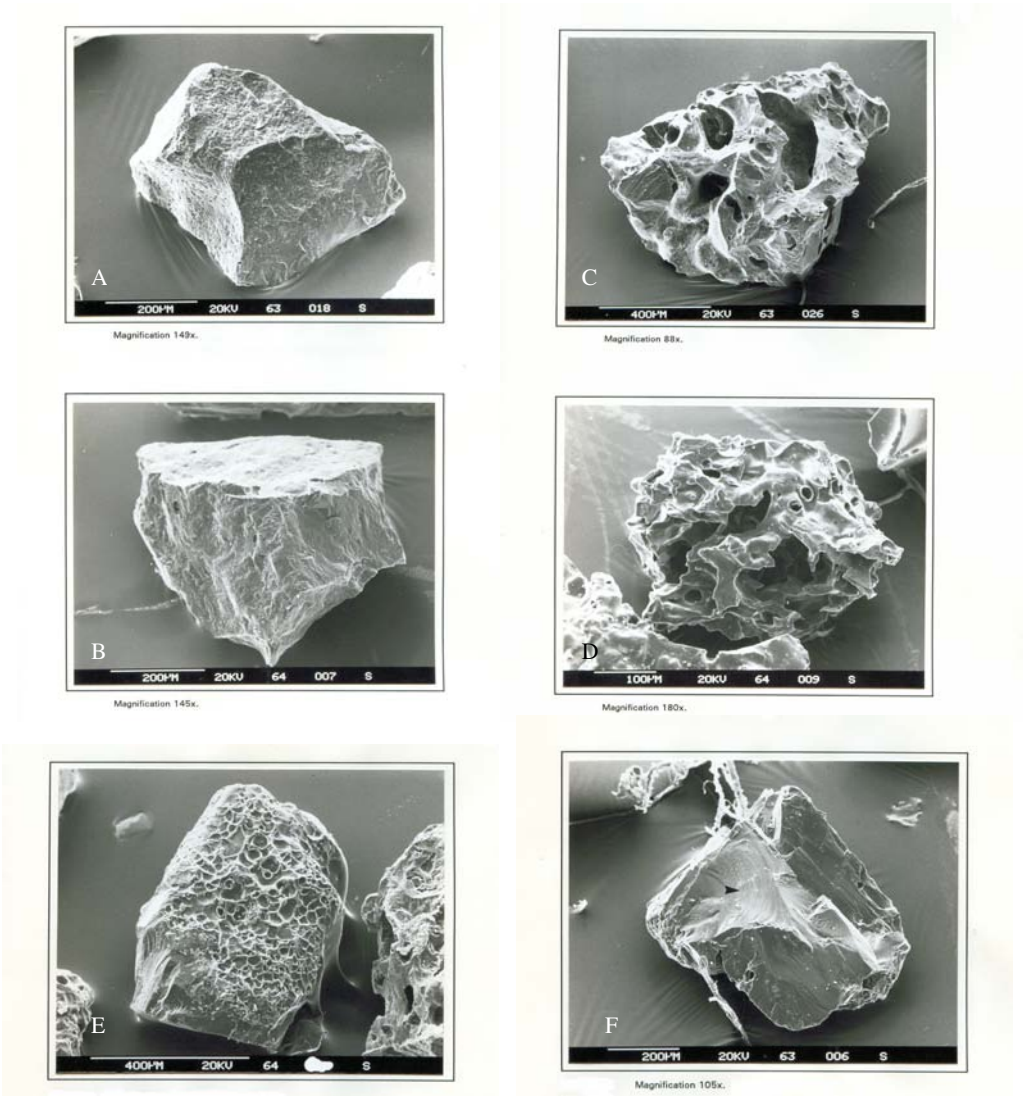

Figure 7.6 Ash grains identified by Donoghue (1991). (A) + (B) poorly vesicular vitric pyroclasts from Tufa Trig Foramtion tephras (c. 1800yr BP – present); (C) + (D) vesicular vitric pyroclasts; (E) broken pyroxene crystal with vesiculated glassy coating; (F) blocky pyroxene crystal showing facial conchoidal fracture patterns (arrows).

7.3 RESULTS

7.3.2 All minerals

Figures 7.7 and 7.8 show some of the microtextures that were identified in this study. The features that were identified to be of diagnostic value for a glacial depositional environment in previous studies (section 7.1.1) have been used, in addition to some common ones identified in this study. However, as no research has been done in this area, the main aim of this part of the study is to identify any possible pattern.

Figure 7.9 shows a frequency plot of the results from the first part of this study, including any grain (except pumiceous particles) found in the samples. The results show a high tendency towards round grains (60%). However, a large portion of grains also show sharp edges (36%), with some instances of sharp and round edges found on the same grain. High (24%) and low relief (24%), conchoidal fracture patterns, (24%) fracture faces (26%) and linear steps (25%) were also relatively common, with the latter three often coinciding together. On many grains adhering particles (14%) can be found, which is associated with glacial grinding (Mahaney *et al.,* 1996). Sharp angular features (17%) and vesiculated glassy coating (16%) are relatively common also, with the vesiculated glassy coating is mainly found on pyroxenes. 2% of this analysis showed V-shaped percussion cracks that are related to subaqueous environments (Krinsley & Doornkamp, 1973). This may have occurred prior to, during, or after glacial transport (Mahaney *et al.,* 1996).

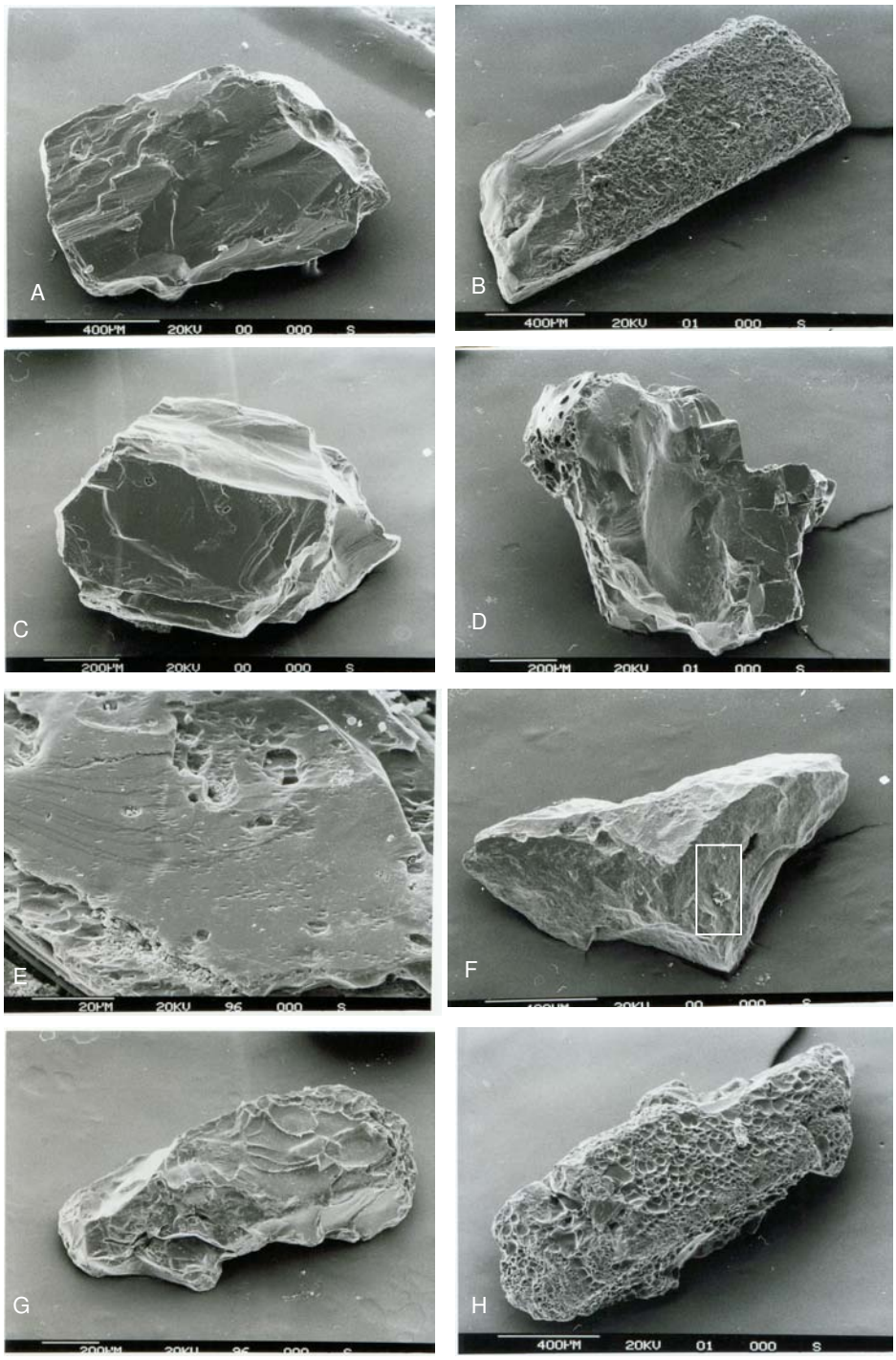

Figure 7.7 Typical micro-morphological textures found in this analysis. (A) Grain shows conchoidal fracture patterns with sub-rounded edges; (B) pyroxene with vesiculated glassy coating and a fracture face; (C) grain with high relief sharp edges; (D) fracture face with sharp edges; (E) V-shaped percussion cracks; (F) angular grain with adhering particles (square); (G + H) pyroxene with vesiculated glassy coating.

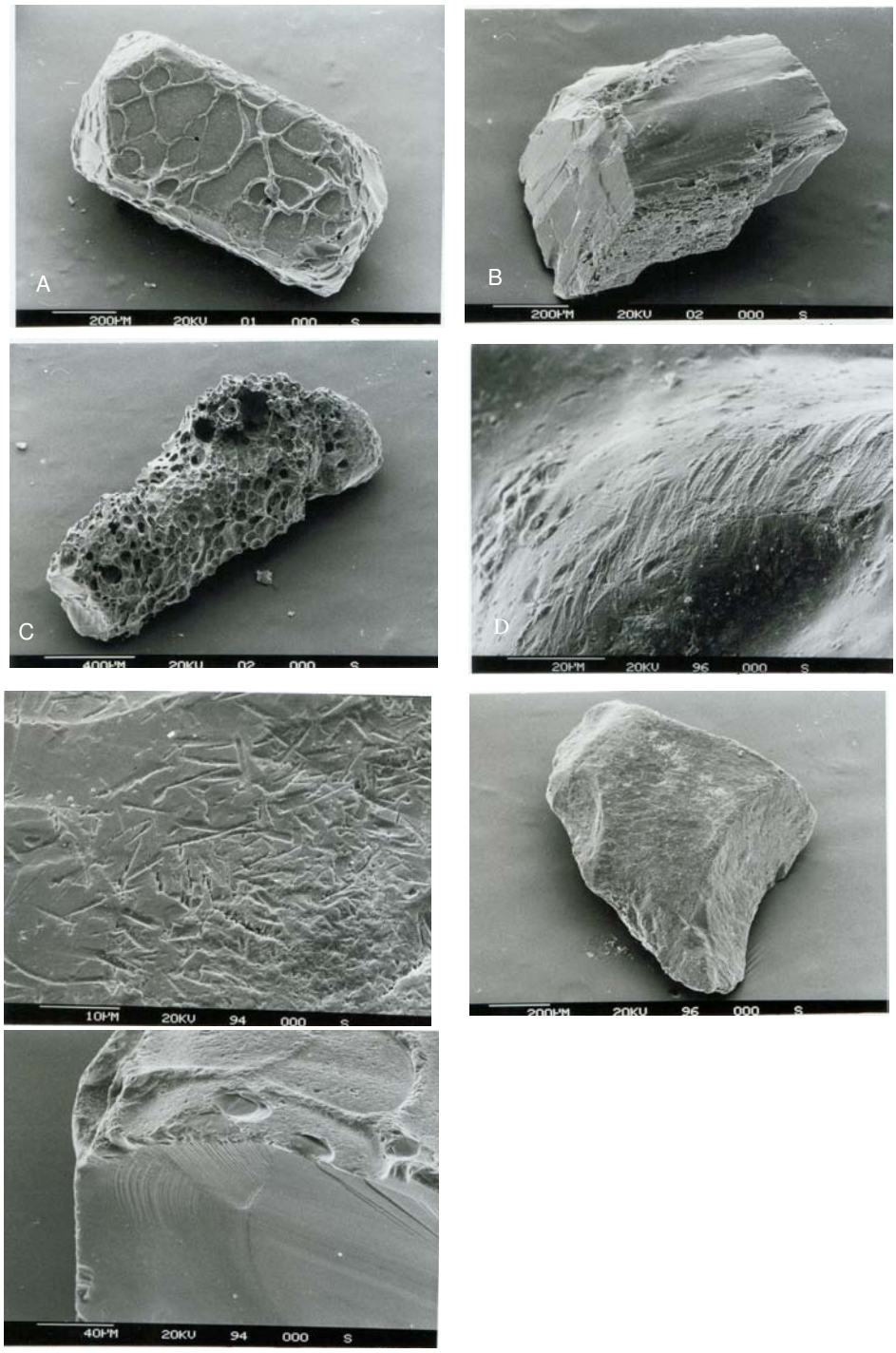

Figure 7.8 Typical micro-morphological textures found in this analysis. (A) Vesiculated glassy coating; (B) angular grain with high relief; (C) vesicular pyroclast; (D+E) abrasion features; (F) grain exhibiting edge rounding; (G) grain with vesiculated glassy coating and a fresh fracture face that shows conchoidal fracture patterns; (H) V-shaped percussion cracks.

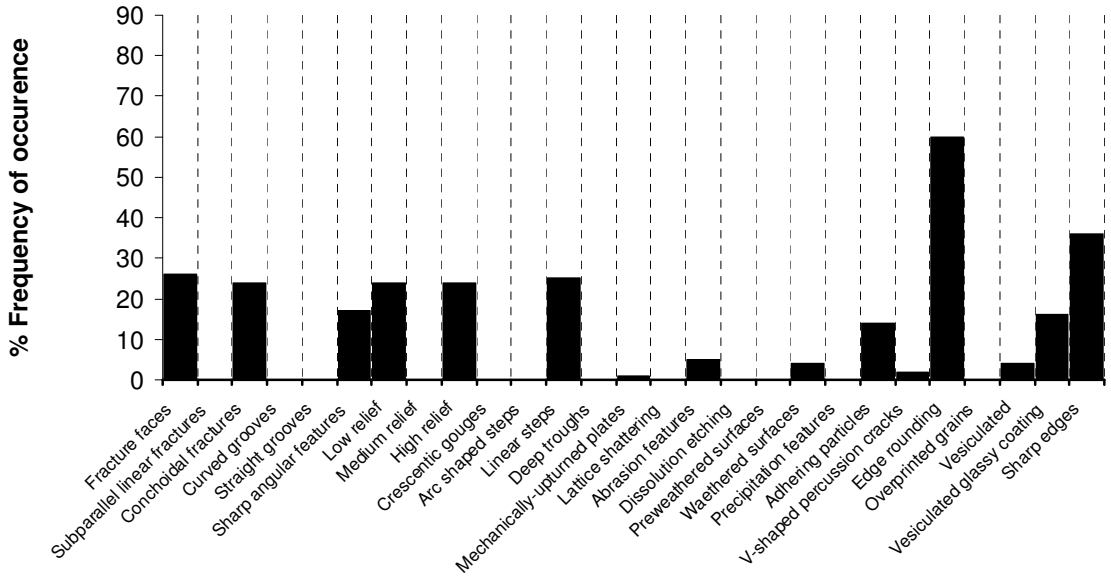

Figure 7.9 Frequency plot of types of microstructures identified for all surface grains studied. Round edges are the most common feature identified. Sharp edges, high and low relief, conchoidal fracture pattern, fracture faces and linear steps are next most abundant features.

7.3.3 Magnetite minerals

As the overall results of this study are difficult to compare with previous studies, it was decided to use magnetite as a proxy to the quartz minerals used in previous work. Magnetite can be separated very easily and has no cleavage and a hardness of about 7.5-8 on the Mohs Scale of Hardness in volcanic ash, which is similar to quartz (hardness of 7). Magnetite is also a heavy mineral (specific gravity of c. 5.2) and therefore less likely to be transported by aeolian and fluvial processes.

Figure 7.10 shows the frequency plot of the magnetite analysis and figure 7.11 shows some of the microtextures that were present. Edge rounding is the most common surface texture identified (86%). This feature was very distinctive in the research done by Mahaney and Kalm (2000), where it was highly abundant in non-cemented sandstone and in glaciofluvial sands, but not in till deposits. The results for the magnetite analysis also show that sharp edges (56%), high relief (52%), adhering particles (44%) and linear steps (34%) are also relatively common. High relief and adhering particles are common microtextures in glacial environments but edge rounding does not occur (Mahaney & Kalm, 2000). However, fewer

features, such as conchoidal fractures or subparallel linear fractures that would suggest mechanical or chemical weathering are present in this study.

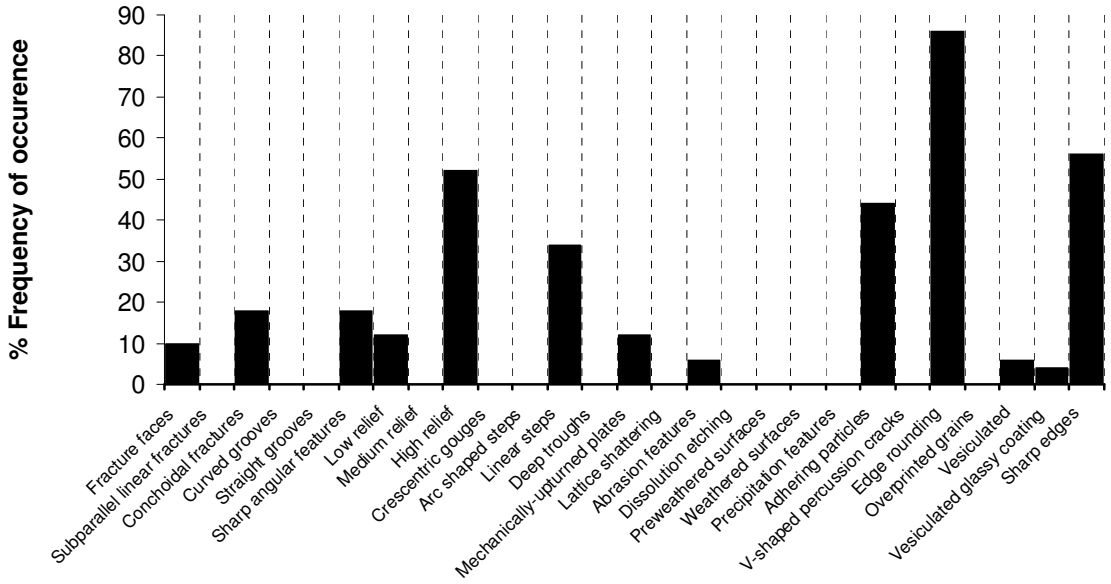

Figure 7.10 Frequency plot of surface features identified on magnetite crystals. Round edges are most common feature identified, next to sharp edges, high relief, adhering particles and linear steps.

7.4 SUMMARY

The results of this study do show some micro-morphological patterns that have been identified in previous research, such as high relief and adhering particles. However, some microtextures have been identified that are less common in glacial transported sediment, for example edge rounding. Conchoidal fracture patterns and subparallel linear fractures are commonly found in glacially derived sediment (Krinsley & Doornkamp, 1973). The present study has identified conchoidal fractures in the bulk of grains but not in magnetite and no grain exhibited subparallel linear fractures.

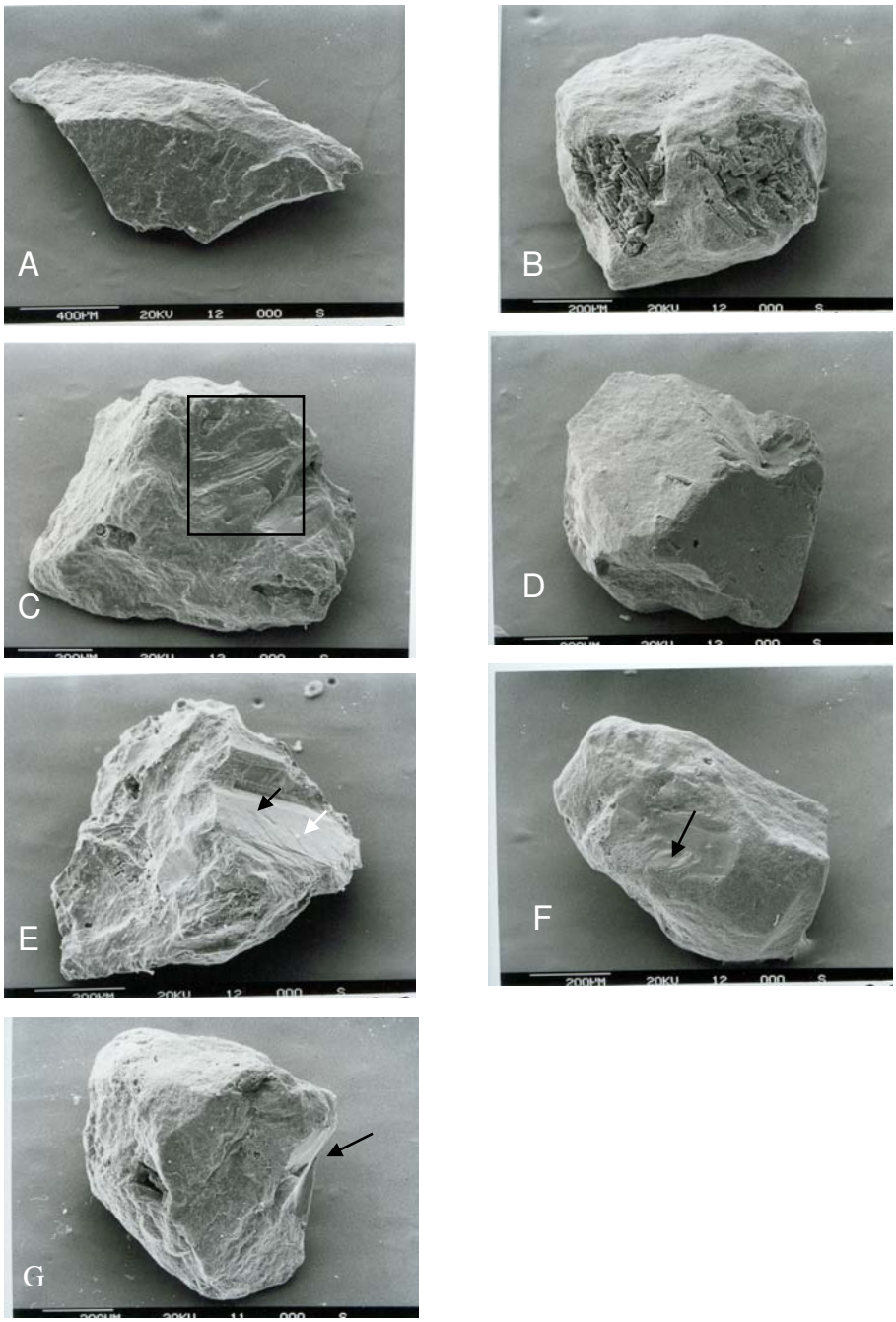

Figure 7.11 Typical micro-morphological features on magnetite. (A) Grain shows low relief and sharp edges; (B) Well rounded particle; (C) Conchoidal fracture pattern and linear steps with adhering particles (in square); (D) Grain exhibits a fresh fracture face; (E) Particle with sharp edges and linear steps (black arrow), some adhering particles (white arrow); (F) Magnetite grain with sub-rounded edges and linear steps (arrow); (G) Well rounded particle with fresh fracture face (arrow).

It is believed that the majority of grains that have been studied are in fact tephra deposits. The samples were primarily collected from the surface (c.5-10cm) of the debris ridges. However, some grains were sampled from an outcrop near the base of the ridge and some at the lower end of the ridge slopes. It could be of an advantage to study these deposits in future only, as it is more likely that they exhibit microtextures produced by glacial activity. Since the LGM there have been numerous eruptions from the Taupo Volcanic Zone. Therefore, the surface of the debris ridges will have been covered with these deposits. The most recent eruption from Mt Ruapehu was in 1995/96. A large number of particles studied here are likely to have derived from this event.

It also could be beneficial if a smaller number of particles are studied in future and to study these under higher magnification and in more detail. This would reduce the possibility of missing important micro-morphological features. Magnetite has not been used in micro-textural studies in the past, but this study has shown the potential of this mineral. In countries, such as Chile and Iceland, where the origin of ridge deposits is unknown and quartz is absent, the SEM analysis of magnetite could help address this problem.

Chapter 8

DISCUSSION

8.1 INTRODUCTION

The summit area of Mt Ruapehu has a very irregular shape. Therefore, it can be assumed that during a time of glaciation the summit was covered by an ice cap, where the ice radiated out in different directions from a central area. During the recession of this ice cap, individual glaciers will have started to appear. At the same time of volcanic activities these glaciers will have continued to shape the landscape. This interplay between volcanic and glacial processes has produced complex landforms. The scientific community has placed its main focus on the volcanic aspects of the region. Although most authors refer to the landforms that appear to be of glacial origin as 'moraines', no actual glacial studies have been undertaken so far to provide the necessary evidence that is needed to support this hypothesis. This study has been an initial attempt at unfolding the glacial history of Mt Ruapehu.

8.1.2 The Transport Pathway of the Wahianoa Glacier

The results of this study do not provide conclusive evidence for the hypothesis that the Wahianoa debris ridges are in fact of glacial origin. However, this study indicates that the hypothesis is correct and that the non-conclusive results are due to the very complex interaction between glacial and volcanic processes. The Wahianoa valley consists of two elongated debris ridges that are constructed of unconsolidated and poorly sorted diamicton of different sizes and lithologies. The only processes that can produce this type of deposit in a volcanic environment are lahars or glacial activities. As the Wahianoa valley has a very pronounced U-shape, it is certain that the deposit has formed due to glacial activities and the deposit is therefore referred to as *glacial till* and the debris ridges as *lateral moraines* from here on. The transport pathway of the Wahianoa Glacier is reflected in these moraines, which have formed due to the deposition of glacigenic sediments and the incision of the Wahianoa River. The river is fed by the Wahianoa Glacier; therefore it is certain that this river has existed as long as the glacier itself.

8.1.3 Supraglacial debris

The contrasting lithologies of the Ruapehu massif result in different erosion rates. Pyroclastic material is more erodable than effusive products. Therefore, the Wahianoa Glacier was probably extensively covered by supraglacial debris. Figure 8.1 shows the Wahianoa Glacier in summer 2006. Although the glacier is currently very small, the photograph illustrates that the glacier is covered by supraglacial debris (arrows) (Fig. 8.1 A). Figure 8.1 B shows the southeastern rock face of the Ruapehu massif. It becomes apparent that a large volume of pyroclastic material forms fan-like deposits at the slopes of the cliffs (arrows). This sediment would have fallen on to the glacier to be transported as supraglacial debris.

Figure 8.1 The Wahianoa Glacier in summer 2006. (A) Pyroclastic material falls on to the glacier to become supraglacial debris (arrows). Girdlestone Peak on the western side of the glacier. (B) The southeastern rock face of the Ruapehu massif. The arrows are pointing at fan-like deposits of pyroclastic products. These very erodable sediments would have fallen on to the glacier when it was more advanced. N.B. note the layers of lava flows of Mitre Peak that are part of the Wahianoa Formation (to the eastern side of the glacier).

Furthermore, lateral moraines are supraglacial landforms that form from the constant supply of frost-shattered debris, or similar. Glacier surfaces are generally slightly convex and supraglacial debris tends to move towards the glacier margins where it rubs against the valley sides and deposits as lateral moraines (Hambrey, 1994). At present, the Wahianoa Glacier is confined by Girdlestone Peak and Mitre Peak. However, when the glacier was more advanced it would have moved down a steep rock face and into a basin (Fig. 8.1 B). There, the ice would have been constrained by the major lava flows of the Wahianoa Formation (section 1.3.7), where the glacier was fed by the more erodable pyroclastic material, frost-shattered debris, rock falls and so on. This debris would have led to the formation of lateral moraines. Further down-valley the glacier was no longer constrained by the valley sides and scoured into the unconsolidated sediments of the ring plain. Because of the constant supply of sediment from the headwall and the valley sides, the moraines continued to form along the margins of the glacier.

8.1.4 Ice flow velocity

As the ring plain of Mt Ruapehu consists mainly of reworked debris, tephra units and coarse laharic volcaniclastic deposits (Hackett & Houghton, 1989; Procter, 2003), the Wahianoa Glacier moved over unconsolidated sediment rather than over hard bedrock. This would have reduced the net amount of friction that is generally produced in the movement of glacial ice. Hence, the glacier possibly moved at a fast rate. However, the gradient of the valley floor is very gentle, which generally reduces ice velocity. The amount of friction varies within a valley glacier and therefore its velocity (Martini *et al.,* 2001). The theoretical horizontal and vertical velocity variations within the Wahianoa Glacier at a time of its greatest extent was presented in figure 3.2. Because the debris that is transported and deposited along the sides and at the base of the glacier exerts more resistance, the ice moves slightly slower in these areas.

8.1.5 Subglacial deformation

As noted before (section 3.1.4.3), subglacial deformation occurs when glacial ice moves over unconsolidated sediment (Hambrey, 1994). As the Wahianoa Valley consists of unconsolidated sediments, it can be assumed that the Wahianoa Glacier caused subglacial

deformation and that a great part of the glacier motion took place in the underlying sediment and not within the ice body. Furthermore, laharic deposits suggest that the Wahianoa River existed during the LGM (Donoghue, 1991; Cronin & Neall, 1997; Donoghue & Neall, 2001). Therefore, it is possible that the basal zone was also strongly influenced by fluvial processes. As mentioned in the introduction (section 1.3.5), lahars were likely to have been more frequent and more severe during the Late Pleistocene, as the laharic deposits are most extensive from that time (Donoghue & Neall, 2001). This leads to the question if the Wahianoa Glacier directed these lahars via the subglacial fluvial system or over the glacier surface. In both cases, glacial debris would have been strongly influenced by these events. Figure 8.2 illustrates the impact of lahars on the Mangaehu (left photograph) and Mangaturuturu (right photograph) Glaciers that occurred during the 1969 eruption of Mt Ruapehu. Both lahars are directed along the surface of the glaciers, but the headwaters of the Whangaehu River join the lahar a short distance from its origin.

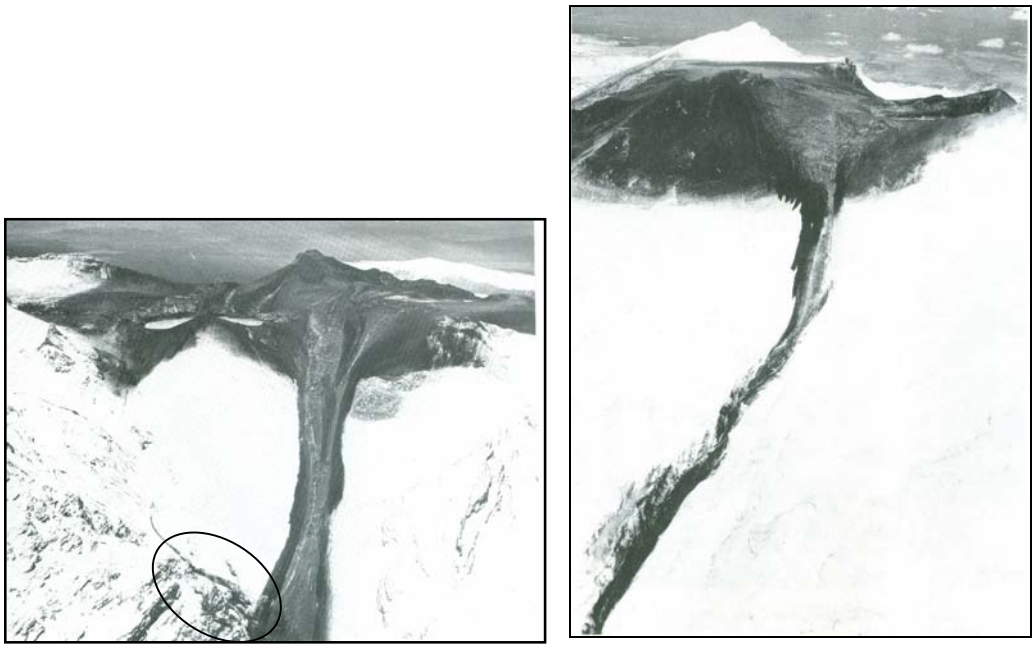

Figure 8.2 The head of the Whangaehu Lahar that was generated during the 1969 eruption of Mt Ruapehu (left) and the Mangaturuturu Lahar (right) from the same eruption. The headwaters of the Whangaehu River and the outlet from Crater Lake are shown at the bottom of the photograph on the left (circled area) (Ruscoe, 1978).

8.1.6 Chemical erosion

The current Crater Lake is warm and highly acidic (currently a pH of about 0.9) due to volcanic gases (Donoghue, 1991; Neall *et al.,* 1999). This means that since the existence of the Crater Lake the processes of chemical erosion by meltwater or laharic medium have possibly played some part in the development of the glaciers of Ruapehu. At present, the Whangaehu River, which originates at the summit of Ruapehu and flows down the Whangaehu valley on the eastern side of the mountain, is contaminated, since water from the Crater Lake leaks into it (Donoghue, 1991). Therefore, the Whangaehu Glacier will currently be strongly influenced by chemical erosion. The exact time of the formation of the Crater Lake is not known. It was suggested that it formed during the last 1800 years BP and is fed by the summit glaciers (Neall *et al.,* 1999).

8.1.7 Possible age of the lateral moraines

Although it is not the objective of this study to date the Wahianoa moraines, some important observations were made. During the field work numerous tephra beds were found in an outcrop at the base of the western ridge. Figure 8.3 shows the location (A + B) and the tephra beds (C). As these tephras are undisturbed, they must have been deposited before the last advance of the glacier (Fig. 8.4).

With the identification of the tephras an absolute date for the moraines could be found. One tephra deposit has been identified as the Taupo Pumice (Fig. 8.5), which is easily recognised by its physical characteristics, such as colour, texture and vesicularity. The Taupo Pumice has been dated at 1718 ±30 cal. yr BP (Alloway *et al.,* 2007) and is the product of a major eruption from the Taupo Volcanic Centre. As the tephra deposits are undisturbed they must be older than the till deposit. Therefore, the Wahianoa lateral moraines appear to be the result of a glacier advance during the LIA (section 2.2.5).

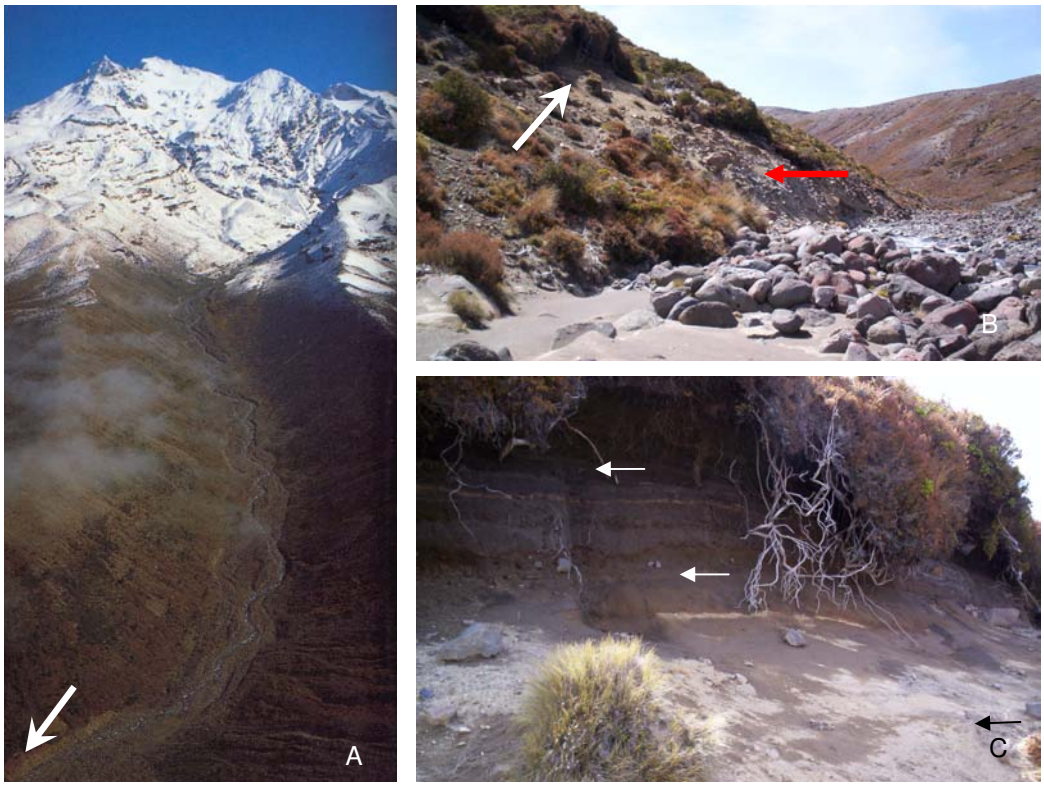

Figure 8.3 The location of tephra beds found in this study. (A) Aerial photograph looking up the Wahianoa Valley (looking North West). The arrow points at the location of tephra beds found at the base of the western ridge (Williams, 2001). (B) Close-up of the location of tephra beds (black arrow). The outcrop is about 15m above the riverbed and is deposited on conglomerate with a sandy matrix (red arrow). (C) Outcrop of tephra beds (arrows).

The Taupo Pumice deposit is relatively thin (c.3cm) at the area of interest (Fig. 8.3 C and Fig. 8.5). Overlying the Taupo Pumice is a layer (c.15cm) of sand (sample 02c-8) with interbedded clasts that are primarily angular to very angular (c.5cm in diameter). The upper boundary of the deposit is strongly oxidised. This is overlain by dark coloured sand and a layer of andesitic tephra. The sand is interbedded by a thin oxidised layer of coarser particles and a layer of light coloured sand that contains fine pumice fragments and imogolites. Overlying the sand deposit is at least one layer of andesitic tephra, which is possibly part of the Tufa Trig Formation (c.1800 yr BP Donoghue, 1991).

Underlying the Taupo Pumice is a thick layer of sand, which is interbedded by at least one smaller deposit of coarser particles. This layer also shows strong oxidation. A thin layer (c.1cm) of rhyolitic tephra is interbedded in the sand deposit. This tephra is very finely grained and white in colour. It is not possible to identify this tephra by its physical

properties alone. It is possible that it is either the Mapara tephra (2100 yr BP, Vucetich & Pullar, 1973) or the Waimihia tephra (3410 ±40 cal. yr BP, Alloway *et al,* 2007) as identified by Donoghue (1991) near the Tufa Trig station (Fig. 1.6). Both tephras are derived from the Taupo Volcanic Centre.

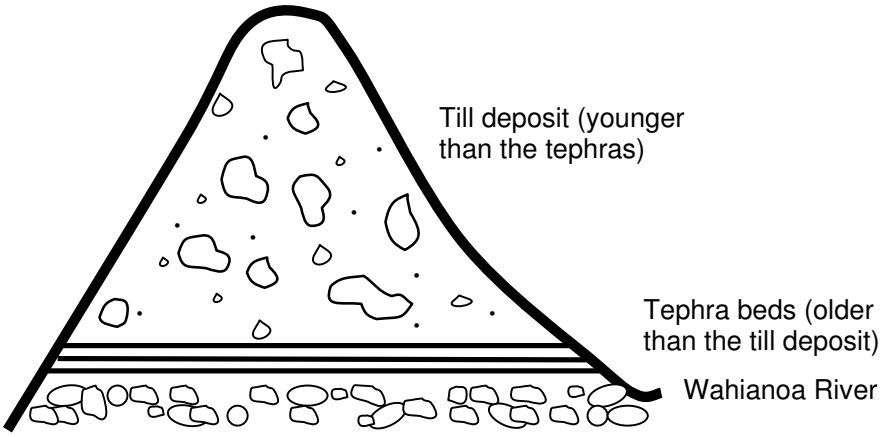

Figure 8.4 Cross-section through the western moraine showing the relationship between tephra beds found at the base of the furthest extent of the western lateral moraine. This relationship shows that the till deposit must be younger than the tephras as they are deposited *in situ*.

The outcrop in question overlies a thick deposit of conglomerate (Fig. 8.3 B). The clasts appear to be primarily sub-angular and sub-rounded. Therefore, it is difficult to determine if the deposit has formed due to fluvial or glacial action. The Wahianoa River is currently cutting into the ridge at that particular point, hence exposing the deposit. It is not certain how deep the river has incised into the sediment as further research is required. During glacial times the river will have transported greater volumes of water and sediments. Because of the larger volumes of ice available during cooler climate phases, lahars were likely to be more frequent and extensive. If the conglomerate deposit is tillite, it would have formed before the first tephra deposit above this unit. No clear boundaries were identified, as the section was unstable and difficult to work on. Therefore, it is not certain if the till deposits are the result of one glacial event or more. It is possible that some older till deposit (such as an end-moraine) was overtopped by a readvance of the glacier. There are further ridges on the eastern side that might be the remnants of Pleistocene glacial advances. However, it appears that the moraines of interest are the result of a glacier advance that occurred during the LIA, possibly at the same time as the South Island readvance (section 2.2.5).

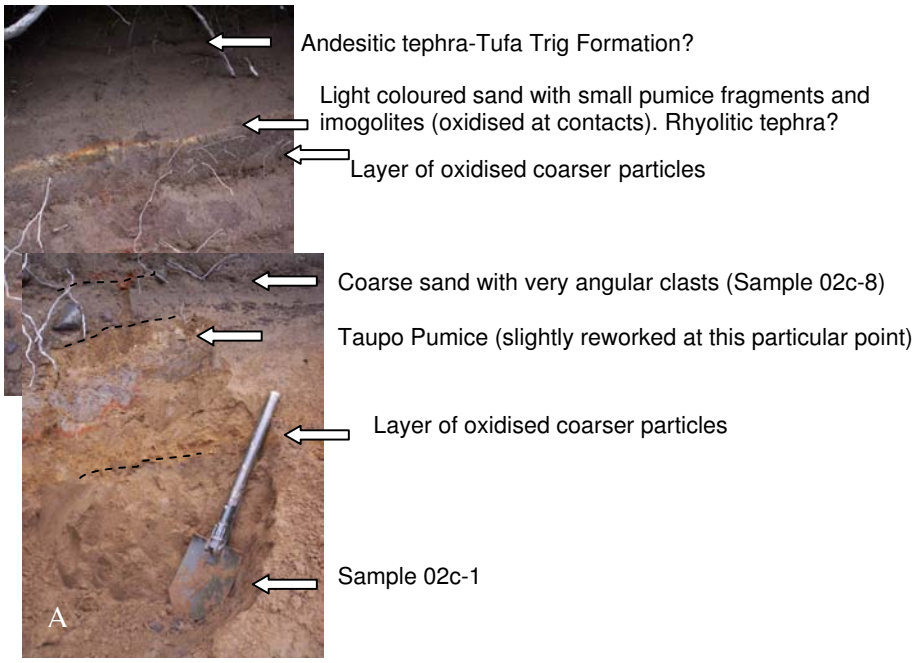

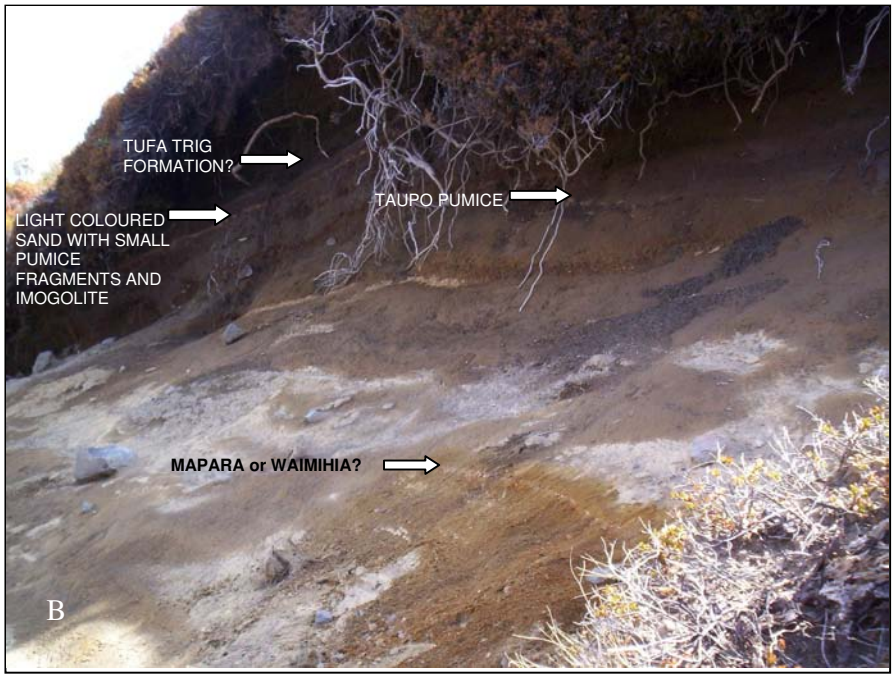

Figure 8.5 Tephra deposits found at the base of the western lateral moraine. The Taupo Pumice is deposited as a thin layer below a unit of angular clasts imbedded in sand. As the tephras are *in situ* they can be used as marker beds to identify the age of the moraines. (A) shows a close-up of the upper section of the outcrop and its individual layers. (B) shows the oldest tephra in context with the upper section. If the andesitic tephra at the upper boundary of this outcrop is part of the Tufa Trig Formation than the upper till deposit is younger than about 1800 yr BP (Donoghue, 1991).

8.1.8 Volcanoes and Glaciers

Many present volcanoes reach altitudes that are above the current snow lines. For example, most of the Cascade volcanoes are covered by glacial ice (Harris, 1988). During an eruption glacial and volcanic processes can interact. Subglacial eruptions are very common in Iceland. For example, the Vatnajökull, the largest glacier of Europe, is underlain by six active volcanoes (Gudmundsson *et al.,* 1997). Subglacial eruptions in Iceland often lead to jökulhlaups, which are major floods of debris-laden glacial meltwater (Schmincke, 2004).

It has been identified that table mountains are the result of subglacial eruptions (Werner & Schmincke, 1999), which first produce a meltwater lake and then the formation of pillow lavas, dikes and hyaloclastites (granulated lava). This is followed by pyroclastic eruptions and the formation of eruption columns. The subaerial stage produces a lava fountain and lava sheets. At that stage the meltwater lake is replaced by massive hyaloclastites. After the glacial ice has retreated, a flat-topped mountain remains. This table mountain has steep upper cliffs and a plateau made of subaerial lava flows (Werner & Schmincke, 1999).

As Mt Ruapehu grew partially in the presence of ice, it is important to consider some of the aspects that arise from this. Stevenson *et al.* (2006) have identified three types of evidence that might be present in a volcanic/glacial environment: i) the interaction of lavas and tephras with meltwater; ii) the confinement of eruptive products by the presence of snow and ice; iii) and the effects of glacial erosion. Gardner *et al.* (1994) also suggest that lahars are very common at glacier-covered stratovolcanoes. It is difficult to evaluate the extent of the ice/fire interactions on Mt Ruapehu as this study focused on the debris deposits of the Wahianoa valley alone and not on the glacier. Because the summit area of Ruapehu is still heavily glaciated it is certain that lavas and tephras have interacted with meltwater. Since the current vent is filled with water that is derived from the glaciers, rising magmas come into contact with the lake water first to cause phreatic and phreatomagmatic eruptions (Hackett & Houghton, 1989). Hydroclastic deposits are typically low in vesicularity, glassy and the ash shards have a strong angularity (Schmincke, 2004).

It is possible that ice or snow confinements have taken place during the history of Ruapehu, but it is beyond this study to provide evidence for this hypothesis. If eruptive products are constrained by thick glacial ice their forward movement is restricted (Mee *et al.,* 2006). Erosion features caused by glacial ice are common on Ruapehu and are the focus of this study. However, no research has been done to provide the necessary evidence to support this hypothesis until now. There is immense potential for further research in glaciology and especially in glacial geomorphology on Mt Ruapehu. It was suggested (Hackett, 1985; Williams, 2001) that volcanic activity together with glacial erosion has shaped the current Ruapehu massif.

Lahars are very common on Mt Ruapehu and represent one of the biggest volcanic hazards (Hodgson, 1993; Neall *et al.,* 1999; Donoghue & Neall, 2001). This is mainly due to the fact that the current vent is filled with a crater lake, which periodically overflows and causes lahars. The Te Heuheu Formation (Fig. 8.6) is the oldest identified laharic deposit (>22ka – 14700 yr BP) (Donoghue & Neall, 2001). It is also the most distributed formation. Lahars must have been extremely common and extensive during that time, which coincides with the LGM and the termination I period (Alloway *et al.,* 2007) (section 2.2). Because of the greater volumes of ice the Crater Lake will have filled much faster than at present. The severity of lahars must have been higher because more ice, snow and meltwater was available to incorporate vast quantities of debris. Furthermore, this lahar surface has been interpreted to represent syn-eruptive sedimentation during a time when Ruapehu was most active (Donoghue & Neall, 2001).

Pseudopillow fractures were found in the Santa Gertrudis lava, Nevados de Chillan volcano, Chile, and have been identified as snow or ice contact features (Mee *et al.,* 2006). When lava flows over an area of snow or ice, the base of the lava cools more rapidly and contraction occurs. Steam rises through the fractures and causes further cooling and contraction. This process leads to primary fractures in the lava. Because of the melting snow/ice, the base of the flow becomes unstable and secondary fractures develop. In the Santa Gertrudis lava it has been suggested that a further pulse of subaerial lava might have emplaced the snow-contact lava (Mee *et al.,* 2006). It can be assumed that this process has

occurred on Mt Ruapehu, especially during the last two major cone forming events: the Mangawhero Formation (60ka-15ka) and the Whakapapa Formation (<15ka) (Fig. 1.11). However, it is beyond this study to provide the necessary evidence.

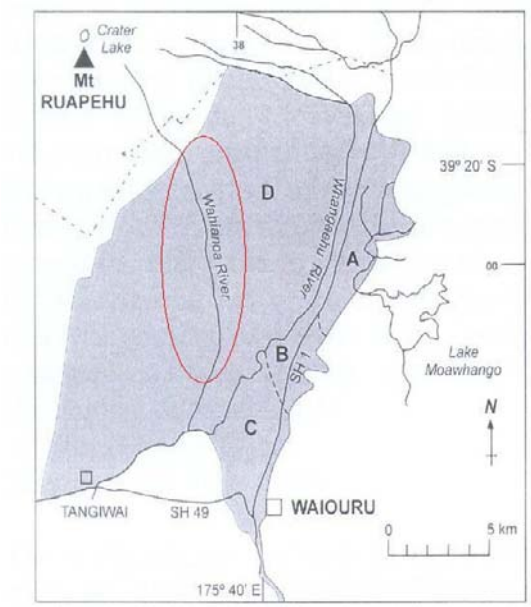

Figure 8.6 The distribution of the Te Heuheu Formation (>22ka – 14700 yr BP). The circled area represents the area of interest (Donoghue & Neall, 2001).

The eruption of St. Helens in 1980 destroyed 70 percent (3.5 billion cubic feet) of the mountain's ice cover (Harris, 1988). Hot ash fell onto the surfaces of the glaciers, which caused rapid melting of the ice. Rock fragments and hot ash mixed with meltwater and major lahars were generated. But air fallen particles do not always cause lahars. If a thin layer of ash covers the surface of a glacier it can enhance ablation rates because the particles absorb heat and melt the ice (Knight, 1999). However, if the supraglacial layer of volcanic ash is thick enough to insulate the ice from incoming solar radiation, the ablation rate will decrease and the glacier advances (Adhikary *et al.,* 2002; Rivera *et al.,* 2006). It is often difficult to measure the ablation rate under a debris/ash layer because the surface is difficult to work on and the ablation rate varies from place to place (Nakawo & Rana, 1999). Therefore, research is often limited.

8.2 CLAST MORPHOLOGY

8.2.2 Co-variance for the lateral moraines

The clast morphology of the two lateral moraines has no particular pattern. The western moraine shows low to medium C_{40}/RA values, whereas the values for the eastern ridge are slightly higher (section 4.5). Because the overall results for shape and roundness are not very conclusive, the C_{40}/RA values were plotted up on a co-variance diagram (Fig. 8.7 and 8.8). Figure 8.7 shows the RA plotted against the C_{40} for the two lateral moraines. The graph shows that the values for the eastern deposit are slightly higher than the ones from the western moraine. In an ideal situation the clasts that were transported passively would be plotted at the highest point of the graph and those that were transported actively at the lowest points (Fig. 4.3).

It is interesting to see that the overall results from the Wahianoa Valley fall on a line between these two extremes, which could suggest that the clasts found on Mount Ruapehu are a mixture of clasts from the two transport zones (active and passive) (Benn & Ballantyne, 1994). The results show that the eastern ridge contains more clasts that appear to have been transported passively (High RAs and high C_{40}) and those on the western ridge actively (low RAs and low C_{40}). This could be due to the fact that the lava flows are more extensive on the eastern side. As discussed in chapter one, the lava flows on Ruapehu form blocky and sheet-like clasts when eroded and if transported in the high level transport zone these clasts will remain blocky and possibly sub-angular to angular. The method developed by Benn and Ballantyne (1994) focused on hard bedrock mainly. The Wahianoa Glacier moved over unconsolidated material and was presumably strongly debris mantled. This study shows that many processes interact in a glacial/volcanic environment and that the morphology of supraglacial debris is determined by provenance and does not always have a slaby or elongated shape.

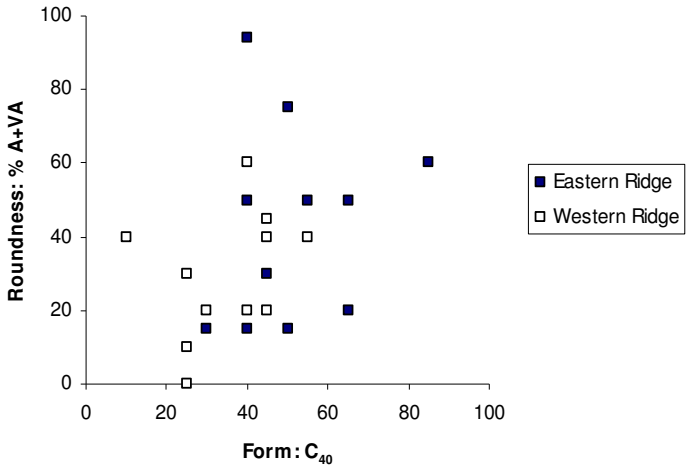

Figure 8.7 Co-variance diagram showing the C_{40}/RA relationship between the ridge deposit. The results form a band, which could suggest a mixture of clasts of both transport zones. The western deposit indicates that more clasts are derived from the active zone and the eastern deposit from the passive zone.

8.2.3 Co-variance for base samples, maximum moraine and a small of on the western ridge

The co-variance diagram for the remaining results (Fig. 8.8) indicates a trend for the small lobe at the distal end of the eastern ridge and the base deposits. However, the results from the small lobe on the western ridge show a vertical trend, indicating a change in roundness but very little in clast shape. This could be due to the fact that these clasts have derived from the main glacial system by overflowing. In order for the clasts to have been moved over the edge of the main ridge, these clasts must have been transported on or near the surface of the ice and definitely not from the base of the glacier. Therefore, according to Benn and Ballantyne (1994) the clasts should have high C_{40} values. However, the results show low values.

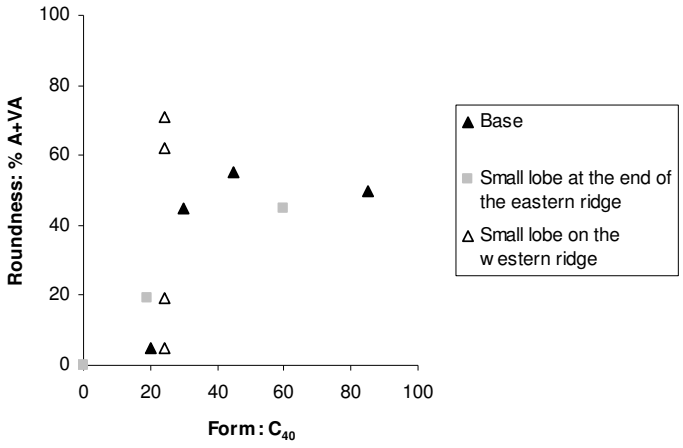

Figure 8.8 Co-variance diagram showing the C_{40}/RA relationship between the possible terminal moraine, the base of the ridges, and the second lobe on the true right. The latter being the only deposit showing a vertical trend. This trend indicates an increase in roundness and little modification in shape.

The roundness increases with distance in the small lobe of the western ridge, which means that the clasts must have undergone great abrasive forces once they had entered the 'miniature' glacial system. The ridges of these 'over flows' are quite high and become thinner away from the source. They also consist mainly of boulders that appear to increase in size down-valley. It is less likely that these boulders are lava bombs, as they are far away from their source and only glacial activity can transport large boulders for long distances.

8.2.4 Discussion

Because the main research in clast morphology has been done in non-volcanic settings (e.g., Benn & Ballantyne, 1993 and 1994), the results might not be comparable. Lava flows form blocky and platy jointing and are therefore very angular and sheet-like when eroded (Hackett, 1985). The majority of clasts identified here is a medium between blocky and elongated (Fig. 4.9 and 4.10). This is especially true for the eastern ridge. This study suggests that a large quantity of debris has been transported supraglacially. Therefore, a low C_{40} value would not necessarily indicate active transport. It is very likely that the moraines represent a mixture of clasts, as a large portion of subglacial sediment was also transported in a deformable bed. Nearly all clasts are sub-angular and sub-rounded (low RA values), which was related to active transport (Benn & Ballantyne, 1994). The matrix of the

till deposit consist of non-cemented sand-size particles (section 6.3), which possibly are derived from the pyroclastic material of the Ruapehu massif, rather than from attrition. It is likely that this has influenced the rate of abrasion on clasts. At the distal end of the western moraine many larger clasts were very rounded (Fig. 8.9), although the results for the smaller clasts identified sub-angularity and sub-roundness. However, the hardness of the rock (mainly andesitic) will have played an important role in roundness.

Figure 8.9 Maximum western moraine, looking down valley. Many clasts show strong roundness.

8.3 MACROFABRICS

8.3.2 Discussion of results

The macrofabrics of the Wahianoa lateral moraines are not very consistent. This can have several reasons. The number of megaclasts increases closer to the mountain. As large lava bombs fall in close proximity to the eruption source, it is very likely that many of the large boulders have originated from such events. Figure 8.10 and 8.11 present some examples. However, some lava bombs may also have fallen on the surface of the glacier and may have been transported as supraglacial debris.

As the moraines consist of unconsolidated diamictons, clasts are naturally more unstable. Therefore, post-depositional processes may have acted on some clasts (e.g. gravity). It also appears that the ice-flow direction of the glacier was not uniform as the moraines indicate (Fig. 5.6). This was possibly caused by variations in sediment supply, the time scale in which the debris was deposited (Matthews & Petch, 1982) and the confinement of the glacier near the accumulation zone.

The morphology of the debris ridges (section 1.3.4) has shown that the western ridge has a much gentler slope on the ice proximal side and the ridges become narrower. The slope gradient of the valley glacier cannot have been very steep, as the base of the valley and the surface of the ridges is quite gentle. The clast morphology results have identified a slight asymmetry, which is possibly caused by different quantities of source rock from each side of the ridges. This, in addition to the fact that the Wahianoa Valley has been (and still can be) a pathway for lahars, will have had a great impact on the fabric of the till deposits. The Wahianoa Glacier was probably strongly debris covered and the majority of clasts did not have to undergo great modification. As less strain is exerted on supraglacial and englacial clasts, they were not forced to re-orientate due to basal processes (Li *et al.,* 2006). Furthermore, when subglacial deformation occurs, a layer of debris rich ice moves together with a layer of deforming till over a region of stable till (Hambrey, 1994). Because this process reduces the strength of the sediment, weaker fabric strengths are associated with deformable beds (Hart, 1994).

8.3.3 Glacier overflow

This research also suggests that the Wahianoa Glacier has breached the top of the confining western lateral moraine. This is shown in numerous smaller lobes that run off the main deposit. The orientation and mean direction of these lobes coincide with the direction of the middle section of the main moraines (Fig. 5.8). It appears as if there was a larger quantity of ice and debris feeding the glacier from the area where the lava flows are thicker and more abundant (eastern ridge, close to headwall). Because Ruapehu was possibly covered by an icecap, ice flow was not valley restricted. It is possible that this has caused a change in ice-flow direction and the overflow of ice over the main moraines. In that situation, clasts on the moraine would have been more orientated towards the area of overflow.

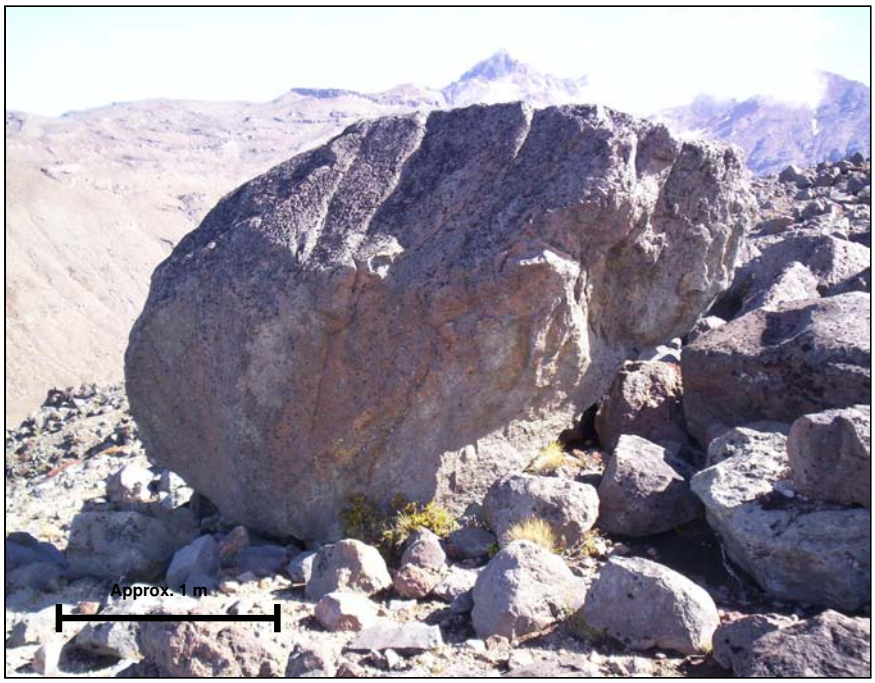

Figure 8.10 A very large boulder deposited in close proximity of the vent of Ruapehu. It is possible that this boulder is the result of a volcanic eruption rather than of glacial activity (looking northwest).

Figure 8.11 An enormous boulder that shows post-depositional welding of pyroclastic fall deposit. N. B. Only the side facing the volcano was influenced by this process.

8.3.4 Problems with method

It was attempted to dig pits into the ridges to take measurements from rock *in situ*. However, it turned out to be nearly impossible, as the ridges consist mainly of clasts (>gravel-size). A hard labour of two hours resulted in one 'pit' of a depth of < 30cm. It was extremely difficult to measure the inclination of boulders as it mostly reflected the slope angle of the moraines and many boulders are resting on other boulders/clasts. Figure 8.10 highlights these problems. The two clasts in the foreground and the boulder on the left of the photograph are resting on smaller clasts. The a-axis of the boulder in the centre is pointing towards the west and the inclination of the same axis is the same as the slope angle of the ridge. Some boulders, as the one on the right in the photograph, are tilted. This made it almost impossible to identify the inclination of the a-axis. Therefore, this study concentrated on the orientation of boulders along the a-axis only.

Figure 8.12 Photograph that shows the problems encountered when the measurement of the inclination of boulders was attempted. Many boulders are resting on other clasts, are tilted or simply reflect the slope angle of the debris ridge.

8.3.5 Mean direction of clasts

The results have shown that the clasts on the eastern moraine have a west/east trend and the clasts from the western ridge are orientated north-west/south-east. The fabric results and the orientation of the moraines suggest that the ice-flow direction was not uniform. This was possibly caused by differences in sediment supply. Figure 8.13 shows the mean direction of all samples of both moraines. The direction is 116.86°/296.86°, which is relatively close to the overall orientation of the lateral moraines (Fig. 5.8). However, the fabric strength is not strong enough to come to a definite conclusion.

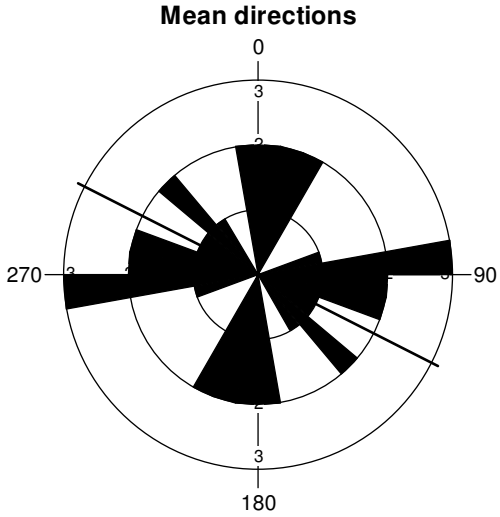

Figure 8.13 Diagram showing the mean vectors or mean directions for the Wahianoa Valley debris ridges. The mean vector is 116.86° - 296.86º.

8.4 GRAIN-SIZE DISTRIBUTION

Variations in grain-size are generally related to different modes of transport and environmental settings (Greenwood, 1969). However, it is also suggested that particle size should be used in conjunction with other criteria, such as clast morphology, fabric analysis and so on (Hoey, 2004; Evans & Benn, 2004). This is because the grain-size distribution in a particular environment depends on other factors, such as lithology and hardness. The results of this study show that the grain-size distribution of the Wahianoa lateral moraines is very similar. Figure 8.14 and 8.15 show summarising diagrams of the results. The grain populations are primarily of sand size and are possibly the result of eroded pyroclastic

material, rather than from attrition. However, the outcrop samples from both moraines are very different from the surface samples. This suggests that different processes have produced the sediments or they are derived from a different source, such as volcanic eruptions.

8.4.2 Ternary diagram of the sand/silt/clay ratios

Figure 8.16 shows the sand/silt/clay ratios in the form of a ternary diagram. Over ninety percent of all samples collected are of sand size, of which about fifty percent is coarse sand, twenty percent medium sand, ten percent fine sand and about five percent very fine sand. Only 0.5 percent of the remaining fractions are of clay size. Subglacial processes generally produce finer sediment (silt size) because of attrition. Only the outcrop samples from the eastern ridge contain silt size grains. The trends of the frequency curves (section 6.3) are very similar for the majority of samples. This suggests that the same processes have acted on the sediments and that the lithologies are similar.

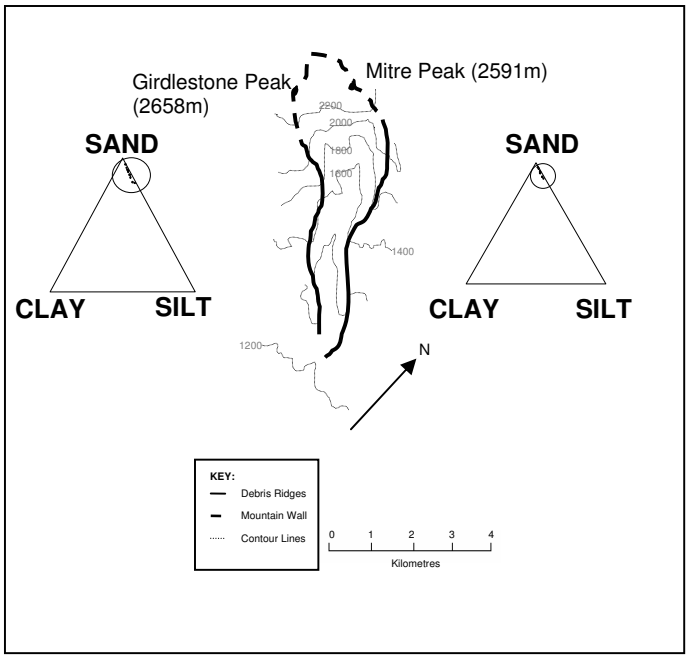

Figure 8.14 The grain-size distribution of the western and eastern ridges. The sediments consist primarily of sand.

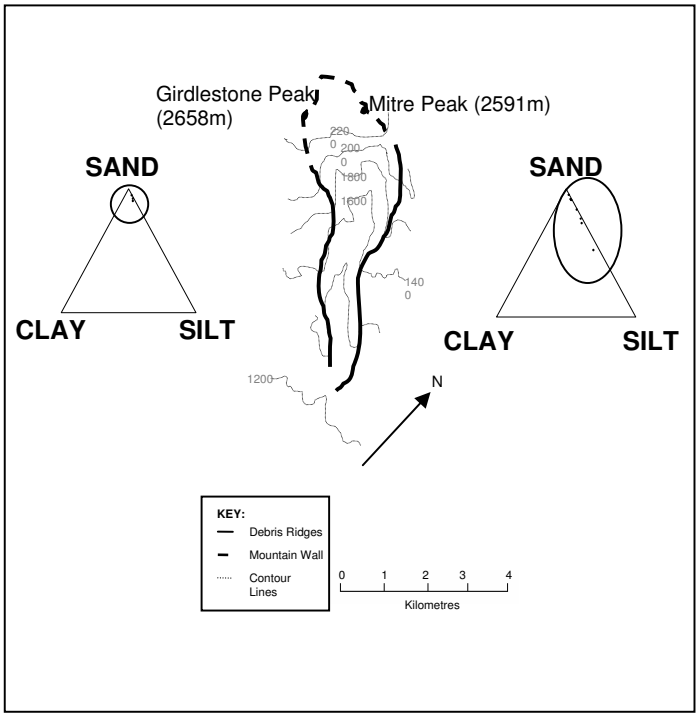

Figure 8.15 The grain-size distribution of the samples found in outcrops of both ridges. The samples from the western ridge are mainly sand. The samples from the eastern ridge are mainly silty sand.

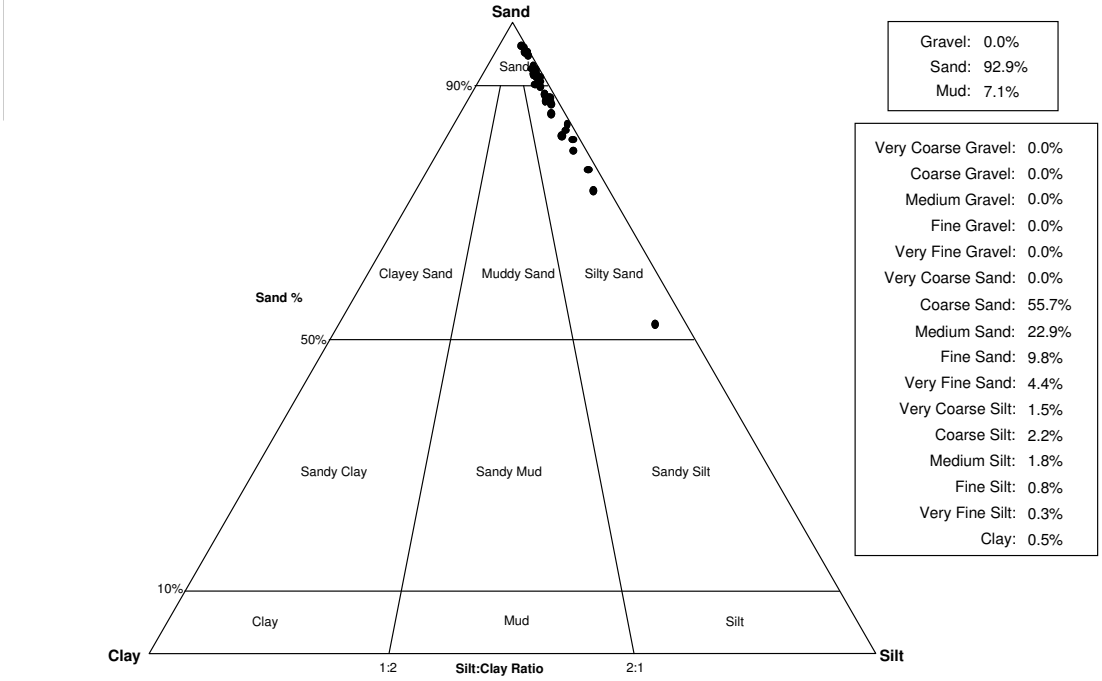

Figure 8.16 Ternary diagram showing the sand/silt/clay ratios for the samples collected from the Wahianoa debris ridges. The majority of samples are coarse to fine sand. Less than 10 percent is of silt size and only 0.5 percent of the total is of clay size.

8.4.3 Mean vs sorting

Figure 8.17 clearly shows a strong clustering around a mean size of two phi and a sorting size of two and three phi. This means that there is a strong increase in mean size but only a very small increase in sorting. The diagram also highlights the difference of the outcrop samples on the eastern ridge. These grain populations in addition to the outcrop samples from the western ridge suggest a difference in processes and possible lithologies compared to the rest of the samples. As mentioned before, only three samples out of a total of sixteen layers are shown here. In section 8.1.7 it was explained that this outcrop contains several layers of tephras and that it must have been deposited before the final advance of the glacier. Therefore, the outcrop deposits have formed during non-glacial times.

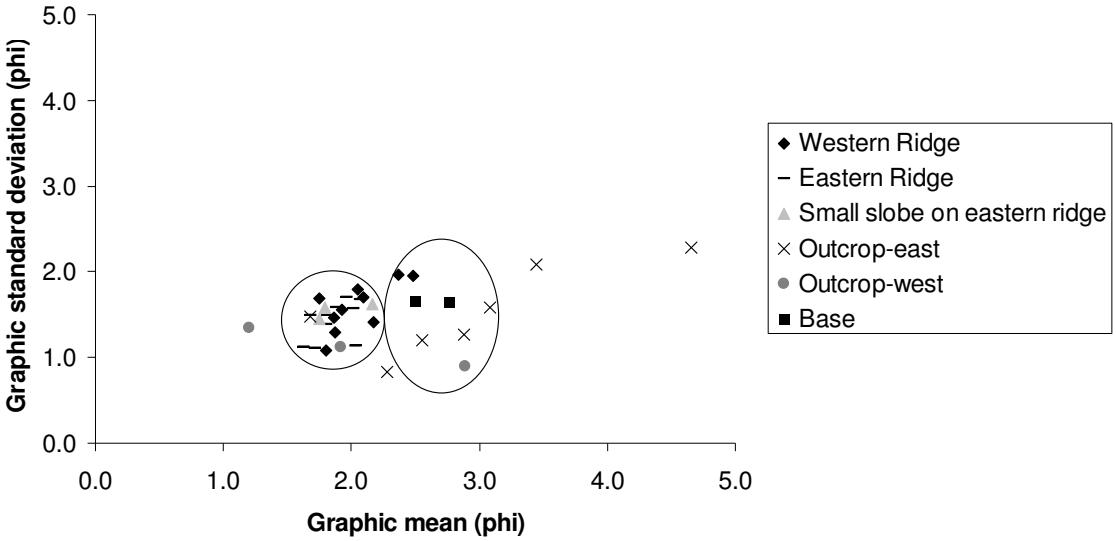

Figure 8.17 A scatter diagram showing the mean plotted against sorting. Overall, there is a dramatic increase in mean sizes but only a very small increase in sorting. The samples are strongly clustered at a mean size of two phi and a sorting size between one and two phi.

8.5 SEM ANALYSIS

The study of microtextures for this research has been done in two analyses. The first analysis looked at the bulk of grains from both moraines. The second analysis studied magnetites only. The results for the SEM analysis have identified that most grains from the Wahianoa moraines exhibit sharp and round edges. The first analysis also identified high and low relief, conchoidal fracture pattern, fracture faces and linear steps. The magnetites have a higher relief than the bulk grains and they also exhibit adhering particles and linear steps. Although some of the features are common in glacial environments (e.g., sharp edges, adhering particles, conchoidal fractures), there are others that are less frequent, such as round edges and low relief (Mahaney & Kalm, 2000).

Previous studies have analysed quartz grains, but because Mt Ruapehu is an andesitic volcano, no quartz is present. Therefore, magnetite was used as it has similar properties to quartz and is easily separated from the bulk of grains. Quartz grains typically show conchoidal fractures, adhering particles, high relief and sharp edges in a glacial environment, especially with increasing ice thickness (Mahaney, 1995). The magnetite grains display most of these features; however, they also show round edges and very few

conchoidal fractures (Fig. 7.11). Therefore, it is not certain if the grains show typical glacial features.

As noted before (section 8.4), it is possible that a large quantity of grains are pyroclasts. Because Mt Ruapehu is partially constructed of pyroclastic material, which is easily erodible, a large amount of smaller particles will have fallen onto the glacier's surface to be transported subglacially and englacially. Therefore, many grains could still exhibit microtextures that were acquired prior to glacial transport and deposition. Microtextures that are typical for glacial environments are produced at the basal zone, due to shear stresses (Clark, 1989). The samples for this study were primarily sampled from the surface of the moraines. It would be more desirable for future research to collect grains from outcrops close to the base. Because the Wahianoa Glacier must have moved over a deformable bed, a large portion of grains will have been transported in the layer of deformable till and within the ice. Shear stresses are generally lower in a deformable bed and there will be little friction (Knight, 1999). Therefore, grains should exhibit fewer glacial microtextures.

Chapter 9
CONCLUSIONS

9.1 OBJECTIVES REVISITED

The focus of this study was the Wahianoa valley, Mt Ruapehu. This study was the first to apply established field techniques in glacial geomorphology on this mountain. Because very little research has been done so far to reveal the glacial history of the volcano, the main objective was to provide evidence that the Wahianoa debris ridges are true moraines. Four diagnostic criteria were used to identify the extent of glacial deposits and to reconstruct the transport pathways of the Wahianoa Glacier: clast morphology, macrofabrics, grain-size distribution and the microtextures of individual particles.

9.1.2 Evidence for glacial activity

The main objective of this study is to provide evidence for the hypothesis that the Wahianoa debris ridges are true glacial moraines and are not the result of volcanic and/or fluvial activity. The Wahianoa Valley has a prominent U-shape, which suggests glacial activity. The debris deposits consist of unconsolidated, poorly sorted diamictons of different lithologies. There are many large boulders along the surface of the deposits. Only two processes could have formed this type of deposit in a volcanic environment: glacial activity or lahars. Although lahars produce unconsolidated and poorly sorted deposits of which clasts can exhibit striae, it is not likely that the Wahianoa debris ridges are the result of such events. This is due to the fact that lahars do not form ridges neither do they produce U-shaped valleys. In addition to the morphological evidence, there are further signs of glacial activity. Many clasts of the debris ridges have faceted and polished surfaces, polished grooves and striae. These features are all typical products of glacial erosion. Therefore, it is certain that the Wahianoa ridge deposits are true lateral moraines that consist of glacial till.

9.1.3 The reconstruction of the transport pathways of the Wahianoa Glacier

The clast morphology results have identified a slight asymmetry in the lateral moraines, which can be related to differences in debris supply feeding the glacier. The majority of

clasts is sub-angular to sub-rounded and has a blocky to elongated shape, which has been related to erosional properties of lava flows on Ruapehu. The direction of the moraines is not uniform and the macrofabrics are not very consistent partially because of that. However, the mean direction of all samples is 116.86°/296.86°, which is similar to the overall orientation of the moraines. The moraines have a more eastward direction (approx. 120°) at the headwall of the glacier. The centre of the moraines is south (approx. 160°) orientated and the maximum moraines have a south-east direction (approx. 140°). There are several smaller lobes running off the western ridge on the ice distal side. The mean direction of those clasts coincides with the direction of the centre of the main moraines. This study suggests that the ice from the Wahianoa Glacier overflowed the western moraine to form smaller moraines on the ice distal side. This is supported by the fact that the roundness of clasts from the lobes increases with distance and because many large erratics can be found at the furthest extend of these deposits. This overflowing must have been caused by a greater ice and sediment supply when the volcano was covered by an ice cap.

The results for the grain-size distribution have shown that the matrix of the till deposit consists primarily of particles of sand size. This means that provenance and the mode of transport and deposition has been the same. The absence of clay particles further supports the hypothesis that the Wahianoa Glacier was strongly debris mantled. The particle sizes from samples collected from two outcrops near the base at the maximum moraines are different from the rest. This has been related to a non-glacial depositional environment. It is possible that the Wahianoa Glacier had greater advances prior to the LIA, but it is beyond this study to provide the necessary evidence for this hypothesis.

The SEM analyses of individual particles from the moraine deposits have shown some similarities with microtextures that are common in glacial environments. However, many non-glacial textures were identified also. It has been concluded from the analyses that it would be of advantage for future studies to collect samples *in situ* only and that magnetite has great potential for research where no quartz is present. The study of microtextures of individual grains is still not completely recognised by glacial geomorphologists and there is

no known research that has used magnetite instead of quartz. Therefore, the results of this part of the study are more speculative than conclusive.

9.1.4 The implications of an active volcano on a glacial system

The fact that Mt Ruapehu is an active volcano had great implications on the Wahianoa glacial system. The poor stability of the Ruapehu massif and laharic events have lead to a ring plain that consists primarily of unconsolidated deposits. Therefore, the Wahianoa Glacier moved over a deformable bed and transported vast volumes of debris. This instability also caused that a large amount of supraglacial and englacial debris was transported by the glacier. This has lead to the formation of high lateral moraines that consist of a mixture of subglacial, supraglacial and englacial debris. Because lava flows tend to produce blocky and sheet-like clasts, many supraglacial clasts exhibit this shape. In addition, the moraines are unstable and clasts tend to move more easily. This has influenced the orientation of clasts. Because Mt Ruapehu is still active, new deposits will have formed over older deposits. The Wahianoa Valley has been the transport pathway for lahars in the past. These will have moved over the ice surface and some might have moved subglacially. This will have affected the orientation of clasts greatly. Individual grains can show volcanic and glacial microtextures as they have been exposed to both processes.

9.1.5 Conclusions

This study has shown that the Wahianoa Glacier has moved over a deformable bed. This means that the glacier has transported large volumes of sediment at the basal zone and possibly at a fast rate. The glacier has also transported large volumes of supraglacial and englacial debris, because of the natural instability of the Ruapehu massif. Lava flows tend to be more angular and sheet-like when eroded. Therefore, the morphology of supraglacial and englacial debris is blockier than in non-volcanic environments. Hence roundness is a greater indicator for the mode of transport than shape. The ice-flow direction has changed possibly due to variations in sediment and ice supplies (possibly from the summit area). This also might have caused the ice to overflow the western moraine to form smaller lobes. Because of the dynamic environment the orientation of clasts is not very consistent. This study was the first to use magnetite as an indicator for microtextures and it has shown some

potential. This study has proposed that the Wahianoa moraines are the result of a LIA advance. However, it is possible that the glacier had more advances during the Pleistocene.

9.2 FUTURE RESEARCH OPPORTUNITIES

This study has identified the great potential for further research. It has been the first attempt to unfold the glacial history of Mt Ruapehu. Previous studies have used topographic and aerial photo analyses, rather than using techniques in glacial geomorphology. The results have shown great complexity because of the interaction between glacial and volcanic processes. This study has focused on the Wahianoa glacial moraines only. There is great potential for further research on the remaining glaciers. For example, there are two debris ridges in front of the Mangaehuehu Glacier that are likely to be lateral moraines from a glacial advance during the LIA.

9.2.2 Tephrochronology

This study has found some tephras that are located near the base of the western lateral moraine of the Wahianoa Glacier. The Taupo Pumice was identified due to its distinctive physical characteristics. It would be of great interest to analyse the remaining tephras to acquire an absolute date for the moraines. It was attempted to microprobe the oldest tephra found but unforeseen circumstances have prevented the completion of the analysis. It also would be important to attempt the correlation of further tephra deposits found in the area of interest. Donoghue (1991) has mapped the southeastern ring plain in detail. Hackett (1985) mapped the extent of the four main lava formations of the volcano. Therefore, the study only concentrated on the Ruapehu massif and not so much on the ring plain. Procter (2003) mapped the Rangipo Planeze, which is located between the eastern moraine of the Wahianoa Glacier and the Whangaehu valley. The purpose of these studies was to place the volcanic history of Mt Ruapehu into a time frame. However, it was not the focus to date the moraines and therefore no samples were collected directly from the moraines.

9.2.3 Optically stimulated luminescence

Optically stimulated luminescence (OSL) is a luminescence dating technique used to date inorganic materials. This technique is only useful in sediment that has been exposed to light

before it was buried. The OSL dating technique of glacigenic sediment is not always successful. Care needs to be taken to which sediment is sampled. Sediment that is transported by a glacier is often not exposed to sunlight (not bleached) before deposition. This makes the sediment unsuitable for the OSL dating technique. However, the technique has been successfully applied by using supraglacially derived and transported sediment that has been deposited due to gravity in frontal and lateral moraines (Benn & Owen, 2002). Sandy and silty sediment from the top of debris-flow units in terminal and lateral moraines have also been successfully dated by using the OSL technique (Richards, 2000). This study has attempted to use the OSL dating technique and two samples from both lateral moraines were collected. However, a delay in the processing of the samples has prevented a successful analysis.

9.2.4 The use of magnetite for the SEM analysis of microtextures

Quartz is the most common used mineral in the analysis of microtextures on individual grains. Because quartz is less common in some countries, such as New Zealand, Iceland, South America, the use of an alternative mineral to identify unknown ridge deposits could be extremely useful. This study has attempted the use of magnetite to identify microtextures that are common in glacial environments. Although the results were not very conclusive, the potential of this mineral has been presented. If magnetite could be used as a discriminator for glacial environments there would be great possibilities for further research in countries where quartz is less abundant.

BIBLIOGRAPHY

1) Addison, K. 1981. The contribution of discontinuous rock-mass failure to glacier erosion. *Annals of Glaciology,* 2:3-10.
2) Adhikary, S., Yamaguchi, Y. & Ogawa, K. 2002. Estimation of snow ablation under a dust layer covering a wide range of albedo. *Hydrological Processes,* 16(14):2853-2865.
3) Adkin, G. L. 1912. The Discovery and Extent of Former Glaciation in the Tararua Ranges, North Island, New Zealand. *Transactions of the New Zealand Institute* 44:308-316.
4) Alloway, B. V., Lowe, D. J., Barrell, D. J. A., Newnham, R. M., Almond, P. C., Augustinus, P. C., Bertler, N. A. N., Carter, L., Litchfield, N. J., McGlone, M. S., Shulmeister, J., Vandergoes, M. J., Williams, P. W. & NZ-INTIMATE members. 2007. Towards a climate event stratigraphy for New Zealand over the past 30 000 years (NZ-INTIMATE project). *Quaternary Science,* 22 (1):9-35.
5) Almond, P. C., Moar, N. T. & Lian, O. B. 2001. Reinterpretation of the glacial chronology of South Westland, New Zealand. *New Zealand Journal of Geology and Geophysics,* 44:1-15.
6) Andrews, J. T. 1971. *Techniques of Till Fabric Analysis.* Technical Bulletins of the British Geomorphological Research Group.
7) Bahr, D. B., Pfeffer, W. T., Sassolas, C. & Meier, M. F. 1998. Response time of glaciers as a function of size and mass balance. *Journal of geophysical research,* 103:9777-9782.
8) Ballantyne, C. K. 1982. Aggregate clast form characteristics of deposits near the margins of four glaciers in the Jotunheimen Massif, Norway. *Norsk Geografisk Tidsskrift,* 36:103-113.
9) Bell, D. 1888. Additional note to Mr. Bell's papers (p.237-261). *Geological Society. Glasgow, Tr.* vol. 8 p.2, p.341.
10) Benn, D. I. 1994. Fabric shape and the interpretation of sedimentary data. *Journal of Sedimentary Research*, A64(4):910-915.
11) Benn, D. I. 1995. Fabric signature of till deformation, Breidamerkurjokull, Iceland. *Sedimentology*, 42:735-747.
12) Benn, D. I. & Ballantyne, C. K. 1993. Short Communication-The Description and Representation of Particle Shape. *Earth Surface Processes and Landforms,* 18: 665-672.
13) Benn, D. I. & Ballantyne, C. K. 1994. Reconstructing the transport history of glacigenic sediments: a new approach based on the co-variance of clast form indices. *Sedimentary Geology,* 91:215-227.
14) Benn, D. I. & Evans, D. J. A. 1998. *Glaciers & Glaciation*. Arnold, London.
15) Benn, D. I. & Gemmell, A. M. D. 2002. Fractal dimensions of diamictic particle-size distributions: simulations and evaluation. *Geological Society of America, Bulletin,* 114:528-532.
16) Benn, D. I., Kirkbride, M. P., Owen, L. A. & Brazier, V. B. 2003. Glaciated Valley Landsystems. In: Evans, D. J. A. (Ed.). *Glacial Landsystems*. Arnold, London, p. 372-406.

17) Benn, D. I. & Owen, L. A. 2002. Himalayan glacial sedimentary environments: A framework for reconstructing and dating the former extent of glaciers in high mountains. *Quaternary International,* 97-98:3-25.
18) Bennett, M. R. & Glasser, N. F. 1996. *Glacial Geology-Ice Sheets and Landforms.* John Wiley & Sons Ltd., England.
19) Bennett, M. R., Waller, R. I., Glasser, N. F., Hambrey, M. J. & Huddart, D. 1999. Glacigenic clast fabrics: genetic fingerprint or wishful thinking? *Journal of Quaternary Science,* 14 (2):125-135.
20) Bennett, M. R., Hambrey, M. J. & Huddart, D. 1997. Modification of clast shape in High-Arctic Glacial Environments. *Journal of Sedimentary Research,* 67(3):550-559.
21) Blakemore, L. C., Searle, P. L. & Daly, B. K. 1987. Methods for chemical analysis of soils. *N.Z. Soil Bureau Scientific Report* 80.
22) Blott, S. J. & Pye, K. 2001. Gradistat: A grain size distribution and statistics package for the analysis of unconsolidated sediments. *Earth Surface Processes and Landforms,* 26:1237-1248.
23) Boggs, S. 2001. (3rd Ed). *Principles of Sedimentology and Stratigraphy.* Prentice Hall, Inc., New Jersey.
24) Boulton, G. S. 1974. Process and patterns of glacial erosion. In: Coates, D. R. (Ed.). *Glacial Geomorphology.* Bingham, New York, p. 41-87.
25) Boulton, G. S. 1976. A genetic classification of tills and criteria for distinguishing tills of different origin. *Geografica,* 65-80.
26) Boulton, G. S. 1978. Boulder shapes and grain-size distributions of debris as indicators of transport paths through a glacier and till genesis. *Sedimentology,* 25:773-799.
27) Boulton, G. S. 1979. Processes of glacial erosion on different substrata. *Journal of Glaciology,* 23:15-38.
28) Boulton, G. S. & Hindmarsh, R. C. A. 1987. Sediment Deformation beneath Glaciers: Rheology and Geological Consequences. *Journal of Geophysical Research,* 92 (B9):9059-9082.
29) Boulton, G.S. and Jones, A.S. 1979. Stability of temperate ice caps and ice sheets resting on beds of deformable sediment. *Journal of Glaciology*, 24:29-44.
30) Brook, M. S. & Brock, B. W. 2005. Valley morphology and glaciation in the Tararua Range, southern North Island, New Zealand. *New Zealand Journal of Geology & Geophysics,* 48:717-724.
31) Brook, M. S., Purdie, H. L. & Crow, T. V. H. 2005. Valley cross-profile morphology and glaciation in Park Valley, Tararua Range, New Zealand. *Journal of the Royal Society of New Zealand,* (4) 35:399-407.
32) Brown, N. E., Hallet, B. & Booth, D. B. 1987. Rapid Soft Bed Sliding of the Pudget Glacial Lobe. *Journal of Geophysical Research*, 92 (B9):8985-8997.
33) Bull, P. 1981. Environmental reconstruction by electron microscopy. *Progress in Physical Geography,* 5:368-397.
34) Burrows, C. J. 1975. Late Pleistocene and Holocene moraines of the Cameron Valley, Arrowsmith Range, Canterbury, New Zealand. *Arctic and Alpine Research,* 7:125-140.

35) Campbell, S. & Thompson, I. C. 1991. Palaeoenvironmental history of Late Plaistocene depostis at Moel Tryfan, North Wales: evidence from scanning electron microscopy. *Proceedings of the Geological Association,* 102:123-134.
36) Chinn, T., Winkler, S., Salinger, M. J. & Haakensen, N. 2005. Recent Glacier advances in Norway and New Zealand: A Comparison of their Glaciological and Meteorological Causes. *Geografiska Annaler,* 87 (A):141-157.
37) Clark, P. U. 1989. Relative differences between glacially crushed quartz transported by mountain and continental ice- some examples from North America and East Africa: Discussion. *American Journal of Science,* 289:1195-1198.
38) Cole, J. W., Graham, I. J., Hackett, W. R. & Houghton, B. F. 1986. Volcanology and petrology of the Quaternary composite volcanoes of Tongariro Volcanic Centre, Taupo Volcanic Zone. In: Smith, I. M. (Ed.). *Late Cenozoic Volcanism in New Zealand,* pp.224-250. Royal Society of New Zealand Bulletin 23.
39) Cronin, S. J. & Neall, V. E. 1997. A late Quaternary stratigraphic framework for the northeastern Ruapehu and eastern Tongariro ring plains, New Zealand. *New Zealand Journal of Geology and Geophysic,*. 40:185-197.
40) Donoghue, S. L. 1991. (Vol. 1-3). *Late Quaternary volcanic stratigraphy of the southeastern sector of the Mount Ruapehu ring plain New Zealand.* Unpublished PhD Thesis. Massey University, Palmerston North.
41) Donoghue, S. L. & Neall, E. V. 2001. Late Quaternary constructional history of the southeastern Ruapehu ring plain, New Zealand. *New Zealand Journal of Geology and Geophysics,* 44: 439-466.
42) Donoghue, S. L., Neall, V. E., Palmer, A. S. & Stewart, R. B. 1995. The volcanic history of Ruapehu during the past 2 millennia based on the record of Tufa Trig tephras. *Bulletin of Volcanology*, 59:136-146.
43) Dowdeswell, J. A., Hambrey, M. J. & Wu, R. 1985. A comparison of clast fabric and shape in Late Precambrian and modern glacigenic sediments. *Journal of Sedimentary Petrology,* 55:691-704.
44) Drewry, D. 1986. *Glacial Geologic Processes*. Edward Arnold, London.
45) Ehlers, J. 1996. *Quaternary and Glacial Geology.* John Wiley & Sons Ltd. England.
46) Evans, D. J. A. & Benn, D. I. 2004. *A Practical Guide to the Study of Glacial Sediments.* Arnold, Great Britain, London.
47) Evans, I. S. & Cox, N. J. 2005. Global variations of local asymmetry in glacier altitude: separation of north-south and east-west components. *Journal of Glaciology,* 51 (174):469-482.
48) Fischer, N. I. 1993. *Statistical Analysis of Circular Data.* Cambridge University Press, Cambridge
49) Fitzharris, B. B., Chinn, T. J. & Lamont, G. N. 1997. Glacier balance fluctuations and atmospheric circulation patterns over the Southern Alps, New Zealand. *International Journal of Climatology,* 17:745-763.
50) Flegler, S. L., Heckman, J. W. & Klomparens, K. L. 1993. *Scanning and Transmission Electron Microscopy-An Introduction.* W. H. Freeman and Company, New York.
51) Folk, R. L. & Ward, W. C. 1957. Brazos River Bar: A study in the significance of grain size parameters. *Journal of Sedimentary Petrology,* 27 (1):3-26.

52) Folk, R. L. & Weaver, C. E. 1952. A study of the texture and composition of chert. *American Journal of Science,* 250:498-510.
53) Friedländer, B. 1898. Some Notes on the Volcanoes of the Taupo District. *Transactions and Proceedings of the New Zealand Institute,* 31: 498-510.
54) Gardner, C. A., Neal, C. A., Waitt, R. B. & Janda, R. J. 1994. Proximal pyroclastic deposits from the 1989-1990 eruption of Redoubt volcano, Alaska: stratigraphy, distribution and physical characteristics. *Journal of Volcanology and Geothermal Research,* 62(1-4):213-250.
55) Glasser, N. F. & Hambrey, M. J. 2002. Sedimentary facies and landform genesis at a temperate outlet glacier: Soler Glacier, North Patagonian Icefield. *Sedimentology,* 49:43-64.
56) Glen, J. W. & Donner, J. J. & West, R. G. 1957. On the mechanism by which stones become orientated. *American Journal of Science*, 255:194-205.
57) Goodsell, B., Hambrey, M. J. & Glasser, N. F. 2005. Debris transport in a temperate valley glacier: Haut Glacier d′Arolla, Valais, Switzerland. *Journal of Glaciology*, 51 (172):139-146.
58) Grange, L. I. 1931. Conical Hills on Egmont and Ruapehu volcanoes. *New Zealand Journal of Science and Technology,* 12:376-384.
59) Greenaway, R. 1998. *The Restless Land-Stories of Tongariro National Park World Heritage Area.* Department of Conservation & Tongariro Natural History Society, Turangi, New Zealand.
60) Greenwood, B. 1969. Sediment parameters and environment discrimination: an application of multivariate statistics. *Canadian Journal of Earth Sciences,* 6:1347-1357.
61) Gundmundsson, M. T., Sigmundsson, F. & Björnsson, H. 1997. Ice-volcnao interaction of the 1996 Gjalp subglacial eruption, Vatnajökull, Iceland. *Nature,* 389(12):954-957.
62) Hackett, W. R. 1985. *Geology and petrology of Ruapehu volcano and related vents*. Unpublished PhD Thesis. Geology Department. Wellington, Victoria University of Wellington.
63) Hackett, W. R. and Houghton, B. F. 1989. A facies model for a Quaternary andesitic composite volcano: Ruapehu, New Zealand. *Bulletin of Volcanology*, 51:51-68.
64) Haldorsen, S. 1981. Grain-size distribution of subglacial till and its relation to glacial crushing and abrasion. *Boreas,* 10:91-105.
65) Hallet, B. 1979b. A theoretical model of glacial abrasion. *Journal of Glaciology*, 23 (89), 39-50.
66) Hambrey, M. 1994. *Glacial Environments*. UCL Press Ltd, London.
67) Hambrey, M. & Ehrmann, W. 2004. Modification of sediment characteristics during glacial transport in high-alpine catchments: Mount Cook area, New Zealand. *Boreas*, 33:300-318.
68) Hamilton, W. & Krinsley, D. 1967. Upper Palaeozoic glacial deposits of South America and Southern Australia. *Geological Society of America Bulletin*, 78:783-800.
69) Hart, J. K. 1994. Till Fabric associated with deformable beds. *Earth Surface Processes and Landforms,* 19:15-32.

70) Hart, J. K. 1995a. Drumlin formation in southern Anglesey and Arvon, north west Wales. Journal of Quaternary Science. 10:3-14.
71) Hart. J. K. 1996. Subglacial deformation associated with a rigid bed environment, Aberdaron, North Wales. *Glacial Geology and Geomorphology.*
72) Hart, J. K., Hindmarsh, R. C. A. & Boulton, G. S. 1990. Different styles of subglacial glaciotectonic deformation in the context of the Anglian ice sheet. *Earth Surface Processes and Landforms*, 15:227-242.
73) Harris, S. L. 1988. *Fire Mountains of the West: The Cascade and Mono Lake Volcanoes.* Mountain Press Publishing Company, Missoula, US.
74) Harrison, W. 1957a. New technique for three-dimensional fabric analysis of till and englacial debris containing particles from 3 to 40mm in size. *Journal of Geology,* 65:98-105.
75) Harrison, W. 1957b. A clay till fabric: its character and origin. *Journal of Geology*, 65:275-308.
76) Heine, A. J. 1962. *Glacier changes on Mt Ruapehu, New Zealand* - 1957-1962. Proceedings of the Symposium on Variations of the Regime of Existing Glaciers, Obergurgl. 10-18 September, 1962, p. 173-7.
77) Hewitt, K. 1988. Catastrophic landslide deposits in the Himalaya. *Science*, 242:64-77.
78) Hicock, S. R. 1991. On subglacial stone pavements in till. *Journal of Geology*, 99:607-619.
79) Hodgson, K. A. 1993. (Vol. 1). *Late Quaternary Lahars from Mount Ruapehu in the Whangaehu River Valley, North Island, New Zealand.* Unpublished PhD Thesis. Massey University, Palmerston North.
80) Hoey, T. B. 2004. The size of sedimentary particles. In: Evans, D. J. A. & Benn, D. I. (Ed.). *A practical guide to the study of glacial sediments.* Arnold, Great Britain, London, p. 52 – 77.
81) Holmes, C. D. 1941. Till Fabric. *Bulletin of the Geological Society of America*, 52:1299-1354.
82) Hooke, R. LeB. (2nd Ed.) 2005. *Principles of Glacier Mechanics*. Cambridge University Press, United England.
83) Hooyer, T. S. & Iverson, N. R. 2000. Clast-fabric development in a shearing granular material: Implications for subglacial till and fault gouge. *GSA Bulletin*, (5) 112:683-692.
84) Hubbard, B. & Glasser, N. 2005. *Field Techniques in Glaciology and Glacial Geomorphology.* John Wiley & Sons Inc. England.
85) Iken, A. 1981. The effect of the subglacial water pressure on the sliding velocity of a glacier in an idealized numerical model. *Journal of Glaciology,* 27(97):407-421.
86) Iken, A., Rothlisberger, A. F. & Haeberli, W. 1983. The uplift of Unteraargletscher at the beginning of the melt season-a consequence of water storage at the bed? *Journal of Glaciology*, (101) 29:28-47.
87) Inman, D. L. 1952. Measures for describing the size distribution of sediments. *Journal of Sedimentary Petrology,* 22:125-145.
88) Iverson, N. R. 2002. Processes of Glacial Erosion. In: Menzies, J. (Ed.). Modern and Past Glacial Environments. Butterworth-Heinemann, Oxford, p. 131-146.

89) Jacka, T. H. 2006. Glacier composition, mechanics and dynamics. In: Knight, P. G. (Ed.). *Glacier Science and Environmental Change*. Blackwell Publishing, UK, p. 284-290.
90) Kaser, G. 2006. Mountain glaciers. In: Knight, P. G. (Ed.). *Glacier Science and Environmental Change.* Blackwell Publishing, UK, p. 268-271.
91) Karlstrom, T. N. V. 1952. Improved equipment and techniques for orientation studies of large particles in sediments. *Journal of Geology*, 60:489-498.
92) Kells, B. R. & Thompson, R. D. 1968. Glaciological Research on Mt Ruapehu. *Compass,* 3(2):1-7.
93) Kells, B. R. & Thompson, R. D. 1970. The Whakapapanui Glacier, Mt Ruapehu – resource or resistance? *Soil & Water,* 6(3+4):34-38.
94) Keys, H. 1988. 1988 Survey of the glaciers on Mt Ruapehu, Tongariro National Park a baseline for detecting effects of climatic change. *Science and Research Internal Report No. 24,* pp. 1-20.
95) Khatwa, A. & Tulaczyk, S. 2001.Microtextural interpretations of modern and Pleistocene subgalcially deformed sediments: the relative role of parent material and subglacial processes. *Journal of Quaternary Science,* 16(6):507-517.
96) Kirkbride, M. P. 2002. Processes of Glacial Transportation. In: Menzies, J. (Ed.). *Modern and Past Glacial Environments*. Butterworth-Heinemann, Oxford, p. 147-169.
97) Kirkbride, M. P. & Brazier, V. 1998. A critical Evaluation of the use of Glacier Chronologies in Climatic Reconstruction, with Reference to New Zealand. In: Owen, L. A. (Ed.). *Quaternary Proceedings, No 6, 1998, Mountain Glaciation.* Wiley & Sons, UK, pp.55-64.
98) Kirkbride, M. P. & Matthews, D. 1997. The Role of Fluvial and Glacial Erosion in Landscape Evolution: The Ben Ohau Range, New Zealand. *Earth Surface Processes and Landforms,* 22:317-327.
99) Kjaer, K. H. 1999. Mode of subglacial transport deduced from till properties, Myrdalsjökull, Iceland. *Sedimentary Geology,* 128(3-4):271-292.
100) Kjaer, K. H. & Krüger, J. 1998. Does clast size infuence fabric strength? *Journal of Sedimentary Research,* 68(5):746-749.
101) Knight, P. G. 1999. *Glaciers.* Stanly Thornes (Publishers) Ltd., United Kingdom.
102) Krenek, L.O. 1959. Changes in the Glaciers of Mt Ruapehu in 1955. New Zealand *Journal of Geology and Geophysics*, (4) 2: 643-653.
103) Krinsley, D. H. & Doornkamp, J. C. 1973. *Atlas of quartz sand surface textures.* Cambridge: Cambridge University Press, UK.
104) Krumbein, W. C. 1938. Size frequency distributions of sediments and the normal phi curve. *Journal of Sedimentary Petrology,* 8:84-94.
105) Krumbein, W. C. 1941. Measurement and geological significance of shape and roundness of sedimentary particles. *Journal of Sedimentary Petrology,* 11(2):64-72.
106) Kuhn, G., Melles, M., Ehrmann, W. U., Hambrey, M. J. & Schmiedl, G. 1993. Character of clasts in glaciomarine sediments as an indicator of transport and depositional processes, Weddell and Lazarev Seas, Antarctica. *Journal of Sedimentary Petrology,* 63:477-487.

107) Lamont, G. N., Chinn, T. J. & Fitzharris, B. B. 1999. Slopes of glacier ELA's inthe Southern Alps of New Zealand in relation to atmospheric circulation patterns.*Global and Planetary Change,* 22:209-219.
108) Landim, P. M. B. & Frakes, L. A. 1968. Distinction between tills and other diamictons based on textural characteristics. *Journal of Sedimentary Petrology,* 38 (4):1213-1223.
109) Larsen, N. K. & Piotrowski, J. A. 2003. Fabric Pattern in a Basal Till Succession and Its Significance for Reconstructing Subglacial Processes. *Journal of Sedimentary Research,* (5) 73:725-734.
110) Lawrence, D. B. 1969. *Recent Variations in Glaciers and Closed-Basin Lakes, Indicators of Climatic Change*. Lecture given to Quaternary Research Institute, University of Canterbury.
111) Lawson, D. E. 1979. A comparison of pebble orientations in ice and deposits of the Matanuska Glacier, Alaska. *Journal of Geology*, 87:629-45.
112) Lawson, W. & Fitzsimons, S. 2001. Glaciers and the Environment. In: Sturman, A. & Spronken-Smith, R. (Eds.). *The Physical Environment-A New Zealand Perspective.* Oxford University Press, Melbourne, p. 269-289.
113) Li, D., Yi, C., Ma, B., Wang, P., Ma, C. & Cheng, G. 2006. Fabric analysis of till clasts in the upper Urumqi River, Tian Shan, China. *Quaternary International*, 154-155:19-25.
114) Mahaney, W. C. 1995. Glacial crushing, weathering and diagenetic histories of quartz grains inferred from scanning electron microscopy. In: Menzies, J. (Ed.). *Modern Glacial Environments: Processes, Dynamics and Sediments*. Oxford, Butterworth-Heinemann, p. 487-506.
115) Mahaney, W. C., Claridge, G. & Campbell, I. 1996. Microtextures on quartz grains in tills from Antarctica. *Palaeogeography, Palaeoclimatology, Palaeoecology,* 121:89-103.
116) Mahaney, W. C., Dirszowsky, R. W., Milner, M. W., Menzies, J., Stewart, A., Kalm, V. & Bezada, M. 2004. Quartz microtextures and microstructures owing to deformation of glaciolacustrine sediments in the northern Venezuelan Andes. *Journal of Quaternary Science*, 19:23-33.
117) Mahaney, W. C. & Kalm, V. 2000. Comparative scanning electron microscopy study of oriented till blocks, glacial grains and Devonian sands in Estonia and Latvia. *Boreas*, 29:35-51.
118) Mark, D. M. 1973. Analysis of Axial Orientation Data, Including Till Fabrics. *Geological Society of America Bulletin,* 84:1369-1374.
119) Marshall, P. 1909. The Glaciation of New Zealand. *Transactions and Proceedings of the New Zealand Institute,* 42: 334-348.
120) Martini, P., Brookfield, M.E. & Sadura, S. 2001. *Principles of Glacial Geomorphology and Geology.* Prentice-Hall, Inc. New Jersey, United States of America.
121) Matthews, J. A. & Petch, J. R. 1982. Within-valley asymmetry and related problems of Neoglacial lateral moraine development at certain Jotunheimen glaciers, southern Norway. *Boreas,* 11:225-247.
122) Mazzullo, J. & Ritter, C. 1991. Influenze of sediment source on the shapes and surface textures of glacial quartz sand grains. *Geology* 19:384-388.

123) McArthur, J.L. & Shepherd, M.J. 1990. Late Quaternary glaciation of Mt Ruapehu, North Island, New Zealand. *Journal of the Royal Society of New Zealand* (20) 3:287-296.
124) McGlone, M., Salinger, M. J. & Moar, N. 1993. Paleovegetation Studies of New Zealand's Climate since the Last Glacial Maximum. In: Wrigh, H. *Global Climates since the Last Glacial Maximum.* University of Minnesota Press, Minneapolis, pp. 294-317.
125) McKinzey, K. M., Olafsdottir, R. & Dugmore, A. J. 2005. Perception, history, and science: coherence or disparity in the timing of the Little Ice Age masimum in southeast Iceland? *Polar Record,* 41(219):319-334.
126) Mee, K., Tuffen, H. & Gilbert, J. S. 2006. Snow-contact volcanic facies and their use in determining past eruptive environments at Nevados de Chillan volcano, Chile. *Bulletin of Volcanology,* 68:363-376.
127) Menzies, J. 2002. Ice Flow and Hydrology. In: Menzies, J. (Ed.). *Modern and Past Glacial Environments*. Butterworth-Heinemann, Oxford, p. 79-130.
128) Miller, H. 1884. *On boulder-glaciation*. Royal Physical Society. Edinburgh, Press. 8:156:189.
129) Mills, S. C. & Grab, S. W. 2005.Debris ridges along the southern Drakensberg escarpment as evidence for Quaternary glaciation in southern Africa. *Quaternary International,* 129:61-73.
130) Moar, N. T. & McKellar, I. C. 2001. Interglacial vegetation in South Westland, South Island, New Zealand. *Journal of Geology and Geophysics*, 44:17-24.
131) Morland, L. W. & Morris, E. M. 1977. Stress in an elastic bedrock hump due to glacier flow. *Journal of Glaciology*. 18:67-75.
132) Nakawo, M. & Rana, B. 1999. Estimate of ablation rate of glacier ice under a supraglacial debris layer. *Geografiska Annaler,* 81A:694-701.
133) Neall, V.E. 2001. Volcanic Landforms. In: Sturman, A. & Spronken-Smith, R. *The Physical Environment-A New Zealand Perspective*. Oxford University Press, Melbourne, 39-60.
134) Neall, V.E., Houghton, B.F., Cronin, S.J., Donoghue, S.L., Hodgson, K.A., Johnston, D.M., Lecointre, J.A. and Mitchell, A.R. 1999. *Volcanic Hazards at Ruapehu Volcano.* Ministry of Civil Defense, Volcanic Hazards Information Series No. 8.
135) Nye, J.F. 1957. The distribution of stress and velocity in glaciers and ice sheets. *Royal Society of London, Proceedings* 239A, 113-133.
136) Odell, N. E. 1955. Mount Ruapehu, New Zealand: Observations on its Crater Lake and Glaciers. *Journal of Glaciology,* Vol.2, 18: 599-605.
137) Owen, L. A. 1994. Glacial and non-glacial diamictons in the Karakoram Mountains and Western Himalayas. In: Warren, W. P. & Croot, D. G. (Eds.). *Formation and Deformation of Glacial Deposits*. Balkema, Rotterdam, p. 9-28.
138) Owen, L. A., Derbyshire, E. & Scott, C. H. 2002. Contemporary sediment production and transfer in high-altitudes glaciers. *Sedimentary Geology*, 155:13-36.
139) Park, J. 1909a. On the Glacial Till in Hautapu Valley, Rangitikei, Wellington. *Transactions and Proceedings of the New Zealand Institute,* 42: 575-580.

140) Park, J. 1909b. Further Notes on the Glaciation of the North Island of New Zealand. *Transactions and Proceedings of the New Zealand Institute,* 42: 580-584.
141) Park, J. 1909c. Some Evidences of Glaciation on the Shores of Cook Strait and Golden Bay. *Transactions and Proceedings of the New Zealand Institute*, 42: 585-588.
142) Park, J. 1909d. The Great Ice Age of New Zealand. *Transactions and Proceedings of the New Zealand Institute,* 42: 589-609.
143) Park, J. 1910. *The Geology of New Zealand-An Introduction to the Historical, Structural, and Economic Geology.* Whitcombe & Tombs, Ltd., Christchurch, New Zealand.
144) Park, J. 1915. On the Occurrence of a Striated Erratic Block of Andesite in the Rangitikei Valley, North Island, New Zealand. *Transactions and Proceedings of the New Zealand Institute,* 48: 135-137.
145) Park, J. (2nd Ed) 1925. *A Text Book of Geology*. Charles Griffin & Companay, Ltd., London.
146) Park, J. 1926. Morainic Mounds on the Waimarino Plain near Ruapehu. *Transactions and Proceedings of the New Zealand Institute*, 56: 382-383.
147) Pelto, M. S. & Hedlund, C. 2001. Terminus Behavior and Response Time of North Cascade Glaciers, Washington, USA. *Journal of Glaciology*. (158)47:497-506.
148) Porter, S. C. 1975. Equilibrium-Line Altitudes of Late Quaternary Glaciers in the Southern Alps, New Zealand. *Quaternary Research,* 5:27-47.
149) Powers, M. C. 1953. A new scale for sedimentary particles. *Journal of Sedimentary Petrology,* 23(2):117-119.
150) Price, R. J. 1973. *Glacial and Fluvioglacial Landforms-Geomorphology Text 5.* Oliver & Boyd, Edinburgh, Great Britain.
151) Procter, J. N. 2003. *The Quaternary Geology of the Southeastern section of Ruapehu Volcano.* Unpublished Master Thesis. Massey University, Palmerston North.
152) Richards, B. W. M. 2000. Luminescence dating of Quarternary sediments in the Himalayas and High Asia: A practical guide to its use and limitations for constraining the timing of glaciation. *Quaternary International,* 65/66:49-61.
153) Richter, K. 1932. Die Bewegungsrichtung des Inlandeis reconstruiert aus den Kritzen und Längsachsen der Geschiebe. *Zeitschrift Geschiebeforschung, Bd.* 8:62-66
154) Richter, K. 1933. Gefüge und Zusammensetzung des norddeutschen Jungmoränengebietes. *Abh. geol.- paleont. Inst. Greifwald. Bd*. 11:1-63.
155) Richter, K. 1936. Gefügestudien im Engebrae, Fondalsbrae und ihren Vorlandsedimenten. *Zeitschrift Gletscherkunde, Bd.* 24:22-30.
156) Rivera, A., Brown, F., Mella, R., Wendt, J., Casassa, G., Acuna, C., Rignot, E. Clavero, J. & Brock, B. 2006. Volumetric changes on active volcanoes in southern Chile. *Annals of Glaciology,* 43:111-122.
157) Rogerson, R. J. & Hudson, H. M. 1983. Quartz surface microtextures and grain-size characteristics of Quaternary sediments in the Porcupine Strand area of Coastal Labrador, Newfoundland, Canada. *Canadian Journal of Earth Sciences*, 20(3):377-387.

158) Rose, R. 1989. Glacier stress patterns and sediment transfer associated with superimposed flutes. *Sedimentary Geology,* 62:151-176.
159) Ruscoe, Q. W. (Ed.) 1978. *DSIR Bulletin No. 217 - The Eruption of Ruapehu New Zealand on 22 June 1969.* Crown Copyright.
160) Salinger, J. 2001. Climate Variation in New Zealand and the Southwest Pacific. In: Sturman, A. & Spronken-Smith, R. *The Physical Environment-A New Zealand Perspective*. Oxford University Press, Melbourne, 131-149.
161) Salinger, M.J. & McGlone, M.S. 1990. New Zealand climate-the past two million years. New Zealand Climate Report 1990, Royal Society of New Zealand, Wellington, pp.11-20.
162) Schmincke, H. 2004. *Volcanism*. Springer-Verlag, Germany.
163) Selby, M. J. 1985. *Earth's changing surface.* Oxford University Press, Great Britain.
164) Sharp, M., Jouzel, J., Hubbard, B. & Lawson, W. 1994. The character, structure and origin of the basal ice layer of a surge-type glacier. *Journal of Glaciology,* 40(135):327-340.
165) Shulmeister, J., Fink, D. & Augustinus, P. C. 2005. A cosmogenic nuclide chronology of the last glacial transition in North-West Nelson, New Zealand – new insights in Southern Hemisphere climate forcing during the last deglaciation. *Earth and Planetary Science Letters,* 233:455-466.
166) Singh, P., Kumar, N., Ramasastri, K. S. & Singh, Y. 2000. Influence of a fine debris layer on the melting of snow and ice on a Himalyan glacier. In: Nakawo, M., Raymond, C. F. & Fountain, A. (Eds.). *Debris-Covered Glaciers* (Proceedings of a workshop held at Seattle, Washington, USA, September 2000). IAHS Publ. no. 264, p. 63-69.
167) Small, R. J. 1987. In: Gurnell, A. M. & Clark, M. J. *Glacio-fluvial sediment Transfer.* John Wiley, Figs. 8.2 and 8.5, pp. 173 and 180.
168) Stevenson, J. A., McGarvie, D. W., Smellie, J. L. & Gilbert, J. S. 2006. Subglacial and ice-contact volcanism at the Öræfajökull stratovolcano, Iceland. *Bulletin on Volcanology,* 68:737-752.
169) Taylor, G. 1927. Notes on the Glaciation of Ruapehu. *Transactions and Proceedings of the New Zealand Institute*,57: 235-237.
170) Te Punga, M. T. 1953. *The Geology of Rangitikei Valley. New Zealand*.Geological Survey, Memoir 8. Owen, R. E., Government Printer, Wellington.
171) Thayyen, R. J., Gergan, J. T. & Dobhal, D. P. 2005. Monsoonal control on glacier discharge and hydrograph characteristics, a case study of Dokriani Glacier, Garhwal Himalaya, India. *Journal of Hydrology,* 306:37-49.
172) Tranter, M. 2006. Glacial chemical weathering, runoff composition and solute fluxes. In: Knight, P. G. (Ed.). *Glacier Science and Environmental Change*. Blackwell Publishing, UK, p. 71-75.
173) Udden, J. A. 1898. *Mechanical composition of wind deposits*. Augustina Library Pub. 1, p.69.
174) Upham, W. 1891. Criteria of englacial and subglacial drift. *American Geology*. 8:376-385.
175) van der Meer, J. J. M. 1993. Microscopic evidence of subglacial deformation. *Quaternary Science Review,* 12:553-587.

176) Vucetich, C. G. & Pullar, W. A. 1973. Holocene tephra formations erupted in the Taupo area, and interbedded tephras from other volcanic sources. *New Zealand Journal of Geology and Geophysics,* 16(3):745-780.
177) Wadell, H. 1932. Volume, shape, and roundness of rock particles. *Journal of Geology,* 40:443-451.
178) Wadell, H. 1933. Spericity and roundness of rock particles. *Journal of Geology,* 42:310-331.
179) Wadell, H. 1935. Volume, shape, and roundness of quartz particles. *Journal of Geology,* 43:250-280.
180) Wentworth, C. K. 1922. A scale of grade and class terms for clastic sediments. *The Journal of Geology,* 30:377-92.
181) Werner, R. & Schmincke, H-U. 1999. Englacial vs lacustrine origin of volcanic table mountains: evidence from Iceland. *Bulletin of Volcanology*, 60:335-354.
182) West, R. G. & Donner, J. J. 1956. The Glaciation of East Anglia and the East Midlands: a differentiation based on stone-orientation measurements of tills. *Quaternary Journal of the Geological Society, London*, 112:69-91
183) Whalley, W. B. & Krinsley, D. H. 1974. A scanning electron microscope study of surface textures of quartz grains from glacial environments. *Sedimentology,* 21:87-105.
184) Williams, K. 2001. *Volcanoes of the South Wind-A Field Guide to the Volcanoes and Landscape of Tongariro National Park.* Tongariro Natural Society, Turangi, New Zealand.
185) Willett, R. W. 1950. Pleistocene Snow Line, Climatic Conditions, and Suggested Biological Effects. *The New Zealand Journal of Science and Technology.* 32 (B): 18-48.
186) Winkler, S. 2004. Lichenometric dating of the 'Little Ice Age' maximum in Mt Cook National Park, Southern Alps, New Zealand. *The Holocene,* 14(6):911-920.
187) Wright, H. E. 1957. Stone orientation in the Wadena drumlin field, Minnesota. *Geogr. Ann*. 39:19-31.
188) Zemp, M., Haeberli, W., Hoelze, M. & Paul, F. 2006. Alpine glaciers to disappear within decades? *Geophysical Research Letters*. 33:L13504.